019776

GEOLOGY AND GEOLOGICAL RESERVES OF THE FARO, GRUM AND VANGORDA DEPOSITS

CURRAGH RESOURCES

MARCH 1987

INTRODUCTION

This document is a summary of the geology of the Anvil District and the Faro Grum and Vangorda deposits. A detailed discussion of the reserve calculations for each deposit is included along with comparisons to previous reserve calculations. For the Faro deposit a comparison of the reserves to 1986 production is presented.

Two appendices provide more detailed information on the geology of the Anvil Range and the regional geology of the southern Yukon.

TABLE OF CONTENTS

INTRODUCTION

3.1 District Geology

3.1.1 Introduction
3.1.2 Regional Geology
3.1.3 District Stratigraphy

3.1.3.1 Introduction

3.1.3.2 The Lower Division

3.1.3.2.1 Mt. Mye formation

3.1.3.2.2 Vangorda formation

3.1.3.2.3 Menzie Creek formation

3.1.4 Deformation, Metamorphism and Phutosism

3.1.5 Ore deposits

3.1.5.1 General Description

3.1.5.2 Description of Sulphide Rock Types

3.1.5.2.1 Massive Pyritic Sulphides

3.1.5.2.2 Baritic Massive Sulphides

3.1.5.2.3 Carbonate bearing Massive Sulphides

3.1.5.2.4 Pyrrhotitic Massive Sulphides

3.1.5.2.5 Ribbon Banded Graphitic Quartzite

3.1.5.2.6 Pyritic Quartzite

3.1.5.3 Alteration

3.1.5.4 Lithologic Terminology

3.1.6 References

3.2 Faro

3.2.1 History

3.2.2 General Geology

3.2.2.1 Stratigraphy and Lithology

3.2.2.2 Structure

3.2.2.3 Deposit Geology

3.2.3 Drilling Density

3.2.4 Reserve Calculation

3.2.4.1 Methods and Procedure - FI Model

3.2.4.1.1 Block Geology and Drillhole Data

3.2.4.1.2 Composite Calculation

3.2.4.1.3 Interpolation

3.2.4.1.4 Reserve Reporting

3.2.4.2 Methods and Procedure - F8608 Model

3.2.4.2.1 Block Geology & Drillhole Data

3.2.4.2.2 Composites

3.2.4.2.3 Interpolation

3.2.4.2.4 Reserve Reporting

3.2.4.3 Results

3.2.4.3.1 Geological Reserves

3.2.4.3.2 Model to Model Comparisons

3.2.4.3.3 Comparison to Blasthole Results

3.2.4.3.4 Conclusions

3.2.5 Additional Work Required

3.3 Grum Geology and Reserves

3.3.1 History

3.3.2 General Geology

3.3.2.1 Lithology

3.3.2.2 Structure

3.3.2.3 Surficial geology

3.3.2.4 Ore deposit geology

3.3.3 Drill definition and information base

3.3.4 Methods and procedure of reserve calculation

3.3.4.1 Introduction

3.3.4.2 Block geology and drillhole information

3.3.4.3 Composite calculation

3.3.4.4 Variogram analysis

3.3.4.5 Interpolation

3.3.4.6 Geological reserve reporting

3.3.5 Results

3.3.5.1 Geological Reserves

3.3.5.2 Model to Model Comparisons

3.3.5.3 Reliability of geological reserves

3.3.6 Additional work needed

3.4 Vangorda Geology and Reserves

3.4.1 History

3.4.2 General Geology

3.4.2.1 Stratigraphy and Lithology

3.4.2.2 Structure

3.4.2.3 Deposit description

3.4.3 Drilling density and information base

3.4.4 Methods and procedure of reserve calculation

3.4.4.1 Introduction

3.4.4.2 Block geology and drillhole information

3.4.4.3 Composite calculation

3.4.4.4 Interpolation

3.4.5 Results

3.4.5.1 Geological reserves

3.4.5.2 Comparison of geological reserves

3.4.5.3 Reliability of geological reserves

3.4.6 Additional work required

APPENDIX A Geology and Sulphide Deposits of the Anvil Range, Yukon

APPENDIX B Geology and Mineral Deposits of Southern Yukon

3.1 District Geology

3.1.1 Introduction

The Anvil Range Pb-Zn-Ag District is located in the central Yukon Territory near the town of Faro (figure 2.1). The district contains one of the world's largest reserves of lead and zinc in several deposits (figure 3.1) including the recently re-opened Faro mine.

3.1.2 Regional Geology

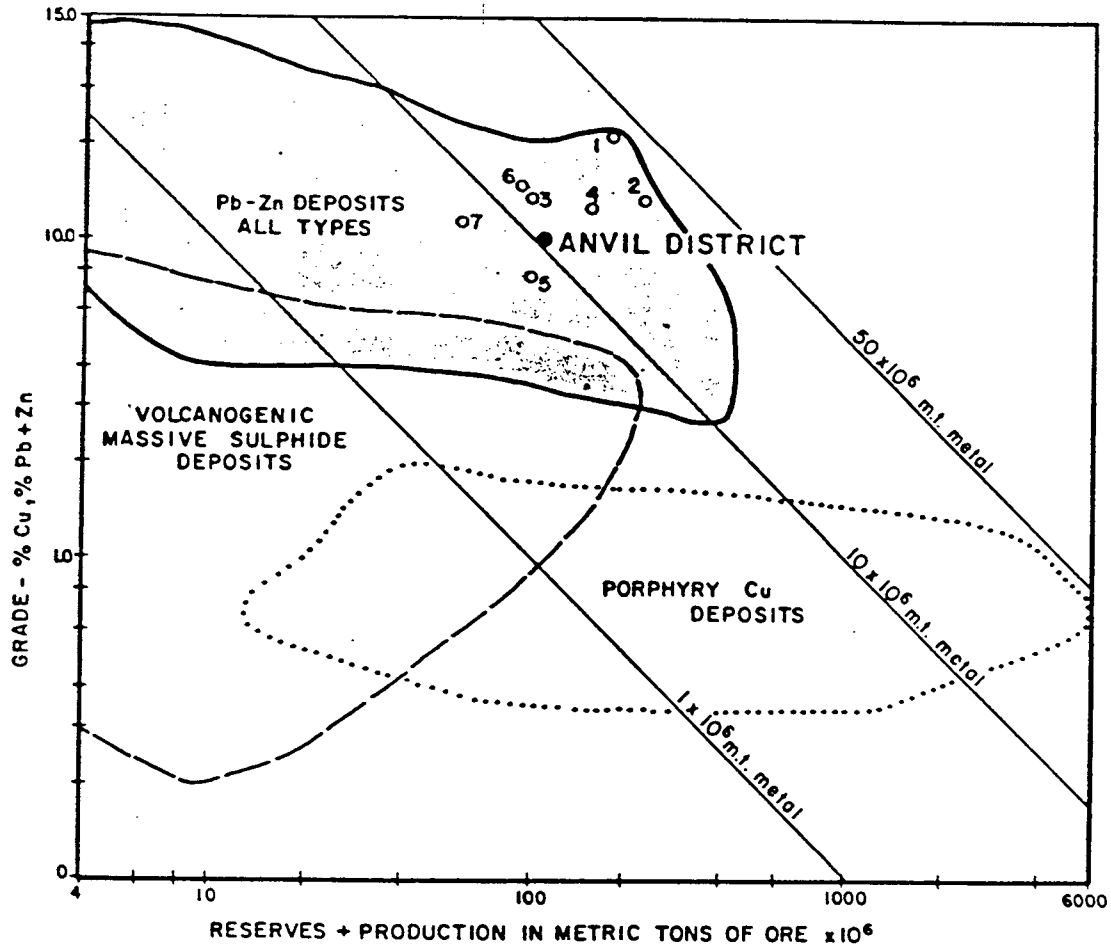
The Anvil District is part of the Selwyn Basin (figure 3.2), a large area of central Yukon where deep water shales accumulated along the ancient North American continental margin during the Paleozoic. The shales of the Selwyn Basin host most of Canada's large stratiform lead-zinc deposits, making it a metallogenic province of world wide significance. Unlike the remainder of the Selwyn Basin, the rocks and ores of the Anvil District are metamorphosed thus the shales are converted to phyllites and schists. The central part of the District in underlain by a large granitic body that cores an enlogate dome exposing the metamorphic sequence (Figure 3.3). The District contains several stratiform, lead-zinc-silver bearing, pyritic, massive sulphide deposits hosted by Cambrian metasediments on the southwest flank of the dome. The Tintina Fault, one of the major right lateral Cordilleran strike slip faults, passes just south of the district (Figures 3.2 and 3.3) but is not directly related to the ores.

3.1.3 District Stratigraphy

3.1.3.1 Introduction

The stratigraphic sequence of Anvil District ranges in age from latest Precambrian to Permian. Two major divisions or assemblages of strata are present. They are separated by a poorly exposed interval of black shale of uncertain affinity which contains late middle Devonian limestone lenses (Tempelman-Kluit, 1972).

The lower division ranges in age from late Precambrian to perhaps Early Silurian. It is approximately 5 km thick and divisible into three major mappable units (fig.3.4). From the base these are non-calcareous metapelite of Mt. Mye formation, calcareous metapelite of Vangorda formation and basalt and black phyllite of Menzie Creek formation. Established formal stratigraphic nomenclature does not apply directly to this area but the rocks are very similar to those of Kechika Group (Gordey, 1981) south of the district in Pelly Mountains. The lead zinc deposits occur within a restricted portion of the lower division.



1 BROKEN HILL, AUSTRALIA

2 MACARTHUR RIVER, AUSTRALIA

3 MT.ISA, AUSTRALIA

4 SULLIVAN, CANADA

5 HOWARDS PASS, CANADA

6 RED DOG, ALASKA

7 MEGGEN, WEST GERMANY

FIGURE 3.1

COMPARISON OF SIZE GRADE CHARACTERISTICS OF SOME MAJOR LEAD-ZINC DEPOSITS

JUNE 1986

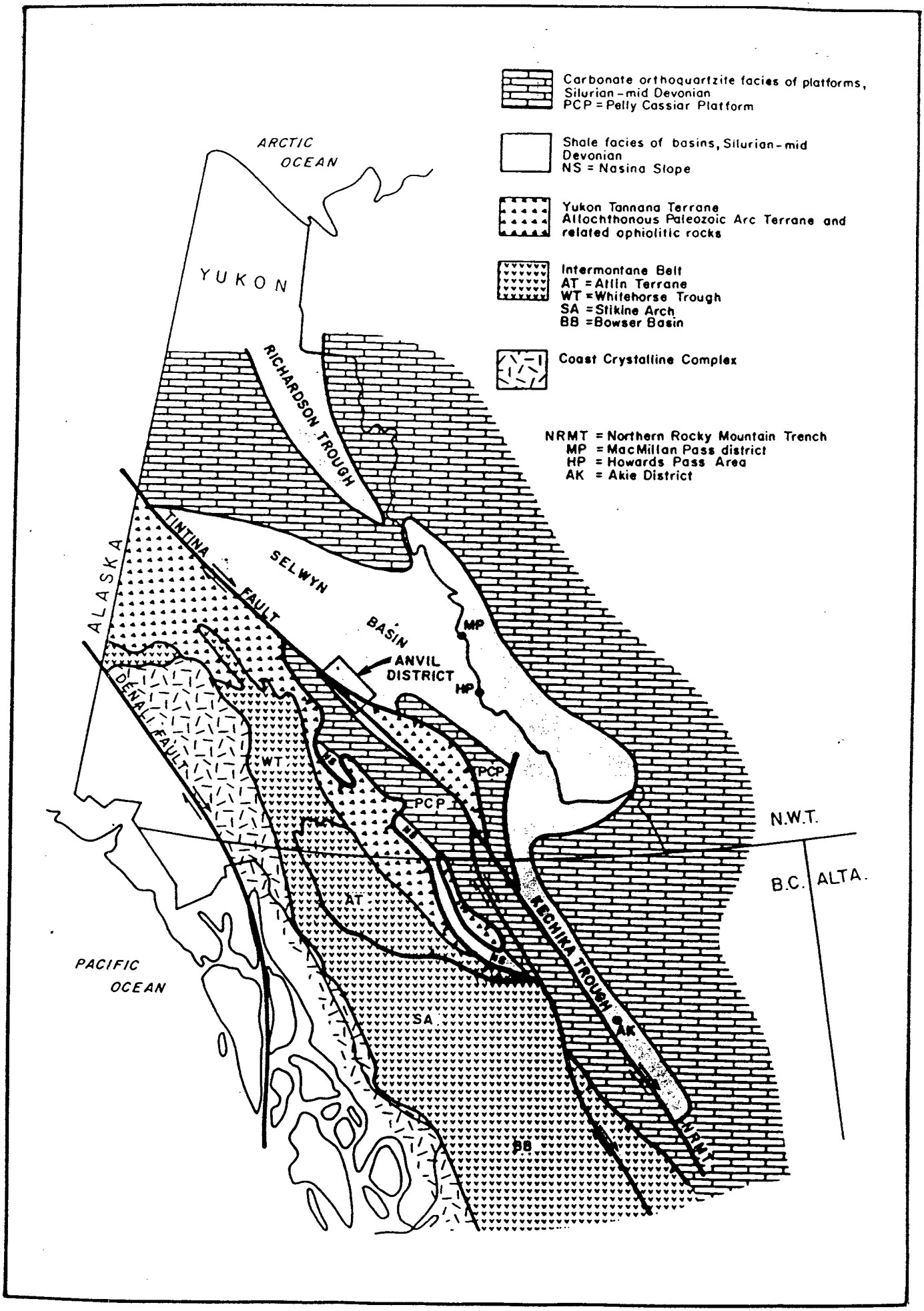

Carbonate orthoquartzite facies of platforms, Silurian-mid Devonian
PCP = Pelly Cassiar Platform
Shale facies of basins, Silurian-mid Devonian
NS = Nasina Slope
Yukon Tannana Terrane
Allochthonous Paleozoic Arc Terrane and related ophiolitic rocks
Intermontane Belt
AT = Atlin Terrane
WT = Whitehorse Trough
SA = Stikine Arch
BB = Bowser Basin
Coast Crystalline Complex
NRMT = Northern Rocky Mountain Trench
MP = MacMillan Pass district
HP = Howards Pass Area
AK = Akie District
ARCTIC OCEAN
YUKON
RICHARDSON TROUGH
TINTINA FAULT
SELWYN BASIN
ANVIL DISTRICT
DENALI FAULT
ALASKA
PACIFIC OCEAN
MP
HP
AK
WT
AT
PCP
SA
BB
NS
KECHIKA TROUGH
NRMT
N.W.T.
B.C.
ALTA.

Figure 3.2

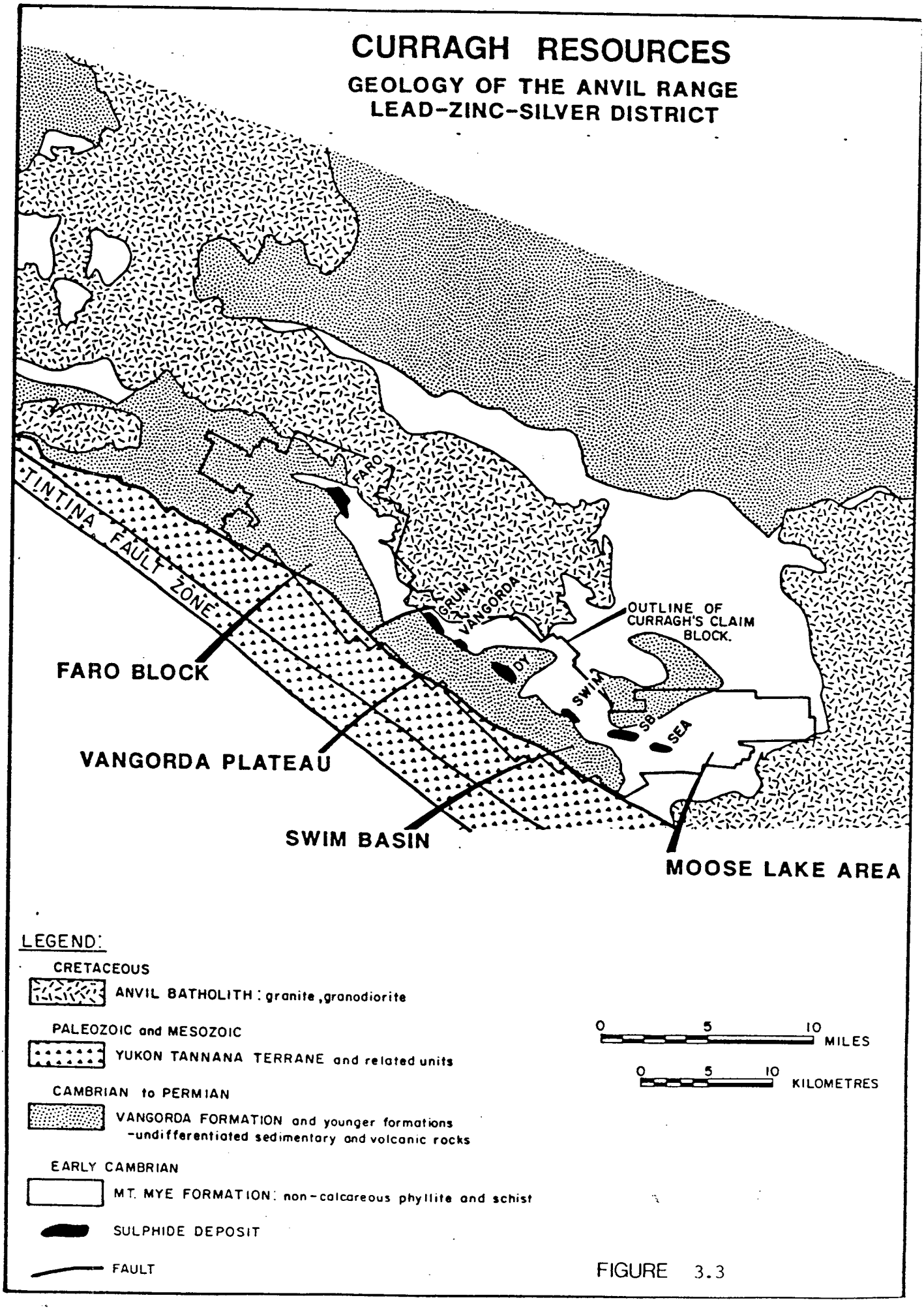

CURRAGH RESOURCES
GEOLOGY OF THE ANVIL RANGE
LEAD-ZINC-SILVER DISTRICT
TINTINA FAULT ZONE
FARO
GRUM
VANGORDA
DY
SWIM
SB
SEA
OUTLINE OF CURRAGH'S CLAIM BLOCK.
FARO BLOCK
VANGORDA PLATEAU
SWIM BASIN
MOOSE LAKE AREA
LEGEND:
CRETACEOUS
ANVIL BATHOLITH: granite, granodiorite
PALEOZOIC and MESOZOIC
YUKON TANNANA TERRANE and related units
CAMBRIAN to PERMIAN
VANGORDA FORMATION and younger formations -undifferentiated sedimentary and volcanic rocks
EARLY CAMBRIAN
MT. MYE FORMATION: non-calcareous phyllite and schist
SULPHIDE DEPOSIT
FAULT
0 5 10 MILES
0 5 10 KILOMETRES

FIGURE 3.3

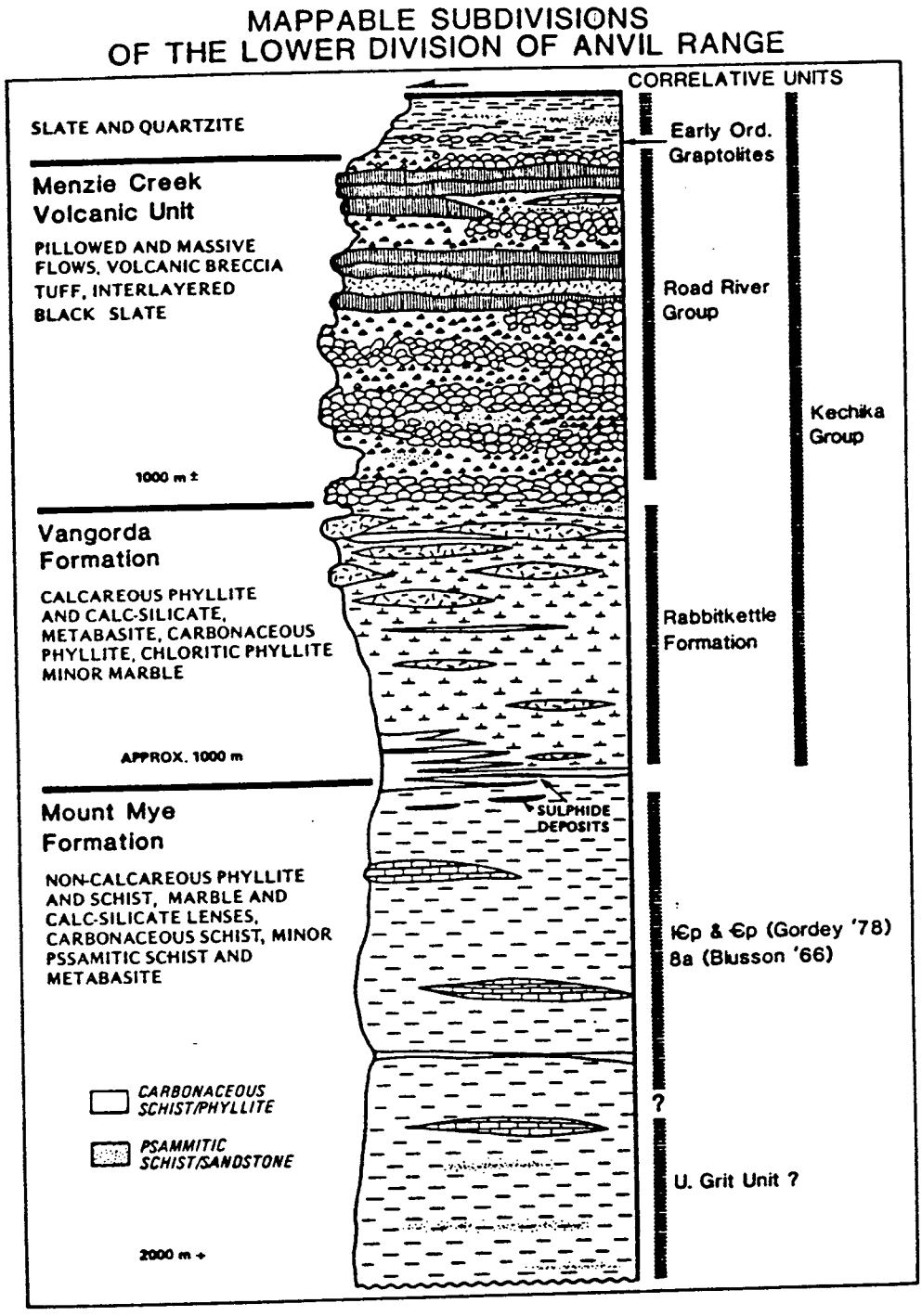


Figure 3.4 Diagramatic stratigraphic section of the lower Paleozoic of Anvil Range showing the ore deposits in relation to stratigraphy. Note that the bulk of the metavolcanics or metabasites are younger than the ore deposits but that the deposits are approximately coincident with the first appearance of substantial mafic igneous material in the section. Note also the anomalous thickness of carbonaceous rocks near the ore deposit trend.

The upper division includes rocks ranging in age from Devonian to Permian. In contrast to the lower division, the upper division is characteristically cherty and conspicuously coarsely clastic. All or part of the upper division may be allochthonous with respect to the lower. The upper division is host to stratiform barite deposits and to a number of interesting geologic problems beyond the scope of this summary.

3.1.3.2 The Lower Division

3.1.3.2.1 Mt. Mye formation

The Mt. Mye formation varies from non-calcareous, biotite-muscovite schist to non-calcareous, weakly carbonaceous, light to medium gray muscovite-chlorite phyllites with lesser, interlayed, black graphitic phyllite, marble, calc-silicate phyllite or schist, metabasite and psammitic schist. At Faro the formation is dominated by schistose variants of these rock types. The formation is at least 2 kilometers thick, its base is not exposed in the district.

The upper portion of the formation is very similar to the buff weathering mudstone and blue-grey mudstone units described by Gordey (1978) to the east near Howards Pass and to unit 8A of Blusson (1966) near Cantung. Correlation with these units would imply the top of the formation is lower Cambrian or possibly middle Cambrian. Parts of the Mt. Mye also resemble rocks underlying those presumed correlative units locally, implying the Mt. Mye probably includes rocks as old as Hadrynian.

3.1.3.2.2 Vangorda formation

The Vangorda formation is characterized by light to medium-gray, calcareous, phyllitic rocks made up of very thin (0.1-2 cm) interlayers of a) medium grey, non-calcareous, weakly carbonceous, muscovite-chlorite pelite and b) light grey, generally calcareous quartz $\pm$ calcite $\pm$ dolomite siltstone. In areas of more intense metamorphism, such as near the Faro deposit, the calcareous phyllite is altered to a harder, banded, green, purplish brown and creme coloured calc-silicate. Other rock types interbedded with the calcareous phyllite include metabasite and meta-tuffs, graphitic phyllite, and phyllitic limestone.

Most metabasite bodies are medium-grained and equigranular, thus they may have been sills; however, locally amygdaloidal margins and a common association with thin bedded, tuffaceous rocks suggests at least some were flows. Whole rock compositional data shows that the metabasites are all of basaltic composition. The bodies range from 1 to 100 meters in thickness and are up to several kilometers in length.

The Vangorda formation varies between 0.5 and 2 kilometers in apparent thickness with basic igneous rocks comprising approximately 15% of the section. The formation becomes more

calcareous up section, paralleling an increase in metabasaltic units. A major carbonaceous member occurs at the base of the formation.

The Vangorda formation is lithologically similar to, though more argillaceous than, Rabbitkettle Formation seen to the east (Gordey, 1978, Gabrielse et al., 1973). Based on this correlation the Vangorda formation may range in age from middle or upper Cambrian through lower Ordovician.

3.1.3.2.3 Menzie Creek formation

The Menzie Creek formation is a unit of basaltic metavolcanic rocks consisting of pillowed and massive flows with comparable amounts of massive, coarse, monolithic breccias and lesser, thin-bedded tuff and/or volcanic sandstone and siltstone. Carbonaceous phyllite and brown siltstone interbeds northeast of the Anvil Batholith contain graptolites of middle Ordovician or lower Silurian age (Tempelman-Kluit, 1972) suggesting correlation with the widespread Road River Formation black shale and chert to the northeast. The Menzie Creek formation varies from zero to about 1.5 kilometers in thickness in and near the district. It has been traced for 100 kilometers along strike and 30 kilometers across strike, showing that it is one of the largest of several basaltic units of its age in and around the Selwyn Basin.

3.1.3.3 Relation of Stratigraphy to ore deposits

The ore deposits of Anvil District are stratiform and stratabound to an approximately 150m thick interval straddling the contact of the Mount Mye and Vangorda formations. The deposits consist of one to five horizons of sulphide mineralization stacked one above the other within this interval. They appear to be related to facies changes involving the basal carbonaceous member of the Vangorda formation.

3.1.4 Deformation, Metamorphism and Plutonism

The structural and metamorphic history of the Anvil Range is complex and of considerable significance to the form and nature of the ore deposits. During mid-Mesozoic, the district suffered two periods of intense fold deformation and concurrent metamorphism during which the gross structure of the mineral deposits was determined.

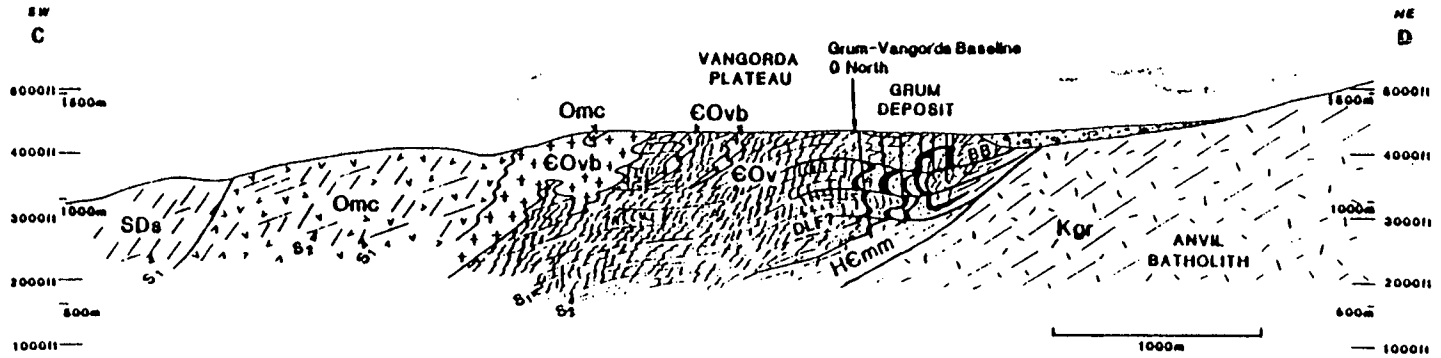
The first deformation (D_1) produced a regional metamorphic foliation (S_1) axial planar to tight to isoclinal mesoscopic folds (F_1) in bedding (S_0). Mesoscopic early folds are rarely preserved in the district. Northeasterly inclined to upright, northeasterly verging megascopic folds with shallow northwesterly or southwesterly plunging axes appear to have formed at that time.

During the second event (D_2), S_1 was strongly crenulated and ubiquitous close to tight mesoscopic folds in S_1 were produced (figure 3.5). Some of the largest megascopic folds known to have been formed during D_2 are those at the Grum Deposit (Figure 3.8) and comparable folds in the Swim Deposit (Figure 3.12). Parallel to the axial planes of these D_2 folds is a crenulation cleavage (S_2) which imparts a well developed lithon structure and pronounced fissility to most rocks of the district, especially the strongly banded phyllites of the Vangorda formation. F_2 axial planes and S_2 dip shallowly, with axes subparallel F_1 axes.

Three later, less intense periods of folding and associated faulting followed. The later events (D_3 through D_5) generally produced open folds and weak crenulations in S_2 related to broad, regional structures. An important exception to this general rule is found in the vicinity of the Faro deposit where the fourth event (D_4) is quite intense. At Faro tight mesoscopic folds are developed in nearly pervasive S_2 with appreciable mica growth along S_4 (see Figure 3.7 for examples of fourth phase affecting outline of the Faro deposit).

During the later stages of the fold deformation history a large granitic body (Anvil Batholith) was intruded into the metamorphic sequence. Anvil Batholith ranges in composition from granodiorite to quartz monzonite and textures include equigranular massive, megacrystic massive and various strongly to weakly foliated variants. Several K/Ar ages on the granitic rocks yield ages of 85-100 ma (Tempelman-Kluit, 1972). Intrusion of the Anvil Batholith further deformed the metamorphic sequence so that the overall structure of the district is an elongate dome cored by the Batholith (Figure 3.2). In the later stages of batholith emplacement large extensional fault displacements occured along its margins. These faults determine the present day limits of several of the deposits (Figures 3.9, 3.11 and 3.12).

Metamorphism was concurrent with deformation and was most intense during the early deformations, especially D_2. Metamorphic facies developed range from middle amphibolite facies to lower greenschist facies in a low pressure Buchan facies series. Metamorphic isograds are roughly concentric about the Anvil Batholith. Faro, close to the Batholith (figure 3.3) is strongly metamorphosed, while deposits such as Vangorda are less intensely metamorphosed. This difference in metamorphism is reflected in decreased grain size, increased degree of mineral intergrowth, and lesser iron content of sphalerite in the less metamorphosed deposits. This has a significant impact on metallurgical performance of Anvil district ores.





DEPOSITION D_1 D_2

Figure 3.5 Cross section through Vangorda Plateau and Grum deposit (86 W). The Grum deposit provides the best example of the D_1/D_2 interference pattern in the district. The deposit is involved in a large Z (or N) shaped D_1 fold refolded by S shaped D_2 folds. The steeply dipping S_1 crenulated by shallowly dipping S_2 is typical of the structural relations on the Vangorda Plateau where greenschist facies rocks dominate. Post D_2 folds gently warp the S_2 foliation. The inserts show the sequential development of Grum from a sequence of stacked en echelon ore layers parallel to S_0 through D_1 and D_2 to produce the geometry observed today.

3.1.5 Ore Deposits

3.1.5.1 General Description

The lead, zinc, silver deposits of Anvil Range are of the sediment hosted, stratiform, massive pyritic sulphide type (Gustafson & Williams, 1981; Large, 1980) or sedex type (Carne and Cathro, 1982). They occur as a single thick sulphide lens with little or no interbanded metasedimentary rocks (e.g. Faro) or as multilayered deposits with several thinner lenses stacked approximately one above the other with substantial metasedimentary or metavolcanic interlayers (e.g. Grum and Dy). An individual mineralized layer was deposited parallel to the bedding of the host sediments. It consisted of an upper, often centrally positioned, lead-zinc rich, massive sulphide facies and a lower and peripheral, lower grade, quartzose, disseminated sulphide facies.

These sulphide sheets, or horizons, have since been deformed into complex fold structures. The deposits are thus elongate parallel to the fold axes and associated lineations in the host metasediments. The Faro deposit, which appears to be an exception to this generalization, actually shows great internal complexity in the geometry of high grade and waste layers.

Present day deposit lengths are generally two to three times widths; unfolded deposit dimensions range up to 4000 m across their ameboid shapes. Individual sulphide horizons commonly are 10 to 40 m in thickness. The upper and lower contacts of sulphide horizons are invariably sharp while laterally the sulphides grade into the enclosing host rocks.

All deposits are composed of a small number of different sulphide rock types. As noted above the suplhide rock types are broadly divisable into massive sulphides and quartzose, disseminated sulphides. There are pyritic, baritic, pyrrhotitic and carbonate bearing variants of massive sulphide types and carbonaceous and non-carbonaceous variants of the quartzose sulphide rock types. The typical spatial distribution of these different types is shown in figure 3.6 with great vertical exaggeration.

The simplified arrangement of the sulphide rock types in the horizons is important since lead-zinc grade and metallurgical performance varies by ore type. The baritic massive sulphides are always high grade, easily grindable and yeild good grade concentrates with good recoveries. On the other hand the lower and distal graphitic quartzites are commonly low grade, hard and produce lower grade concentrates or low recoveries. Other ore types exhibit intermediate characteristics and performance.

All deposits show a variably developed, white mica-dominant, alteration overprint in the wallrocks.

There are presently five known lead zinc bearing mineral deposits along a prominant curvilinear trend on the south flank of Anvil Arch (Figure 3.3). From northwest to southeast they include Faro, Grum, Vangorda, Dy and Swim. Additionally two lead-zinc deficient sulphide occurances, the SB and Sea, are also known. Diagramatic sections through each of the major deposits are shown in Figures 3.7 through 3.12.

3.1.5.2 Description of Sulphide Rock Types

3.1.5.2.1 Massive Pyritic Sulphides: (Unit 2E / 2F)

The massive sulphides consist of banded to homogenous, usually weakly foliated and/or lineated, massive pyrite with lesser sphalerite and galena. Total sulphide content is at least 60%, generally greater than 80% and commonly nearly 100%. Gangue consists of quartz and/or barite and/or carbonates (calcite, dolomite, ankerite). Accessory minerals include pyrrhotite, chalcopyrite, magnetite, arsenopyrite and marcasite. At amphibolite facies metamorphic grade, this rock type commonly develops a buckshot porphyroblastic texture of pyrite in a matrix of dark reddish brown to black lead-zinc sulphides. This texture usually is restricted to rocks with economic lead-zinc grades (Unit 2F). Hard, barren, massive pyrite, commonly with disseminated, black, magnetite porphyroblasts, is widespread at Faro particularly in the northeast part of the deposit.

3.1.5.2.2 Baritic, Massive Pyritic Sulphides:

The baritic sulphides (Unit 2G) are strongly and thinly banded massive sulphide/sulphate rock consisting of pyrite, galena, sphalerite and commonly magnetic in a gangue of off-white barite and lesser carbonates (calcite, dolomite, ankerite and probably barytocalcite). The amount of barite may be as high as 50%; non-sulfidic, massive barite does not occur in the Anvil deposits. There is a complete gradation between this and the above facies with 10% visible barite by volume being the dividing line. This facies is usually quite high grade (10-15% combined lead-zinc). Sphalerite is characteristically honey coloured to reddish brown. Pyrrhotite is not commonly seen in the baritic facies except in the Faro deposit where overall pyrrhotite is more abundant.

3.1.5.2.3 Carbonate-bearing, Massive Pyritic Sulphides:

The carbonate bearing sulphides (Unit 2K) are similar to massive pyritic sulphides but contain greater than 10% carbonate (calcite, dolomite, ankerite) either as interstitial gangue or as coarse patches and irregular blebs. This is a minor facies and is not known with certainty to always be an original composition variant. The most common occurance of coarse pinkish beige to tan, ankerite patches may represent recrystallized original carbonate or re-worked pre/syn-metamorphic veins. This variant is generally lead-zinc

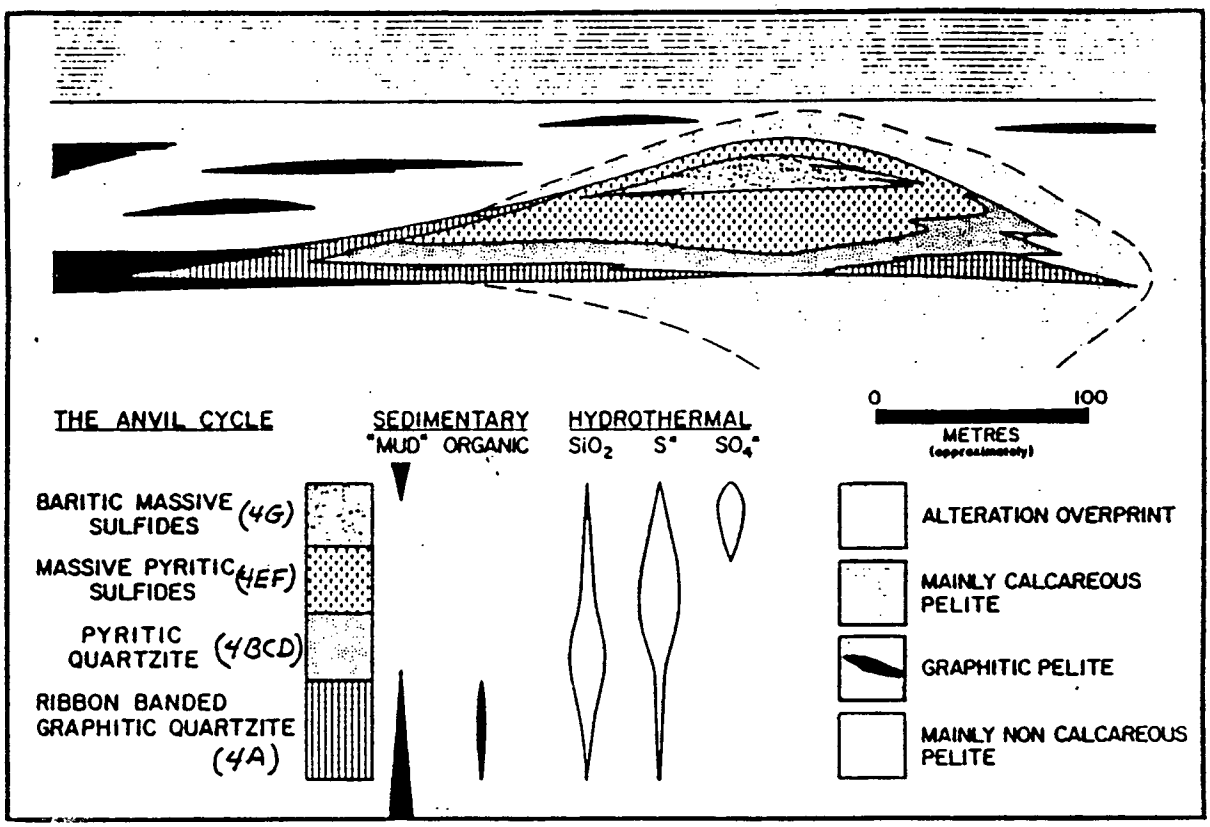


Figure 3.6 An idealized Anvil deposit based on cross sections of the Faro deposit. Such lateral and vertical zoning can be found in all deposits of the district. Massive sulphides are the central and upper lithofacies with pheripheral and lower quartzose disseminated lithofacies.

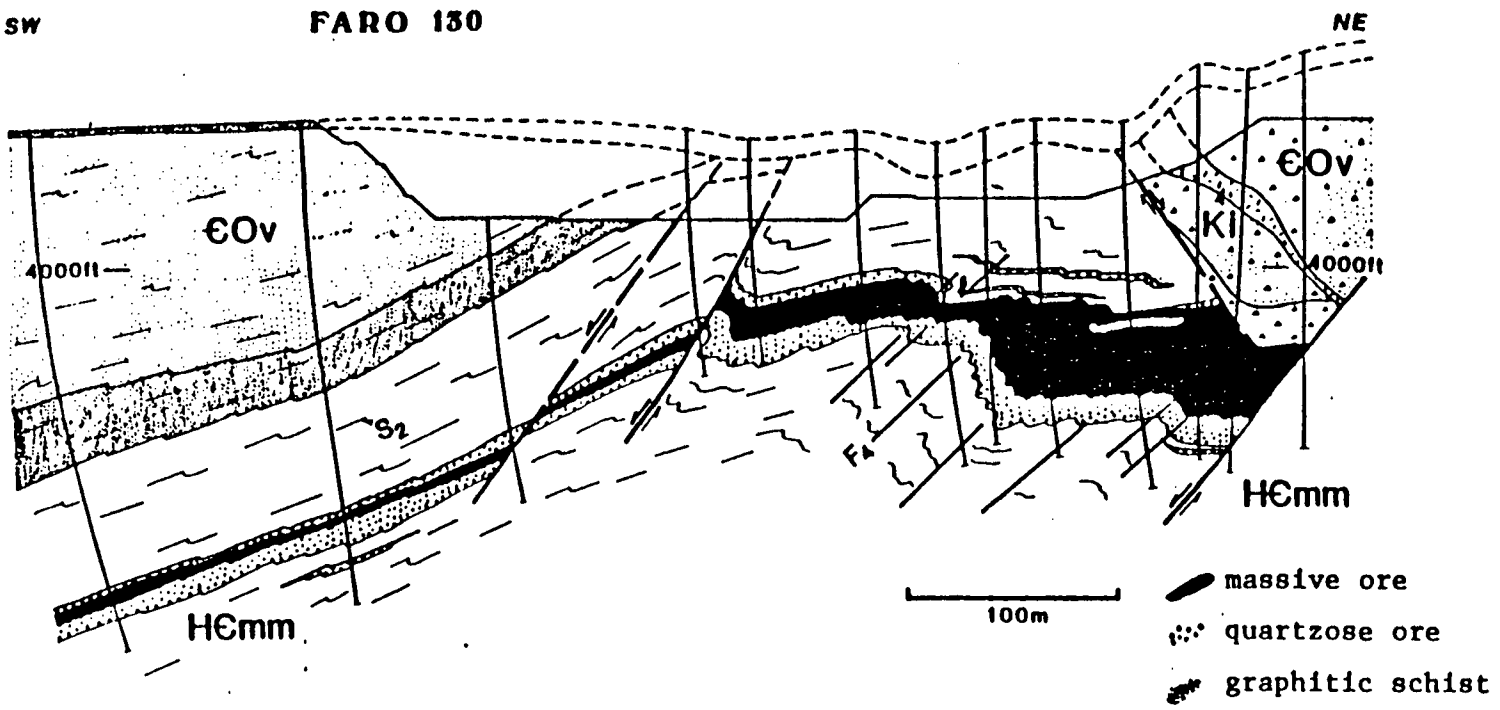


Figure 3.7 Cross section 130 through the southeast end of Faro zone 3. The pit outline shown is the present outline (as of June 1982 at suspension of mining). The faults are part of the Big Indian Fault set that separated zone 2 from zone 3, they are normal faults and cut across the section at a small angle. The triangular symbols at the northeast end of the section indicate the "breccia cap", a large body of post metamorphic breccia apparently formed by explosive activity during dyke emplacement.

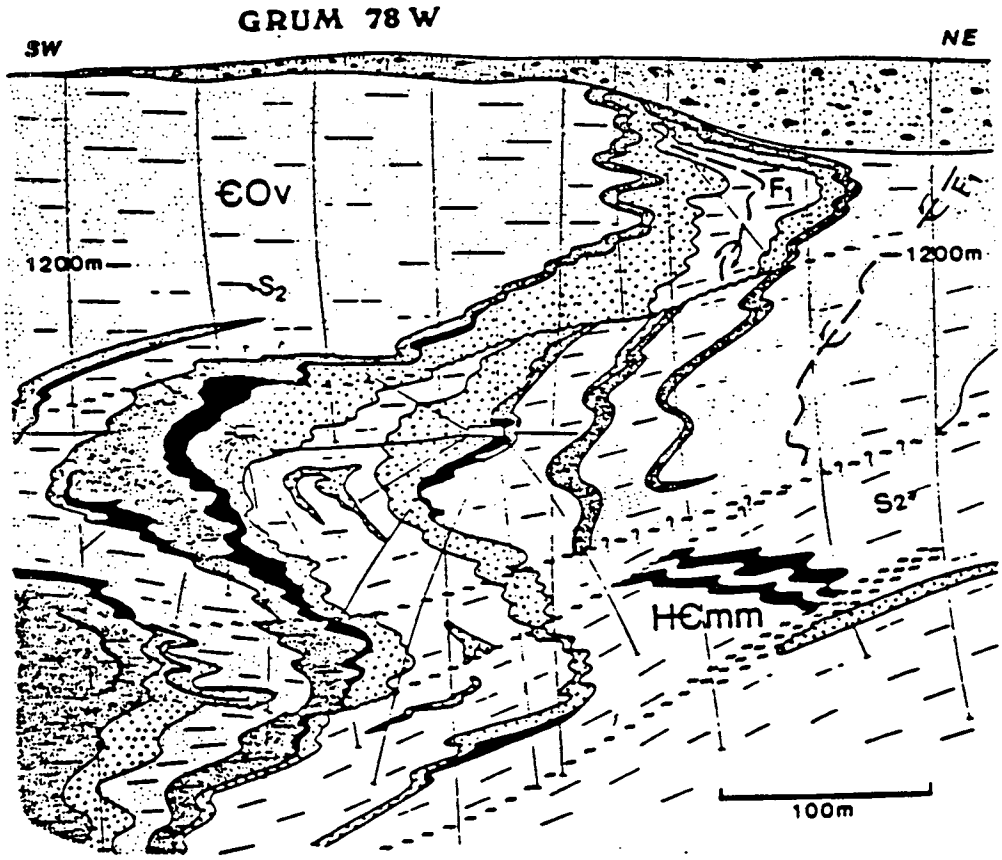


Figure 3.8. Cross section 78 W through the Grum deposit. The deposit forms a complex D_1/D_2 interference pattern which, despite the density of drilling, is not yet completely resolved. The faults appear to have slip lines directed across the plane of the cross section such that they "telescope" different deposit domains and appear not to make good sense on an individual section. The F_1 closure just beneath the overburden is confirmed on several densely drilled sections to the northwest down fold plunge.

massive ore

quartzose ore

graphitic phyllite

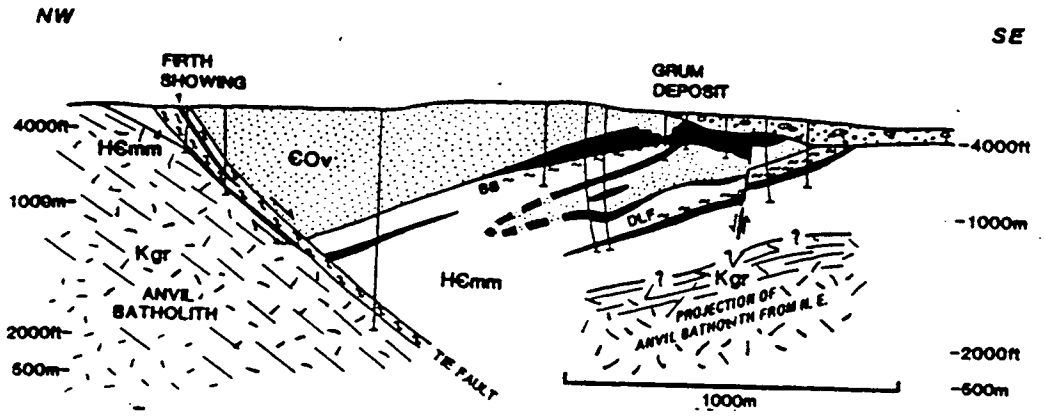


Figure 3.9 A diagramatic longitudinal showing the plunge of the Grum folded structure and the relation of the Grum deposit to the Firth showing. Firth appears to represent slivers of Grum caught in a large extensional fault, the Tie Fault, that separates footwall amphibolite facies metamorphic and granitic intrusive rocks from hangingwall greenschist facies

all sulphide lithofacies

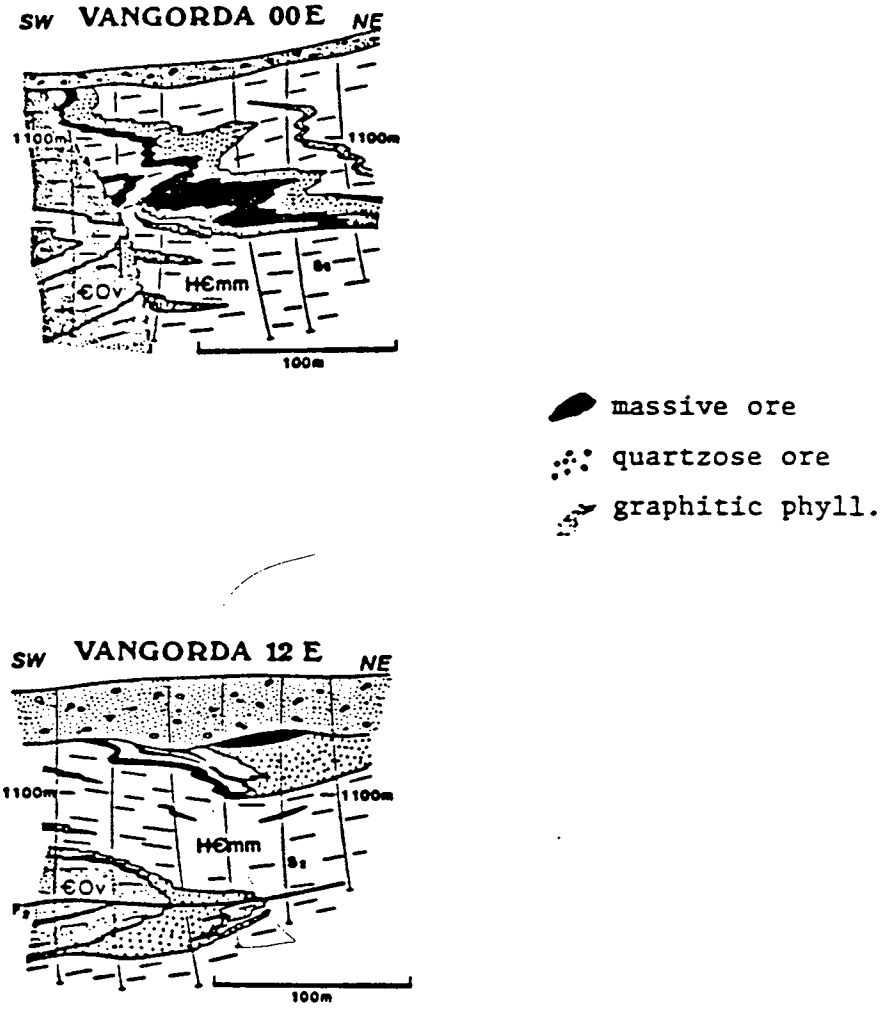


Figure 3.10 Cross sections 0E and 12E through the Vangorda deposit.

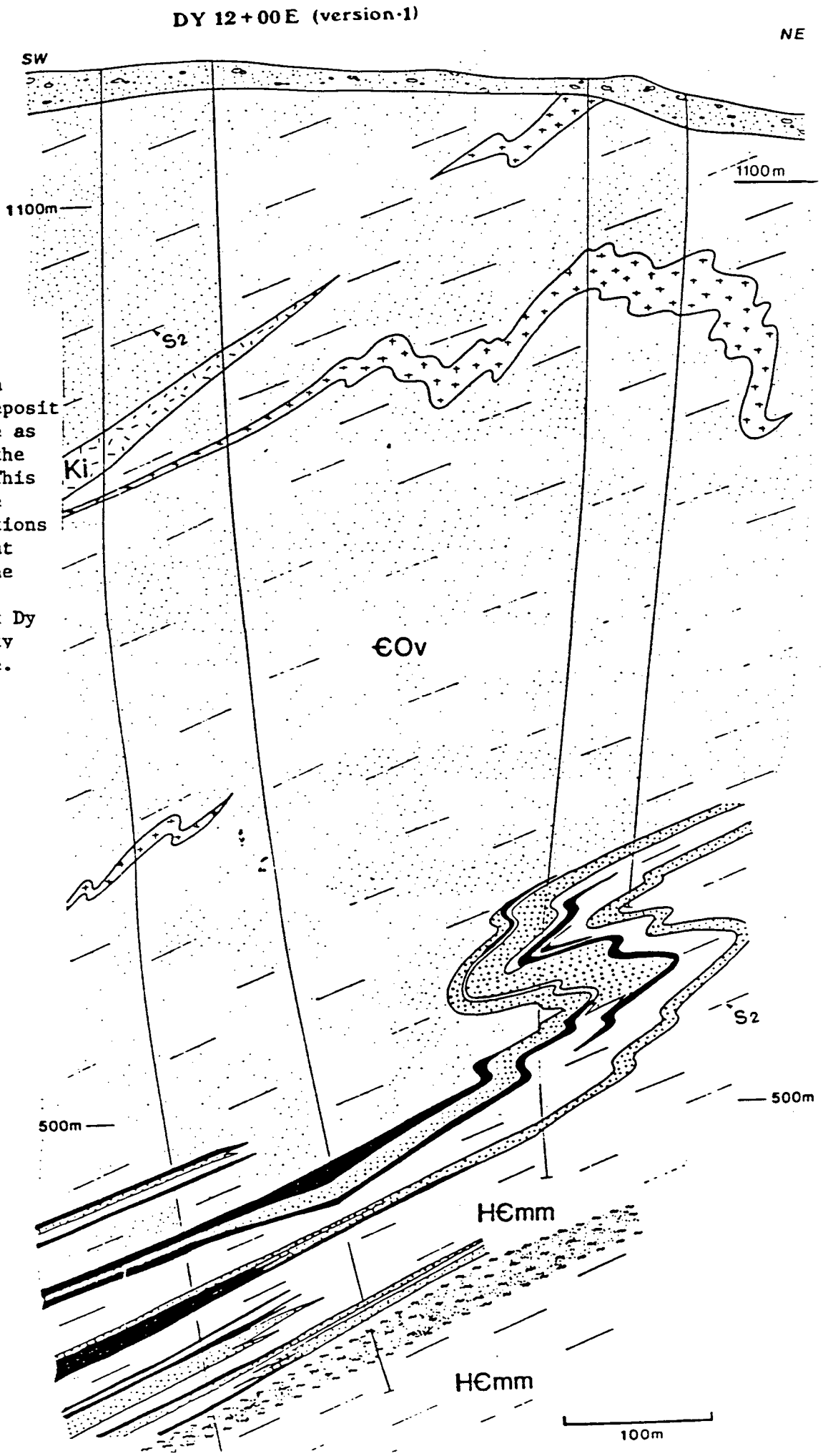
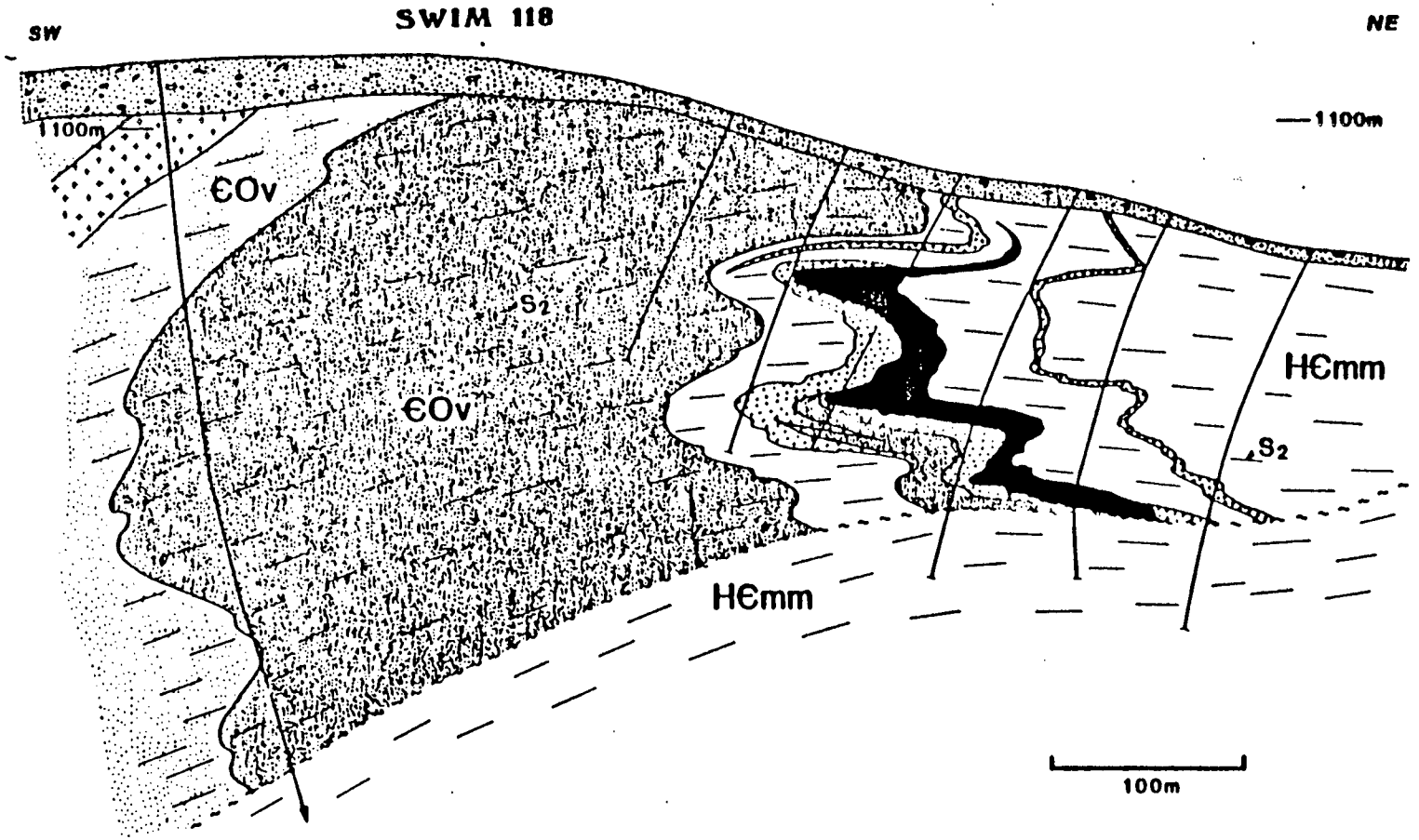


Figure 3.11

Schematic section through the DY deposit at the same scale as the sections of the other deposits. This is not one of the best drilled sections of the deposit but it illustrates the relative paucity of information at Dy and the difficulty of obtaining more.



massive ore
quartzose ore
graphitic phyll
metabasite

Figure 3.12 Cross section 118 through the Swim deposit. The basal massive sulphides in the main horizon are divisible into an upper baritic portion and a lower non baritic which is underlain locally by a thin quartzose unit thus the appearance of a reversed cycle is not real. The upper quartzose mineralization presumably represents the onset of a second incomplete (on this section at least) cycle. Displacement on the fault at the base of the deposit does not appear to be in the plane of the section, the resolution of this problem is a matter for furthur exploration.

poor. The variants with white interstitial gangue can be high grade and locally they texturally resemble the baritic sulphides

3.1.5.2.4 Pyrrhotitic Massive Sulphides:

This rock type (Unit 2H) consists of massive, finely crystalline, usually well foliated pyrrhotite with less than 50% pyrite porphyroblasts and highly variable amounts of sphalerite and galena. Minor chalcopyrite is characteristic of this relatively copper-rich facies. Rounded to angular, rotated, foliated quartzite or quartz-vein clasts 2 cm or less in diameter are typical. This is a minor facies and is not known with certainty to be primary as some pyrite in the massive facies may invert to pyrrhotite during regional metamorphism. At Faro the pyrrhotitic facies is more volumetrically important than the other deposits. Pyrrhotite rich ores are generally much finer grained than non pyrrhotitic ores at Faro.

3.1.5.2.5 Ribbon banded, "graphitic", pyritic quartzite:

This unit (Unit 2A)is a dark grey to black, well banded, sulphide-bearing quartzite (metamorphic usage). Bands are: (a) dark grey, very fine grained carbonaceous phyllitic quartzite to siliceous phyllite (presumed metachert) and (b) light grey, quartz-sulphide (pyrite-sphalerite-galena) bands. These bands are usually 2 mm to 2 cm thick. Total sulphide content of unit 2A is usually between 10 to 30% but ranges from 2% to 60%. Pyrite is usually the dominant species but higher grade examples have sub-equal pyrite and lead-zinc sulphides. Lead-zinc dominant variants with little pyrite occur but are not common unless total sulphide content is low. Strong sulphide species differentiation between bands, such that barren pyrite bands are adjacent to or near sphalerite or galena rich bands, occurs but is not generally the case.

3.1.5.2.6 Pyritic quartzite:

The pyritic quartzites (Units 2B, C, D)are light to medium grey, generally poorly banded, moderately to weakly foliated, micaceous quartzites with highly variable lead-zinc and pyrite contents. Pyrite contents are generally 10% to 40% ranging between 2 and 60%. Although there is a complete gradation from massive to quartzose ores there is usually little problem in separating this facies from the massive pyritic sulphides as the vast majority of examples have less than 40% total sulphides. A minor variant of this facies (unit 2B) shows low pyrite (< 5%) content with lead-zinc sulphides predominant. Barite in major amounts is uncommon in the quartose this facies; carbonate species are not typical but locally are abundant. Chalcopyrite, pyrrhotite and magnetite-bearing varieties are common. Sphalerite in the high grade examples is characteristically a vibrant reddish brown. At Faro the more sulphide rich variants of this facies are well developed along the northeast edge of zone 3. They are spectacularly barren but contain elevated copper contents and are rich in magnetite. A similar facies is developed at Vangorda and locally at Grum where the rocks are

also quite gold rich and more clearly in the deposit footwall.

3.1.5.3 Alteration

Both wallrocks and certain ore facies of the Anvil deposits are overprinted by a prominent, easily recognized, light beige, white mica dominant alteration assemblage (Units 2L and 1D4). This overprint facies is not a depositional unit and may form as a reaction product between wallrocks and deposit forming hydrothermal fluids, or as a metamorphic reaction envelope unrelated to ore forming fluids or as combination of these processes. In the multi-layered deposits, this alteration overprint appears discontinuous and often best developed in the footwall of a given lens or deposit as a whole. At Faro, a continuous envelope of this lithology encloses the entire deposit with local (especially Zone 1) best development in the hanging wall. The more intensely developed alteration assemblages can cause frothing problems in the mill since they contain talc or sericite that acts like talc

3.1.5.4 Lithologic Terminology

A consistent alphanumeric code for lithology for all Anvil District deposits was introduced a number of years ago to facilitate storage of lithology data in a computerized database. Since occasional reference to these codes is made in the following sections a brief note of explanation is in order. The system works on the basis of a number followed by a letter and then a series of numbers and or symbols. The first number refers to metamorphic grade and hence structural level: 2 means amphibolite facies (Faro) and 4 means greenschist facies (all other deposits). The letter refers to the major lithology as shown in Table 3.1. The remaining letters and symbols are modifiers as outlined in Table 3.2. Thus 4A4 is a lead-zinc rich carbonaceous pyritic quartzite; 2A479 would be the same from Faro with pyrrhotite and chalcopyrite.

In some cases it is preferable to refer to a combination of sulphide rock types, particularly in a mining context. In such cases the letters are combined with the dominant component listed first. Thus 2EG would be mixed 2E and 2G; 2BCD refers to all non carbonaceous quartzites regardless of sulphide species.Another common combination is 2CE which can refer both to mixed 2C and 2E and semimassive sulphides between 2C and 2E in character. At Faro there are now three ore types mined: 2A, 2BG and 2H. In this case 2BG means all the detailed sulphide types from B through G.

The mine models generally require an integer lithologic code and it has generally not been possible to use the same codes for all models; these codes are explained below for each model.

TABLE 3.1 THE ALPHA PART OF THE LITHOLOGIC CODE FOR SULPHIDE ROCK TYPES

A	thinly banded carbonaceous pyritic quartzite
B	weakly to non-pyritic quartzite
C	lead-zinc poor pyritic quartzite
D	lead-zinc rich pyritic quartzite
E	pyritic massive sulphide
F	buckshot textured pyritic massive sulphide
G	pyritic massive sulphide with >10% barite gangue
H	pyrrhotitic massive sulphide
J	non-pyritic or pyrrhotitic massive sulphide or massive magnetite
K	pyritic massive sulphide with >10% carbonate gangue
Q	foliated vein type quartz with sulphides

TABLE 3.2 LITHOLOGIC MODIFIERS FOR SULPHIDE ROCK TYPES

0	normal
1	siliceous
2	coarse porphyroblastic pyrite bearing
3	fine pyrite rich
4	lead-zinc rich
5	carbonaceous
6	barite bearing
7	pyrrhotitic
8	magnetite bearing
9	chalcopyrite bearing
*	undifferentiated carbonate bearing
#	calcite bearing
@	ankerite bearing
$	dolomite bearing

3.1.6 Geology of the Vangorda Plateau

The Grum and Vangorda deposits are located in a part of the Anvil District referred to as the Vangorda Plateau. The Plateau is defined as the area between the headwaters of Rose Creek on the northwest and Blind Creek on the southeast. It is essentially the drainage basin of Vangorda Creek.

The Plateau is low rolling country between the rugged topography of the Mt. Mye massif and Sheep Mountain. The bedrock exposure is very poor, there are several areas where glacial overburden is many tens of metres thick. The area is heavily tree covered below 1220 m (4000 feet) elevation with thick brush above that.

The geology of the northwest part of the Plateau is outlined on three 1:5000 scale maps that cover the portion of the area to be affected by development of the Grum and Vangorda deposits. Three additional maps show the distribution of drill holes in the same area. The maps and the sections noted below are available in supporting documents filed at Curragh's Whitehorse and Toronto offices.

The stratigraphy is as outlined previously. Most of the Plateau is at greenschist facies with the high grade metamorphic rocks in the core of the Anvil Arch and the granitic rocks of the Anvil Batholith being separated from the low grade phyllites by a complex system of extensional faults. The geological boundary between the Vangorda Plateau and the Faro Block is the Tie fault, one of these extensional faults with about 1 km of throw.

The structure of the metamorphic sequence underlying the Vangorda Plateau is indicated on a set of cross sections also at a scale of 1:5000.

The stratigraphic position of the ores is indicated on those sections. The available drilling and mapping indicates the presence of a large isoclinal, S shaped, second phase fold which overturns the stratigraphic sequence in the vicinity of the trend of ore deposits. Because of this the depth to the favourable horizon increases rapidly to the southwest of the line of deposits and open pit potential in that area is nil. All available deep drillholes (at least those deep enough) southwest of the line of ore deposits have intersected a thick sequence of siliceous graphitic phyllite with minor disseminated pyrite and traces of sphalerite but none of the mineralized facies typical of the deposits. All indications are that the deposits are associated with the linear zone of the thickening of this graphitic phyllite and that the phyllite itself southwest of the line of thickening has limited potential. Northwest of the line of deposits stratigraphic levels exposed are deeper than the ore horizons thus the potential in that area is also limited.

Along the line of deposits there are several areas requiring further drill testing. Several holes will be required northeast of the Vangorda deposit where a blind second phase fold hinge is

predicted which could repeat the ore horizon and offer potential for additional reserves. Between Vangorda and Grum is an uplifted fault block that exposes the hinge of the large overturned fold. There are several drill holes in this area but few of them have fully tested the favourable stratigraphy. This area being an upthrown block, is underlain by the more southwesterly portions of the favourable horizon as traced through the S shaped second phase folds. At both Grum and Vangorda the thickness and grade of mineralization in the deeper more southwesterly part of the favourable horizon decreases substantially from that in the main deposit area while the thickness of graphitic phyllite increases. The limited sulphide intersections in the upthrown block between Grum and Vangorda are consistent with this observation in both the adjoining downthrown blocks since thick graphitic phyllite is found at the favourable stratigraphic horizon. Nonetheless at Dy, southeast of this area, it appears that a second mineralized center is developed southwest of the main deposit line with thick sections of good grade mineralization. This observation along with the fact that Anvil type deposits are characterized by rapid, highly unpredictable facies changes shows that there is a possibility of a completely isolated separate mineralized centre within this fault block. It is highly unlikely that such a mineralized center could be found in an open pit environment however. Only a few holes would be required to evaluate the area between Grum and Vangorda prior to construction of waste dumps. It is essential that this be done because this area is some of the most attractive exploration ground in the Anvil Range.

3.1.7 References

Blusson, S.L., 1966, Frances Lake, Yukon Territory and District of Mackenzie; Geol. Surv. Canada, Map 8-1967.

Carne, R.C., and Cathro, R.J., 1982, Sedimentary exhalative (sedex) zinc-lead-silver deposits, northern Canadian Cordillera: Can. Inst. Min. Metall. Bull., v.75, p. 66-78.

Gabrielse, H., Blusson, S.L. and Roddick, J.A. 1973, Geology of Flat River, Glacier Lake and Wrigley Lake map areas; Geol. Surv. Canada, Memoir 366, 153 p.

Gordey, S.P., 1978, Stratigraphy and structure of the Summit Lake area, Yukon and Northwest Territories; in Current Research, Part A, Geol. Surv. Canada, Paper 78-1A, p.43-48.

Gordey, S.P., 1981 Stratigraphy, structure and tectonic evolution of southern Pelly Mountains in the Indigo Lake area, Yukon Territory; Geol. Surv. Canada, Bulletin 318, 44p.

Gustafson, L.B., and Williams, N. 1981, Sediment-hosted stratiform deposits of copper, lead, and zinc: Econ. Geol., 75th Anniversary Volume, p. 139-178.

Kuo, S.L., 1976, Geology and geochemistry of stratabound ore deposits in south central Yukon Territory and southwestern District of Mackenzie, Northwest Territories; Ph.D. dissert., Univ. of Alberta, Edmonton.

Large, D., 1980, Geological parameters associated with sediment-hosted submarine exhalative Pb-Zn deposits: Geologisch. J., Reike D, Heft 40, p.49-129.

Tempelman-Kluit, D.J., 1972, Geology and origin of the Faro, Vangorda and Swim concordant zinc-lead deposits, central Yukon Territory; Geol. Surv. Canada, Bulletin 208, 73p.

3.2 Faro Geology and Reserves

3.2.1 History

The Faro deposit was discovered in 1964 while drill testing airborne electro-magnetic anomalies supported by other indications. Mining at Faro began in late 1969 and continued until 1982 when high costs and falling prices forced temporary closure of the mine.

In November 1985, Curragh Resources bought the Faro mine and other deposits in the Anvil Range from Cyprus Anvil Mining Corporation. Waste removal from the Faro pit resumed in early 1986. The Faro concentrator resumed production in June 1986. During 1986 1,842,000 tonnes or high and low grade ore was mined.

3.2.2 General Geology

3.2.2.1 Stratigraphy and lithology

The Faro deposit occurs approximately 100m beneath the Mt. Mye/Vangorda formation boundary. Stratigraphically this may equate to the position of the lowest horizons in the Vangorda Plateau deposits.

The immediate host rock of the orebody is biotite-muscovite-andalusite schist (unit 1D) that grades downwards into a coarse, gneissic botite-muscovite schist (unit 1C). A discontinuous graphitic phyllite unit about 6 m thick is interlayered with the schists about 25 m above the ore deposit. There are also several thin interbands of strongly foliated chlorite actinolite schist, or bleached and carbonated equivalents of this mafic schist, above the orebody.

The Vangorda formation at Faro is represented by hard, dense, banded calc-silicates (unit 3D) rather than the calcareous phyllite that characterizes the Vangorda Plateau. This fact is of considerable importance in blasthole drilling at Faro because of the rocks hardness. Amphibolite up to 10 m thick is interbanbed with the calc-silicates and there are several thin graphitic phyllite layers. The basal unit of the Vangorda formation in the Faro deposit area (unit 3A) consists of graphitic phyllite, amphibolite and calc-silicates mixed in subequal amounts.

Post metamorphic igneous intrusive rocks are more widely developed at Faro than elsewhere in the district. There are two clans of importance: a) a equigranular to subporphyritic hornblende diorite to quartz diorite clan (unit 10E) and b) a quartz-feldspar porphyry clan (unit 10F). The former occurs as a large dyke truncating the deposit at its northwest end, a smaller dyke along the fault between zones 1 and 3, an inferred sill beneath the breccia cap (see below) and several smaller dykes. The latter forms highly irregular and unpredictable intrusive bodies in the north part of zone 3.

Associated with these dykes, or irregular intrusive bodies, and the intersection of two important faults is a large mass of heavily silicified post metamorphic breccia at the northeast edge of the deposit in Zone 3. This "breccia cap" exaggerates the problems of blast hole drilling because of its extreme hardness.

3.2.2.2 Structure

Faro is deeper in the structural sequence than other parts of the Anvil District. Consequently the structural picture is rather different. The second deformation (D_2) effect is very strong at Faro. Virtually all sign of the first deformation has been completely overprinted by D_2.

The D_2 axial planar schistosity (S_2) is strongly developed and is the plane of greatest fissility in all metamorphic rocks of the Faro area. S_2 dips 10° to 20° towards the southwest or west. Second phase folds are generally isoclinal with shallowly northwest or southeast plunging axes. D_2 is so strongly developed that the structural sequence can be essentially viewed as a stratigraphic sequence with bedding parallel to S_2. The ore deposit is a tabular body parallel to compositional layering and S_2; internal layering in the ores is also parallel to S_2.

Three generations of later folds deform S_2, compositional layering and the ore deposit into close to tight northeasterly verging folds with axial planes dipping 45° to 60° towords the southwest and generally west or northwest plunging axes. The late folds commonly have amplitudes of approximately one m and folds of several tens of m are inferred in the base of the deposit (Figure 3.7). The size of these folds and the extent to which the deposit margin and internal banding geometry is defined by late folds as opposed to faults is one of the major uncertainties in ore reserve estimation at Faro.

Faults postdating the fold deformation (and concurrent metamorphism) are widely developed at Faro. Two sets are particularly important: 1) a N20°W striking and steeply west dipping set and 2) a East or N60°E striking and generally steeply to moderately south dipping set. These two sets define a graben structure. Zone 3, which contains the remaining reserves, is the central downtwrown block and Zones 1 and 2, now largely mined out, are the upthrown blocks. Many other fault sets are more locally developed, particularly in the area of the JB phase. Seemingly random faults with small but cumulatively significant displacement pose one of the most serious limitations on accurate local bench reserve estimation from exploration drillhole information.

S_2, along with joints and small gouge zones parallel to S_2, is the primary element for consideration in slope stability. The shallow to moderate southwest dip means that the northeast wall of the pit is relatively unstable. Failures to date appear to be surficial and involve platy rock fragments bounded by S_2

sliding slowly towords the pit. The possibility of larger scale failures involving slip on S_2 backed by some of the larger faults dipping towords the pit cannot be dismissed. The relatively more massive and stronger rock mass of the northeast edge of the sulphide deposit is expected to butress the northeast pit wall as the pit deepens.

3.2.2.3 Deposit Geology

Before mining, the Faro deposit was 2000 m along strike, 800 m across strike and from a few meters to 90 m thick. The deposit is a flat-lying, elongate, asymmetric lens with a thick northeast side and a thin tapering southwest side.

There is essentially one thick horizon at Faro although this horizon contains numerous cycles and several thin phyllite waste bands are included. Locally a thin upper horizon is differentiated from the main mass of the deposit, generally this is too thin to be mineable. Low grade sulphide interbanding with high grade ore is widespread especially in the northeast part of the deposit. The low grade or waste sulphides pose a major dilution problem, unlike phyllitic waste they can not be visually differentiated thus are much more difficult to control. Only blasthole assays can define sulphide waste. The thickness of high grade and sulphide waste or low grade interbanding is commonly less than the 6 m (20 ft.) bench height particularly in the northeast part of the deposit. This places basic limits on dilution control using the current methods of ore sampling and deliniation.

Ore type zoning is particularly strong at Faro. It follows the scheme outlined above with a massive variably baritic upper portion and a quartzose variably carbonaceous lower part (figures 3.6 and 3.7). In addition there is a prominent very low grade semi-massive zone along the northeast edge of zone 3 and unusually abundant (compared to other Anvil district deposits), but erratically distributed, pyrrhotitic mineralization in the southwest part of the deposit. Grade zoning follows ore type zoning so that the base and northeast edge of the deposit contains the lower grade mineralization whereas the upper and southwest portion contains the higher grade mineralization. Zoning was also obvious in plan view at Faro. Zone 1 was rich in baritic ores thus high grade, zone 2 at the other end of the deposit was rich in carbonaceous quartzose ore types thus low grade and metallurgically undesireable. Zone 3 has intermediate characteristics.

The greatest continuity in the deposit is along the deposit elongation. Across this trend the horizontal continuity is relatively poor with gradual changes in rock type and grade in the northeast half of the deposit and less abrupt grade variation in the southwest half. The vertical continuity is poor since there are rapid changes in rock type and grade across the sub-horizontal layering. The ore deposit thus has a feather edge assay boundary along its northeast edge. A better defined lower assay boundary and a relatively sharply defined upper

boundary. The southwest limit of the ore is defined by the gradual thinning of the deposit and the gentle southwest dip.

It is easy to make generalizations such as those above in order to convey an impression of the deposit however the Faro deposit shows very complex internal variation. Between drillhole variability is so great that commonly the rock type and assay distribution in adjacent drillholes seem to bear no relation to one another. This great variability places some basic limits on the reliability of local reserve estimates.

3.2.3 Drilling Density

The Faro deposit was drilled off on 43 m (141 feet) spaced sections with holes spaced nominally at 43 m along the sections. Most holes were vertical. In some parts of the deposit fill in drilling to 43 m has not been completed. In 1986 additional fill in (to about 25 m) was added to the northeast side of the AY phase because of difficulties in making accurate projections with available data. The results of this new drilling are not yet in a form suitable for mine planning.

3.2.4 Reserve Calculation

3.2.4.1 Method and Procedure - "FI" Model

The reserves used for Faro mine planning are derived from the "FI" mine model, generated from October to December 1985 by Cyprus Anvil Mining Corporation. The FI model is one of several computer block models of the Faro deposit; reference to some others will be made herein. The F3 and T3 date from 1981 and prior to completion of the FI model were the most recent complete models available. The F4 is more recent but was never completed and thus is not useable for mine planning. The FI model is an interim model that combined parts of the F3 and F4 and incorporated extensive drilling results postdating completion of the F3 and T3 models. The 1985 Kilborn analysis of the Faro mine project used the T3 model results.

3.2.4.1.1 Block geology and drillhole information

The FI Model is a computer based block model with block size 15.25m X 15.25m X 6.1m high (50 ft. X 50 ft. X 20 ft. high). The blocks are oriented North-South and East-West, at 45° to the elongation of the ore deposit and the geological sections. The Mintec Medsystem release 10 software package was used to generate the model and derived reserves. The model has since been imported to Curraghs software package, PC Mine, but all model building calculations have were done by Mintec's software. Reserves for Curragh's newly defined mining phases are calculated by PC Mine.

The geological interpretive base was derived from two sources. In the southeast part of Zone 3 (Sections 124 to 133) the geological interpretation is the most up to date possible (1983) and is the same as that used for the F4 model. In the remainder

of Zone 3 (Sections 117 to 123) this new geological interpretation was not yet available thus the interpretation used was that developed in 1981 for the F3 and T3 models. This did not take advantage of 1984 drilling. The interpretations differ in the relative importance of folds and faults which results in significant differences in bench to bench geology, but for an overall section thru the deposit the cross-section area, hence the volume, is not very different. There are some artificial discontinuities evident in the resulting model where the two interpretations join (this is largely in the CY phase ore).

Block geological code assignment was based on 6 m (20 foot) spaced bench plans of the geology. A block whose area is underlain by more than 50% sulphide rock type was coded as an ore type otherwise it was coded as waste. The actual block geological code was defined by the unit occupying the maximum plan view area within the block. One rock code was assigned to each block and that code was assumed to apply uniformly to the entire block. The rock codes used are listed on table 3.3.

TABLE 3.3 LITHOLOGIC CODES USED FOR THE FI MODEL

Rock Code	Description		Density Used *
0	air	tonnes/BCY	0
1	undifferentiated sulphides	2.295	0.085
2	2A ribbon banded graphitic quartzite	2.241	0.083
3	2BCD pyritic quartzite	2.43	0.090
4	2CE semi-massive sulphides	2.673	0.099
5	2EF pyritic massive sulphides	2.889	0.107
6	2GE baritic massive sulphides	3.024	0.112
7	2H pyrrhotitic massive sulphides	2.808	0.104
10	WASTE all types except calc-sil or sulph.	2.052	0.076
11	WASTE calc-silicates 3D		0.076
12	WASTE in blocks partially above topography		0.076

* Density is in tonnes per cubic foot

The drill hole database used includes all holes in the deposit to the time of model construction; thus all holes prior to Curragh's acquisition of Faro but none of Curragh's 1986 holes are included.. In the northwest half of the deposit the geology has not been adjusted to reflect holes put down since 1981 but the assays were used for interpolation.

All drillholes were relogged to a common standard between 1982 and 1984 and extensive checking of the assay and survey data for consistency was carried out by Cyprus Anvil's staff. Not all holes have been surveyed for downhole deviation. In these cases an average deviation based on nearby surveyed holes was used. As discussed below there are now known to be errors in the collar locations of some holes on the order of 50 feet laterally. This is apparently due to a small angular error in restablishing survey control at some time and cannot be corrected now. The error is largest in the more southeasterly holes thus is significant in the JB phase and especially zone 2 but is thought to be less important in the AY phase. Apparently not all holes in the JB are affected. Holes postdating the mid 70's are thought to be consistent with the current survey control.

3.3.4.1.2 Composite Calculation

Drill hole assays were composited on a 6 m (20 ft.) bench basis. Assays, were weighted by length within the bench and specific gravity of the constituent samples. High assay valves were rolled back to the 95th percentile level before compositing. Internal waste (3 m or 10 feet thick or less) was included in the composites at zero grade. Composites were again clipped to the 95th percentile before interpolation. External waste and waste bands greater than 1/2 bench height (3 m or 10 feet) were not included in the composite intervals resulting in a composite shorter than 6 m (20 feet) long. This was done on the premise that waste or ore thicker than half a bench height could be separated during mining. This assumption is of questionable validity and the method of composite calculation will lead to grades that require a higher dilution in order to quote mill feed than a calculation that averages an entire bench regardless of material type. Part of the rationale in this method of compositing is that a given composite will be used on more than one bench thus a composite from the margin of the deposit will be used to estimate the grade of the interior of the deposit and in that case it would not be appropriate to have averaged in a large amount of unmineralized material. All previous Anvil District models have followed exactly the same compositing scheme. Thus this is not an explanation of differences between model reserves.

A major improvement over previous models (particularly the T3) was made in geological coding of the composites. Each composite was checked manually to ensure that it was coded consistantly with the sectional geology rather than machine coded by detailed

logged geology. Since large interpreted units often encompass several smaller intervals of different geology, this procedure insured that the composite would be used to interpolate only relavant units. The implications of this coding are discussed in the next section.

3.2.4.1.3 Interpolation

Interpolation search volume was 69 m (225 ft.) along strike, 46 m (150 ft.) along dip and 8 m (25 ft.) vertically. Composites were selected for interpolation on the basis of block geology being equivalent to composite geology coding. No composite less than 2.4 m (8 feet) long was used in the interpolation to avoid biasing large blocks with small data points. One composite per drillhole was allowed for interpolation to minimize vertical averaging across banding in the stratiform deposit.

Interpolation was carried out in five passes starting with strict matching requirements and a small search volume then gradually loosening the restrictions to interpolate values into blocks missed on previous passes without affecting the values already assigned. The search volume was enlarged to as much as 76 m (250 ft.) X 53 m (175 ft.) X 32 m (105 ft.) high.

Where more than one composite was available to estimate a given block they were weighted isotropically by the inverse square of distance to the point being estimated as well as by the length of the composite. The length weighting of composites was done to avoid biasing large volumes of ore with assays representative of only a small amount of material. In retrospect this proceedure appears to have deweighted the assays from the margins of the deposit relative to those in the core of the deposit. Because of the grade zoning in the deposit this probably has led to an overestimation of grade in marginal situations but has little or no effect in the core of the deposit. This proceedure is different from all previous Faro deposit models except the little known F4 and probably is the reason that the FI model differs from other calculations in marginal benches and has tended to overestimate grade in the JB phase (see below).

The implications of the geological matching requirement during interpolation have not been tested due to lack of time however some statements can be made in light of the rock type - grade correlations and grade zoning described above. Since massive ores tend to be higher grade than disseminated ores and massive ores are more central and higher in the deposit than disseminated ores, there will be a tendency to average grade both by rock type and in space if there is no matching required. The use of matching will tend to make massive ores higher grade and disseminated ores lower grade than would be the case without matching. Because of the geometry of the deposit and its zoning the higher grade ore will be more central and higher in elevation in the case of matching than it would be without matching. When a cutoff is applied to the block values computed through geological code matching the tonnage above cutoff will

be lower and the average grade higher than a reserve computed without a matching requirement furthermore the limits of ore will be higher in elevation and closer to the centre of the deposit. Because of these rock type and zoning characteristics of the Faro deposit it is considered essential to use matching to produce an accurate picture of grade distribution. It is however inescapable that a reserve computed through geology matching will require a higher dilution factor than one computed without matching. It is however considered more realistic for dilution calculations to be made after the model is constructed rather than during interpolation when it will occur in uncontrollable and unpredictable fashion.

Specific gravity was treated as an assay and interpolated into blocks. This is due to the variability of SG by rock type and by grade as well as regional variations of SG within one rock type. Sulphide blocks outside of interpolation range were assigned an average specific gravity based on rock type. The SG values used for interpolation were the pulp SG not the whole rock SG thus the value did not reflect porosity in the insitu intact material. A number of comparative SG tests have been done on Anvil District ores to determine the degree of overstatement of SG. In light of the results of these tests block SG values were reduced by 5% for quartzose ore types or 10% for massive ore types to correct for porosity in the insitu whole rock. Previous Faro models have not had this correction made if pulp SG was used (such as the F3 and T3 - these models actually used an average SG derived from the pulp SG data not an interpolated SG). Cyprus Anvil's practice in quoting model results as mill feed predictions was generally to reduce the grade by 5% but not to adjust the tonnage; since the tonnage was already overstated by use of the pulp SG value this was nearly the same as adding 5% dilution. Curragh's approach is to attempt to estimate the insitu tonnage and apply an appropriate dilution factor later rather than attempt to make two sets of corrections at once.

3.2.4.1.4 Reserve Reporting

Reserves were computed for 6 ore types: 2A, 2BCD, 2CE, 2GE, and 2HE. Geological reserve computation was by a weighted average of all blocks in the model below topography that exceed a ceretain arbitrary lead and zinc content. Pit reserves are reported by computing the weighted average of all blocks above cutoff lying between two surfaces gridded on the same block grid as the block model. The two surfaces are an upper surface representing topography or the previous phase bottom and a lower surface representing the current phase bottom. Blocks partly above or below the surface are multiplied by the fraction of the block that is between the surface elevations for that block when computing the weighted average.

3.2.4.2 Methods and Procedure - F8608 Model

In August and September 1986 a new computer model of the AY and

BY phases, the F8608 model, was constructed. This was largely in reaction to the poor performance of the FI model in the JB phase and concerns over the base geologic interpretation in the AY and BY phase areas as well as some of the computational methodology used for the FI model. This model only covered the northwest portion of Zone 3 thus has not been used for long range planning, it is only included here for comparison purposes in order to help quantify the uncertainty of estimation of the FI model on which the planning is based.

3.2.4.2.1 Block Geology and Drillhole Data

The F8608 model is a 3D block model made using PC Mine software. Block size was 10.7 m (35 feet) along the deposit, 7.6 m (25 feet) across the deposit and 6 m (20 feet) high. The coordinate grid was rotated 45° so that rows of blocks are parallel to the geological cross sections of the deposit rather than the mine survey grid.

The geological control used in the model is based on new cross and longitudinal sections for the northwest part of zone 3 completed by R.S. Tolbert in early 1986. The 43 m (141 foot) spaced sections were simplified and intermediate cross sections created at 21.5 m (70.5 foot) intervals (or 10.7 m (35 foot) where required). These sections provided geological control for block geology rather than geological bench plans as have been used for all previous Faro deposit models. This was done not only because it is a quicker process to make cross sections but also because a flat lying stratiform deposit is more logically viewed in section perpendicular to its direction of predictability. The sectional model approach also allows the use of different bench heights without changing the geological bench plans so that bench height optimization could be studied. A drawback to this approach is that if section to section geology has not been closely coordinated and a control section is not provided for each row of blocks then the bench plans of grade distribution and ore type have a patchy appearance with obviously angular contacts parallel to the sections. This is the case with the F8608 model but this problem is largely due to having rushed the model to completion without taking time to refine the base geologic interpretation. The effect on reserves is not thought to be great but the lack of "smoothly flowing" bench plans could cause problems in the mine planning stage.

As in all other models a block is considered homogenous and of one material type. Block coding was based on digitized geological sections with the geology at the centre of the block assigned to the entire block. Assignments were made entirely by machine and checked manually. In most cases 2 rows of blocks were assigned according to the geology of one section since the sections were 21.5 m (70 feet) apart in most cases.

Rock types used were the same as those used for the FI model with the exception of the waste lithologies where several additional units were used (Table 3.4).

TABLE 3.4 LITHOLOGIC CODES USED FOR THE F8608 MODEL

Rock Code	Description	Density Used *
0	air	0
1	undifferentiated sulphides	0.085
2	2A ribbon banded graphitic quartzite	0.083
3	2BCD pyritic quartzite	0.090
4	2CE semi-massive sulphides	0.099
5	2EF pyritic massive sulphides	0.107
6	2GE baritic massive sulphides	0.112
7	2H pyrrhotitic massive sulphides	0.104
8	WASTE schist and phyllite 1D, 1CD and 1C	0.076
9	WASTE calc-silicate 3D	0.076
10	WASTE calc-silicate breccia 3Dbx	0.076
11	WASTE intrusive rocks 10E and 10F	0.076
12	WASTE bleached schist envelope 2L and 1D4	0.076
13	WASTE unconsolidated overburden	0.060
14	WASTE graphitic phyllite 1E and Unit 3A	0.076
20	WASTE in blocks partially above topography	0.076

* Density is in tonnes per cubic foot

Drillhole data used was that already imported into the PC Mine for the FI model and is described above.

3.2.4.2.2 Composites

The composites used were those generated for the FI model since they had geological codes assigned and considerable time was saved by cutting this corner. The length of the composite was not used in PC Mine. A significant drawback to this approach was that the geologic codes of the composites do not correspond exactly with the sectional geology. In general the massive and quartzose ore type distinction is close but subdivisions within massive or quartzose are not necessarily. This necessitated changes to the geological matching scheme during interpolation. Note that problems with non full bench height compositing of external and internal waste still would be present with this composite data set.

3.2.4.2.3 Interpolation

Variogram analysis of Faro composites was not generally sucessful. A tendency of a larger along deposit than across deposit range was indicated. The search volume (and hence anisotropy) used was tailored to be a close approximation to that used for the FI Model with the exception that the search ellipsoid was tilted to follow the layering of the deposit in three domains. First pass interpolation used a seach ellipsoid looking 69 m (225 ft.) along the deposit trend 46 m (150 ft.) across it and 7.6 m (25 ft.) vertically. This was enlarged to 91 m(300 ft.) along the deposit, 61 m (200 ft.) across and 11.3 m (37 ft.) vertically in 3 passes.

hor factor .667

vert 10.7 4 5.3

Because to FI model composite data set was used geological matching had to be relaxed from that used in the FI model considerably in order to avoid large numbers of uninterpolated blocks. Generally any massive ore type could accept the assay value of any other massive ore type. The distinction between carbonaceous and non-carbonaceous quartzose ore types was dropped. Massive sulphide assays were not allowed to influence quartzose sulphide blocks and vice versa. Semi-massive (2CE) blocks were allowed to accept quartzose and pyritic massive ore type assays.

A minimum of 2 composites was required to interpolate a block; the maximum number of composites allowed was 6. There was no limit possible on the number of composites from a single drillhole but the flat search ellipsoid used precludes more than two.

Composite values were weighted by the inverse square of the distance to the point being estimated. There was no weighting by length of composite and no minimum length of composite stipulated.

A large number of test interpolations were run using different

interpolation parameters to check the grade distribution achieved versus the number of blocks that could not be interpolated. The most faithful reproduction of known grade distribution was acomplished by using a flat search ellipsoid so that only composites along the layer being estimated could be used. More spherical search volumes create a false impression of homogenous grade distribution by assigning high grades across strata to areas known to be barren. To have a flat search ellipsoid in PC Mine requires the use of a high degree of vertical anisotropy. The logic of the software treats anisotropy by adjusting distance in different directions. An apparent distance equal to the actual distance divided by the anisotropy factor is calculated and used for search and weighting criteria. This results in every point on the edge of the search ellipsoid being treated as if it were the maximum radius of the ellipsoid away from the point being estimated. Points a small distance off the principal plane of the search ellipsoid are considered further away from those on the plane in cases of a high vertical factor. Test interpolations and trace blocks run during the tests did not reveal any problems arising from this treatment of distance but this is one of the major differences between the F8608 and FI model methodologies.

Specific gravity is treated as an assay and interpolated into blocks. This is due to the variability of SG by rock type and by grade as well as regional variations of SG within one rock type. Prior to interpolation the composite pulp SG's were reduced by 5% for quartzose ore types or 10% for massive ore types to correct for porosity in the insitu whole rock. Uninterpolated blocks were assigned the density 0.096 tonnes/cu. ft. (see Table 3.4)

3.2.4.2.4 Reserve reporting

Geological reserves were not computed since the model only covers the part of the deposit between sections 117 and 125. Pit reserves are reported by computing the weighted average of all blocks lying between two surfaces gridded on the same block grid as the block model. The two surfaces are an upper surface representing topography or the previous phase bottom and a lower surface representing the current phase bottom. Blocks partly above or below the surface are multiplied by the fraction of the block that is between the surface elevations for that block.

3.2.4.3 Results

3.2.4.3.1 Geological Reserves

Geological reserves calculated from the FI model are given in Table 3.5 along with some previous figures of a comparable nature. The Dome hand calculation covers a larger area than the FI model thus cannot be compared directly. Since nearest neighbor sectional calculations such as the Dome one tend to report higher grades than inverse distance squared interpolated models the difference in grade may not be significant.

The 1985 Kilborn Report gives a rather large geological reserve with an unstated cutoff grade or source. The source is presumably the Cyprus Anvil F3 model but no printouts could be found to confirm it. It is not clear how this number can be consistent with the Dome figure let alone the FI model. The authors predjudice is to favor the Dome sectional calculation reserve as the geological reserve for the Faro deposit since it covers a larger area than the current model and is well documented.

TABLE 3.5 GEOLOGIC RESERVES FOR THE FARO DEPOSIT-ZONE THREE
all values are undiluted and unadjusted

grade category	ore (tonnes)	Pb (%)	Zn (%)	Pb+Zn (%)	Ag (g/t)
FI COMPUTER MODEL					
+5%Pb+Zn	22,793,000	3.28	5.14	8.41	41.5
4-5%Pb+Zn	3,770,000	1.72	2.78	4.50	27.3
+4%Pb+Zn	26,563,000	3.06	4.81	7.86	39.5
total metal at +4% Pb + Zn cutoff= 2,088,000 tonnes					
DOME SECTIONAL HAND CALCULATION					
+4%Pb+Zn	29,251,000	3.13	5.03	8.16	40.8
total metal at +4% Pb + Zn cutoff= 2,387,000 tonnes					
CYPRUS ANVIL (F3 COMPUTER MODEL ?)					
+4%(?)Pb+Zn	33,000,000	3.0	4.6	7.6	35.7
total metal at +4%(?) Pb + Zn cutoff= 2,508,000 tonnes					

3.2.4.3.2 Model To Model Comparisons

Table 3.6 compares the FI model (actually the reserves computed before the SG reduction so that the numbers are comparable) with three computer calculated valves for phase A (for old phase A not the current AY) all based on the same geology but varying in computational methodology and in the case of FI for the assay database. Also shown is a hand calculated reserve for phase A based on a geologic interpretation done by the author in September 1985 incorporating all drilling data available and using a fault dominant as opposed to fold dominant geological interpretation. In this phase the FI model reports a lower tonnage at a higher grade that previous models. This is likely due to more restrictive application of geology matching during interpolation due to the greater availability of composites and the more rigorous coding but may be partly due to length weighting of composites during interpolation.

The comparison of hand calculated reserves using new geology to FI reserves is the most critical as it deals with estimates derived from very different approaches. As shown on Table 3.6, the FI model reports 9% higher tonnage than the hand model at 5% lower grade. Much of the grade reduction may be due to the comparison of a nearest neighbor to an inverse squared distance interpolation but at the worst this comparison suggests the reserves compare within 10% and within 4% on total metal.

The other phases do not compare as favorably as the A phase. The comparison of the FI, T3 and F3 models for the old A through D phases of the Faro pit is shown on table 3.7. In every phase the FI model reserve contains fewer tonnes but higher grade. The grade increase in the B to D phases is not however large enough to compensate for the drop in tonnage and there is a drop in total contained metal ranging from 7% to 10% averaging 6% for the entire pit. The reasons for this drop in total metal and the comparable drop between the F3 and T3 models is not totally clear; the most likely explanation is the restrictions on interpolation caused by the requirement for matching geology codes. The most direct test of this inference would be to reinterpolate the FI model without geology matching however this has not been done. A clue to what is happpening is found in the relative proportions of ore types above cutoff. One would expect that the grades being assigned to disseminated ore types without good geologic control would be on the average too high, consequently too much would be considered ore at a given cutoff; the converse would be expected for the massive ore types. This is the trend shown in Table 3.8.

TABLE 3.6 COMPARISON OF SEVERAL RESERVE ESTIMATES FOR CYPRUS ANVILS A PHASE

DATE	MODEL	TONNES +6% Pb+Zn	Pb (%)	Zn (%)	Ag (g/t)	Pb+Zn (%)	TOTAL METAL (tonnes)
1985	HAND	3,290,317	3.95	5.98	49	9.93	326,728
1985	F1	3,595,315	3.83	5.62	48	9.45	339,757
1982	T3	3,668,154	3.63	5.37	42	9.00	330,281
1981	F3	4,051,087	3.61	5.33	43	8.93	361,884

TABLE 3.7 COMPARISON OF THREE COMPUTER BASED MINE MODEL RESERVES FOR CYPRUS ANVIL'S A-D PIT DESIGN, FARO ZONE 3
(all values unadjusted except where noted otherwise)

**********PRELIMINARY**********

		TONNES +6% ORE	Pb (%)	Zn (%)	Ag (g/t)	Pb+Zn (%)	TOTAL METAL (tonnes)	UNINTERPOLATED BLOCKS (tonnes)
PHASE A								
FI		3,595,315	3.83	5.62	48	9.45	339,757	
T3		3,668,154	3.63	5.37	42	9.00	330,281	85,951
F3		4,051,087	3.61	5.33	43	8.93	361,884	43,996
PHASE B								
FI		4,457,843	3.78	5.32	48	9.10	405,664	
T3		5,129,659	3.69	5.12	45	8.81	451,923	43,775
F3		5,201,360	3.62	5.11	44	8.73	454,079	23,928
PHASE C								
FI		3,681,852	3.60	5.33	48	8.93	328,789	
T3		4,127,797	3.56	4.98	44	8.54	352,308	162,654
F3		4,694,443	3.42	4.92	43	8.34	391,704	26,797
PHASE D (includes JB phase)								
FI		3,906,211	3.38	5.57	40	8.95	349,606	
T3		4,510,291	3.21	5.30	36	8.51	383,690	252,307
F3		5,036,489	3.13	5.17	36	8.29	417,676	31,100
TOTAL A-D PIT								
FI		15,641,221	3.65	5.45	46	9.10	1,423,816	0
T3	*	17,435,901	3.52	5.19	42	8.71	1,518,201	544,687
F3		18,983,378	3.44	5.13	41	8.56	1,625,343	125,821
TOTAL A-D PIT RESERVES EXPRESSED AS EXPECTED MILLFEED (adjustments per users customary practice, see below)								
FI	#	16,345,076	3.32	4.96	42	8.28	1,352,625	
T3	@	17,435,901	3.35	4.93	40	8.27	1,442,291	
F3	@	18,983,378	3.26	4.87	39	8.13	1,544,075	

* compared to 17,180,000 quoted by Kilborn in 1985 report
F3 and T3 numbers in this table taken directly off Mintec printouts.

\# 95% mining recovery and 10% dilution at zero grade

@ minus 5% to grades, no change to tonnage

Table 3.8 PROPORTIONS OF VARIOUS ORE TYPES ABOVE CUTOFF IN THE T3 AND FI MODELS

ore type	percent of total +6% ore	
	FI model	T3 model
A	3.9	3.4
BCD	12.3	19.9
CE	8.2	10.2
EF	51.4	49.5
GE	9.6	8.7
HE	14.5	8.3

Table 3.9 compares the expanded JB phase (again not exactly the same as the current JB phase) as calculated by the FI model and with a calculation done by Cyprus Anvil using the same assay data and geologic interpretation. Cyprus Anvil's approach was to compute the actual area of geologic units on the benches and make the most appropriate assay assignment to these areas by manual means. This comparison thus addresses the question of how adequate the block representation of the geology is and how the machine algorithms and computations compare human reasoning and manual computations. The comparison is good; the major difference being in tonnage which is probably at least in part due to the inability of 15 m (50 ft.) X 15 m (50 ft.) blocks to show every geologic unit.

The results from the FI and F8608 models the AY and BY Phases are compared in table 3.10 A to D. The F8608 computed tonnages are very close to those of the FI model or slightly higher. The grades are fairly consistently lower. The total metal for both phases is within 2.2% of that calculated by the FI model. Despite the close comparison on a large volume basis, the bench to bench variance is quite large with many benches being within only $\pm$30% (see Table 3.10 B and D). As might be expected the larger benches in the core of the deposit compare well.

3.2.4.3.3 Comparison To Blasthole Results

The acid test of a model is to compare to actual production data. The FI model was not designed to accurately predict small domains but was intended to acheive some degree of accuracy when dealing with at best quarterly production. The model has not fared well by comparison to blasthole results. This has been traced back to two definite problems a) very high dilution by low grade sulphides caused by high grade bands that rarely occupy a full bench height and b) incorrect DDH locations; and a third possible problem, c) the length weighting of composites during interpolation.

The actual comparison of model results to JB phase blastholes is detailed in table 3.11. The table gives both the raw model and diluted model results, the 5% mining loss is not taken for this comparison since both estimates refer to the resource in the ground. The model predicts more metal than was actually blocked out; 10% more for high grade ore (combination of some +6% and some +5%) and 4% more at a 4% cutoff. The model over predicted high grade tonnage by 6.5% and grade by 5.3%. At a 4% Pb + Zn cutoff the model underpredicted tonnage by 4.4% and overpredicted grade by 7.7%. Despite these fairly close results for two quarters production the bench by bench comparison is rather poor. In the upper benches the model grossly overpredicted tonnage and under predicted grade; in the lower benches the converse was true. The upper benches model complex fault bounded slices in the Big Indian Fault Zone; this area was expected to prove to be difficult to estimate because the geology was difficult to define using the exploration drillholes. On the 3850 bench the model performed worse than

TABLE 3.9 COMPARISON OF FI MODEL TO CYPRUS ANVIL'S HAND CALCULATION FOR THE CYPRUS ANVIL JB EXTENDED PHASE

DATE	MODEL	TONNES +6% Pb+Zn	Pb (%)	Zn (%)	Ag (g/t)	Pb+Zn (%)	TOTAL METAL (tonnes)
1985	FI	816,017	3.81	6.19	50	10.00	81,602
1984	CANC HAND	858,887	3.80	6.10	52	9.90	85,030

TABLE 3.10 A

CURRAGH RESOURCES
Comparison of FI and FB608 models - FOR AY PHASE ONLY

September 24, 1986

NO ADJUSTMENTS FOR DILUTION OR MINING LOSS

**********NEW MODEL (FB608)**********

BENCH NUMBER	TOE ELEV.	TONNES +6% ORE	Pb (%)	Zn (%)	Ag (g/t)	Pb + Zn (%)	LEAD METAL (tonnes)	ZINC METAL (tonnes)	SILVER METAL (grams)	TOTAL METAL (tonnes)
17	3750	3,840	3.97	5.87	79.04	9.84	152	225	303521	378
18	3730	33,320	4.15	5.13	71.75	9.28	1382	1710	2390743	3092
19	3710	49,290	3.81	5.00	54.99	8.81	1876	2464	2710654	4340
20	3690	77,620	3.42	5.66	45.75	9.07	2651	4390	3551115	7041
21	3670	51,530	3.20	5.15	38.07	8.35	1648	2653	1961953	4302
22	3650	43,590	3.14	4.16	37.53	7.30	1367	1813	1636029	3180
23	3630	76,680	3.16	4.26	37.33	7.42	2420	3266	2862771	5686
24	3610	141,460	3.13	4.88	32.90	8.01	4426	6909	4654458	11335
25	3590	121,260	2.91	4.74	31.34	7.65	3524	5749	3799682	9273
26	3570	79,820	2.91	4.84	36.36	7.74	2322	3859	2902574	6181
27	3550	205,690	3.25	5.09	44.78	8.34	6681	10466	9211004	17146
28	3530	365,850	3.61	5.27	47.45	8.88	13211	19291	17358485	32502
29	3510	499,220	3.56	5.27	44.84	8.83	17762	26299	22386522	44061
30	3490	469,190	3.87	5.41	49.20	9.28	18158	25369	23082271	43527
31	3470	361,350	3.76	5.28	45.78	9.03	13572	19068	16541158	32641
32	3450	314,490	3.17	4.67	43.67	7.85	9982	14699	13734722	24681
33	3430	253,690	3.72	5.72	45.15	9.43	9427	14498	11454357	23926
34	3410	42,300	2.79	4.27	25.95	7.06	1181	1806	1097474	2987
35	3390	16,880	2.97	4.14	23.57	7.11	501	699	397929	1200
TOTALS/AVERAGES:		**3,207,070**	**3.50**	**5.15**	**44.29**	**8.65**	**112244**	**165235**	**142037415**	**277479**

**********OLD MODEL (FI)**********

BENCH NUMBER	TOE ELEV.	TONNES +6% ORE	Pb (%)	Zn (%)	Ag (g/t)	Pb + Zn (%)	LEAD METAL (tonnes)	ZINC METAL (tonnes)	SILVER METAL (grams)	TOTAL METAL (tonnes)
17	3750	3,110	6.50	5.94	105.00	12.44	202	185	326550	387
18	3730	10,630	3.86	4.73	59.64	8.58	412	505	636923	917
19	3710	62,910	3.14	4.61	46.73	7.74	1972	2900	2939784	4872
20	3690	53,469	3.31	5.11	45.41	8.42	1770	2731	2427565	4501
21	3670	43,050	3.98	5.79	48.25	9.77	1714	2493	2077033	4207
22	3650	47,850	4.22	5.02	48.87	9.24	2021	2400	2338573	4421
23	3630	71,320	4.18	5.49	49.99	9.66	2980	3912	3565501	6892
24	3610	150,670	3.24	5.68	30.47	8.92	4885	8557	4591518	13441
25	3590	84,600	2.89	5.35	27.01	8.24	2441	4528	2284792	6969
26	3570	81,450	3.71	5.79	48.87	9.50	3019	4719	3980706	7738
27	3550	260,620	3.70	5.59	53.89	9.29	9640	14574	14043509	24214
28	3530	417,040	3.89	5.72	48.30	9.61	16240	23855	20142198	40094
29	3510	566,280	3.98	5.77	47.88	9.75	22555	32674	27111788	55229
30	3490	426,680	4.27	6.00	52.05	10.27	18211	25609	22209121	43820
31	3470	375,390	3.85	5.29	44.89	9.14	14441	19854	16852008	34296
32	3450	295,120	3.38	4.91	48.57	8.29	9975	14490	14334569	24465
33	3430	212,300	3.69	5.75	45.71	9.44	7828	12207	9703808	20035
34	3410	32,740	2.79	4.35	24.31	7.14	912	1425	795942	2337
35	3390	17,630	2.85	4.23	22.71	7.08	503	745	400289	1247
		3,212,900	**3.79**	**5.55**	**46.92**	**9.34**	**121,719**	**178,363**	**150,762,176**	**300,082**

TABLE 3.10 B

Variance between the F8608 and F1 models for the A1 phase

TONNES +6% ORE	Pb (%)	Zn (%)	Ag (%)	Pb + Zn (%)	LEAD METAL (%)	ZINC METAL (%)	SILVER METAL (%)	TOTAL METAL (%)	BENCH NUMBER	TOE ELEV.
PERCENT VARIANCES ((NEW-OLD)/OLD)										
23.5%	-38.9%	-1.2%	-24.7%	-20.9%	-24.6%	22.0%	-7.1%	-2.3%	17	3750
212.0%	7.6%	8.5%	20.3%	8.1%	235.8%	238.6%	275.4%	237.4%	18	3730
-21.6%	21.4%	8.5%	17.7%	15.7%	-4.9%	-15.0%	-7.8%	-10.9%	19	3710
45.2%	3.1%	10.7%	0.8%	7.7%	49.8%	60.7%	46.3%	56.4%	20	3690
19.7%	-19.7%	-11.1%	-21.1%	-14.6%	-3.8%	6.4%	-5.5%	2.2%	21	3670
-8.9%	-25.8%	-17.0%	-23.2%	-21.0%	-32.4%	-24.4%	-30.0%	-28.1%	22	3650
7.5%	-24.5%	-22.4%	-25.3%	-23.3%	-18.8%	-16.5%	-19.7%	-17.5%	23	3630
-6.1%	-3.5%	-14.0%	8.0%	-10.2%	-9.4%	-19.3%	1.4%	-15.7%	24	3610
43.3%	0.7%	-11.4%	16.0%	-7.2%	44.4%	27.0%	66.3%	33.1%	25	3590
-2.0%	-21.5%	-16.6%	-25.6%	-18.5%	-23.1%	-18.2%	-27.1%	-20.1%	26	3570
-21.1%	-12.2%	-9.0%	-16.9%	-10.3%	-30.7%	-28.2%	-34.4%	-29.2%	27	3550
-12.3%	-7.3%	-7.8%	-1.8%	-7.6%	-18.7%	-19.1%	-13.8%	-18.9%	28	3530
-11.8%	-10.7%	-8.7%	-6.3%	-9.5%	-21.2%	-19.5%	-17.4%	-20.2%	29	3510
10.0%	-9.3%	-9.9%	-5.5%	-9.7%	-0.3%	-0.9%	3.9%	-0.7%	30	3490
-3.7%	-2.4%	-0.2%	2.0%	-1.1%	-6.0%	-4.0%	-1.8%	-4.8%	31	3470
6.6%	-6.1%	-4.8%	-10.1%	-5.3%	0.1%	1.4%	-4.2%	0.9%	32	3450
19.5%	0.8%	-0.6%	-1.2%	-0.1%	20.4%	18.8%	18.0%	19.4%	33	3430
29.2%	0.2%	-1.9%	6.7%	-1.1%	29.5%	26.8%	37.9%	27.8%	34	3410
-4.3%	4.0%	-2.0%	3.8%	0.4%	-0.4%	-6.2%	-0.6%	-3.8%	35	3390
-0.2%	-7.6%	-7.2%	-5.6%	-7.4%	-7.8%	-7.4%	-5.8%	-7.5%	AVERAGE VARIANCE	

TONNES +6% ORE	Pb (%)	Zn (%)	Ag (%)	Pb + Zn (%)	LEAD METAL (tonnes)	ZINC METAL (tonnes)	SILVER METAL (ounces)	TOTAL METAL (tonnes)	BENCH NUMBER	TOE ELEV.
ACTUAL VARIANCES ((NEW-OLD)/OLD)										
730	-2.53	-0.07	-25.96	-2.60	-50	41	-672	-9	17	3750
22,640	0.29	0.40	12.11	0.70	971	1205	51212	2176		
(13,620)	0.67	0.39	8.26	1.06	-96	-436	-6691	-531		
24,160	0.10	0.55	0.34	0.65	881	1659	32808	2540		
8,480	-0.78	-0.64	-10.17	-1.43	-66	160	-3360	94		
(4,260)	-1.09	-0.85	-11.34	-1.94	-654	-586	-20515	-1241		
5,360	-1.02	-1.23	-12.66	-2.25	-560	-646	-20520	-1206		
(9,210)	-0.11	-0.80	2.43	-0.91	-458	-1648	1838	-2106		
36,660	0.02	-0.61	4.33	-0.59	1083	1221	44235	2304		
(1,630)	-0.80	-0.96	-12.51	-1.76	-697	-860	-31481	-1556		
(54,930)	-0.45	-0.50	-9.10	-0.96	-2960	-4108	-141109	-7068		
(51,190)	-0.28	-0.45	-0.85	-0.73	-3029	-4563	-81284	-7592		
(67,060)	-0.43	-0.50	-3.03	-0.93	-4793	-6375	-137978	-11168		
42,510	-0.40	-0.59	-2.86	-0.99	-53	-240	25496	-293		
(14,040)	-0.09	-0.01	0.88	-0.10	-869	-786	-9077	-1655		
19,370	-0.21	-0.24	-4.90	-0.44	7	209	-17516	216		
41,390	0.03	-0.04	-0.56	-0.01	1600	2291	51116	3891		
9,560	0.01	-0.08	1.63	-0.08	269	381	8805	650		
(750)	0.12	-0.08	0.87	0.03	-2	-46	-69	-48		
(5,830)	-0.29	-0.40	-2.64	-0.69	-9475	-13127	-254763	-22603		

TABLE 3.10 C

CURRAGH RESOURCES
Comparison of F1 and F8608 models - FOR BY PHASE ONLY

September 3rd, 1996

NO ADJUSTMENTS FOR DILUTION OR MINING LOSS

			********** NEW MODEL (F8608) **********								********** OLD MODEL (F1) **********							
BENCH NUMBER	TOE ELEV.	TONNES +6% ORE	Pb (%)	Zn (%)	Ag (g/t)	Pb + Zn (%)	LEAD METAL (tonnes)	ZINC METAL (tonnes)	SILVER METAL (grams)	TOTAL METAL (tonnes)	BENCH NUMBER	TOE ELEV.	TONNES +6% ORE	Pb (%)	Zn (%)	Ag (g/t)	Pb + Zn (%)	LEAD METAL (tonnes)	ZINC METAL (tonnes)	SILVER METAL (grams)	TOTAL METAL (tonnes)
20	3690	2,770	2.55	6.17	25.05	8.72	71	171	69383	242	20	3690	0	0.00	0.00	0.00	0.00	0	0	0	0
21	3670	11,930	3.14	7.75	27.81	10.89	374	925	331797	1299	21	3670	0	0.00	0.00	0.00	0.00	0	0	0	0
22	3650	0	0.00	0.00	0.00	0.00	0	0	0	0	22	3650	2,360	6.18	7.81	61.00	13.99	146	184	143960	330
23	3630	0	0.00	0.00	0.00	0.00	0	0	0	0	23	3630	0	0.00	0.00	0.00	0.00	0	0	0	0
24	3610	3,650	3.78	5.42	47.62	9.19	138	198	173809	336	24	3610	0	0.00	0.00	0.00	0.00	0	0	0	0
25	3590	51,360	3.79	5.76	51.14	9.55	1948	2958	2626756	4906	25	3590	1,420	3.59	4.44	50.00	8.03	51	63	71090	114
26	3570	120,300	3.74	4.83	54.03	8.57	4499	5809	6499328	10309	26	3570	105,810	4.32	5.41	54.45	9.73	4574	5725	5761566	10300
27	3550	176,490	3.93	4.76	56.83	8.69	6931	8403	10029927	15333	27	3550	181,470	4.31	4.73	63.08	9.04	7816	8584	11446220	16399
28	3530	252,270	3.52	4.62	54.13	8.14	8877	11660	13655880	20537	28	3530	267,200	4.40	5.18	69.03	9.58	11757	13833	18444549	25590
29	3510	319,950	4.26	5.60	63.46	9.86	13636	17908	20304987	31544	29	3510	272,490	4.18	5.47	66.52	9.65	11390	14905	18126307	26295
30	3490	471,560	4.03	5.55	55.40	9.59	19018	26181	26125839	45199	30	3490	471,420	4.32	5.77	61.81	10.09	20342	27220	29137999	47562
31	3470	745,720	4.24	5.83	56.23	10.07	31633	43461	41929598	75094	31	3470	751,690	4.13	5.70	56.51	9.83	31045	42846	42474243	73891
32	3450	560,290	4.06	5.54	49.38	9.59	22737	31012	27666000	53749	32	3450	489,640	4.13	5.71	55.03	9.84	20207	27973	26945379	48181
33	3430	529,670	3.61	5.22	40.87	8.83	19116	27638	21648143	46754	33	3430	503,770	3.68	5.34	39.35	9.02	18534	26896	19824861	45430
34	3410	679,850	3.13	4.84	31.59	7.97	21273	32884	21476462	54157	34	3410	706,020	3.30	5.06	34.35	8.36	23299	35746	24252493	59044
35	3390	428,320	3.02	4.65	29.36	7.68	12948	19934	12576332	32882	35	3390	450,190	3.07	4.38	36.45	7.45	13816	19736	16408075	33553
36	3370	305,530	2.96	4.89	26.96	7.85	9053	14943	8236172	23996	36	3370	243,000	2.96	4.79	31.70	7.76	7203	11642	7702128	18845
37	3350	109,550	2.78	5.26	29.86	8.03	3040	5761	3270725	8801	37	3350	148,630	2.88	5.28	34.04	8.17	4286	7849	5059811	12136
38	3330	14,410	2.62	5.20	43.80	7.82	377	750	631086	1127	38	3330	28,830	2.61	4.92	39.32	7.52	751	1417	1133624	2168
TOTALS/AVERAGES:		4,783,620	3.67	5.24	45.42	8.91	175668	250596	217252222	426264			4,623,940	3.79	5.29	49.08	9.08	175,217	244,620	226,932,216	419,837

TABLE 3.10 B

Variance between the FB608 and FI models for the BY phase

PERCENT VARIANCES ((NEW-OLD)/OLD)										
TONNES +6% ORE	Pb (%)	Zn (%)	Ag (%)	Pb + Zn (%)	LEAD METAL (%)	ZINC METAL (%)	SILVER METAL (%)	TOTAL METAL (%)	BENCH NUMBER	TOE ELEV.
ERR	ERR	ERR	ERR	ERR	ERR	ERR	ERR	ERR	20	3690
ERR	ERR	ERR	ERR	ERR	ERR	ERR	ERR	ERR	21	3670
-100.0%	-100.0%	-100.0%	-100.0%	-100.0%	-100.0%	-100.0%	-100.0%	-100.0%	22	3650
ERR	ERR	ERR	ERR	ERR	ERR	ERR	ERR	ERR	23	3630
ERR	ERR	ERR	ERR	ERR	ERR	ERR	ERR	ERR	24	3610
3516.9%	5.6%	29.7%	2.3%	19.0%	3720.4%	4592.2%	3599.7%	4202.4%	25	3590
13.7%	-13.5%	-10.8%	-0.8%	-12.0%	-1.6%	1.5%	12.8%	0.1%	26	3570
-2.7%	-8.8%	0.7%	-9.9%	-3.9%	-11.3%	-2.1%	-12.4%	-6.5%	27	3550
-5.6%	-20.0%	-10.7%	-21.6%	-15.0%	-24.5%	-15.7%	-26.0%	-19.7%	28	3530
17.4%	2.0%	2.3%	-4.6%	2.2%	19.7%	20.1%	12.0%	20.0%	29	3510
0.0%	-6.5%	-3.8%	-10.4%	-5.0%	-6.5%	-3.8%	-10.3%	-5.0%	30	3490
-0.8%	2.7%	2.2%	-0.5%	2.4%	1.9%	1.4%	-1.3%	1.6%	31	3470
14.4%	-1.7%	-3.1%	-10.3%	-2.5%	12.5%	10.9%	2.7%	11.6%	32	3450
5.1%	-1.9%	-2.3%	3.9%	-2.1%	3.1%	2.8%	9.2%	2.9%	33	3430
-3.7%	-5.2%	-4.5%	-8.0%	-4.7%	-8.7%	-8.0%	-11.4%	-8.3%	34	3410
-4.9%	-1.5%	6.2%	-19.4%	3.0%	-6.3%	1.0%	-23.4%	-2.0%	35	3390
25.7%	0.0%	2.1%	-15.0%	1.3%	25.7%	28.4%	6.9%	27.3%	36	3370
-26.3%	-3.8%	-0.4%	-12.3%	-1.6%	-29.1%	-26.6%	-35.4%	-27.5%	37	3350
-50.0%	0.4%	5.9%	11.4%	4.0%	-49.8%	-47.1%	-44.3%	-48.0%	38	3330
3.5%	-3.1%	-1.0%	-7.5%	-1.9%	0.3%	2.4%	-4.3%	1.5%	AVERAGE VARIANCE	

ACTUAL VARIANCES ((NEW-OLD)/OLD)										
TONNES +6% ORE	Pb (%)	Zn (%)	Ag (%)	Pb + Zn (%)	LEAD METAL (tonnes)	ZINC METAL (tonnes)	SILVER METAL (grams)	TOTAL METAL (tonnes)	BENCH NUMBER	TOE ELEV.
2,770	2.55	6.17	25.05	8.72	71	171	2026	242	20	3690
11,930	3.14	7.75	27.81	10.89	374	925	9688	1299	21	3670
(2,360)	-6.18	-7.81	-61.00	-13.99	-146	-184	-4204	-330	22	3650
0	0.00	0.00	0.00	0.00	0	0	0	0	23	3630
3,650	3.78	5.42	47.62	9.19	138	198	5075	336	24	3610
49,940	0.20	1.32	1.14	1.52	1897	2895	74628	4792	25	3590
14,490	-0.58	-0.58	-0.43	-1.16	-75	84	21543	9	26	3570
(4,980)	-0.38	0.03	-6.25	-0.35	-885	-181	-41356	-1066	27	3550
(14,930)	-0.88	-0.55	-14.90	-1.44	-2879	-2173	-139829	-5052	28	3530
47,460	0.08	0.13	-3.06	0.21	2246	3002	63617	5249	29	3510
140	-0.28	-0.22	-6.41	-0.50	-1324	-1039	-87955	-2363	30	3490
(5,970)	0.11	0.13	-0.28	0.24	589	614	-15904	1203	31	3470
70,650	-0.07	-0.18	-5.65	-0.25	2529	3039	21042	5568	32	3450
25,900	-0.07	-0.12	1.52	-0.19	582	742	53240	1324	33	3430
(26,170)	-0.17	-0.23	-2.76	-0.40	-2026	-2861	-81060	-4888	34	3410
(21,870)	-0.05	0.27	-7.09	0.22	-868	198	-111887	-671	35	3390
62,530	0.00	0.10	-4.74	0.10	1850	3301	15594	5152	36	3370
(39,080)	-0.11	-0.02	-4.19	-0.13	-1246	-2088	-52241	-3334	37	3350
(14,420)	0.01	0.29	4.47	0.30	-374	-667	-14674	-1041	38	3330
159,680	-0.12	-0.05	-3.66	-0.17	452	5975	-282656	6427	AVERAGE VARIANCE	

TABLE 3.11 COMPARISON OF FI MODEL PREDICTED BENCH RESERVES WITH 1986 MINE PRODUCTION IN JB PHASE AS BLOCKED OUT BY BLASTHOLES

	bench	high grade tonnes	Pb (%)	Zn (%)	Ag (g/t)	Pb+Zn (%)	tonnes total metal	low grade tonnes	Pb (%)	Zn (%)	Ag (g/t)	Pb+Zn (%)	tonnes total metal	all grades (+4%) tonnes	Pb (%)	Zn (%)	Ag (g/t)	Pb+Zn (%)	tonnes total metal
BLASTHOLE RESULTS																			
*	3890	44,180	3.10	4.70		7.80	3,446	0				0.00	0	44,180	3.10	4.70	0	7.80	3,446
*	3870	20,378	3.30	5.30		8.60	1,753	8,333	1.61	3.05		4.66	389	28,711	2.81	4.65	0	7.46	2,141
*	3850	29,549	2.41	3.83		6.24	1,844	7,140	1.42	2.94		4.36	311	36,689	2.22	3.66	0	5.87	2,155
*	3830	81,920	2.79	4.51		7.30	5,980	19,627	2.12	2.45		4.57	897	101,547	2.66	4.11	0	6.77	6,877
*	3810	99,840	3.19	4.41		7.60	7,588	20,480	1.89	2.51		4.40	901	120,320	2.97	4.09	0	7.06	8,489
	3790	184,320	3.44	4.94		8.38	15,446	5,760	1.94	2.66		4.60	265	190,080	3.39	4.87	0	8.27	15,711
	3770	217,600	2.73	4.43	35	7.16	15,580	34,560	1.89	2.69	24	4.38	1,514	252,160	2.59	4.19	33	6.78	17,094
	3750	208,249	3.11	4.60	47	7.71	16,056	65,813	1.78	2.98	33	4.76	3,133	274,062	2.79	4.21	39	7.00	19,189
	3730	261,111	2.99	4.66	42	7.65	19,975	82,667	2.00	3.34	34	5.34	4,414	343,778	2.75	4.34	40	7.09	24,389
	3710	115,662	2.95	4.60	38	7.55	8,732	49,378	1.73	3.07	32	4.80	2,370	165,040	2.58	4.14	36	6.73	11,103
	TOTAL	1,262,809	3.03	4.61		7.64	96,479	293,758	1.84	2.99		4.83	14,189	1,556,567	2.81	4.30		7.11	110,667
MODEL PREDICTIONS (NO DILUTION)																			
	3890	28560	3.71	5.01	54	8.72	2,490	0					0	28,560	3.71	5.01	54	8.72	2,490
	3870	10050	3.17	4.78	46	7.95	799	4500	3.37	3.18	37	5.55	250	14,550	2.92	4.29	43	7.21	1,049
	3850	45500	4.33	7.64	52	11.97	5,446	8950	1.85	3.18	31	5.03	450	54,450	3.92	6.91	49	10.83	5,897
	3830	76000	3.98	6.55	51	10.53	8,003	8250	2.06	2.87	32	4.93	407	84,250	3.79	6.19	49	9.98	8,410
	3810	83390	3.92	6.32	52	10.24	8,539	22970	1.66	2.94	35	4.62	1,061	106,360	3.44	5.59	48	9.03	9,600
	3790	115150	4.37	7.28	54	11.65	13,415	13950	1.36	3.2	28	4.56	636	129,100	4.04	6.84	51	10.88	14,051
	3770	184900	3.42	5.61	49	9.03	16,696	16550	1.06	3.31	22	4.37	723	201,450	3.23	5.42	47	8.65	17,420
	3750	222400	3.14	4.98	44	8.12	18,059	25200	1.55	3.06	36	4.61	1,162	247,600	2.98	4.78	43	7.76	19,221
	3730	233320	3.05	5.07	37	8.12	18,946	12290	1.52	3.14	30	4.66	573	245,610	2.97	4.97	37	7.95	19,518
	3710	228710	2.71	4.57	35	7.28	16,650	14710	2.23	2.51	36	4.74	697	243,420	2.68	4.45	35	7.13	17,347
	TOTAL	1,227,980	3.36	5.52	44	8.88	109,045	127,370	1.65	3.03	32	4.68	5,961	1,355,350	3.20	5.29	43	8.49	115,006
MODEL PREDICTIONS DILUTED																			
		100 PERCENT MINING RECOVERY																	
		10 PERCENT DILUTION																	
		0 LEAD GRADE (%) OF DILUTANT																	
		0 ZINC GRADE (%) OF DILUTANT																	
		0 LEAD + ZINC GRADE (%) OF DILUTANT																	
		0 SILVER GRADE (g/t) OF DILUTANT																	
	3890	31,416	3.37	4.55	49	7.93	2,490						0	31,416	3.37	4.55	49	7.93	2,490
	3870	11,055	2.88	4.35	42	7.23	799	4,950	2.15	2.89	34	5.05	250	16,005	2.66	3.90	39	6.55	1,049
	3850	50,050	3.94	6.95	47	10.88	5,446	9,845	1.68	2.89	28	4.57	450	59,895	3.57	6.28	44	9.84	5,897
	3830	83,600	3.62	5.95	46	9.57	8,003	9,075	1.87	2.61	29	4.48	407	92,675	3.45	5.63	45	9.07	8,410
	3810	91,729	3.56	5.75	47	9.31	8,539	25,267	1.53	2.67	32	4.20	1,061	116,996	3.12	5.08	44	8.21	9,600
	3790	126,665	3.97	6.62	49	10.59	13,415	15,345	1.24	2.91	25	4.15	636	142,010	3.68	6.22	47	9.89	14,051
	3770	203,390	3.11	5.10	45	8.21	16,696	18,205	0.96	3.01	20	3.97	723	221,595	2.93	4.93	43	7.86	17,420
	3750	244,640	2.85	4.53	40	7.38	18,059	27,720	1.41	2.78	33	4.19	1,162	272,360	2.71	4.35	39	7.06	19,221
	3730	256,652	2.77	4.61	34	7.38	18,946	13,519	1.38	2.85	27	4.24	573	270,171	2.70	4.52	33	7.22	19,518
	3710	251,581	2.46	4.15	32	6.62	16,650	16,181	2.03	2.28	33	4.31	697	267,762	2.44	4.04	32	6.48	17,347
	TOTAL	1,350,778	3.05	5.02	40	8.07	109,045	140,107	1.50	2.75	29	4.25	5,961	1,490,885	2.91	4.81	39	7.71	115,006

* High grade is +6% Pb+Zn and low grade is 4-6%; on all other benches high grade is +5% and low grade is 4-5%

usual; this has been traced back to a drillhole which is now known to be in the wrong place by comparison of pit geology to the drillhole results. This errant drillhole caused the width of a fault bounded panel to be twice what it actually was with a corresponding overestimate of tonnage. The lower benches model larger parts of the deposit in areas less affected by faulting and the model produces better results there. The last bench is starting to show the effect of another drillhole in the wrong place causing the elevation of the base of the ore zone to be estimated lower than it actually is with a resulting shortfall of tonnage. The cause of the generally greater overprediction for zinc compared to lead is not understood.

Table 3.12 shows a similar comparison for the FI model and the blasthole results in the AY phase. The tendency to underpredict the tonnage and overpredict the grade is clear. Table 3.14 shows the same comparison for high grade ore and the F8608 model. For the few benches mined this model seems to give a fair approximation of the pit reserves; it is within 1% on total metal and ore tonnage but 11% high on lead and 6% low on zinc.

3.2.4.3.4 Conclusion

The conclusion of these comparisons is that the FI model compared reasonably well to other calculations on the basis of total metal and for a large enough volume of material was within 10% of actual production statistics. Despite this, it was unuseable for bench by bench predictions whithout an appropriate dilution factor. The grade predictions of the FI model are too high probably as a result of inappropriate methodology but mainly too low a dilution factor. Most importantly, dilution is not average throughout the deposit and the choice of factor must take account local deposit structure in order to provide reasonable predictions of millfeed. Furthermore without accurate drillhole data, accurate modeling is impossible regardless of calculation sophistication. On the average the FI model will probably give a reasonable approximation of the long term mill feed at a dilution of 10% however local dilution factors should be tried in order to attempt to better reflect the short term and sensitivity to higher dilutions should be carried out at least on the marginal benches. The newer modeling techniques should be extended to the remainder of the deposit a soon as practical.

3.2.5 Additional Work Required

In order to provide reliable estimates of reserves on a short term basis it will be necessary to drill additional fill in holes. To fill in the current pattern to 43 m (141 ft.) minimum on the main 43 m (141 ft.) spaced sections will require 32 additional holes totalling 4270 m (14000 feet). Of this total 20 holes totaling 2300 m (7500 feet) are in the AY and early BY phases and have considerable urgency.

To upgrade the drilling pattern significantly beyond the level outlined above would be prohibitive in terms of cost and the

TABLE 3.12 COMPARISON OF FI MODEL PREDICTED BENCH RESERVES WITH 1986 MINE PRODUCTION IN AY PHASE AS BLOCKED OUT BY BLASTHOLES

	bench	high grade tonnes *	Pb (%)	Zn (%)	Ag (g/t)	Pb+Zn (%)	tonnes total metal	low grade tonnes *	Pb (%)	Zn (%)	Ag (g/t)	Pb+Zn (%)	tonnes total metal	all grades (+4%) tonnes	Pb (%)	Zn (%)	Ag (g/t)	Pb+Zn (%)	tonnes total metal
BLASTHOLE RESULTS																			
	3750	0	0.00	0.00	0	0.00	0	0	0.00	0.00	0	0.00	0	0	ERR	ERR	ERR	ERR	ERR
#	3730	11,520	2.04	3.89	32	5.93	683	8,333	1.63	2.69	34	4.32	360	19,853	1.87	3.39	33	5.25	1,043
	3710	123,056	2.67	4.49	40	7.16	9,057	7,140	1.46	3.14	24	4.60	328	130,196	2.79	4.42	39	7.21	9,385
	3690	116,252	2.52	4.65	36	7.17	8,335	19,827	1.75	2.97	25	4.72	526	135,879	2.41	4.41	29	6.82	9,262
	TOTAL	250,828	2.67	4.54	35	7.21	18,085	35,100	1.62	3.04	25	4.66	1,636	285,928	2.54	4.26	34	6.80	19,720
MODEL PREDICTIONS (NO DILUTION)																			
	3750	3110	6.5	5.94	105	12.44	387	0					0	3,110	6.50	5.94	105	12.44	387
	3730	10660	3.85	4.72	58	8.57	915	4500	2.37	3.18	37	5.55	250	15,160	3.41	4.26	52	7.67	1,165
	3710	80410	3.02	4.27	46	7.29	5,862	8950	1.85	3.18	31	5.03	450	89,360	2.90	4.16	44	7.06	6,312
	3690	73260	3.08	4.63	42	7.71	5,648	8250	2.06	2.87	32	4.93	407	81,510	2.96	4.45	41	7.43	6,055
	TOTAL	167,460	3.16	4.45	46	7.65	12,811	21,700	1.65	3.03	32	4.68	1,016	189,160	2.99	4.32	44	7.31	13,826
MODEL PREDICTIONS DILUTED																			
		100 PERCENT MINING RECOVERY																	
		10 PERCENT DILUTION																	
		0 LEAD GRADE (%) OF DILUTANT																	
		0 ZINC GRADE (%) OF DILUTANT																	
		0.00 LEAD + ZINC GRADE (%) OF DILUTANT																	
		0 SILVER GRADE (g/t) OF DILUTANT																	
	3750	3,421	5.91	5.40	95	11.31	387						0	3,421	5.91	5.40	95	11.31	387
	3730	11,748	3.50	4.29	54	7.79	915	4,950	2.15	2.89	34	5.05	250	16,698	3.10	3.86	48	6.96	1,165
	3710	88,451	2.75	3.88	42	6.63	5,862	9,845	1.68	2.89	28	4.57	450	98,296	2.64	3.76	40	6.42	6,312
	3690	80,586	2.80	4.21	36	7.01	5,648	9,075	1.87	2.61	29	4.48	407	89,661	2.71	4.05	37	6.75	6,055
	TOTAL	184,206	2.87	4.08	42	6.95	12,811	23,870	1.50	2.75	29	4.25	1,016	208,076	2.72	3.93	40	6.64	13,826

* High grade is +5% Pb+Zn and low grade is 4-5%

Includes ore mined from 3750 since 3730 was mined on a 40 foot lift

TABLE 3.13 COMPARISON OF FI MODEL PREDICTIONS TO ACTUAL BLASTHOLE RESULTS FOR 1986 PRODUCTION IN AY AND JB PHASES OF FARO DEPOSIT, ZONE 3

	ORE TONNES	Pb	Zn	Ag	Pb+Zn	TONNES TOTAL METAL	PERCENT VARIANCE OF TOTAL METAL FROM THE MODEL PREDICTION
BLASTHOLES							
JB PHASE							
high grade	1,262,809	3.03	4.61		7.64	96,479	-11.5% from predicted
low grade	293,758	1.84	2.99		4.83	14,189	138.3% from predicted
both grades	1,556,567	2.81	4.30		7.11	110,667	-3.7% from predicted
AY PHASE							
high grade	250,828	2.67	4.54	35	7.21	18,085	41.2% from predicted
low grade	48,688	1.62	3.04	25	4.66	2,269	33.7% from predicted
both grades	299,516	2.50	4.30	34	6.80	20,354	40.3% from predicted
ALL 1986 PRODUCTION							
high grade	1,513,637	2.97	4.60		7.57	114,563	-6.0% from predicted
low grade	342,446	1.81	3.00		4.81	16,457	115.1% from predicted
both grades	1,856,083	2.76	4.30		7.06	131,021	1.2% from predicted
FI MODEL PREDICTION (10% dilution at 0% grade, no mining loss)							
JB PHASE							
high grade	1,350,778	3.05	5.02	40	8.07	109,008	
low grade	140,107	1.50	2.75	29	4.25	5,955	
both grades	1,490,885	2.90	4.81	39	7.71	114,962	
AY PHASE							
high grade	184,206	2.87	4.08	42	6.95	12,806	
low grade	42,647	1.66	2.32	23	3.98	1,697	
both grades	226,853	2.64	3.75	38	6.39	14,503	
ALL 1986 PRODUCTION							
high grade	1,534,984	3.03	4.91	40	7.94	121,814	
low grade	182,754	1.54	2.65	28	4.19	7,652	
both grades	1,717,738	2.87	4.67	39	7.54	129,466	

TABLE 3.14 COMPARISON OF F8608 MODEL PREDICTIONS FOR AY PHASE TO 1986 MINE PRODUCTION AS BLOCKED OUT BY BLASTHOLES

bench	tonnes +5%	Pb (%)	Zn (%)	Ag (g/t)	Pb + Zn (%)	tonnes total metal
BLASTHOLES						
3750	0					
3730	11,520	2.04	3.89	32	5.93	683
3710	123,056	2.87	4.49	40	7.36	9,057
3690	116,252	2.52	4.65	30	7.17	8,335
TOTAL	250,828	2.67	4.54	35	7.21	18,085
F8608 MODEL (UNDILUTED)						
3750	3,480	3.97	5.87	79	9.84	342
3730	34,880	4.08	5.01	70	9.09	3,171
3710	65,250	3.58	4.39	53	7.97	5,200
3690	122,570	2.93	4.79	40	7.72	9,462
TOTAL	226,180	3.31	4.73	49	8.04	18,185
F8608 MODEL WITH 10% DILUTION AT ZERO GRADE						
3750	3,828	3.61	5.34	72	8.95	342
3730	38,368	3.71	4.55	64	8.26	3,171
3710	71,775	3.25	3.99	48	7.25	5,200
3690	134,827	2.66	4.35	36	7.02	9,462
TOTAL	248,798	3.01	4.30	45	7.31	18,185

logistics of both drilling and data analysis.

While this core is still fresh it could be used for additional metallurgical testing if required.

As noted above, the remainder of the deposit modeling should be upgraded to at least F8608 model standards. A new modeling technique that treats PC Mine blocks not as homogenous single geologic entities but as the sum of two or more material types has been devised but not yet put into practice. This modeling technique could help significantly with the treatment of low grade and waste dilution and should tried soon. Work is already underway on both these objectives. The first priority however is to produce an updated AY anbd BY (or BZ) model incorporating the 1986 drilling which will help evaluate the gains from additional drilling by comparison to the F8608 model.

3.3 Grum Geology and Reserves

].3.1 History

The Grum deposit was discovered in 1973 by AEX Minerals in joint venture with Kerr Addison Mines. Discovery was as the result of drill testing a gravity anomaly in an area down fold plunge from the Vangorda deposit along what was then a, as yet, poorly defined favourable trend.

Surface drilling in 1973 and 1974 indicated a significant deposit; in 1975 and 1976 an underground sampling and drilling program, along with further surface diamond drilling, was carried out to further define it.

Kerr Addison sold the deposit, along with Vangorda and Swim, to Cyprus Anvil Mining Corporation in 1979. From 1980 to 1982 Cyprus Anvil drilled additional holes in and around the deposit and reloged all existing holes in it. All available sulphide intersections were re-sampled and re-assayed at that time.

3.3.2 General Geology

3.3.2.1 Stratigraphy and lithology

The Grum deposit consists of three to five highly contorted layers of massive and disseminated sulphide mineralization within a 150m section of barren phyllite. The most important mineralized horizon occurs just beneath the basal carbonaceous member of the Vangorda formation. There are thin low grade horizons within the Vangorda formation and more important horizons in the upper part of the Mt. Mye formation.

At Grum, the Vangorda formation consists of soft, highly fissile, calcareous phyllites. Metabasites in the Grum area are minor and tend to be highly foliated chlorite phyllite rather than blocky, massive greenstones that typify the Vangorda formation elsewhere. The basal carbonaceous member of the formation (unit 5A) thickens across the deposit from about 10m in the northeast to as much as 80 or 100 m southwest of the deposit. The sulphide horizons appear to be associated with the northeast pinchout of this unit. Immediately above the main ore horizon the carbonaceous rocks are soft, highly sheared and gouged but elsewhere they are moderately hard, highly fractured, black siliceous phyllites.

The Mt. Mye formation also consists of soft phyllites which are distinguished from those of Vangorda formation be being non-calcareous and less distinctly banded.

There are no significant post metamorphic dykes at Grum. The Anvil Batholith crops out 1.5 km northeast of the deposit but is separated from it by major faults. The batholith is unrelated to the deposit and does not appear to have significantly affected it.

3.3.2.2 Structure

The ore layers at Grum are contorted into a complex, shallowly northwest plunging, polyphase fold structure. The prominant S shaped folds (figure 3.8) are second phase structures. They are superimposed on a larger Z shaped first phase fold. The dominant plane of fissility (S_2) in the phyllites at Grum is axial planar to the second phase folds and dips shallowly (10^0 to 30^0) generally to the southwest. This fissility is a major factor in assessing slope stability for a Grum pit. The overall deposit elongation parallels the axial direction of the second phase folds (315^0 trend 11^0 plunge).

There are several important faults at Grum. The largest displacements occur on moderately (35^0 - 45^0) dipping structures that truncate the deposit at both its northwest and southeast ends (figure 3.9). Neither of these structures would crop out in an open pit but smaller subparallel faults will be found in the pit. A steeply northwest dipping fault trending about 060^0, passes between sections 70W and 72W and downdrops the deposit about 60 m to the northwest. A myriad of smaller faults were mappped underground by Kerr Addison trending on the average 080^0 and dipping steeply. Joints mapped underground and on surface tend to strike 060^0 and dip subvertically.

3.3.2.3 Surfical Geology

The subcrop of the ore deposit is covered by up to 100 m of morainal material (tills) and better sorted galciofluvial silts, sands and gravels. These unconsolidated sediments are water saturated and may contain pockets of permafrost. The northeast wall of any pit designs at Grum must contend with thick sections of these sediments. Dewatering in advance of stripping may help increase stability substantially as well as simplify operations in the pit.

3.3.2.4 Ore Deposit Geology

As with other deposits in the Anvil Range a given ore horizon at Grum tends to have a massive sulphide upper and central portion and a quartzose, disseminated sulphide lower and perhiperal portion. The horizons can be up to 30 m thick but are mostly 15 m or less thick. Grade is strongly partitioned into massive, particularly baritic, sulphides thus the tops of horizons tend to be high grade and the bottoms low grade (except of course where the horizons are overturned). The sulphide horizons are separated by significant thicknesses of barren phyllite. Interfaces between ore and waste tend to be sharp at the stratigraphic hanging wall contact against barren phyllite and gradational both at the footwall and laterally against sulphide waste.

Grum, like Vangorda and Dy, has several characteristics that distinguish it from Faro. In large part this is due to the lower metamorphic grade the deposit has reached. The most outstanding difference between Grum, and all the other Vangorda

Plateau deposits, as opposed to Faro is the form of the deposit. The Vangorda Plateau deposits consist of several distinct, highly contorted horizons separated by barren phyllite waste. Faro on the other hand is essentially one thick horizon in overall outline with lesser phyllitic waste but substantial barren sulphide waste banding. This implies that dilution by phyllite will be higher at Grum than at Faro. Faro however contains considerable internal sulphide waste thus its dilution is higher than might appear at first glance. It is none the less inescapable that Grum has more potential dilution and will have more complex mining problems than Faro. On the positive side, the dilutant at Grum will be more commonly easily identifiable phyllite rather than low grade sulphides as at Faro. Experience at Faro shows that phyllite dilution is much easier to control than low grade sulphides. Grum's higher grade if diluted at 3 times the historical 5% dilution used at Faro still gives Grum a higher average grade.

The next most obvious difference is a finer grain size and more complex mineral intergrowth, necessitating finer grinding than Faro ores. Cyprus Anvil Mining Corporation had already made modifications to its mill to accomodate this fine grind prior to shutdown in 1982. When a large proportion of feed comes from Grum it will be necessary to utlize this grinding capability at the expense of tonnage throughput.

At a given Pb + Zn cutoff grade, ores at Grum are higher grade than those remaining at Faro, particularly in precious metals relative to base metals. The average gold content of Grum is several times higher than Faro. Similarily, other elements that tend to be geochemical associates of gold: mercury and arsenic, tend to be higher at Grum. The sphalerite at Grum, and likely other Vangorda Plateau deposits, is richer in zinc due to lower metamorphic grade and resulting lesser iron content. This will help counteract higher pyrite-sphalerite middlings expected with Grum ores.

A feature unique to Grum among the Vangorda Plateau deposits is the relative abundance of quartzose ore types, particularily carbonaceous pyritic quartzites (4A) which comprise about 35% of the reserves above 4% Pb + Zn. It will undoubtedly create challenges for maintaining good lead concentrate grades, and probably necessitate stockpiling and planning campaigns of 4A during which depressants are used.

3.3.3 Drill Definition & Information Base

The Grum deposit extends from section 52W in the southeast to section 112W in the northwest. The deposit has been most densely drilled between 62W and 86W and it is this portion of the deposit for which proven geologic reserves are reported.

Most of the deposit southeast of 88W has been drilled from the surface on at least a 61m X 30.5 m (200' X 100') pattern. Most surface holes are vertical.

Between sections 62W and 86W the deposit has also been explored by 15,000 m of underground drilling in fans from a pair of parallel inclines following the deposit trend. The strike length of the deposit examined from underground is 700 m, underground workings, now flooded, total 2900 m. The fans are most complete on even numbered sections (ie: spaced 61 m apart); on the odd numbered sections in between some fill in drilling has also been done from underground. The overall density of drilling is on the order of 15 m X 30 m with local areas being much in excess of that.

In the southeast part of the deposit additional fill in drilling was done by Cyprus Anvil in 1980-1982 from the surface to more closely define shallow ore for early production.

Total drilling at Grum is 67,200 m of which 15,000 m is underground drilling and 52,200 m is surface drilling. Between 62W and 86W there is a total of 53,600 m of drilling in 372 drill holes (154 surface and 218 underground) of which 344 are used in the current model. The remainder not included in the model are underground holes that are at high angles to the geological sections and some short holes that did not intersect ore.

Without question Grum is the best drill defined deposit in the Anvil District.

There are 9000 samples in the Grum deposit assay database. Assay intervals generally average 1.5 m in length and are keyed as closely as possible to sulphide rock types. 90% of these were determined for Cyprus Anvil by Kamloops Research and Assay Labs between 1980 and 1983. For most of these samples Pb, Zn, Cu, and Ag assays are available. For 2/3 of these samples there is also insoluble Fe, soluble (in hot concentrated HCL) Fe, Au, and pulp SG. All assays were determined using a set of Anvil District ore type standards for control. Rejects and N_2 purged pulps (by now somewhat oxidized) have been retained for additional analytical work. There are no BaO or Mn assays available nor is there systematic data available for Hg, As, Cd or any other elements.

The remaining 10% of the assays are from Kerr Addison samples for which Pb, Zn and Ag only are available. Many of these samples are from the holes not used in the ore deposit model.

3.3.4 Methods and Procedure of Reserve Calculation

3.3.4.1 Introduction

For the purpose of this evaluation a new block model, the G8606 model, was constructed in June and July 1986. New reserves were calculated for the the deposit in two portions, one, from surface (1336m maximum elevation) to 1088.5 m elevation and a second from 1088.5 to 868.0 m. elevation. This was due to software and hardware limitations bought about by a low bench height (4.5m) and correspondingly larger number of benches.

The PC Mine software package was used for grade interpolation and reserve calculation. The block geology and composites had been previously calculated using Mintec's Medsystem release 10. The results of the calculation are outlined in Table 3.19 and discussed below.

3.3.4.2 Block Geology and Drillhole information

The reserves are calculated from a computer based 3D block model based on a set of cross-sections produced by Cyprus Anvil geologists in 1982. The sections are parallel to the columns in the mine model and perpendicular to the elongation of the deposit. The cross sections are 61m apart (200 feet) and provide the only geologic control for the mine model. These are the same sections used for the sectional calculation by Cyprus Anvil in 1983 (the Simpson-Adamson calculation) recalculated by Dome in 1984. All sections are available in a supporting document available at Curragh's Toronto and Whitehorse offices.

The logging and drill hole orientation data used were the most current available for the deposit. The interpretation of the geologic detail is known to need improvement in a number of areas particularly concerning the correlation of certain horizons and the treatment of faults. A new set of more closely spaced cross and longitidinal sections is being prepared to address these points of detail. For the time being however these shortcomings are of little consequence as most of the deposit is so densely drilled that there is little scope for variations in geologic interpretation to change the volume of the deposit significantly. The details of ore distribution on a given bench can however change significantly. For the purposes of annual projections of production the current geological model is considered adequate.

The block geology was generated manually by laying a grid over the geologic sections and hand coding the rock types. Block dimensions are 4.5 m high, 8.0 m across deposit trend and 15.0 m along deposit trend. These block sizes provide a reasonable approximation of the complex structure of Grum. Codes were assigned by visual estimation of the arealy most abundant rock type. If the block was more than 50% sulphides it was coded as a sulphide type, otherwise the block was considered waste. One code is assigned per block and that code is assumed to apply homogenously to the entire block. The sectional codes were plotted, checked and edited for each section. The blocks in overburden or air were assigned from interpolated grids representing topography and bedrock surfaces based on digitized contour maps. Blocks more than 50% above topography were coded as air and more than 50% between topography and bedrock as overburden. One generic waste code was carried for the remainder of the model not coded as air, overburden or sulphide.

The rock types used in the Grum model are summarized in table 3.15. Since there is a large amount of low grade quartzose mineralization in the footwall of mineralized horizons at Grum

it was judged desireable to carry a separate code for base metal poor and base metal rich lithologies. This is inherrent in the lithologic codes of 4C and 4D however exactly the same distinction is made by the modifiers 4A0 and 4A4 (the latter being the base metal rich variant). A similar distinction was made between 4E0 and 4E4. The purpose of this distinction is to avoid undue averaging of grade into the footwall (and vice versa) and to improve modeling of the relatively sharp grade separation within mineralized horizons.

Sectionally assigned codes were applied to 2 columns of blocks on either side of the section. Since the Grum deposit plunges to the northwest this assignment would create a stairstep appearance in long section. By coincidence the diagonal of two blocks in long section is parallel to the deposit plunge thus a "plunge correction" was made by raising the first column of blocks one level (southeast of the section) and lowering the 4th column of blocks one level (northwest of the section). The second and third columns of blocks are kept the same. This has no affect on deposit reserves. All this block coding was done outside of PC Mine either using the Mintec Medsystem release 10 software package or by manual means. The block codes were reformated to suit PC Mine then imported.

DDH data was imported directly to PC Mine from Mintec output files after reformating but not used since composites were also imported from reformated Mintec output files.

Table 3.15

86-06 Mine Model Rock Type	Lithologic Code	Description
1	4A0	low grade, ribbon banded, graphitic, pyritic quartzite
2	4A4	high grade ribbon banded, graphitic, pyritic quartzite
3	4C	low grade pyritic quartzite
4	4D	high grade pyritic quartzite
5	4E0 & 4K	low grade massive pyritic sulphides (K = carbonate bearing)
6	4E4, 4J, 4F	high grade massive pyritic sulphides
7	4G	baritic massive sulphides
8	4H	pyrrhotitic massive sulphides
9	4L	mineralized altered wallrock phyllites
10	all waste	phyllite
11	overburden	gravel, sand & silt

3.3.4.3 Composite Calculation

Composites were calculated by Medsystem on a 4.5 m bench basis for holes steeper than 45°. For holes shallower than 45°, composites were based on 4.5 m horizontal intervals from the drillhole collar. Composite intervals can range from 4.5 m to 6.5 m depending on borehole orientation. Waste intervals less than 1/2 bench height (2.25 m) were considered internal waste and included in the composite interval. Intervals greater than 1/2 bench height were external waste and not included. This procedure was intended to accurately represent the grade of ore in blocks of all settings but does not automatically include all dilution in marginal composites. Such dilution adjustments must be made separately.

Drill hole assay data were clipped to the 95th percentile levels to avoid assigning unusually high assays to large blocks. These levels are listed in table 3.16. Intervals with no measured S.G. were assigned an SG depending on rock type as listed in table 3.17. These are based on statistical analysis of the measured data.

Composite calculation was carried out for the mineralized sections using this modified assay data and weighting by length and specific gravity. The length of the composite within a mineralized band was carried as well as the values since only the length of the mineralized part of an interval was composited.

Table 3.16

Maximum Permitted Assay Values and SG Values

Pb	11.0%
Zn	20.0%
Ag	175.0 g/tonne
Au	2.8 g/tonne
Cu	0.4%
Pulp SG	5.0

Table 3.17

SG Values Assigned For Each Major Ore Type
In Case of Missing Analytical data

Ore Type	SG
4A0	3.23
4A4/4AE	3.31
4B	3.00
4C	3.45
4D	3.53
4E	4.32
4G	4.42
4H	3.86
4J	3.87
4K	3.84
4L0	3.11
4L4/4LE	3.29

Table 3.18

Maximum Permitted Assay and SG
For DDH Composites

PB	9.00%
ZN	17.00%
AG	150.00 G/tonne
AU	2.30 G/tonne
CU	0.34%
PSG	4.80

The final composites can be as short as 0.1 m if only a small part of a mineralized band is within a composite interval. When the composites were imported to PC Mine the length data could no longer be carried. After calculation, the composites were also clipped to the 95th percentile level as outlined in Table 3.18. Every composite was manually checked against the cross-sections to insure that the codes applied to sectional units were consistent with the composite codes.

The modeling process up to this point is described in more detail in documentation of Cyprus Anvil's "G2" model produced in 1982 by P.I. Clarke and in 1984 by L.C. Pigage. Composite calculation was the last step carried out with Medsystem, the remaining calculations, reporting and analysis was done through PC Mine.

3.3.4.4 Variogram analysis:

Experimental variograms were calculated for the Grum composites in vertical, across deposit (model 000^0) and along deposit (model 090^0) directions. As was expected the variograms are generally ambiguous. Those for lead are shown in figure 3.13 to 3.15. The variogram analysis shows the range along the deposit is about 40 m and is greater than either vertically or across the deposit. The approximately 20 m across deposit range is uncertain but it can be argued that the along deposit range is about twice the across deposit. This conforms to what was expected on geologic grounds.

3.3.4.5 Interpolation:

The geostatisitcal analysis done was not adeqaute to use kriging as as interpolation method thus inverse square distance weighting was used following precedent set at Faro. The search volume was an ellipsoid with major axis of 150 m parallel to the deposit plunge and with a diameter in cross section of 106 m. The elipsoid centered on the block being interpolated thus the maximum distance a sample can be used to weight a block is 75 m. A horizontal and vertical anisotopy of 1.41 was used. This results in samples along trend being weighted twice as heavily as those across trend (with an anisotopy of 1.41 a sample 53 m across strike is weighted the same as one 75 m along plunge because the sample is treated as if it is 53 X 1.41 or 75 m from the block center, once this apparent distance is squared the factor of 2 ($= 1.41^2$) appears). A search volume radius much larger than the range was used in order to insure that the blocks in the less intensely drilled part of the deposit would get grades assigned. Multi pass interpolation used for the F8608 model was not available when the Grum model was built.

The most important test that a sample within the search volume must pass before being used to interpolate a block is the equivalance of geological codes. This is important in Anvil district deposits because of the strong ore type zoning and

TWO DIMENSIONAL VARIOGRAM

EXTRACTION DATA USED :

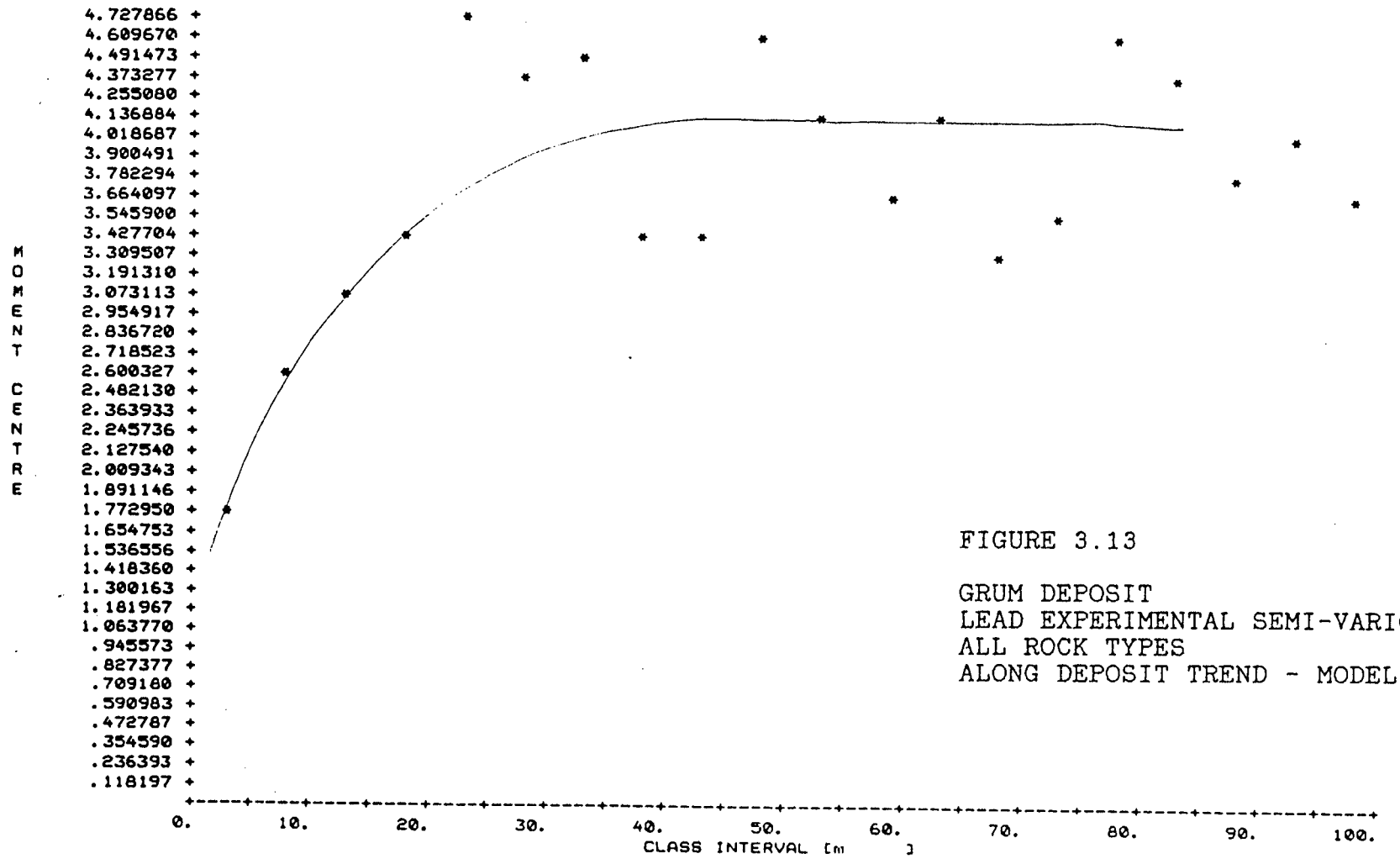


FIGURE 3.13

GRUM DEPOSIT
LEAD EXPERIMENTAL SEMI-VARIOGRAM
ALL ROCK TYPES
ALONG DEPOSIT TREND - MODEL 090

TWO DIMENSIONAL VARIOGRAM

EXTRACTION DATA USED :

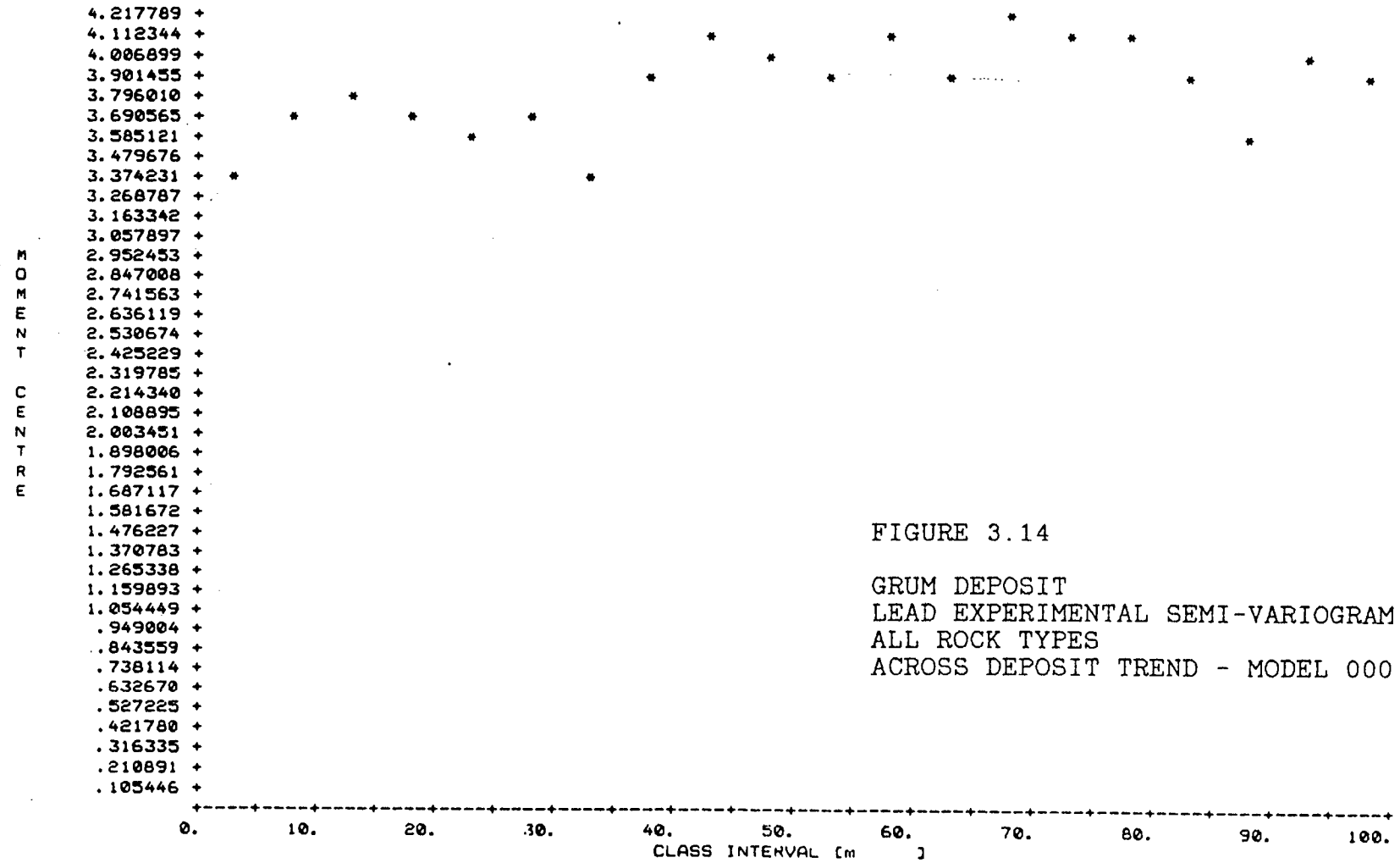


FIGURE 3.14

GRUM DEPOSIT
LEAD EXPERIMENTAL SEMI-VARIOGRAM
ALL ROCK TYPES
ACROSS DEPOSIT TREND - MODEL 000

THE SYMBOL "*" INDICATES LESS THAN 30 SAMPLES IN THAT CLASS

DOWN-THE-HOLE VARIOGRAM - SAMPLE DATA

BOREHOLE USED : AVERAGE FOR ALL SELECTED HOLES FOR LABEL NO : 2 Pb %

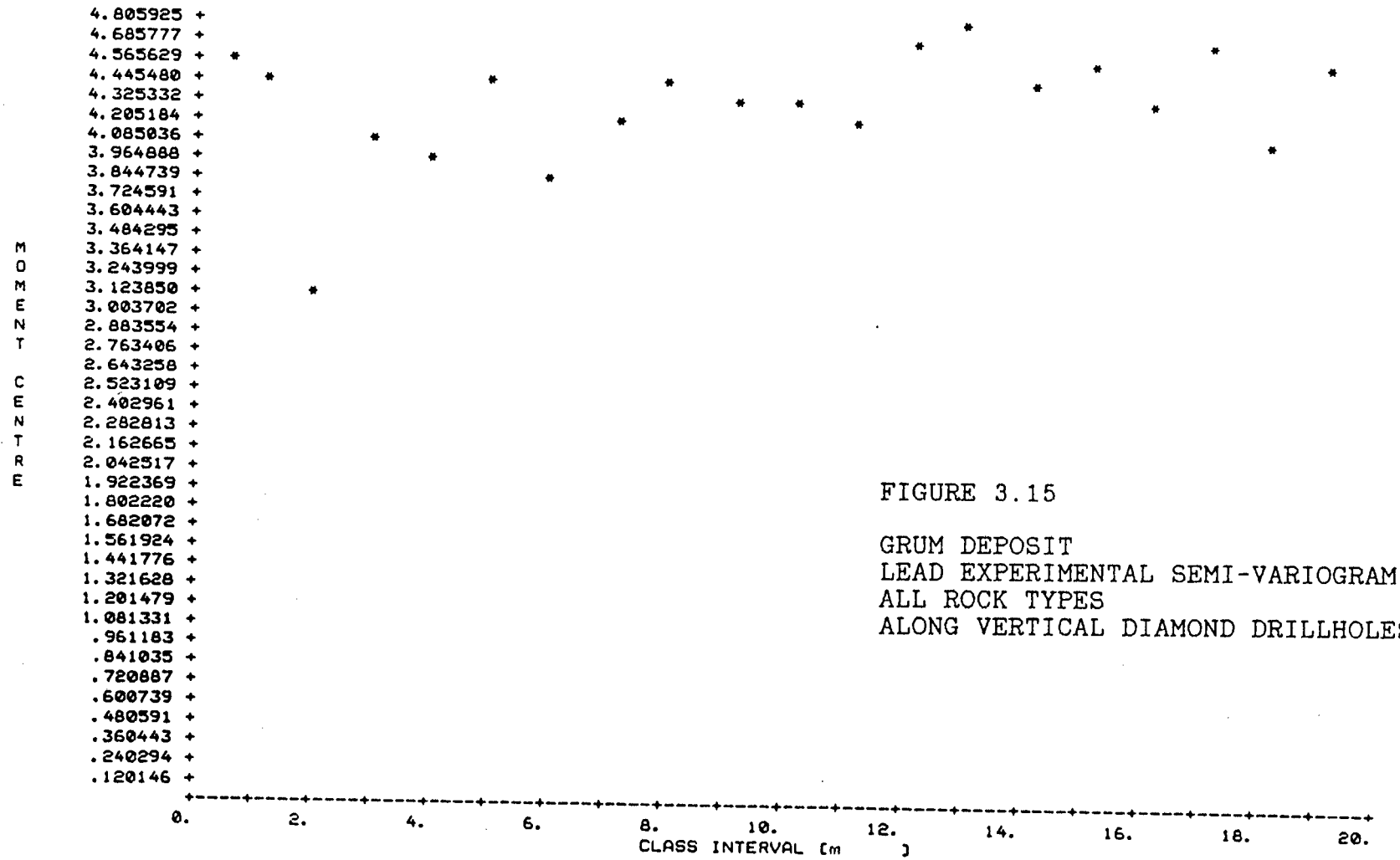


FIGURE 3.15

GRUM DEPOSIT
LEAD EXPERIMENTAL SEMI-VARIOGRAM
ALL ROCK TYPES
ALONG VERTICAL DIAMOND DRILLHOLES

THE SYMBOL "*" INDICATES LESS THAN 30 SAMPLES IN THAT CLASS

coupled grade zoning. The implications of this restrictive code matching for use of the model are very significant and discussed below.

The minimum number of composites required to interpolate a block was set at 2, the maximum at 8. The minimum limit was set to avoid the possibility that one very short composite could bias an entire block, the possibility that two very short composites could be used cannot be excluded however in most cases a very short composite will be near a longer one.

Specific gravity was interpolated in the same fashion as other assays. Uninterpolated sulphide blocks were assigned an SG of 2.7. SG was reduced by 5% in the final model in order to correct the pulp SG to in-situ whole rock SG. The average SG's for the Grum deposit are given with the geological reserves in tables 3.19 and 3.20.

3.3.4.6 Geological Reserve Reporting

Reserves were calculated by the weighted average of block values for all blocks that exceed an arbritrary % lead plus % zinc cutoff value. Geologic reserves are the sum of all blocks in the model below topography but irrespective of any pit outlines.

Since there are two Grum models the results of the two models were combined by a spreadsheet.

Sectional geological reserves were also computed for each cross section by reporting the reserves within a plan view polygon representing the area of influence of each section (± 30.5m from the section line). The sectional reserves were needed to compare to previous calculations which are largely sectional hand calculations.

3.3.5 Results

3.3.5.1 Geological Reserves

The geological reserves calculated for Grum are summarized in table 3.19 for the two constituent models and for the entire deposit. Sectional geological reserves are summarized in table 3.20 for the entire deposit.

Southeast of section 62W the Champ zone is estimated to contain a additional 1.7 milliion tonnes averaging 3.5% Pb, 4.3% Zn and 46 g/t Ag. This figure is based on sectional calculation and quoted at a 4% Pb+Zn cutoff with no adjustment to reflect dilution. Northwest of 86W there may be an additional 5 to 10 million tonnes of deep mineralization not yet completely drilled off.

3.3.5.2 Model to Model Comparisons

Table 3.21. and 3.22 A to D compare the newly calculated reserves (G8606 model) to previous calculations on a whole

TABLE 3.19

68606 MODEL GEOLOGICAL RESERVES FOR THE TWO CONSTITUENT MODELS
AND FOR THE ENTIRE DEPOSIT

GRADE CATEGORY	VOLUME (bcm)	S.G.	ORE (tonnes)	LEAD (%)	ZINC (%)	Pb + Zn (%)	SILVER (g/t)	GOLD (g/t)
ABOVE GRUM (1336.0 m to 1088.5 m)								
+6 %	4,677,480	3.37	15,765,300	3.84	6.50	10.34	64.0	0.92
4 - 6%	1,942,920	3.12	6,065,990	1.90	3.10	4.99	33.0	0.77
+4 %	6,620,400	3.30	21,831,290	3.30	5.56	8.85	55.4	0.88
UNDER GRUM (1088.5 m to 868.0 m)								
+6 %	1,880,820	3.75	7,057,100	4.04	6.36	10.40	68.5	1.18
4 - 6%	522,720	3.37	1,760,770	2.12	2.76	4.88	35.5	0.99
+4 %	2,403,540	3.67	8,817,870	3.66	5.64	9.30	61.9	1.14
TOTAL DEPOSIT (1336.0 m to 868.0 m)								
+6 %	6,558,300	3.48	22,822,400	3.90	6.46	10.36	65.4	1.00
4 - 6%	2,465,640	3.17	7,826,760	1.95	3.02	4.97	33.6	0.82
+4 %	9,023,940	3.40	30,649,160	3.40	5.58	8.98	57.2	0.95
COMPARISON TO CYPRUS ANVIL/DOME (SIMPSON - ADAMSON) HAND CALCULATION Uncorrected - see Tables 3.14 B and D								
+4 %	8,225,911	3.96	32,611,000	3.48	5.72	9.20	59	
VARIANCE new to old	9.7%x	-14.3%x	-6.0%*	-2.2%	-2.5%	-2.4%	-3.0%	

NOTES:

* Part of this difference in tonnage is due to uninterpolated blocks. There are 707 such blocks in under grum and 316 in above grum, not all of this material will be ore however. Each block represents about 1900 tonnes of material thus there is about 2,000,000 tonnes of un accounted for sulphides.

x The large variance in volume and specific gravity between the two calculations is explained in the text and the notes for Tables 3.22 B and D.

TABLE 3.20

GEOLOGICAL RESERVES BY CROSS SECTION FROM GB606 COMPUTER MODEL, 1986
TOTAL DEPOSIT, 4% Pb + Zn CUTOFF GRADE

SECTION	VOLUME	SPECIFIC GRAVITY	TONNAGE	LEAD	ZINC	SILVER	GOLD	Pb+Zn	TOTAL METAL
	(bcm)		(tonnes)	(%)	(%)	(g/t)	(g/t)	(%)	(tonnes)
86 W	684,180	3.09	2,116,210	2.60	4.99	46.0	0.44	7.59	160,592
84 W	584,820	3.16	1,849,610	2.80	4.90	47.6	0.60	7.70	142,432
82 W	787,860	3.40	2,680,540	3.19	5.55	56.5	0.84	8.73	234,069
80 W	1,297,080	3.35	4,340,270	3.10	4.85	51.8	1.05	7.95	345,081
78 W	975,780	3.27	3,195,500	3.16	5.50	54.7	1.04	8.66	276,762
76 W	907,200	3.36	3,048,860	3.49	5.80	58.6	1.07	9.29	283,135
74 W	1,013,040	3.45	3,498,640	3.72	6.20	62.3	1.05	9.92	347,146
72 W	748,440	3.45	2,584,690	3.64	5.77	61.2	1.02	9.41	243,256
70 W	694,980	3.52	2,449,940	3.86	6.57	63.6	1.04	10.43	255,415
68 W	355,320	3.70	1,314,260	4.10	6.27	66.7	1.00	10.37	136,297
66 W	442,260	3.69	1,632,190	4.14	5.75	66.7	0.99	9.90	161,507
64 W	301,860	3.61	1,091,070	3.79	5.52	61.2	0.99	9.30	101,466
62 W	178,200	3.69	657,640	3.39	5.03	54.8	1.10	8.42	55,347
	8,971,020	3.40	30,459,420	3.41	5.60	57.3	0.95	9.00	2,742,527

* The slight difference (0.1%) in tonnage between this figure and that on table 3.19 is due to a small amount of material outside the area limits set for the cross sections when computing these reserves.

deposit and sectional basis respectively.

Unfortunately the calculations listed in table 3.21 are not exactly comparable. The first 3 (A-C) are all based on Kerr-Addison's geological interpretation and assay data. The Cyprus Anvil computer models differs in that some new assay data was used but the bulk of the data was the same as A and B.

The last 2 (D & E on table 3.21) are based on the current geological interpretation and the current assay information which nearly completely replaces Kerr-Addison's data. These two calculations reflect some ore in the northwest part of the deposit that was drilled off in 1982, this amounts to about 3,000,000 tonnes largely of low grade material on sections 78W to 86W.

The early computer models did not use geologic control on interpolation which tends to average grade between disseminated and massive mineralization resulting in a larger tonnage of lower grade material than a comparable sectional calculation with sharp grade distinctions (compare A to B and C on table 3.21).

The G8606 model has attempted to counter this averaging effect by restricting the choice of composites to the same rock type as the block being estimated. The result is a closer comparison in grade to the corresponding sectional calculation (compare D to E on table 3.21). The G8606 model however was not able to assign a grade to every block due to the stringent matching requirements and local paucity of assay information. Thus there 1023 uninterpolated blocks representing about 2,000,000 tonnes of sulphides distributed through the deposit. Only a portion of this is likely to be over 4% Pb + Zn in reality but for the purposes of the current model all of it is assigned a zero grade and included as sulphide waste. Much of this material (about 700,000 tonnes in 423 blocks) is in the lower part of section 86W partly accounting for the poor comparison to the hand calculation on that section (table 3.22D). The distribution of uninterpolated blocks by section in the two constituent models is given in table 3.23.

A further complication in comparing the current model to the hand calculated reserves obtained from the same geological interpretation is that two problems were encountered with the Cyprus Anvil/Dome calculation: a) there were some calculation errors involving volumes above cutoff and to a lesser extent tonnes on sections 78W to 86W and b) the SG used for sections 82W-86W was assumed to be 3.6 (because assay data was not complete at the time the calculation was made)rather than the measured SG that was used for the rest of the deposit. In retrospect the assumed value was too high as much of the mineralization on those sections is considerably lighter. These points have been adjusted for in Table 3.22B. Table 3.22D shows the section by section variance between calculations. Between the Cyprus Anvil/Dome calculation and the current one the grade is almost always slightly down. In large part of this is

TABLE 3.21

COMPARISON OF PREVIOUS CALCULATIONS OF THE GEOLOGIC RESERVES TO THE FB608 MODEL
4% Pb + Zn CUTOFF GRADE

	CALCULATION		ORE (tonnes)	Pb (%)	Zn (%)	Pb+Zn (%)	Ag (g/t)	TOTAL METAL (tonnes)
A	KERR ADDISON - 1977 sectional hand calculation		26,083,000	4.1	6.4	10.5	62	2,738,715
B	KERR ADDISON / NORANDA - 1978 computer block model		27,650,000	3.1	4.9	8.0	48	2,212,000
C	CYPRUS ANVIL - 1981 "81" computer block model		30,781,000	3.1	4.9	8.0	49	2,462,480
D	CYPRUS ANVIL / DOME -1983 sectional hand calculation (uncorrected, see table 3.22)	*	32,611,000	3.5	5.7	9.2	59	3,000,212
D	CYPRUS ANVIL / DOME -1983 sectional hand calculation (corrected, see table 3.22)	*	31,615,000	3.5	5.7	9.2	59	2,918,065
E	CURRAGH RESOURCES - 1986 "FB608" computer block model	*	30,649,000	3.4	5.6	9.0	57	2,758,410

* Includes on the order of 2,000,000 to 3,000,000 tonnes of sulphides in the northwest part of the deposit drilled off in 1982 after the other calculations were done.

TABLE 3.22 A

RESULTS OF KERR ADDISON SECTIONAL CALCULATION, 1977
TOTAL DEPOSIT (both Vangorda Mines and AEX option) 4% Pb+Zn CUTOFF

SECTION	VOLUME (bcm)	SPECIFIC GRAVITY	TONNAGE (tonnes)	LEAD (%)	ZINC (%)	SILVER (g/t)	GOLD (g/t)	Pb+Zn (%)	TOTAL METAL (tonnes)
86 W	n/a	n/a	1,678,746	3.59	5.80	55.0	n/a	9.39	157,634
84 W	n/a	n/a	1,375,120	3.33	5.60	53.0	n/a	8.93	122,798
82 W	n/a	n/a	2,185,447	4.06	7.30	69.0	n/a	11.36	248,267
80 W	n/a	n/a	3,039,373	3.67	5.71	56.0	n/a	9.38	285,093
78 W	n/a	n/a	2,918,497	3.79	6.45	50.0	n/a	10.24	298,854
76 W	n/a	n/a	2,732,810	4.08	6.24	61.0	n/a	10.32	282,026
74 W	n/a	n/a	2,778,449	4.15	6.63	66.0	n/a	10.78	299,517
72 W	n/a	n/a	2,223,718	4.10	6.46	63.0	n/a	10.56	234,825
70 W	n/a	n/a	2,226,492	4.77	7.45	67.0	n/a	12.22	272,077
68 W	n/a	n/a	1,736,341	4.55	6.38	73.0	n/a	10.93	189,782
66 W	n/a	n/a	1,377,921	4.81	6.55	67.0	n/a	11.36	156,520
64 W	n/a	n/a	1,164,762	4.34	6.74	67.0	n/a	11.08	129,056
62 W	n/a	n/a	630,266	3.94	6.01	55.0	n/a	9.95	62,711
62W to 86W	n/a	n/a	26,067,842	4.07	6.43	61.50	n/a	10.51	2,739,161

TABLE 3.22 B

RESULTS OF CYPRUS ANVIL/DOME SECTIONAL CALCULATION (SIMPSON-ADAMSON), 1983
TOTAL DEPOSIT, 4% Pb + Zn CUTOFF GRADE

SECTION	VOLUME (bcm)	SPECIFIC GRAVITY	TONNAGE (tonnes)	LEAD (%)	ZINC (%)	SILVER (g/t)	GOLD (g/t)	Pb+Zn (%)	TOTAL METAL (tonnes)
86 W	997,045 *	3.23	3,221,532	2.88	5.21	49.0	n/a	8.09	260,622
84 W	776,317 *	3.20	2,486,855	2.86	4.83	48.0	n/a	7.69	191,239
82 W #	989,573 *	3.29	3,256,446	3.00	5.10	52.0	n/a	8.10	263,772
80 W #	1,118,740	3.38	3,783,293	3.31	5.41	56.0	n/a	8.72	329,903
78 W #	994,148	3.11	3,093,642	3.37	5.96	59.0	n/a	9.33	288,637
76 W	886,940	3.39	3,006,734	3.61	6.06	62.0	n/a	9.67	290,751
74 W	934,978	3.46	3,237,299	3.66	5.97	61.0	n/a	9.63	311,752
72 W	659,715	3.62	2,389,111	3.80	6.11	65.0	n/a	9.91	236,761
70 W	656,848	3.69	2,425,119	4.06	6.62	68.0	n/a	10.68	259,003
68 W	386,618	3.73	1,440,349	4.54	6.88	73.0	n/a	11.42	164,488
66 W	446,215	3.62	1,613,702	4.41	5.95	71.0	n/a	10.36	167,180
64 W	282,918	3.64	1,028,545	3.84	5.75	62.0	n/a	9.59	98,637
62 W	170,190	3.72	632,340	3.32	5.66	63.0	n/a	8.98	56,784
62W to 86W	9,300,243	3.40	31,614,967	3.49	5.74	59.1	n/a	9.23	2,919,529

* An assumed value for S.G.of 3.6 was used on these sections.
This is too high and has been reduced by 10% for comparison purposes.

\# Volumes above cutoff have been recalculated due to an error
in the original calculation.

TABLE 3.22 C

PERCENT VARIANCE OF GB608 (TABLE 3.20) TO KERR ADDISON (TABLE 3.22 A) [(NEW-OLD)/OLD]
TOTAL DEPOSIT, 4% Pb + Zn CUTOFF GRADE

SECTION	VOLUME	SPECIFIC GRAVITY	TONNAGE	LEAD	ZINC	SILVER	GOLD	Pb+Zn	TOTAL METAL
	(bcm)		(tonnes)	(%)	(%)	(g/t)	(g/t)	(%)	(tonnes)
86 W			26.1%	-27.6%	-14.0%	-16.4%		-19.2%	1.9%
84 W			34.5%	-15.9%	-12.5%	-10.2%		-13.8%	16.0%
82 W			22.7%	-21.5%	-24.0%	-18.0%		-23.1%	-5.7%
80 W			42.8%	-15.6%	-15.0%	-7.5%		-15.2%	21.0%
78 W			9.5%	-16.7%	-14.7%	9.4%		-15.4%	-7.4%
76 W			11.6%	-14.5%	-7.1%	-3.9%		-10.0%	0.4%
74 W			25.9%	-10.3%	-6.5%	-5.6%		-8.0%	15.9%
72 W			16.2%	-11.2%	-10.7%	-2.8%		-10.9%	3.6%
70 W			10.0%	-19.2%	-11.8%	-5.1%		-14.7%	-6.1%
68 W			-24.3%	-9.9%	-1.7%	-8.7%		-5.1%	-28.2%
66 W			18.5%	-13.9%	-12.2%	-0.5%		-12.9%	3.2%
64 W			-6.3%	-12.8%	-18.2%	-8.6%		-16.1%	-21.4%
62 W			4.3%	-14.1%	-16.3%	-0.3%		-15.4%	-11.7%
62W to 86W			16.6%	-16.3%	-13.0%	-6.8%		-14.3%	0.1%

TABLE 3.22 D

PERCENT VARIANCE OF GB608 (TABLE 3.20) TO SIMPSON -ADAMSON/DOME (TABLE 3.22 B) [(NEW-OLD)/OLD]
TOTAL DEPOSIT, 4% Pb + Zn CUTOFF GRADE

SECTION	VOLUME	SPECIFIC GRAVITY	TONNAGE	LEAD	ZINC	SILVER	GOLD	Pb+Zn	TOTAL METAL
	(bcm)		(tonnes)	(%)	(%)	(g/t)	(g/t)	(%)	(tonnes)
86 W *	-31.4%	-4.3%	-34.3%	-9.6%	-4.2%	-6.2%		-6.2%	-38.4%
84 W *	-24.7%	-1.3%	-25.6%	-2.0%	1.4%	-0.8%		0.1%	-25.5%
82 W *	-20.4%	3.4%	-17.7%	6.2%	8.6%	8.7%		7.8%	-11.3%
80 W *	15.9%	-1.0%	14.7%	-6.4%	-10.3%	-7.5%		-8.8%	4.6%
78 W	-1.8%	5.2%	3.3%	-6.3%	-7.7%	-7.3%		-7.2%	-4.1%
76 W	2.3%	-0.9%	1.4%	-3.3%	-4.3%	-5.5%		-4.0%	-2.6%
74 W	8.3%	-0.2%	8.1%	1.7%	3.9%	2.1%		3.0%	11.4%
72 W	13.4%	-4.6%	8.2%	-4.2%	-5.5%	-5.8%		-5.0%	2.7%
70 W	5.8%	-4.5%	1.0%	-5.0%	-0.8%	-6.5%		-2.4%	-1.4%
68 W	-8.1%	-0.7%	-8.8%	-9.7%	-8.9%	-8.7%		-9.2%	-17.1%
66 W	-0.9%	2.0%	1.1%	-6.0%	-3.3%	-6.1%		-4.5%	-3.4%
64 W	6.7%	-0.6%	6.1%	-1.4%	-4.1%	-1.3%		-3.0%	2.9%
62 W	4.7%	-0.7%	4.0%	2.0%	-11.1%	-12.9%		-6.3%	-2.5%
62W to 86W	-3.5%	-0.1%	-3.7%	-2.5%	-2.5%	-3.0%		-2.5%	-6.1%

* See explanation in text-comparison of models at 0% cutoff

probably due to the clipping of the extreme high end of the assay and composite population which was not done in the Cyprus Anvil/Dome calculation. The large variance in volume on sections 80W-86W is partly due to uninterpolated blocks but must be mainly due to differences in calculation method. The computer model interpolated grade into each block whereas the hand calculation averaged a large number of intersections to arrive at the grade for large panels of ore. In light of the relative paucity of drillhole information for some panels such large variances are not surprising. The interpolation method would be expected to give a more realistic picture of grade distribution.

A check on the volume of sulphides above 0% Pb+Zn grade shows that the volumes are essentially identical for the two calculations: 11,125,546 cu. m for the Cyprus Anvil/Dome versus 11,166,660 cu. m for the present model. The comparison for tonnage above cutoff for the two calculations with adjustment for a lower S.G. on sections 82W to 86W gives 37,415,941 tonnes for Cyprus Anvil/Dome versus 37,329,090 tonnes for the current model (the original Cyprus Anvil/Dome calculation using their S.G. gave 38,536,557 tonnes above 0%). Thus it is clear that the reserves only become inconsistent when a cutoff grade above 0% is used.

Table 3.15

UNINTERPOLATED BLOCKS IN G8608
GRUM COMPUTER MODEL

	86 W	84 W	82 W	80 W	78 W	76 W	74 W	72 W	70 W	68 W	66 W	64 W	62 W	TOT
Above Grum	32	1	1	32	19	4	8	21	62	74	46	12	0	312
Under Grum	423	23	38	52	54	23	13	36	10	14	1	0	0	687
Total	455	24	39	84	73	27	21	57	72	88	47	12	0	999

3.3.5.3 Reliability of Reserves

The reliability of geological reserves is a difficult matter to quantify at this time. The inadequate geostatistical knowledge of the deposit has precluded determination of block estimation variance. Thus quantification of overall deposit variance was not possible.

The density of drilling is sufficient to limit the possibility of major changes in deposit volume due to variance in interpretation. Volume ranges of ±10% would be possible. Variance possible due to calculation methods is also not quantified but changes of a few percent would be possible through adjustment of interpolation parameters such as anisotropy, weighting scheme and range and perhaps more by altering the geology matching scheme.

Based on the reproducability of geological reserve calculations for the Grum deposit and the central position of the current model in the range of values it is concluded that the geological reserves presented herein for the entire deposit are reliable within ± 10%, as such can be considered proven. Local reserves or bench reserves on the other hand can not be as reliable. In the vicinity of the dense drill pattern around the underground workings the local reserves are probably reasonably accurate however towards the periphery there is considerably more possible variance.

The earliest production comes from a long troughlike pit following the subcrop of the ore horizons. This part of the deposit is the most densely dilled from the surface but only the part southeast of 72W has been drilled from underground. The drill density is at least one hole every 30.5 m (100 feet) on 61 m (200 foot) spaced sections, close to the current density of Vangorda drilling. There is room for improvement especially in light of the complex structure involving steeply dipping ore layers. In general the earliest production is from an area that is only moderately reliable but it is underlain by highly reliable deeper reserves.

How well the reported reserves will relate to mill feed depends on the type and degree of dilution allowed. It is recommended to use a dilution of no less than 10% at zero grade with alternate dilutions ranging to about 25% at 3% Pb + Zn depending on the extent of low grade sulphide dilution experienced. As a starting point 15% at zero grade would be reasonable but sensitivity to dilution should be considered. As is the case for Faro dilution will be site specific and a constant average dilution will be an oversimplification.

The need to use a higher dilution than the historic 5% used for Anvil District deposits in the past is brought on largely by the restrictive geology matching during interpolation. This matching was not done previously thus the models tended to dilute themselves in unpredictable ways during interpolation. In order to present a more realistic portrayal of grade

distribution especially with respect to grade averaging into otherwise barren sulphides, particularly footwall sulphides, the modeling technique was changed. It is however necessary to change dilution practice at the same time. This was not done at Faro when using the FI model with the result that prdicted tonnages were far too low and grade far too high compared to blasthole indicated tonnage and grade.

The other major problem with the Faro FI model in the JB phase has been traced back to drillholes now known to be in the wrong place due to a survey error many years ago. This became apparent by comparing drillhole geology to pit geology. At Grum similar problems are not expected since more careful surveying has been done and survey calculations have been checked for errors; those found have been corrected. At Grum the drillhole collars are still present thus surveyed locations could be checked if desired. This was not the case at Faro.

3.3.6 Additional Work needed

The complex geology of the Grum deposit and its multi-horizon nature creates a great deal of difficulty in producing an interpretation that it is consistent from section to section. Horizons are indistiguishable from one another in drill core thus it is only the iterative process of section by section interpretation and comparison that can potentially solve this problem. The current interpretation has several inconsistencies that should be corrected. Additionally 60.5m spaced sections are too far apart and do not take account of all drillhole information available. A new interpretation is needed that will provide the basis for a better and more reliable model. 30m spaced sections should be made and longitudinal sections as well as cross sections should be interpreted in order to better portray fault problems. This interpretation has already been started and should be finished at the earliest possible date.

The Champ zone should be included in the overall deposit model since mining that area might influence the overall pit economics by lowering the main pit exit. Considering both zones together might enhance the economics of both.

The geostatistical treatment of Anvil District deposits has always been inadequate. This is largely due to the wide spacing of drill holes. At Grum the drill pattern is dense enough to produce meaningful analysis once the basic geologic data is organized by the above interpretation. Such analysis should allow better interpolation methods to be used than the simple inverse square method used to date.

One of the major inadequacies of geologic data at Grum is geotechnical data. There is reason to believe that the S_2 foliation under Doal Lake (in the northeast part of the proposed pit) may be dipping northeast rather than southwest. This could have significant implications for slope stability and the size of the area required to be pre-stripped. A program of oriented core drilling is required to evaluate this question. These

holes should also sample the overburden to evaluate its clay content and hydogeology. If the overburden is amendable to dewatering and can be kept dry then steeper slopes will be possible than in the current water saturated state.

There is little known geotechnically of the proposed waste dump sites; the foundation conditions in these areas should be studied.

More metallurgical work is required particularly on the 4A carbonaceous ore type. Its abundance at Grum could have a serious impact on mine reserves if an economic treatment scheme cannot be worked out. Separate consideration of the optimum grind for 4A should be given since in hand specimen 4A is not noticably finer grained than 2A (unlike the massive ores) and fine grinding exaggerates the problems of treating 4A. The northwest half of the ore in the first years pit will be almost entirely 4A.

The frequency distribution of specific gravity for Grum ores is strongly bimodal with modes corresponding to the quartzose and massive ores. Consideration should be given to the possibility of mechanical separation of the bulk of the ore types using this density contrast rather than relying on separation during mining.

It may be necessary to carry out fill in drilling in the area of early production to further delineate and detail bench reserves there. This work could be coordinated with the collection of metallurgical samples.

3.4 Vangorda Geology and Reserves

3.4.1 History

Vangorda was the initial discovery in the Anvil Range. The deposit was drill tested from 1953 to 1955 by Prospector Airways, a predecessor to Kerr Addison Mines. This drilling showed a significant deposit existed but a production decision was not warranted at that time. The deposit remained idle for the following decade. Minor additional drilling was done by Kerr Addison, largely for metaullurgical sampling, until the deposit was sold to Cyprus Anvil in 1979. Cyprus Anvil geologists examined the available drill core and concluded that it would be necessary to redrill the deposit to provide adequate material to re-evaluate it.

In 1979 the portion of the deposit from 2W to 12E was re-drilled with NQ core holes. Scattered core holes were put down in the southeast part of the deposit. Because of anticipated poor recoveries in this area it was judged advisable to drill this part of the deposit with rotary methods. This fill in drilling was done in 1981. Since 1981 no additional drilling has been done.

3.4.2 General Geology

3.4.2.1 Stratigraphy and lithology

The Vangorda deposit consists of one major sulphide horizon about 50 to 120 m beneath the basal carbonaceous member of the Vangorda formation. The host rocks for the deposit are dominantly non-calcareous phyllites, probably part of the Mt. Mye formation, however formational assignments near this deposit are ambiguous. The reason for the ambiguity is largely due to the strong wall rock alteration developed around the deposit. Most phyllites, especially in the deposit footwall, are bleached, locally silicified and/or chloritic and sulphide bearing.

A number of thin sulphide horizons occur above the main horizon; one at the base of the carbonaceous phyllites southwest of (stratigraphically above) the deposit may equate to the main horizon at Grum. In general these horizons are too thin or too low grade to be mineable.

3.4.2.2 Structure

The Vangorda deposit occurs in the hinge of a large second phase fold. Overall the deposit has the shape of a reclining M or a 3 in cross section, however there is considerable uncertainty in the details of fold morphology. The deposit is elongate in the northwest-southeast direction parallel to F_2 fold axes. It has been traced over a 1300 m X 200 m area.

The northwest half of the deposit plunges about 10° towards the northwest but the southeast half has a sub-horizontal plunge.

The S_2 foliation dips shallowly toward the southwest as at Grum but is locally quite variable.

The deposit is truncated by a steep normal fault at its northwest end. Many gouge zones were observed in drill core but the orientation of the structures responsible for them is not known. A number of faults parallel to S_2 are predicted. These are "required" to make the structure and stratigraphy fit. These low angle structures are best thought of as sheared out fold limbs, they are not generally gouge zones and will pose no more serious a problem for slope stability than the S_2 foliation itself and the myriad of small gouge zones that parallel it. Several analogous structures are thought to be present at Grum.

3.4.2.3 Deposit Geology

The deposit is quite shallow, in most places subcroping beneath glacial till. The till blanket is up to about 30 m thick in the northwest part of the deposit but thin in the southeast. Northwest of Vangorda Creek till cover is also quite thin. Locally the basal overburden and uppermost broken bedrock are cemented by iron oxides into a tough breccia.

The deposit consists of the same sulphide rock types as the other deposits but two types are particularly prominant. In the footwall (also the interpreted stratigraphic footwall) of the deposit is a sulphide rich quartzite (4C and 4EC). This quartzite grades downwards into siliceous phyllite and ultimately altered phyllite. Parallel to this downward decrease in silica is a downward decrease in the abundance of sulphides from quartz rich semi-massive sulphide (4EC) at the top to weakly pyritic altered phyllite at the base (4L). Most of the sulphides in the quartzite are pyrite, however pyrrhotite is generally present and locally abundant or dominant. Magnetite is unusually well developed in the quartzite. The quartzite contains only minor lead and zinc but is relatively rich in copper and unusually high in gold (see Table 3.24). The quartzite is similar to the semi-massive zone along the northeast edge of Zone 3 at Faro and one of the lower ore panels at Grum. From a reserve estimation point of view, The significance of the barren pyritic quartzite is that it is beneath and sharply delinated from high grade massive sulphides. For this reason it is important to restrict the selection of assay composites during grade interpolation to equivalent, geology otherwise excessive averaging of grade into the deposit footwall and lowering of the overall deposit grade will occur. Previous models of Vangorda have been subject to this averaging effect, resulting in a larger tonnage of lower grade than more selective calculations and creating the impression of ore deeper than it actually extends.

The massive sulphides that overlie the pyritic quartzite are commonly baritic and rich in lead and zinc. The unit is actually a mixture of about 50% 4E and 50% 4G ore types but separate treatment of pure types at Vangorda is not realistic from either the point of view of mining or the level of detail

carried in this model. Metallurgical predictions must take into account the mixed nature of this dominant ore type compared to the relatively pure samples on which test work was done. Of the mineralization exceeding 6% Pb & Zn, 90% is barite bearing massive sulphides (4EG). Most pyritic quartzite (4C and 4EC) is sulphide waste on the basis of lead zinc content (see Table 3.24).

Of the other sulphide rock types only 4A is of any importance. As is usual for these deposits it tends to be low grade and peripheral to the deposit. Much of the 4A is actually part of the upper horizon associated with the carbonaceous phyllite.

The shallow depth of burial of the deposit may create metallurgical difficulties because of oxidation. Early metallurgical work seemed to show this however later work done by Cyprus Anvil on fresh core achieved better results. The limited core observed by the writer was not visibly oxidized and oxidation is not extensively described in most drill logs below the first few meters of bedrock. Recoveries in massive sulphides are generally good except locally near Vangorda creek and in the southeast end of the deposit (at Faro oxidized massive sulphides yield poor core recoveries). In much of the southeast end of the deposit it is not possible to give recoveries based on recent drilling but old holes did not core well and it seems prudent to assume that the portion of the deposit southeast of 12E, where till cover is thin, will be oxidized. This could affect as much as 1,900,000 tonnes of baritic sulphide or 37% of the baritic sulphides in the geological reserves.

3.4.3 Drilling Density and Information Base

In the portion of the deposit from 2W to 12E there are 53 diamond drill holes in a 60 m X 30 m pattern. All holes are vertical and all are NQ diameter. Collar locations have been surveyed, checked and appear accurate. Assay intervals are 1.5 to 2 m long and are where possible are confined to one rock type.

In the remainder of the deposit there are 8 recent NQ or HQ drill holes but the bulk of the drilling (45 holes) is by rotary methods. The pattern is also 60 m X 30 m. There appears to have been a sampling problem with some of the rotary holes that has resulted in unreasonable assays. These holes have not been used in the current reserve calculation but they cast doubt on the remainder of the rotary holes. For this reason, where a Prospector Airways hole was also available and good recovery was obtained, the older hole has been used in preference to a rotary hole.

For most assay intervals there are Cu, Pb, Zn, Ag, Au., soluble (in hot HCl) Fe, insoluble Fe and BaO assays. Old diamond drill holes generally only have Pb, Zn and Ag. The newer assays are the same as those described for Grum.

The lead assays from the older holes are suspect because a correction for barium interference was not made.

3.4.4 Methods and procedure of reserve calculation

3.4.4.1 Introduction

The Vangorda deposit reserves were generated using a computer based 3D block model, the V8607 model, made during June and July 1986. The PC MINE software package was used for all stages of model construction.

3.4.4.2 Block geology and drillhole information

The model was generated using geologic control provided by 60m spaced cross sections. The cross sections were newly interpreted for this model in order to provide a uniform structural concept for the entire deposit. The assumptions used in cross section construction were:

1.) The deposit must fit the overall structural setting of this part of the Vangorda Plateau as defined by surface mapping and deep drilling nearby. This work shows that the deposit is in the hinge region of a large recumbent second phase fold.

2.) Stratigraphic facings implied by Anvil cycles were followed wherever possible. Of particular importance was the barren pyritic quartzite (units 4C and 4EC) which shows strong indications of being a footwall facies.

3.) Symmetric sulphide intersections were taken to imply folds.

4.) The dominant deformation episode would be the second phase implying a deposit shape similar to Grum but different from Faro.

Assumption 1 and 2 together require highly attenuated folds in order to produce a consistant interpretation. The resulting fold shapes are consistent with the deformation style observed in nearby outcrops on a small scale and with the inferred shapes of more closely controlled folds at Grum. All sections are included in supporting documents at Curragh's Toronto and Whitehorse offices.

At the density of drilling at Vangorda it is not realistic to produce interpretations that differ widely in deposit volume (changes in volume of ±10% to 15% may be possible due to interpretation) thus the current interpretation is adeqaute for long term planning even if there is disagreement on the treatment of structural detail.

The rotary drilling results in the southeast part of the deposit

proved to be difficult to interpret because the rock type logging was not as precise or reliable as the diamond drilled part of the deposit. As a result of this uncertainty in the base data there in more uncertainty in the geologic sections of this part of the deposit.

The cross sections were digitized and block assignments made by machine from digitized outlines. The logic used for block assignment is based on the geology at the center of a block. The block is assigned one geology code and the block is thereafter considered to be entirely that rock type.

Block size used was 4.5 m high, 4.5 m across strike and 10.0 m along strike. This is essentially the smallest block size practical that allows maximum resolution of geologic detail. Rows of blocks are parallel to the geologic sections. The same geological codes were applied to 3 rows of blocks on either side of a section so that the blocks are essentially 60 m long but each 10 m segment is treated separately for purposes of interpolation. There are 45 levels in the model extending from 1209.5 m to 1007.0 m elevation (1979 CAMC Datum).

Drill hole data was imported as ASCII files into the mine modelling system from the Hewlett Packard HP3000 based database for Vangorda drillhole information. A number of reformatting steps were needed.

3.4.4.3 Composite calculation

The assays were composited on the basis of geology with an attempt to conform to a 4 to 6 m length. This composite coding ensures that an interpreted geologic unit will only be assigned an assay from a length of drill core that was actually used to define the unit. In some cases these defined units will actually contain two or more different geological types but this simplification was necessary in order to produce units that would be reasonable from a mining point of view with the minimum number of necessary ore types. In general these mixed types are related for example: mixed 4E and 4G or mixed 4C and 4A. The minimum composite length was about 1 m. Internal waste was included in the composites at a 0% assay valve. Unlike most previous models, except the F4, bench composites were not used.

Assays were weighted by length of the sample but not by its specific gravity. Since composite intervals tend to be restricted to one ore type SG weighting would have relatively little effect. There was no "clipping" of assay valves to arbitrary maxima prior to compositing calculations.

3.4.4.4 Interpolation

Interpolation was done in essentially the same fashion as the Grum G8606 model described previously. Experimental variograms calculated from these composites showed only nugget effect due to the relatively large drill hole spacing. For this reason the anisotopy developed for Grum was used at Vangorda with a

slightly larger search volume.Search volume parameters were:

elongation: ~~model~~ 090° (ie: along deposit trend)
plunge: - 10° (ie: 10° northwest plunge)
horizontal anisotopy: 1.41
vertical anisotopy: 1.41
maximum range: 90 m (1.5 X section spacing)
minimum # composites used for a block :2
maximum # composites used for a block :8

Composites were weighted by the inverse square of the distance from the composite center to the block center. A composite could be used to interpolate a block only if its geologic code matched the code of the block being estimated.

These interpolation parameters allowed most of the blocks to be assigned a value. Two rock types proved difficult to interpolate, 2EH and 2E. Since there is relatively little of this material it was generally not possible to find 2 composites within a search volume. For these rock types the lower limit was reduced to one composite. Any remaining uninterpolated blocks (total of 97) were assigned an SG of 3.0 and grades were left at 0.0% (ie: the blocks do not get counted in reserves).

Specific gravity was treated as an assay and interpolated into blocks based on measured pulp SG of composite intervals. These SG's were determined by air pycnometer on assay pulps consequently do not account for void space. For tight quartzose ore types these SG's are high by about 5% and for vuggy, porous, massive ore types they are high by as much as 10% based on comparison of whole rock and pulp SG's done on Grum, Faro and Dy ores. In order to recast the SG data in terms of whole rock values the SG was reduced by 5% in the final model.

Geological reserves were computed by weighted average of block values between certain Pb plus Zn grades for all levels below topography.

3.4.5 Results

3.4.5.1 Geological Reserves

Geological reserves at a 4% and 6% Pb+Zn cutoff grade are summarized in Table 3.24. The results quoted are for all mineralization regardless of potential pit outlines. There has been no allowance made for dilution or mining recovery in the geological reserves.

3.4.5.2 Comparison of Geological Reserves

Two hand calculations have been done for the entire Vangorda deposit. Both are based on the old drilling and assays for the deposit. Table 3.25 compares these results to the present model.

The oldest one by Prospector Airways is based on the triangular

TABLE 3.24 GEOLOGICAL RESERVES FOR VANGORDA DEPOSIT FROM V8607 MODEL - NO DILUTION

rock type		% of ore type	tonnes (x1000)	density (tn/bcm)	Pb (%)	Zn (%)	Pb + Zn (%)	Ag (g/t)	Au (g/t)
PLUS 6 % Pb + Zn									
4A	1	7.1	382.33	2.81	3.17	4.66	7.83	39.74	0.68
4C	2	0.0	1.42	3.50	6.40	1.01	7.41	57.51	1.77
4EC	3	0.4	21.41	3.65	2.97	3.79	6.75	46.65	0.80
4E	4	0.1	4.16	3.43	2.57	4.12	6.69	46.50	0.63
4EG	5	90.8	4,917.88	3.96	4.51	5.83	10.34	64.03	0.75
4EH	6	1.7	90.23	3.65	6.82	5.05	11.87	83.15	0.54
TOTAL		100.0	5,417.43	3.88	4.45	5.72	10.17	62.55	0.74
4 % TO 6 %									
4A	1	58.6	1,194.40	2.83	1.86	3.02	4.88	26.48	0.46
4C	2	9.5	194.12	3.27	2.34	2.08	4.42	25.82	0.79
4EC	3	14.1	286.99	3.68	2.28	2.40	4.68	33.18	0.85
4E	4	10.2	207.58	3.76	1.90	2.87	4.77	37.94	0.14
4EG	5	6.7	137.28	3.75	2.47	2.76	5.23	36.96	0.76
4EH	6	0.9	19.13	3.78	2.43	2.95	5.38	34.31	0.41
TOTAL		100.0	2,039.51	3.16	2.01	2.81	4.83	29.30	0.53
MINUS 4 %									
4A	1	36.2	3,721.08	2.92	0.90	1.44	2.34	12.48	0.33
4C	2	42.8	4,393.21	3.27	0.79	1.00	1.79	14.50	0.65
4EC	3	17.9	1,842.51	3.67	1.33	1.34	2.67	21.57	0.94
4E	4	2.9	299.17	3.65	1.50	1.40	2.90	17.48	0.28
4EG	5	0.1	5.88	3.23	0.67	0.86	1.53	11.66	0.65
4EH	6	0.1	9.09	2.99	0.39	0.49	0.88	5.95	0.08
TOTAL		100.0	10,270.94	3.23	0.95	1.23	2.18	15.12	0.57
TOTAL DEPOSIT (all grades)									
4A	1	29.9	5,297.81	2.89	1.28	2.03	3.31	17.60	0.38
4C	2	25.9	4,588.75	3.27	0.86	1.04	1.90	15.00	0.66
4EC	3	12.1	2,150.90	3.67	1.47	1.51	2.98	23.37	0.93
4E	4	2.9	510.92	3.69	1.67	2.02	3.69	26.03	0.23
4EG	5	28.5	5,061.05	3.96	4.45	5.74	10.19	63.24	0.75
4EH	6	0.7	118.46	3.62	5.62	4.36	9.98	69.33	0.48
TOTAL		100.0	17,727.88	3.42	2.14	2.78	4.92	31.24	0.62
PLUS 4 %									
4A	1	21.1	1,576.72	2.83	2.18	3.42	5.60	29.69	0.51
4C	2	2.6	195.54	3.27	2.37	2.07	4.44	26.05	0.80
4EC	3	4.1	308.40	3.68	2.32	2.50	4.82	34.11	0.84
4E	4	2.8	211.75	3.75	1.91	2.90	4.81	38.11	0.15
4EG	5	67.8	5,055.17	3.96	4.45	5.74	10.20	63.30	0.75
4EH	6	1.5	109.36	3.67	6.05	4.68	10.74	74.60	0.52
TOTAL		100.0	7,456.94	3.68	3.78	4.92	8.71	53.46	0.69

method. The comparison to the present model is quite close. The large variance in lead grade is expected as it is known that the older lead assays were low probably because a correction for barium was not made. The areal extent of this calculation is not known but it may extend as far as 40E. The amount of ore in the far southeast sections (between 30E and 40E) is slight but this detracts from the comparison since the V8607 model only extends to 29E.

The Kerr Addison reserves are based on a sectional calculation by J. Paxton using sections between 4W and 30E by C.L. Smith in 1966.

These sections show unconnected enechelon pods of ore thus the tonnage should be lower than the current model where the assumptions outlined above imply the pods should be connected into fold patterns.

Previous computer models of Vangorda have only covered the northwest end of the deposit (2W-13E). For purposes of comparison to these models a separate reserve calculation was made for the area covered by these models. The results are given in Table 3.26 and 3.27.

As expected the current model reports higher grades but somewhat unexpectedly the tonnage is higher or comparable. This may be due to the fold interpretation used since zones that might be thought of as disconnected pods are connected into continuous horizons. The tonnage of the V8607 is higher than the 80-01 model (Table 3.27) because the volume of 4% material is about 10% higher, this tends to confirm the above inference and is within the realm of expected variance for the density of drilling.

3.4.5.3 Reliability of Geological Reserves

As a check on model computations, the areas of geological units output during digitizing of unit outlines was used to compute the volume of the overall deposit at a 0% combined cutoff grade. The average SG's of the ore types was used to calculate tonnes of mineralization. This calculation gave a total deposit tonnage of 18,921,000 tonnes compared to 18,660,930 from the block model (all these tonnages are prior to SG reduction), or 18,732,000 if the 97 uninterpolated blocks are included. No check calculation of the grades was done.

There was not sufficient time available to compute reserves with different sets of interpolation parameters. During test interpolation, increasing the degree of anisotopy tended to increase the spread in extreme block values. The effect on the average is not known but presumably above a given cutoff the average grade would increase.

On a small gold deposit modeled with PC Mine (P. Clarke, personal communication, 1986) changing only the anisotopy parameters from isotropic to about the same anisotopy used for

TABLE 3.25 EARLIER GEOLOGICAL RESERVE ESTIMATES FOR THE ENTIRE DEPOSIT COMPARED TO THE V8707

	tonnes (x1000)	density (tn/bcm)	Pb (%)	Zn (%)	Pb+Zn (%)	Ag (g/t)	Au (g/t)	total metal (tonnes)
PROSPECTORS AIRWAYS / CHISHOLM ET AL. (extent unknown - may be 4W to 40E)								
high grade (+4%?)	8,528	4.0 ?	3.16	4.96	8.12	60.33	0.69	692,474
low grade	11,431	----------	----------	not determined	----------	----------	----------	
total deposit	19,959							
KERR-ADDISON / PAXTON (recalculated to 3W to 29E)								
high grade (+4%?)	6,942	4.0 ?	-------nd---------		8.67	--------nd--------		601,871
low grade	9,139	3.5 ?	----------	not determined	----------	----------	----------	
total deposit	16,081							
THIS CALCULATION (3W to 29E)								
high grade (+4%)	7,457	3.68	3.78	4.92	8.71	53.46	0.69	649,224
low grade (-4%)	10,271	3.23	0.95	1.23	2.18	15.12	0.57	
total deposit	17,728	3.42	2.14	2.78	4.92	31.24	0.62	

TABLE 3.26 EARLIER GEOLOGICAL RESERVE ESTIMATES FOR THE NORTHWEST PART OF THE DEPOSIT COMPARED TO THE V8607 MODEL

	tonnes (x1000)	density (tn/bcm)	Pb (%)	Zn (%)	Pb+Zn (%)	Ag (g/t)	Au (g/t)	total metal (tonnes)	% variance (new-old)/old
79-09 MODEL (i.e. the Vangorda Plateau AFE model)									
high grade (+4%)	6,751	4.20	3.5	4.6	8.1	50.7		546,331	-11.4
low grade (-4%)									
total deposit									
60-10 MODEL (i.e. the V1 model)									
high grade (+4%)	5,209	3.83	3.3	5.2	8.5	54.5	0.65	441,608	9.8
low grade (-4%)	4,165								
total deposit	9,375	3.70							
KERR ADDISON / PAXTON (recalculated to 3W to 13E)									
high grade	4,906	4.00			8.6			420,796	15.2
low grade	5,831								
total deposit	10,738								
THIS CALCULATION (3W TO 13E)									
high grade (+4%)	5,471	3.59	3.9	5.0	8.9	55.6	0.72	484,718	
low grade (-4%)	5,695								
total deposit	11,166	3.39	2.4	3.1	5.5	36.7	0.74		

TABLE 3.27 COMPARISON OF COMPUTER MODELS FOR THE NORTHWEST PART OF THE VANGORDA DEPOSIT - V8607 TO 81-10 (or V1)

The 81-07 model was a computer based 3D block model based on more detailed geologic interpretation resulting in geologic bench plans rather than just sections. Block size was 12m X 12m X 6m. Measured S.G. was used.

	81-10 MODEL	86-07 MODEL	VARIANCE (NEW-OLD)/OLD
4.0 % CUTOFF			
TONNES	5209.5	5470.9	5.0
S.G.	3.77	3.59	-4.8
Pb (%)	3.31	3.88	17.1
Zn (%)	4.34	4.98	14.8
Ag (g/t)	47.8	55.6	16.3
Au (g/t)	0.74	0.72	-2.7
METAL (tonnes)	398.5	484.5	21.6
VOLUME (bcm)	1381.5	1524.6	10.4

NOTE: in both 3.27 there is some doubt as to the limit of the volume modeled to the NW. The 86-07 model is definitely quoted for 3W to 13E, the older model may only cover 2W to 13E or possibly 2W to 12E. In the former case the 86-07 tonnage would be about 35,000 tonnes too high, in the latter they would be about 160,000 tonnes too high. In the latter case the deposit volume and tonnage would be within 1%.

Vangorda and Grum increased the tonnage above cutoff by about 5% and the average grade above cutoff by 1 to 2%. This may have no relevance to Vangorda but it does give some idea of the effect of changing only computational parameters.

The above considerations along with concerns about the adequacy of drill spacing suggest that the reliability of Vangorda reserves is between ±10% to ±20%. Much of this uncertainty is due to the southeast part of the deposit where ±50% might be a more realistic estimate of possible variance to be expected.

When reporting reserves as mill feed it will be necessary to use a high dilution as at Grum.

3.4.6 Additional Work Required

The major shortfall in the work at Vangorda is the drill density. While the density may appear adequate in plan view the picture in section is another matter. On some sections holes have deviated away from one another creating a relatively large gap between the ore intersections. Some of these problems unfortunately occur where large proportions of the tonnage are inferred to exist.

The 200' X 100' drill pattern is probably adequate to define large deposits on a global basis however Vangorda is a small high grade target. Everything rests on the accuracy of the high grade reserves inferred to exist. The current drill density is not adequate to reliably predict the reserves of such a small body. Fill-in sections and fill-in holes on the current sections must be put down at the earliest possible time before final startup of the project. A staggered triangular pattern should be drilled rather than the current retangular pattern.

The question of reliability of the rotary drilled part of the deposit must be answered. Effort should be made to core this part of the deposit using large diameter core and heavy use of modern artificial mud ingredients.

Considerable metallurgical work on the fill-in drill core should be carried out in order to answer the question of the extent of oxidation of Vangorda massive sulphides, especially in the southeast part of the deposit.

Metallurgical work should be done on the mixed massive sulphide ore types used in the reserve definition rather than the pure logging ore types that previous work has been keyed to.

APPENDIX A

Geology and sulphide deposits of Anvil Range, Yukon

D.S. JENNINGS
Northern Dynasty Explorations Ltd.
Vancouver, British Columbia
and
G.A. JILSON
Curragh Resources
Whitehorse, Yukon

ABSTRACT

Anvil District is underlain by 5 km of polydeformed, late Precambrian to upper Paleozoic, metasedimentary and metavolcanic rocks intruded by a Cretaceous granitic plutonic suite. Most rocks of the district are almost certainly North American and have strong affinities with well-known Selwyn Basin stratigraphy representing the most southwestern (outboard) present-day examples. The uppermost unit, however, is suspect and may be allochthonous. The southwestern margin of the district is defined by two major faults separating it from adjoining terranes.

The Late Proterozoic and (?) Lower Cambrian Mt. Mye formation, monotonous, non-calcareous pelites at least 2 km thick, forms the basal stratigraphic unit in the district. Mt. Mye strata are correlated with unnamed, lithologically similar assemblages beneath Rabbitkettle Formation toward Mackenzie Platform northeast of the district. Calcareous phyllites and lesser basaltic extrusive and intrusive rocks of the Cambrian and Ordovician(?) Vangorda formation overlie the Mt. Mye with narrowly gradational contact. An important carbonaceous phyllite member occurs at the base of the formation. The 1 km thick Vangorda sequence is correlated with the more calcareous Rabbitkettle Formation eastwards toward Mackenzie Platform. A 1 km thick basaltic metavolcanic sequence named Menzie Creek formation overlies and is interleaved with Vangorda formation. Carbonaceous phyllites, slates and siltstones containing lower Ordovician to lower Silurian graptolite fauna are interbanded with the diverse Menzie Creek volcanic facies and overlie them. These metasediments are lithologically and faunally similar to strata of Road River Group with which the Menzie Creek is correlated. This lower portion of the Anvil district stratigraphic sequence represents deep marine sediments which accumulated on a trailing continental margin subject to episodic extensional tectonism resulting in the emplacement of the basaltic component of the section.

A thick (1 km) Devonian(?) to Permian(?) sequence of varicoloured, phyllitic cherts, chert conglomerate, and local stratiform barite capped by massive alkaline basalts occurs along the southwest edge of the district. This chert-rich sequence is in part similar to Earn Group, but the upper portion of this chert package and overlying basalts comprise the type section of Anvil Range Group. A distinct structural discontinuity between these sequences is not locally recognized, but regional relationships outside the district suggest Anvil Range Group, at least, formed in an oceanic basin outboard of North America and is allochthonous.

Anvil District has a complex polydeformational/polymetamorphic history. Two overlapping Mesozoic regional metamorphic and folding events are recognized in low pressure, Buchan-type facies series ranging from greenschist to amphibolite facies grade. Metamorphic zones decrease in grade radially outward and stratigraphically upward from a granite-cored central metamorphic/plutonic culmination termed Anvil Arch which domes the entire stratigraphic sequence into an open, doubly-plunging antiform. Subsequent events are regionally non-penetrative, brittle folding and faulting episodes superimposed on earlier fabrics. An episode of major extensional faulting may record the final stages of uprise of the plutonic core of the district.

Five stratifrom, pyritic lead-zinc-silver-(barite) deposits associated with anomalous thicknesses of graphitic phyllite are developed in a 150 m thick interval straddling the contact of Mt. Mye and Vangorda formations. The bulk of this mineralization occurs in uppermost Mt. Mye formation, but the highest horizons in multi-layered deposits are hosted by basal Vangorda formation. A pre-mining geological reserve of 120 000 000 tonnes of 3.7% lead, 5.6% zinc and approximately 45 - 50 g/tonne silver applies to the aggregated five deposits.

A cyclic arrangement of sulphide lithofacies is common in deposits of the district. Graphitic to non-carbonaceous, disseminated sulphide-bearing quartzites form the basal and/or marginal facies of a deposit which are succeeded upwardly and inwardly by massive pyritic sulphides, then baritic massive pyritic sulphides. This recurring facies arrangement may occur on the scale of an entire deposit cross section to a 1 m length of drill core. This idealized arrangement is commonly interrupted, truncated or imperfectly developed.

Sulphide deposits have a variably developed, white mica-dominant alteration envelope, commonly best developed in a deposit footwall. This alteration may represent hot ore fluid/wallrock interaction along the ore fluid pathway; a metamorphic reaction envelope between the sulphides and enclosing sediments or a combination of these origins. Demonstrable feeder zones for Anvil deposits are absent.

In plan, the known sulhpide deposits of Anvil district describe a northwest-southeast trending curvilinear array. Graphitic phyllites associated with the Mt. Mye/Vangorda contact thicken abnormally southwest of this deposit line. Additionally, the first major pulse of basaltic volcanism in the Anvil pile is recognized near this contact. These features taken together are consistent with a genetic model involving extensional tectonism, rifting and passive basaltic volcanism with episodic focussed exhalation of evolved, metalliferous, basinal brines along synsedimentary growth faults into local, reduced basins. Sulphide facies cyclicity may result from repetitively occurring physicochemical factors at the site of sulphide deposition, at the site of ore fluid evolution, or in the manner of ore fluid escape.

Introduction

The Anvil Range lead-zinc-silver district is located 200 km northeast of Whitehorse, Yukon (Fig. 1). There are five deposits with defined reserves in the district. Open-pit mining from Cyprus Anvil Mining Corporation's Faro deposit at rates up to 10 000 tonnes per day began in late 1969; this is the only deposit that has yet sustained production. The Anvil Mine constitutes

CIMM SPECIAL VOLUME 39 1986

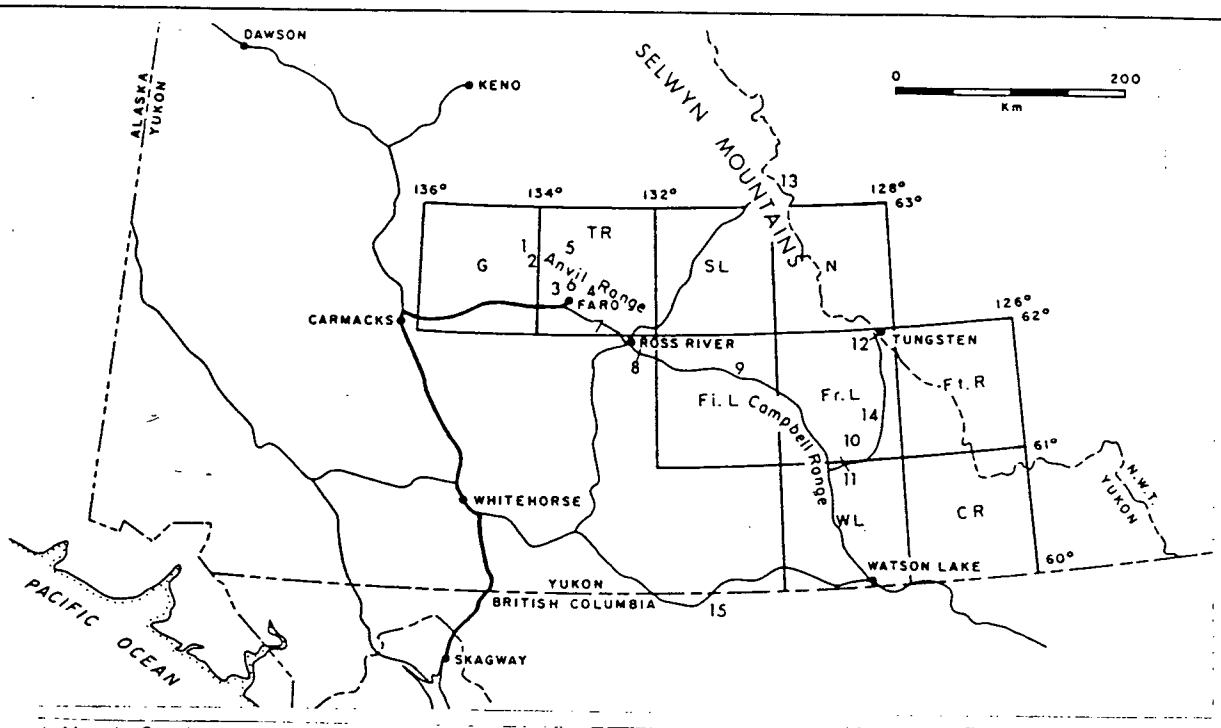


FIGURE 1. The southern Yukon showing the location of the Anvil Range and Anvil Mine (location 6) in relation to the Yukon highway system. The heavy line shows the route of concentrate shipment from the mine to tide water at Skagway, Alaska. Also shown are various localities and map sheets cited in the test.

Yukon's largest mining operation and is one of the largest lead-zinc-silver mines in Canada. Present remaining geological reserves for all five deposits in the district total 96 million tonnes of 8.9% combined lead-zinc with 51 g/tonne silver. In the district, there is an estimated total of 225 million tonnes of sulphide-bearing rock if all sulphide lithofacies are considered irrespective of grade.

These stratiform, stratabound, pyritic, massive sulphide deposits occur in a well defined curvilinear trend within a restricted 150 m thick upper Proterozoic to Cambrian stratigraphic interval straddling the boundary of the underlying Mt. Mye and overlying Vangorda formations. Discussion of the deposits is given in the context of a stratigraphic and structural analysis of the Anvil District. A synsedimentary, exhalative, genetic model consistent with Selwyn Basin evolution and lead isotope systematics is presented.

The first systematic geological mapping in the Anvil District was that of Roddick and Green (1961). After discovery of the Faro and Swim deposits in 1964-65, a more detailed geological study was undertaken by Tempelman-Kluit (1972). This work includes some descriptive detail on the Faro, Vangorda and Swim deposits.

Exploration methods in the District are discussed by Aho (1966, 1969), Brock (1973), Chisholm (1957) and Morton (1973).

Work on ore deposits of the district has not been extensive. An early study on the Faro deposit is that of Campbell and Ethier (1974). The Grum Deposit, particlarly the sulphide isotopes of the ores, has been studied by Modene (1982).

Several studies have included Anvil District ores within a larger context: Le Couteur (1973), Kuo (1976), Kuo and Folinsbee (1974), Godwin and Sinclair (1982) and most recently, McClay and Ellis (1983).

This study is the result of work in the district by the authors and many co-workers during the period 1971-1983.

Regional Geology

The ore deposits of the Anvil District formed in the shale-rich, outboard, portion of the early Paleozoic - late Proterozoic North American miogeocline. The local basin of interest is Selwyn Basin (Fig. 2), a major northeasterly convex embayment in the present-day distribution of peri-cratonic platformal carbonate and orthoquartzite strata of Mackenzie Platform, coeval with the basinal shales. Selwyn Basin passed through several evolutionary stages which are reflected in the basin filling sediments as large-scale compositional sequences.

The basin appears to have been initiated by complex Proterozoic rifting which formed the ancient continental margin (Eisbacher, 1981). The oldest unit exposed (in the basin) is the late Proterozoic to early Cambrian "Grit Unit" (Gabrielse *et al.*, 1973). This unit consists of turbidites (Gordey, 1979) and can be viewed as a huge fining upward sequence of coarse, poorly sorted, quartz + feldspar, sandstone and pebble conglomerate with interbedded shales. Locally important interbedded limestone and dolomite is developed in the upper part of the unit, and minor mafic volcanics occur locally. The shale component is commonly drab olive green, but a belt of red and green shale near the top of the unit runs the length of the southern part of the basin (Fig. 2). The varicoloured shales are co-extensive with, but largely younger than, a belt of the largest limestone and dolomite bodies. The shales of the red and green belt change gradually through maroon and green into dark grey shales (largely the Phyllite Unit of Gabrielse *et al.*, 1973) to the northeast and the uppermost shales intertongue with the sandstones of the Backbone Ranges Formation (Gabrielse *et al.*, 1973). To the southwest of the red belt, the shales appear also to grade laterally through maroon into grey colours but there is little exposure of this interval.

The shales at the top of the "Grit Unit" pass upwards into early and middle Cambrian drab brown and black shales (Gordey,

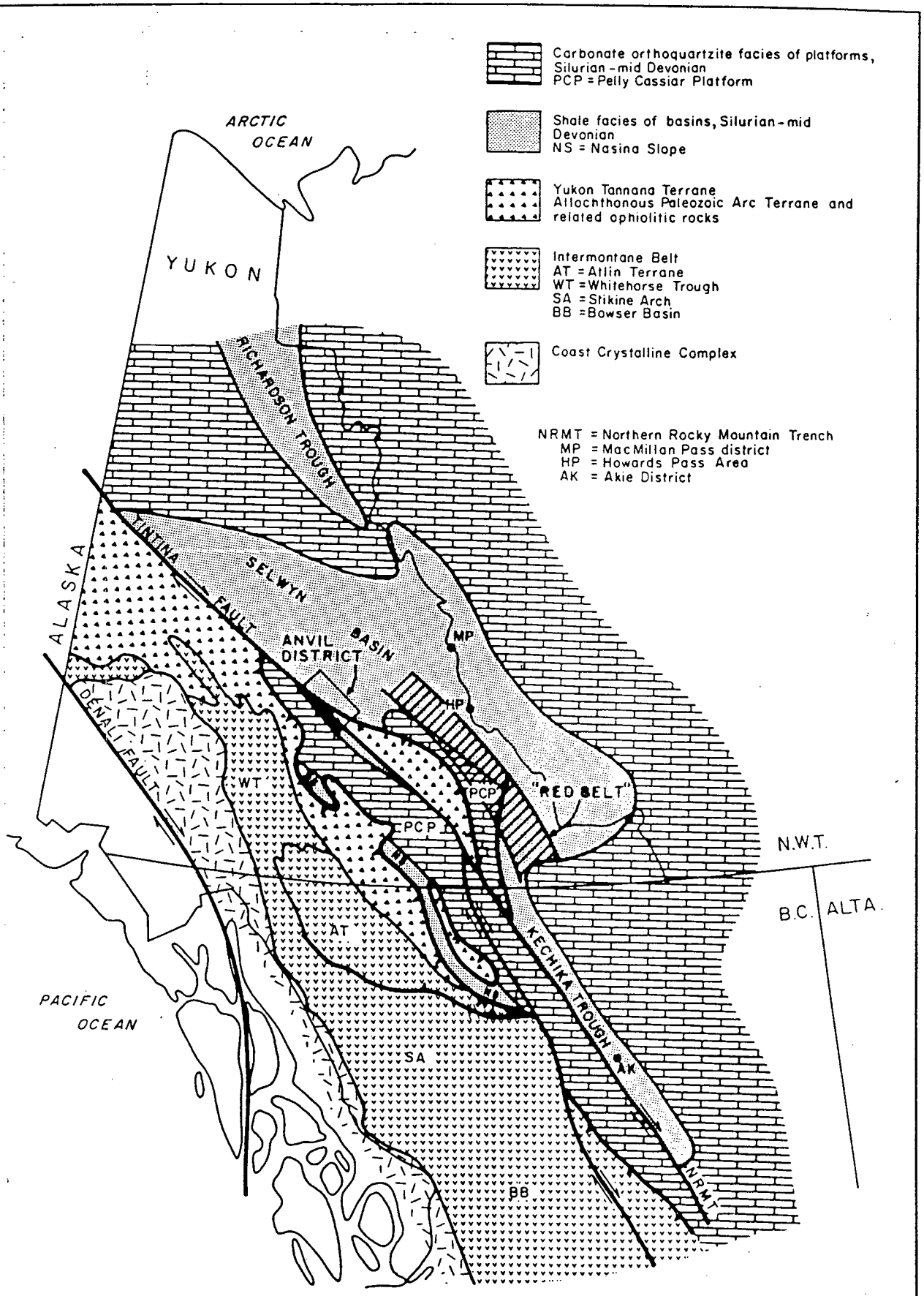


FIGURE 2. The Anvil District in relation to the Selwyn Basin and other major tectonic features outboard of platformal carbonates and basinal shales of strong North American affinity. The "red belt" shows the distribution of red shales and large carbonate bodies in the upper Grit Unit based largely on mapping by the authors and co-workers.

Legend

Tertiary – Paleocene?

Tsv	basalt, quartz feldspar porphyry, sandstone, conglomerate, shale
Ts	conglomerate, sandstone
Tv	rhyolite plug

Cretaceous

Ki	Anvil Dyke Suite: diorite, quartz diorite, quartz feldspar porphyry
Kgr	Anvil Plutonic Suite: granodiorite, quartz monzonite

Triassic (and younger?)

Tr	polymict conglomerate, micaceous quartz sandstone, greywacke, black shale, limestone (Tr? may be younger and uncomforably overlie Tr)

Permian and older

uYTT	undifferentiated rocks of Yukon Tanana Terrane: micaceous quartzite, gritty micaceous quartzite, black phyllite, marble, metabasite, felsic metavolcanics, phyllitic chert

Pennsylvanian and Permian (and older?)

PPc	calcitic and dolomitic marble, limestone

age unknown: upper Paleozoic? (associated with PPa)

mi	mafic intrusive rocks: gabbro, diabase
um	ultramafic rocks: serpentinite, harzburgite, rodingite, quartz carbonate fuchite altered ultramafics

Pennsylvanian and lower Permian?

PPav	Anvil Range Group: basalt
PPat	Anvil Range Group: red and green chert, tuffaceous chert

Devonian and Mississippian

Mk	Kalsas Formation: limestone
uDM	Earn Group: chert, siltstone, shale, chert pebble conglomerate, barite (uDM+: probably includes older rocks and some younger)

Ordovician to Devonian?

S q	quartzite (age unknown, could belong to uDM locally)
SD a	laminated dolomitic quartz siltstone, dolomite, quartzite, dark grey shale (resembles basal Askin Group and lower Earn Group)
SD s	black phyllite with middle Devonian limestone lenses (may belong entirely in lower Earn Group)
OSrr	black and grey slate, quartzite, minor dolomite (may equate partly to Road River and older rocks - probably partly equivalent to SDs and SDa

lower Ordovician (and younger?)

Omc	Menzie Creek formation : basalt, black phyllite

Cambrian to lower Ordovician (?)

€Ov	Vangorda formation: calcareous phyllite, metabasite, calc-silicate (€Ov+ includes H€mm locally or Omc locally)

lower Cambrian and Hadrynian (?)

H€mm	Mt Mye formation: noncalcareous phyllite and schist

FIGURE 3. Geological map of the Anvil District. The major sulphide deposits are indicated in black. Section C-D is Figure 19. See Figure 20 for location of additional cross sections.

1978 and 1979; Blusson, 1966). This sequence appears to thin over the red belt and is easily distinguished from the underlying "Grit Unit" shales in that area, but to the southwest and northeast, the sequence is thick and difficult to separate from the "Grit Unit". A widespread archeocyathid-bearing limestone conglomerate (Gordey, 1978) apparently derived from the earliest Paleozoic shallow water carbonates of the Mackenzie Platform occurs in this sequence.

In southeastern Selwyn Basin, the next major compositional unit is the thin banded, medium grey, silty argillaceous limestone of the upper Cambrian to lower Ordovician Rabbitkettle Formation (Gabrielse *et al.*, 1973). This sequence is best developed east of the red belt of the "Grit Unit" where it is very thick and dominantly limestone. Over the red belt, the sequence is thin and to the southwest, it is shale-rich and recessive; it is commonly represented there by calcareous phyllite. An important unconformity is present at the base of this sequence east of (Gabrielse *et al.*, 1973; Gordey, 1979) and probably above the red belt of the "Grit Unit" but there is no evidence of the unconformity to the southwest where exposure is poor.

In middle Ordovician, episodes of mafic volcanism occurred locally around and within Selwyn Basin (Gabrielse *et al.*, 1973; Cecile, 1982), accumulating to considerable thickness at several places. At about the same time, the basin filling sediments became black and chert rich. This carbonaceous sequence characterizes the basin until mid-Devonian and is largely known as the Ordovician and Silurian Road River Group and early and middle Devonian Basal Earn Group (Gordey *et al.*, 1982).

From late early Silurian to middle Devonian, a belt of shallow water limestone, dolomite and quartz sandstone accumulated along the present southwest edge of Selwyn Basin just outboard of and sub-parallel to the former red belt of the "Grit Unit". These are the sediments that characterize the Pelly-Cassiar Platform (Fig. 2). Between this platform and the Mackenzie Platform facies equivalent dark shale and chert and lesser dolomitic siltstone continued to be deposited in Selwyn Basin (Gordey, 1979).

In late Devonian and Mississippian, an episode of extensional tectonism disrupted this segmented basin and intrabasinal or westerly derived chert and quartz-rich coarse clastics accumulated interbedded with black shale and chert (Gordey, 1979). These sediments form the upper part of the Earn Group (Gordey *et al.*, 1982).

A Mississippian through Triassic sequence including shale, sandstone, siltstone and chert succeeded the Earn Group. These sediments are not conspicuously dark coloured and mark the return of aerated conditions to the basin (Gordey *et al.*, 1982 and Gordey, pers. comm., 1984).

The Anvil deposits are associated with carbonaceous phyllites within a transition from strata of the second and third sequences outlined above. In the Anvil District, strata of the second sequence are represented by the Mt. Mye formation, largely non-calcareous phyllite and schist, and the third sequence by the Vangorda formation, largely calcareous phyllite and metabasite. Basalt and carbonaceous phyllite of the Menzie Creek formation represents one of the largest centres of mafic volcanism associated with the fourth sequence. Other major lead-zinc deposits in the vicinity (Howards Pass and Macmillan Pass, Fig. 2) occur within the younger, black, shale-rich sequences.

The district is part of the Omineca Crystalline Belt, the easterly of two major granitic and metamorphic welts that run the length of the Canadian Cordillera (Monger *et al.*, 1982). In the area, the Omineca Belt is a series of uplifts exposing polydeformed and metamorphosed equivalents of the older parts of the stratigraphy outlined above. The uplifts are cored by 100 Ma, late to syn-kinematic granites and are commonly partly bounded by extensional faults. The Anvil Batholith (Fig. 3) is one of the larger of these granitic bodies. The complex structural and metamorphic history of the district has had a profound effect on textures and structures of its ore deposits.

The Anvil District is just inboard of one of the larger suspect terranes of the Yukon, the Yukon Tanana Terrane, (Coney *et al.*, 1980) and because of its complex tectonic history, should be considered as a possible suspect terrane itself. The strong similarities between the lower parts of the structural/stratigraphic sequence of the district and well known Selwyn Basin stratigraphy argues against this possibility. Although rocks of the district may be allochthonous (Gordey, 1983) or displaced, such translation is probably not large. The uppermost unit of the district, basalt and chert of the Anvil Range Group (Tempelman-Kluit, 1972), however, does not fit well into Selwyn Basin stratigraphy and appears to be an allochthonous exotic oceanic assemblage. The Yukon Tanana Terrane is faulted against the Anvil District sequence along the Vangorda Fault (Fig. 3). This structure is thought to be part of a transpressive suture developed during oblique collision of the Yukon Tanana Terrane with the North American continental margin (Mortensen and Jilson, 1985) which initiated the metamorphism and deformation of the district and culminated in intrusion of the Anvil Batholith (Tempelman-Kluit, 1979).

One of the most prominent of the longitudinal lineaments of the Canadian Cordillera, the Tintina Trench, passes just southwest of the district. The Trench is the locus of the late Cretaceous or early Tertiary right lateral strike-slip fault with 450 km to 500 km displacement (Tempelman-Kluit, 1970a). The association of this lineament with the district is thought to be a consequence of it having been controlled by a major crustal weakness that has repeatedly exerted its influence over the evolution of the district. We speculate below that the oldest example is the control over ancient faults that bounded sub-basins, channeled ore fluids and resulted in the linear array of ore deposits we see today.

Stratigraphy

Introduction

The stratigraphic sequence of the Anvil District ranges from latest Precambrian to Permian. The ore deposits occur within a 150 m thick section of the pre-Ordovician part of that sequence. This study consequently focusses on the lower portion of the sequence.

Three informal formational names are used to describe the Ordovician or older strata of the district (Fig. 4).

Mt. Mye Formation

Introduction

The Mt. Mye formation is the oldest map unit in the district. Drilled intersections and cross sections suggest an approximate thickness of at least 2 km. Excellent exposures of Mt. Mye formation are found on the south slopes of Mt. Mye northeast of the Vangorda and Dy deposits and between the Grum and Faro deposits along the access road to the Anvil Mine (Fig. 5). Lower portions of the formation occur in the core of Anvil Arch northeast of Blind Creek (Fig. 5). The formation crops out widely near Tay Mountain (Fig. 1).

Lithology

The two dominant rock types of the formation are non-calcareous biotite, muscovite, quartz, plagioclase, ± garnet, ± staurolite schist in areas of amphibolite facies metamorphism and non-calcareous muscovite, chlorite, quartz, plagioclase phyllite in areas of lower grade metamorphism. Important interlayered rock types are: (a) carbonaceous, muscovite, quartz phyllite; (b) calcitic marble and limestone; (c) thinly banded diopside, quartz, plagioclase, biotite ± calcite calc-silicates; and (d) weakly to strongly foliated actinolite, chlorite ± calcite schists and amphibolites or metabasites.

The typical non-calcareous phyllite of the Mt. Mye is medium to dark medium grey and weathers rusty brown with a rust flecked foliation surface. The rocks are commonly banded with dark grey micaceous folia 1 mm to 10 mm thick separating lighter grey finely crystalline quartz-rich layers two to five times thicker. In general, the unit has smaller and less well developed lithon structure than the overlying Vangorda formation. Soft, homogeneous, mica-rich phyllites are also widespread in the unit.

GENERALIZED GEOLOGICAL MAP OF THE ANVIL LEAD-ZINC DISTRICT CENTRAL YUKON TERRITORY

MAPPED BY: D.S. JENNINGS & G.A. JILSON 1971-1979, 1980, 1983; L.C. PIGAGE 1979, 1980; J.B. HESLOP 1971, 1972; P.F. LEWIS 1972-1974; D.J. HANSEN 1977-1978; J.P. FRANZEN 1978;

ymbols

- contact
- sulphide deposit
- strike slip fault
- normal fault, ball on downthrown side
- moderately or shallowly dipping fault of unknown sense of displacement
- thrust fault
- form line of S_2 foliation, or in uYTT form line of flaser fabric; (former dip mostly less than 45°, latter mostly more than 45°)
- bedding strike and dip direction (mostly 45° or less)
- axis of antiform
- e eclogite locality

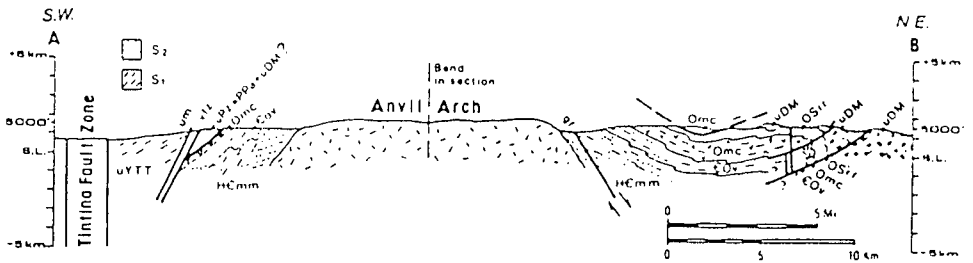
Faults

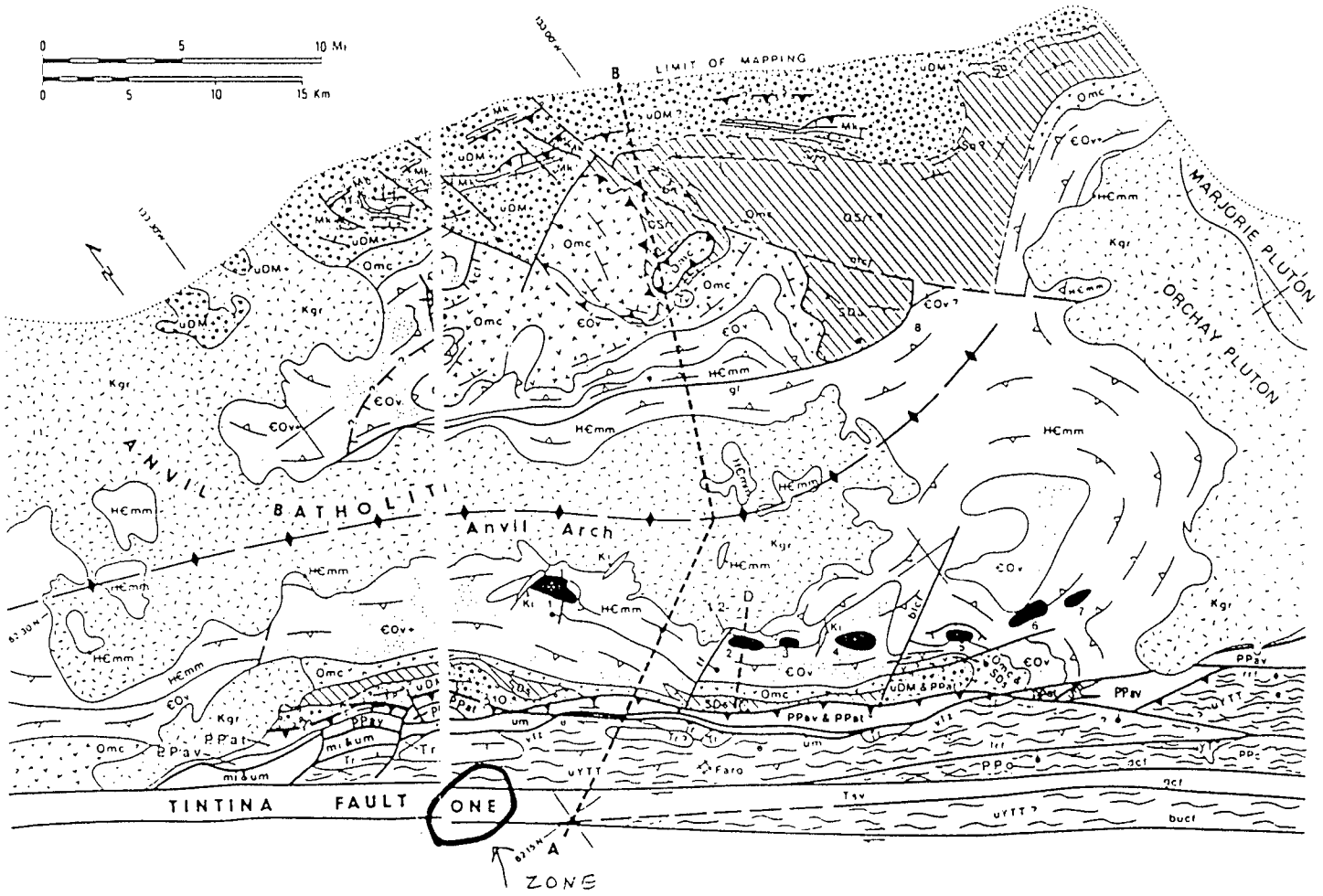
- vfz : Vangorda Fault zone
- tf : Tie Fault
- ilcf : Blind Creek Fault
- mcf : Mye Creek Fault
- gf : Graphite Fault
- kcf : Klunk Creek Fault
- lrf : Lapie River Fault
- bucf : Buttle Creek Fault
- gcf : Grew Creek Fault
- dcf : Danger Creek Fault
- rrf : Ross River Fault

Strands of Tintina Fault

Mineral Occurrences & Sulphide Deposits

1.	Faro	Zn, Pb, Ag, Au, Cu; stratiform
2.	Grum	" "
3.	Vangorda	" "
4.	Dy	" "
5.	Swim	" "
6.	SB	Cu, Zn, Fe; stratiform
7.	Sea	Cu, Zn, Fe; stratiform?
8.	Ace	Cu, Zn, Fe; stratiform
9.	KD	Zn, Cu; volcanogenic stringer?
10.	Urn	barite, stratiform
11.	Dana	Zn, Pb, Cu, Ag; replacement?
12.	FIRTH	ZnPb, modified stratiform





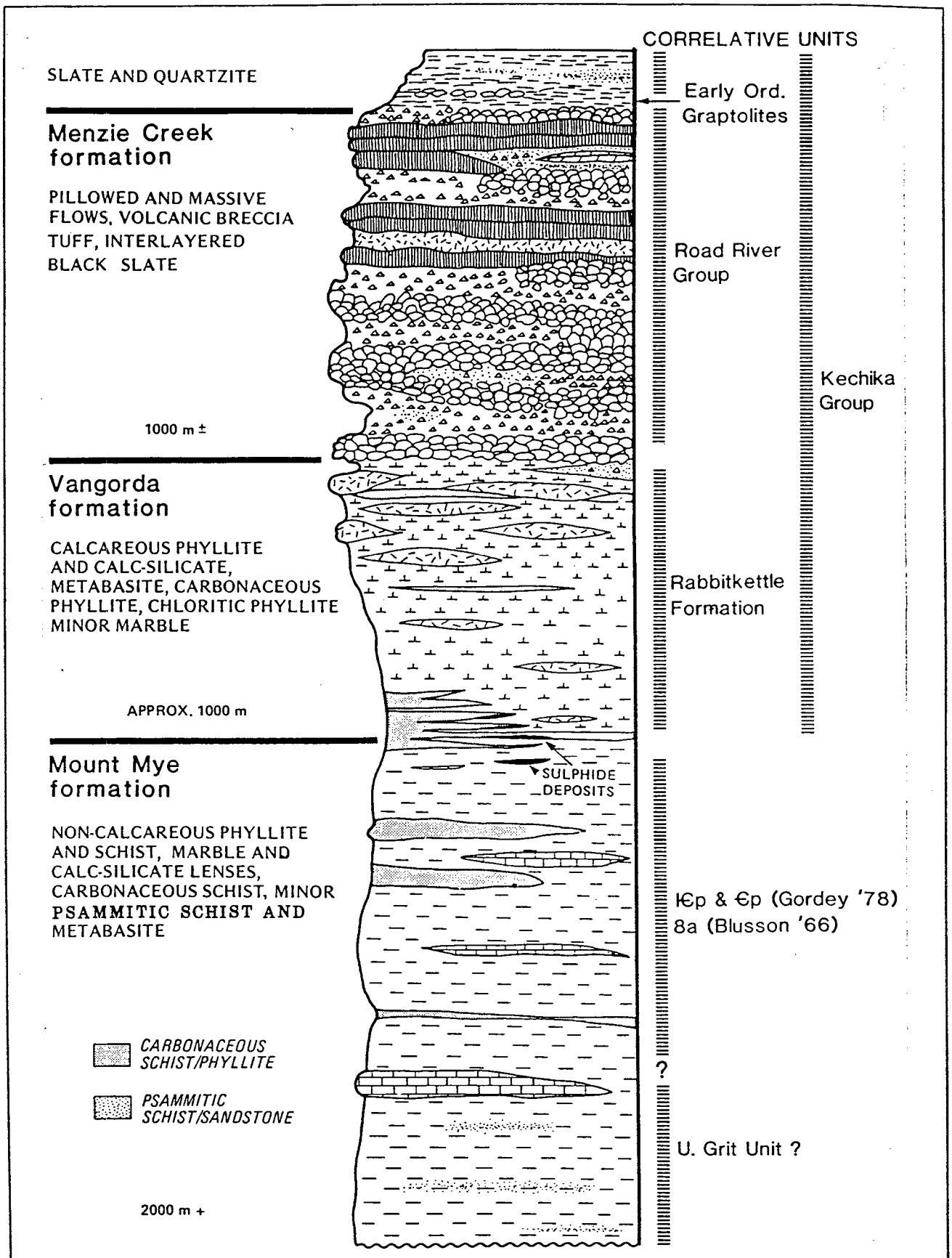


FIGURE 4. A schematic column of the older portion of the stratigraphy of the Anvil District. The sulphide deposits consist of several horizons in the upper Mt. Mye and lower Vangorda formations. The thickening of carbonaceous phyllite near the ore deposits is represented as if viewed looking northwest. The over-all section is rich in mafic volcanic and subvolcanic material but most is younger than the ore deposits.

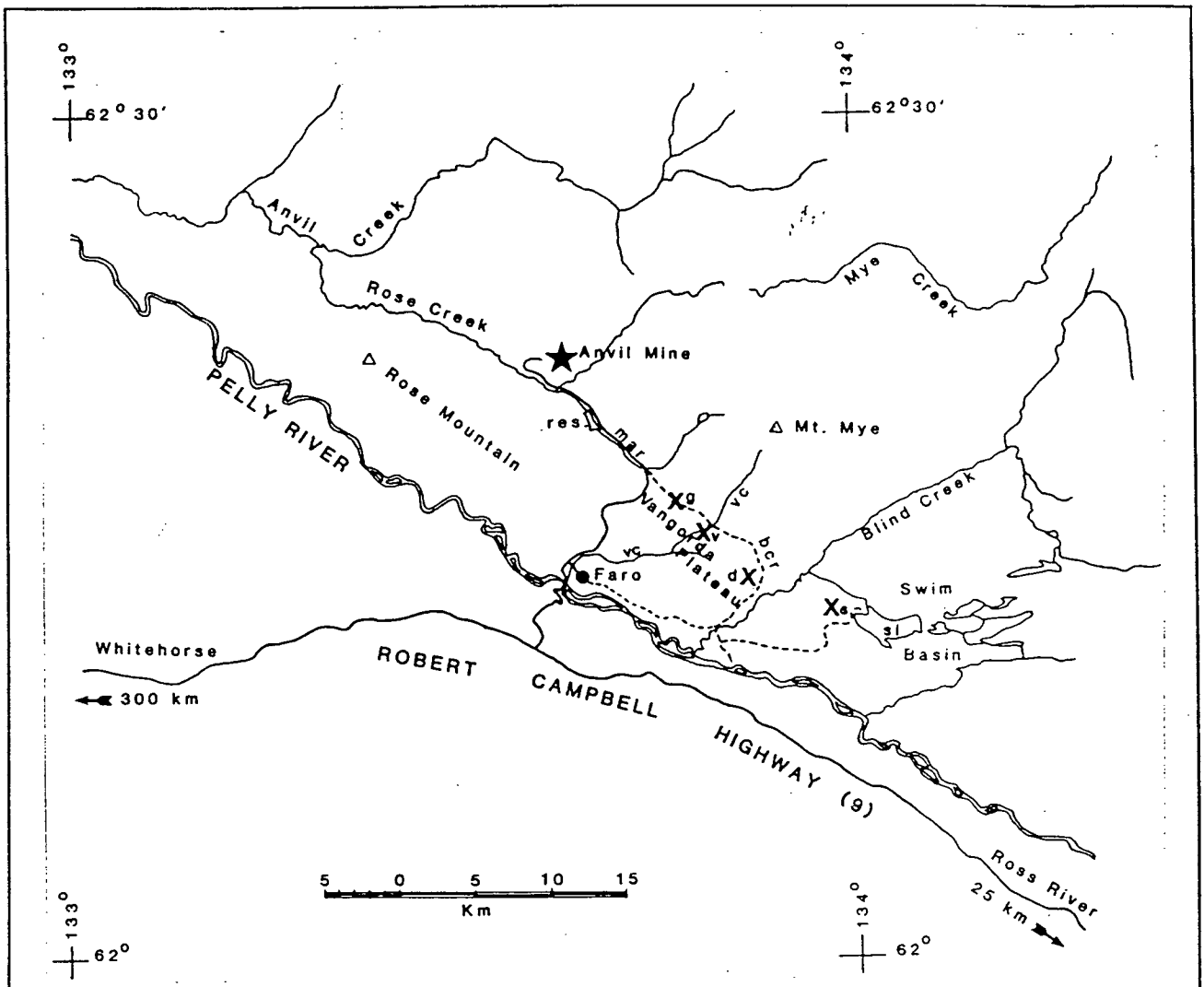


FIGURE 5. The southwest quarter of Tay River map sheet (Fig. 1) showing the location of the major Pb-Zn-Ag-bearing sulphide deposits (g = Grum, v = Vangorda, d = Dy, s = Swim) and other localities cited in the text (sl = Swim Lake, vc = Vangorda Creek, bcr = Blind Creek road, mar = mine access road, res. = mine water supply reservoir). Heavy solid lines are all-weather gravel highways, dashed lines are secondary roads. Swim Basin is a structural basin between the Blind Creek Fault and the Orchay Batholith (Fig. 3). Vangorda Plateau is defined as the area between the Tie Fault and Blind Creek Fault (Fig. 3).

Mineralogically, the Mt. Mye phyllites average 60% quartz, 30% muscovite, the rest being chlorite, biotite, and plagioclase or dolomite. The average bulk composition of 18 examples of this phyllite is shown in Table 1, Col. A. Its composition is closer to the average shales of Shaw (1956) and Clarke (1924) than to greywacke composition (Middleton, 1960 and Pettijohn, 1963), a protolith with which it might be confused (Table 1, Col. H and I).

In areas of higher grade metamorphism, the pelite of the Mt. Mye is a fine to coarse, medium grey-brown to purplish brown schist with colour depending on relative proportions of carbonaceous material and biotite. Its weathering colour, a reddish to purplish brown, is similar to the fine-grained phyllites. The schists are generally pervasively foliated with lithon structure seen only in thin section. Quartzo-feldspathic and micaceous compositional banding parallel to foliation is increasingly developed at higher metamorphic grade.

There are two major schist variants. The first is a fine-grained, medium dark brownish grey schist (Table 1, Col. B) composed dominantly of quartz, muscovite and biotite with lesser garnet and andalusite. Pseudomorphs (after andalusite?) are conspicuous on the foliation surface as dark greenish grey, irregular, feather-like chloritic patches, 1 cm to 20 cm in length. The second major variant is a non-carbonaceous, coarse, well banded schist composed of quartz, muscovite and biotite with garnet and staurolite porphyroblasts and andalusite clots. The composition of these variants and an intermediate schist unit is shown on Table 1 where it is seen that the schist variants are similar to one another and to the phyllites. The schists and phyllites represent the same pelite package at various metamorphic grades.

Dark grey to black carbonaceous quartz, muscovite and chiastolite phyllites and schists are interlayered with and grade into less carbonaceous Mt. Mye pelites. These darker coloured rocks comprise only about 10% of the formation but are important because of their association with sulphide deposits and their electromagnetic response. Carbonaceous interbands appear to be more abundant in the upper 200 m of the formation where the background pelite also appears slightly more carbonaceous.

Marble and calc-silicate schist are interlayered with pelite of the formation and comprise about 10% of the unit. The most commonly occurring lithologies are: (a) light grey, medium crystalline, calcitic marble with boudins of biotite schist and calc-silicate, and; (b) thinly banded light green, cream and brown quartz, tremolite, biotite ± diopside ± garnet ± calcite ± epidote calc-silicates. The marble bodies may be up to about 75 m thick but generally are only a few tens of metres thick. The largest bodies can be traced several kilometres. Smaller bodies are less continuous. Some thickness variation may be due to unmapped isoclinal folds. The calc-silicates are spatially

TABLE 1. Comparison of Mt. Mye formation average composition with average pelites and greywackes

	Average - this study								
	A phyllite (N = 18)	B coarse biotite - muscovite - andalusite schist ± garnet ± staurolite (N = 32)	C biotite-muscovite-andalusite schist (N = 47)	D grey biotite - muscovite - andalusite schist (N = 65)	E weighted[1] average of Mt. Mye formation (A—D) (N = 162)	F average pelite (Shaw, 1956)	G average shale (Clarke, 1924)	H average greywackes (Pettijohn, 1963)	I average eugeosynclinal greywackes (Middleton, (1960)
SiO_2	56.89	56.82	55.57	57.33	56.67	61.54	58.38	66.75	65.67
TiO_2	0.78	0.69	0.70	0.54	0.64	0.82	0.65	0.63	—
Al_2O_3	20.53	19.39	20.29	19.99	20.02	16.95	15.47	13.54	12.73
Fe_2O_3	9.08	9.57	9.02	8.30	8.85	2.56	4.03	5.53	5.09
FeO	—	—	—	—	—	3.90	2.46	—	—
MnO	0.08	0.07	0.10	0.08	0.08	—	—	0.05	—
MgO	2.29	2.29	2.11	2.06	2.15	2.52	2.45	2.15	2.40
CaO	1.19	0.66	0.99	0.88	0.90	1.76	3.12	2.54	4.20
Na_2O	1.17	0.64	0.88	0.70	0.79	1.84	1.31	2.93	3.04
K_2O	4.37	4.07	4.07	3.77	3.98	3.45	3.25	1.99	1.87
P_2O_5	0.15	0.14	0.12	0.17	0.15	—	—	0.16	—
H_2O	—	—	—	—	—	3.47	5.02	—	—
CO_2	—	—	—	—	—	1.67	2.64	—	—
S	0.04	0.79	0.28	0.40	0.40	—	—	—	—
LOI	3.44	4.98	5.87	5.78	5.38	—	—	—	—
Total	100.01	100.11	100.00	100.00	100.01	100.48	98.78	96.34	95.00

1 Weighting on the basis of number of samples, N = number of samples.
2 LOI = loss on ignition.
3 A—D are averages of analyses by Bondar-Clegg, Vancouver, British Columbia, using XRF.

TABLE 2. Mt. Mye formation metabasites

Sample Number	812	1025	1907	1552	788	1863	Average
SiO_2	50.80	49.40	48.80	51.60	54.10	48.10	50.47
TiO_2	2.58	1.81	2.66	1.09	1.31	1.00	1.74
Al_2O_3	13.30	15.50	15.00	15.50	15.00	15.90	15.03
Fe_2O_3*	13.80	11.70	13.80	11.30	11.70	12.10	12.40
MnO	0.17	0.15	0.17	0.17	0.13	0.16	0.16
MgO	6.70	6.20	5.60	7.10	6.20	6.30	6.35
CaO	10.00	9.80	10.60	10.50	7.30	9.90	9.68
Na_2O	1.10	3.50	1.70	2.70	3.55	2.75	2.55
K_2O	0.15	0.40	0.25	0.15	0.10	0.40	0.24
P_2O_5	0.27	0.23	0.34	0.09	0.15	0.25	0.22
S	0.18	0.01	0.26	0.01	0.02	0.59	0.18
LOI	0.62	1.19	0.44	—	0.38	1.41	0.80
Total	99.67	99.89	99.02	100.21	99.94	98.86	
Zr ppm	153	95	170	43	82	109	109
Y ppm	17	14	20	17	16	16	17
Normalized for total = 100% and LOI + S = 0%							
SiO_2	51.38	50.06	49.33	51.50	54.35	49.66	51.05
TiO_2	2.61	1.83	2.69	1.09	1.32	1.03	1.76
Al_2O_3	13.45	15.71	15.16	15.47	15.07	16.42	15.21
Fe_2O_3*	13.96	11.86	13.95	11.28	11.75	12.49	12.55
MnO	0.17	0.15	0.17	0.17	0.13	0.17	0.16
MgO	6.78	6.28	5.66	7.09	6.23	6.50	6.42
CaO	10.11	9.93	10.72	10.48	7.33	10.22	9.80
Na_2O	1.11	3.55	1.72	2.69	3.57	2.84	2.58
K_2O	0.15	0.41	0.25	0.15	0.10	0.41	0.25
P_2O_5	0.27	0.23	0.34	0.09	0.15	0.26	0.22
Total	99.99	100.01	99.99	100.01	100.00	100.00	

* Includes FeO calculated as Fe_2O_3.
LOI = loss on ignition.
Analyses by Bondar-Clegg using XRF with Y checked by neutron activation.
All values are weight per cent unless otherwise noted.

associated with the marbles and are one to three times more voluminous. The most widespread marble/calc-silicate horizon is about 200 m to 400 m below the top of the formation and may correlate with the widespread Early Cambrian limestone conglomerate of Selwyn Basin (Gordey, 1978). Minor carbonaceous finely crystalline mable is interlayered with carbonaceous pelite above this unit.

Metabasites interpreted as either flows or sills occur in the Mt. Mye but are volumetrically significant only near its top where they comprise a few per cent of the unit. These rocks are generally strongly foliated, dark green amphibole, plagioclase, quartz schists lacking relict igneous texture. Metabasite bodies are generally only a few metres to tens of metres thick and have small to moderate lateral dimensions (up to a few hundred metres). Thin (10 cm to 1 m), variably calcareous, green, amphibole-rich schists, possibly derived from tuffs, occur interlayered with pelites near the top of the formation. The composition of Mt. Mye metabasites (6 analyses, Table 2) is that of a sub-alkaline basalt (Figs. 6-9). These metabasites are compositionally similar to, though less alkaline than, the more altered but less metamorphosed mafic rocks of the Vangorda formation and Menzie Creek formation to which they may be related as subvcolcanic feeders.

Little unequivocal data on the depositional environment of the Mt. Mye is found in Anvil District. The fine-grained, thinly banded monotonous nature of the metapelites and their regional setting is felt to be consistent with accumulation in relatively deep water on or at the foot of a continental rise.

Age and Correlation

Mt. Mye formation is similar to Cambrian strata mapped by Gordey (1978—units ϵp and lϵp) in Selwyn Mountains (Fig. 1) near Howards Pass. Early Cambrian strata similar to the upper portion of the Mt. Mye have also been mapped by Blusson, (1966—Unit 8a) near Cantung (Fig. 1). Grey to brown phyllites of Early Cambrian or Hadrynian age below these units and

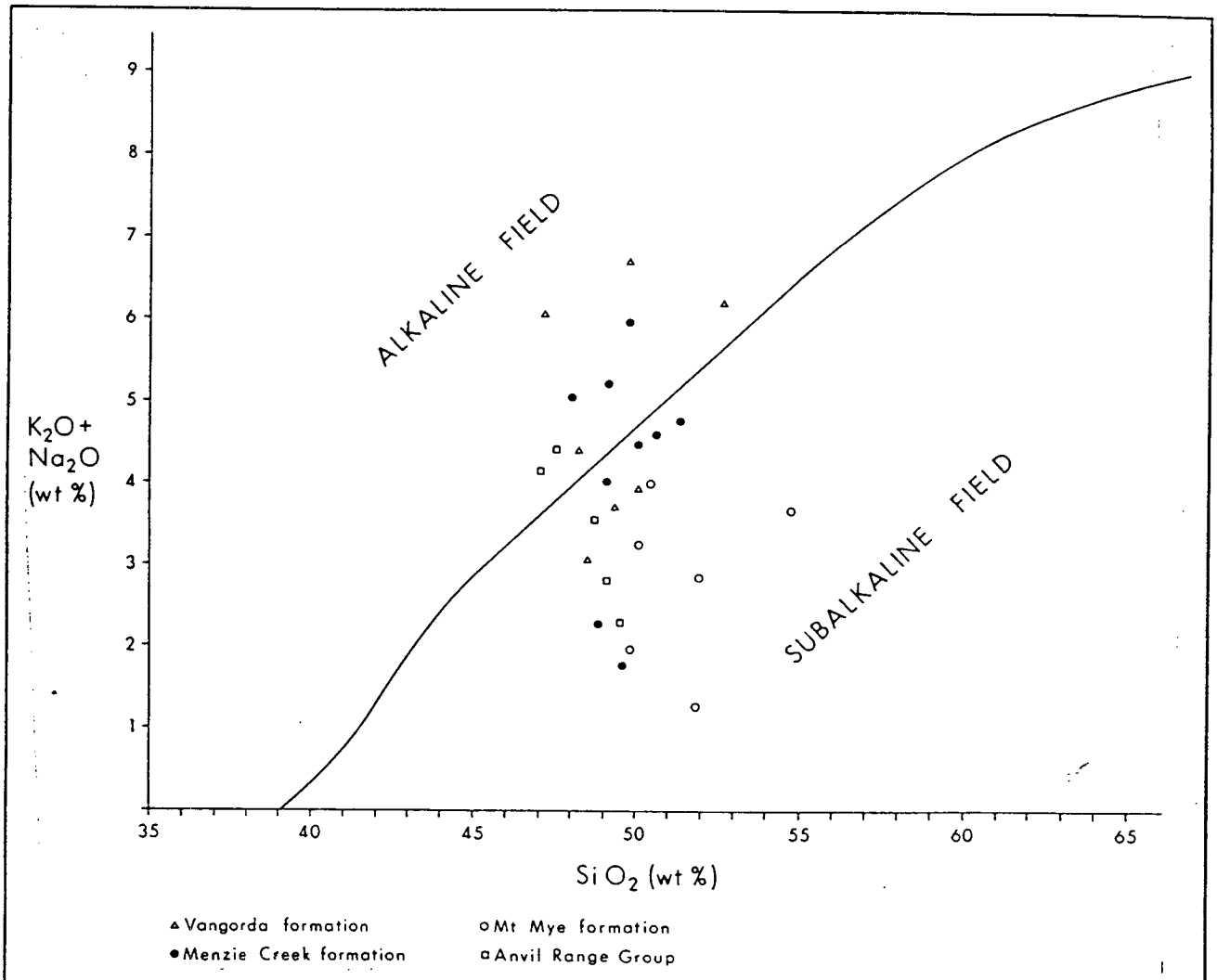


FIGURE 6. Alkali-silica diagram showing analyses of various mafic lithologies given in Tables 2, 3, 5 and 6. The alkaline-subalkaline field boundary is after Irvine and Baragar (1966). The metabasites of the Mt. Mye formation are least carbonated and tend to plot in the subalkaline field. The more strongly carbonated Vangorda and Menzie Creek formation metabasites plot toward the alkaline field.

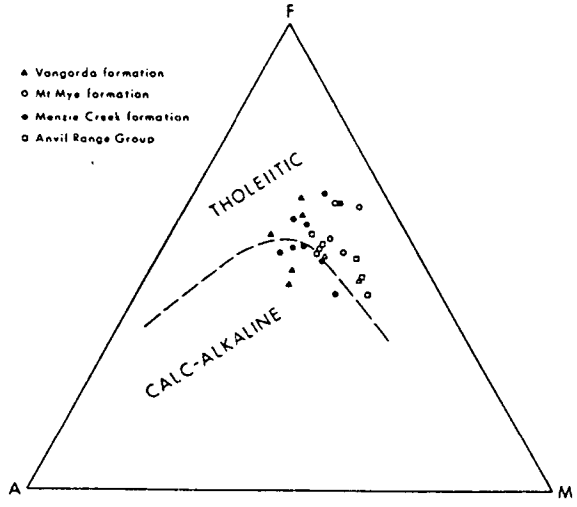


FIGURE 7. AFM plot of same analyses as Figure 6 definition of A, F and M as well as field boundary is after Irvine and Baragar (1966). With the exception of the Anvil Range Group basalts, all rocks are sufficiently strongly altered to carbonate-bearing assemblages to render inferences from this diagram and Figure 6 highly suspect.

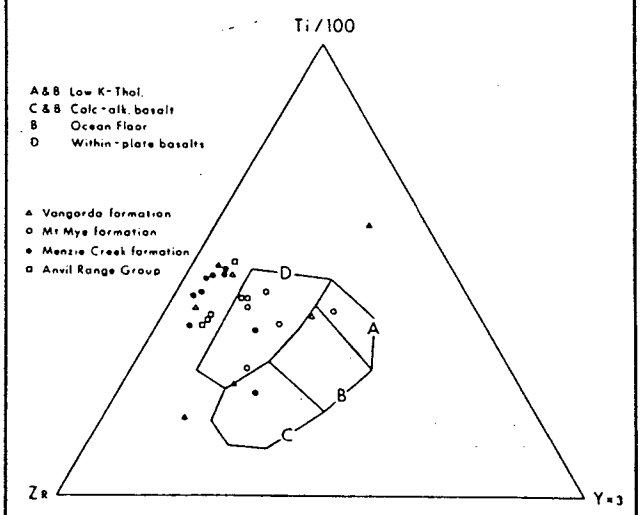


FIGURE 8. A Ti-Zr-Y discriminant diagram after Pearce and Cann (1973). The tendency of the least carbonate altered metabasites (of Mt. Mye formation) to plot in the within plate basalt field may be meaningful but the over-all scatter of analyses casts doubt on the general applicability of the inference to other formations.

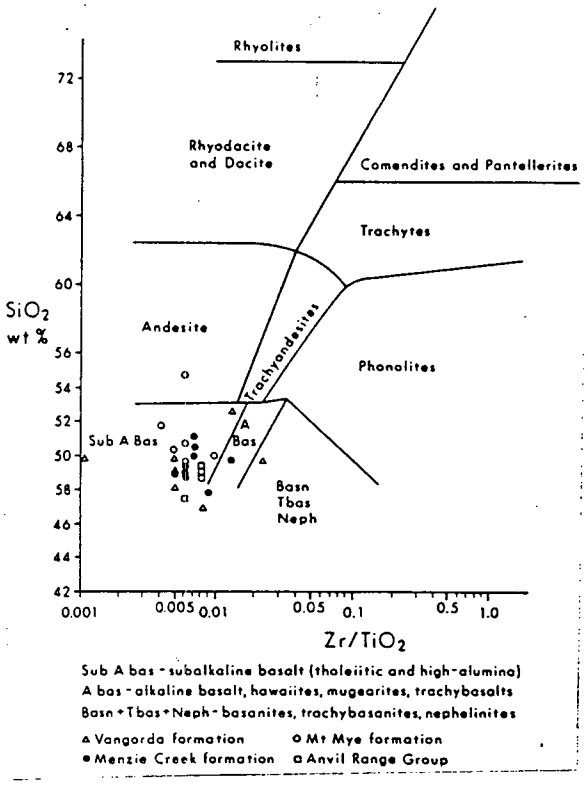


FIGURE 9. An SiO_2-Zr/TiO_2 discriminant plot after Floyd and Winchester (1977). Most analyses plot in the subalkaline basalt field but probable silica mobility renders the plot ambiguous.

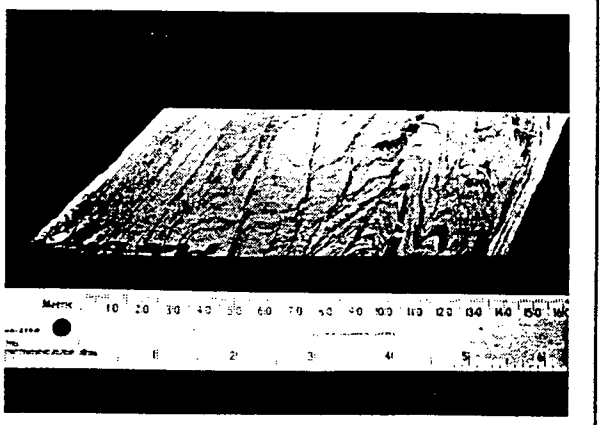


FIGURE 10. Calcite-rich Vangorda formation phyllite in drill core. S_2 (Table 7) is at about 80 degrees to the core axis. The thin compositional banding parallel to S_1 and the typical lithon structure of the phyllites is evident. The light-coloured bands are the quartz- and calcite-rich recrystallized siltstone bands; the darker micaceous bands are non-calcareous.



FIGURE 11. Green, laminarly banded phyllite (possible metatuffs or hornfelsed calcareous pelite) found adjacent to metabasites (just out of photo to the right) of the Vangorda formation, S_2 is inclined gently from left to right. S_0 and S_1 are parallel and steeply dipping (Table 7 for clarification of structural terminology).

similar rocks in Flat River map area (Fig. 1, part of phyllite unit of Gabrielse *et al.*, 1973) also resemble Mt. Mye formation and may be equivalent. On the basis of lithologic similarity to these better dated units, the Mt. Mye formation is thought to be lower (perhaps middle) Cambrian and possibly late Hadrynian.

The Mt. Mye formation includes the lower quartz-rich division of unit 3 and all of unit 3b of Tempelman-Kluit (1972). Most of unit 2 (*op. cit.*) is also part of the Mt. Mye, though amphibolite facies Vangorda formation is also included.

Vangorda Formation

Introduction

Vangorda formation is a thick sequence of recessive, generally calcareous phyllite, intercalated with lesser, basic, meta-igneous rock. The calcareous phyllites are locally metamorphosed to calc-silicate assemblages. A carbonaceous member occurs at the base of the formation. The existence of a mappable upper calcareous division in the phyllites of the Anvil District was first clearly demonstrated by Roberts (Brock and Roberts, 1971).

Strong internal deformation in the district adds great uncertainty to estimates of thickness of the formation. The thickness indicated from cross sections is about 1000 m, but this can vary considerably depending on the treatment of local structural detail.

The best readily accessible exposures of Vangorda formation are found along the road paralleling Blind Creek in the vicinity of the Dy deposit (Fig. 5), where both phyllite and metabasite can be examined. Good exposures of phyllite can also be seen southeast of the Firth showing (Fig. 12, Mineral Occurrence No. 12). Calc-silicates of Vangorda formation are best examined in the walls of the Faro pit (Anvil Mine) and in surface exposures northwest of the Faro deposit. Excellent exposures of the basal carbonaceous unit can be seen in the Faro pit and on the road to Swim Lake south of the Swim deposit (Fig. 5).

Weathering of the unit is distinctive and generally aids mapping the formations, especially from the air. Most outcrops are covered with a light grey druse and are light brownish grey or tan with conspicuous lustrous grey phyllite chips nearby. The formation is easily distinguished from rusty brown weathering Mt. Mye formation.

Lithology

Phyllites

Vangorda formation is characterized by medium grey phyllite very thinly interlayered with light grey quartz- and calcite-rich bands thought to be derived from siltstone beds and laminae (Fig. 10). The phyllitic bands are one-half cm to 1 cm thick and the quartz and calcite bands are 1 cm to several cm thick. The phyllitic bands are generally non-calcareous and homogeneous though internal colour gradations in shades of grey occur. The quartz-calcite bands are usually parallel laminated; grading occurs rarely; cross lamination is also rare and is generally preserved only in lower grade equivalents outside the district. The thin bands that form this rock are usually intricately folded on a hand specimen scale with an axial planar crenulation cleavage forming the dominant plane of fissility of the phyllites.

This rock type has many variants due to variations in the composition of the constituent bands. The over-all colour of the muscovite-chlorite phyllitic bands ranges from light olive, greenish-grey to medium grey (the dominant colour) to black

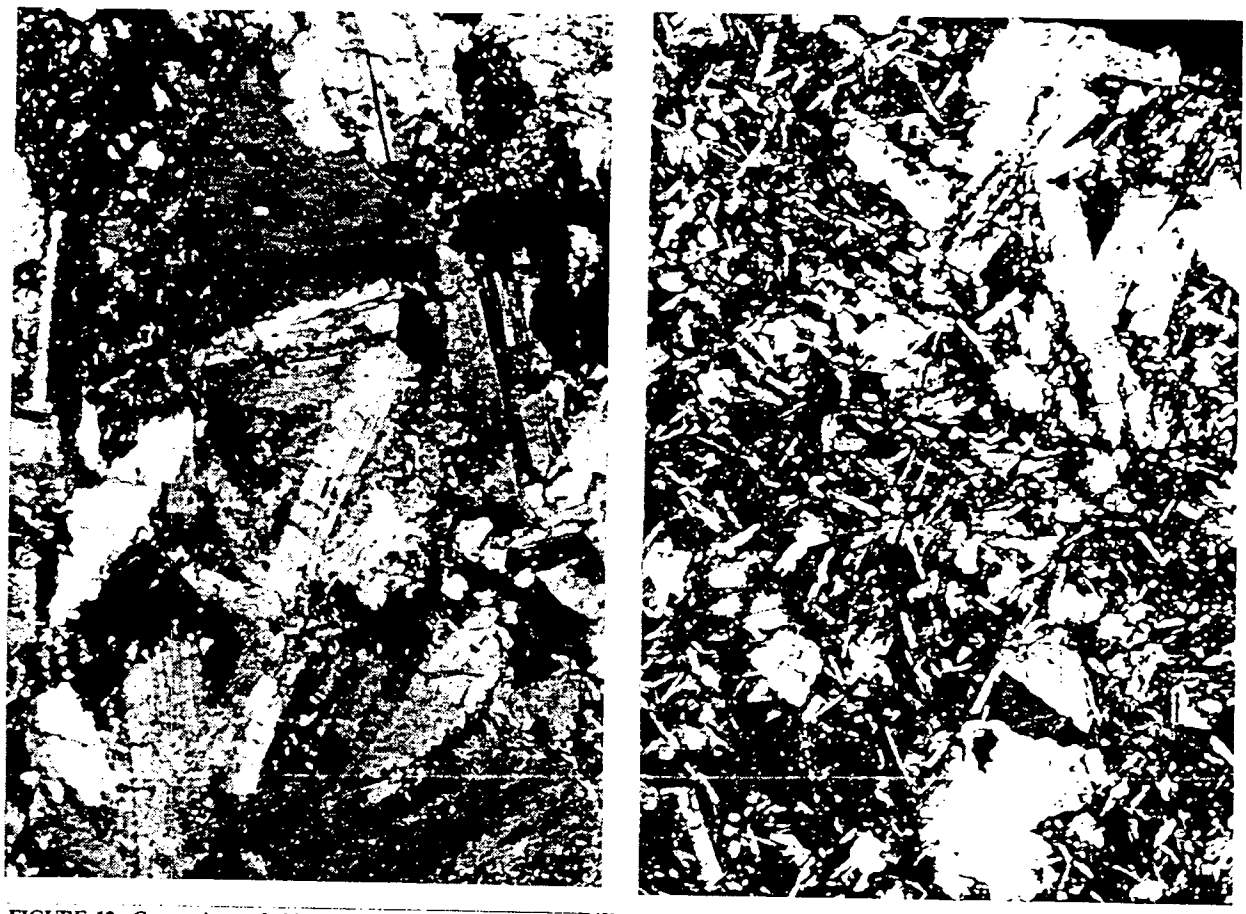


FIGURE 12. Comparison of thin sections of a typical specimen of metabasite from Vangorda formation—(A) crossed nicols—and a metavolcanic from Menzie Creek volcanic unit—(B) crossed nicols. Clear volcanic textures which typify the Menzie Creek are not found in Vangorda metabasites. Rather, they are coarser and more equigranular. Each view is 2 mm by 3 mm.

depending essentially on the amount of carbonaceous material. The siltstone bands, though always quartz-bearing, can have calcite and/or dolomite contents varying from 0% to 70%.

The most important Vangorda phyllite variants are (a) black, variably calcareous and commonly dolomitic, thinly layered, quartzose phyllite; (b) soft, medium grey to black, homogeneous, non-calcareous phyllite (lacking in quartz siltstone layers); (c) medium grey, non-calcareous phyllite thinly interlayered with quartz siltstone similar to the dominant Mt. Mye lithology; and (d) medium grey phyllite with thin quartz dolomite layers. None of these variants comprise more than 10% to 15% of the unit and they are clearly subordinate to the medium grey calcareous version which forms about 50% of the volume of the formation.

In addition to the black phyllite variant noted above, pervasively foliated, homogeneous, variably siliceous, hard, fine-grained black phyllites with minor (1%) disseminated pyrite and pyrrhotite are also developed, particularly near the base of the formation. Near ore deposits, these rocks are harder, more siliceous, more sulphide-rich and more abundant than elsewhere. They appear to be derived from black, siliceous shales laterally equivalent to black, sulphide-bearing, ribbon-banded, graphitic quartzite ore facies (see deposits section).

Dimensions of the carbonaceous members of Vangorda formation are poorly known. The thickest and most extensive member is at the base of the formation and can be traced discontinuously through the district and beyond as far as correlative exposures near the Nahanni Range Road on the west flank of Mt. Billings Batholith, 300 km southeast (Fig. 1). It is typically only a few tens of metres thick but near ore deposits can be up to 100 m thick. Electromagnetic conductors that define this unit can be followed continuously for several kilometres to a few tens of kilometres. It is not certain whether the lack of continuity of this member is caused by unappreciated structural complications or is depositional. Carbonaceous phyllite is developed as a subordinate lithology through the remainder of the formation where it is less areally extensive and thinner than the basal member.

Relatively pure marble is a very minor lithology in Vangorda formation. These marbles are mostly calcitic, medium bluish grey and the fine to medium crystalline; they are generally thin interbands and tend to occur in association with abundant and very calcite-rich siltstone bands. Rare, rusty orange weathering, medium crystalline, dolomitic marbles also occur locally. Black, slightly fetid, finely crystalline, calcitic marble is a minor constituent particularly in association with the basal carbonaceous member of the formation.

Green phyllitic rocks are common in Vangorda formation. These green phyllites are of considerable importance because of their implications for the extent to which volcanic rocks are present in the formation. Of particular interest is a striking, thinly laminated green and white, generally calcareous, phyllite that resembles a bedded tuff (Fig. 11). Locally, these rocks appear to be cherty and are hard. These green, laminated phyllites are rarely seen except adjacent to metabasites (described below) and most metabasites have them associated. In many instances, these phyllites grade outward from the metabasites into green or greenish grey, texturally normal Vangorda formation calcaerous phyllites. These greenish grey phyllites may result from a volcanic admixture to normal Vangorda formation pelites or from a weak bleaching (due to oxidation of background carbon in the normal pelites?) and/or chlorite alteration superimposed on the formation during intrusion of the spatially associated metabasites. The strongly laminated green rocks may thus be an

TABLE 3. Vangorda formation metabasites

Sample Number	5531	692	1402	1497	1487	5564	5596	Average
SiO_2	46.80	50.40	47.00	46.80	47.40	44.40	47.00	47.11
TiO_2	4.70	2.28	2.38	1.58	1.84	2.20	3.20	2.60
Al_2O_3	15.40	16.80	14.40	14.90	19.90	18.50	13.00	16.12
Fe_2O_3*	5.00	11.70	10.60	10.80	11.50	3.60	4.70	12.76
FeO	9.50	—	—	—	—	8.90	9.90	—
MnO	0.21	0.08	0.13	0.15	0.04	0.16	0.19	0.14
MgO	5.60	6.10	8.60	6.20	6.40	4.20	4.80	5.99
CaO	4.80	2.65	11.00	11.40	1.80	6.20	7.00	6.41
Na_2O	4.00	4.70	2.90	3.45	4.35	5.35	3.50	4.47
K_2O	0.25	1.20	0.10	0.05	2.05	0.40	0.20	0.61
P_2O_5	0.58	0.56	0.32	0.21	0.70	0.45	0.47	0.47
S	—	0.04	0.03	0.07	0.01	—	—	0.04
LOI	3.30	3.26	2.37	4.43	3.79	5.15	6.55	4.12
Total	100.14	99.77	99.83	100.04	99.78	99.81	100.51	
Zr ppm	260	317	26	80	430	175	175	209
Y ppm	16	41	24	23	32	(5)	6	21
Normalized for total = 100% and LOI + S = 0%								
SiO_2	48.33	52.24	48.24	48.98	49.39	47.22	50.02	49.20
TiO_2	4.85	2.36	2.44	1.65	1.92	2.32	3.41	2.71
Al_2O_3	15.90	17.41	14.78	15.60	20.73	19.54	13.84	16.83
Fe_2O_3*	5.16	12.13	10.88	11.30	11.98	3.80	5.00	13.33
FeO	9.81	—	—	—	—	9.40	10.54	—
MnO	0.22	0.08	0.13	0.16	0.04	0.17	0.20	0.14
MgO	5.78	6.32	8.83	6.49	6.67	4.44	5.11	6.23
CaO	4.96	2.75	11.29	11.93	1.88	6.55	7.45	6.69
Na_2O	4.13	4.87	2.98	3.61	4.53	5.65	3.72	4.21
K_2O	0.26	1.24	0.10	0.05	2.14	0.42	0.21	0.63
P_2O_5	0.60	0.58	0.33	0.22	0.73	0.48	0.50	0.49
Total	100.00	99.98	100.00	99.99	100.01	99.99	100.00	

* Includes FeO calculated as Fe_2O_3 if FeO not given separately.
LOI = loss on ignition.
Analyses by Bondar-Clegg using XRF with Y checked by neutron activation.
( ) indicates less than the detection limit within parentheses.
All values are weight per cent unless otherwise noted.

altered facies of normal Vangorda pelites rather than tuffs. A second type of distinct, green, calcareous phyllite is described below with the metabasites to which it is more directly related.

Metabasites and Derived Rocks

The most abundant subordinate lithology of Vangorda formation is mafic meta-igneous rock: metabasite or greenstone. Even though this sub-unit accounts for only about 15% to 20% of the formation, it is particularly conspicuous because it is resistant. Thus it, and its associated green phyllite, make up a high proportion of outcrops. Metabasites occur throughout the formation but are most abundant in its upper part where they may amount to 50% of the unit. Metabasite occurs in lens-shaped bodies with massive interiors commonly preserving relict diabasic or medium-grained, ophitic texture (Fig. 12). The margins of metabasites are pervasively recrystallized and strongly foliated. Metabasite bodies are 1 m to 100 m in thickness and can be as much as several kilometres in length. Most are smaller, commonly foliated and appear to parallel original compositional layering in Vangorda formation but are locally cross-cutting in detail. Whole rock analyses show that metabasites are of basaltic composition (Table 3, Figs. 6-9).

A commonly occurring, widespread but volumetrically minor lithology of Vangorda formation related to the metabasites is olive green, calcareous, chlorite-rich phyllite. These rocks are more homogeneous than the green, laminated phyllites noted above. They commonly contain 0.1 cm to 5 cm thick, foliaform, white, quartz ± calcite bands of more irregular thickness than quartz ± calcite bands in normal Vangorda pelites and these bands are considerably more coarsely grained. These bands are more akin to vein material and merge locally with foliaform veins. The remainder of the rock is a homogeneous or a weakly, thickly colour laminated, fine-grained aggregate of chlorite + quartz + calcite + plagioclase + muscovite. Locally, relict feldspars and or pyroxenes and/or amygdules have been identified. Some specimens show an indeterminate mottled texture that could be clastic. These chloritic phyllites are very similar to the fine-grained margins of metabasites and to chloritic phyllites found in the overlying Menzie Creek formation (see below). They have mafic igneous compositions and may be small, fine-grained, metabasite bodies that are pervasively foliated throughout. However, some appear to have been tuffs or mafic flows. The dimensions of individual chloritic phyllite units is not well known. They are generally not more than a few metres thick and many examples are only a few centimetres thick. Some bodies have been traced for several hundred metres at approximately the same stratigraphic interval. These chloritic phyllites are generally readily distinguished from the medium grey, calcareous, pelitic phyllites that typify Vangorda formation but the two rock types become very difficult to separate where they are intimately interlayered and the pelites are highly altered. A large complex of these green phyllites of diverse origin occurs with metabasites at the northeast edge of the Dy and Grum deposits.

Two significant variants of the metabasic rocks in the district deserve mention. The first is variably serpentinized pyroxenite that occurs locally associated with otherwise normal metabasites. These appear to be pyroxene cumulates related to the metabasites, and like them have foliated margins showing their pre-D_1 age. The second is a rusty weathering, light tan quartz-sericite-dolomite or ankerite rock commonly bearing minor amounts of a bright green possible serpentine or clay mineral (Modene, 1982) resembling fuchsite. These rocks are common in the Grum deposit and are found more rarely in other deposits. They are heavily carbonated metabasites resembling quartz-carbonate altered, metabasic rocks described worldwide. Black, carbonaceous ore types are commonly bleached off-white adjacent to these rocks. Less intensely altered, carbonated metabasites that retain a green colour occur widely in the district. Indeed, most metabasites in the Vangorda formation are carbonated to some degree, a fact that adds considerable ambiguity to interpretation of whole rock geochemical data in Table 3.

The origin of the metabasites and allied green rocks is controversial. In hand specimen and in thin section, most metabasites are texturally like fine-grained intrusive rocks (Fig. 12). Local, crosscutting, contact relationships also support an intrusive origin. Pillows have not been observed in the metabasites and fine-grained, amygdaloidal texture that typify the overlying

TABLE 4. Comparison of average whole rock analytical data for calcareous phyllite and all calc-silicates of Vangorda formation

	A[3] calcareous phyllite (N = 8)	B[3] "ordinary" calc-silicate (N = 9)	C[3] "cherty" calc-silicate (N = 3)	D average calc-silicate B and C (N = 12)	E A normalized for LOI = 0	F B normalized to LOI = 0	G C normalized to LOI = 0	H D normalized to LOI = 0
SiO_2	49.86	51.27	52.11	51.48	55.06	53.90	53.32	53.77
TiO_2	0.29	0.46	0.47	0.46	0.31	0.48	0.47	0.48
Al_2O_3	16.34	17.14	15.87	16.83	17.99	18.01	16.23	17.57
[1]Fe_2O_3	6.75	7.04	6.54	6.92	7.39	7.38	6.67	7.21
MnO	0.09	0.09	0.06	0.08	0.10	0.09	0.06	0.08
MgO	3.21	3.54	3.89	3.63	3.52	3.71	3.96	3.77
CaO	9.51	10.96	13.34	11.56	10.63	11.50	13.76	12.06
Na_2O	1.70	1.38	1.33	1.37	1.87	1.44	1.35	1.42
K_2O	2.69	3.13	3.87	3.32	2.97	3.30	3.95	3.46
P_2O_5	0.16	0.18	0.20	0.19	0.17	0.19	0.20	0.19
[2]LOI	9.42	4.80	2.32	4.18	—	—	—	—

1 Total iron as Fe_2O_3.
2 LOI = loss on ignition.
3 Averages of analyses by Bondar-Clegg, Vancouver, British Columbia, using XRF (N = number of samples).

Menzie Creek flows are restricted to the margins of larger equigranular bodies. The metabasites are texturally identical to dykes and plugs intrusive into the overlying Menzie Creek volcanics. The above considerations suggest that the metabasites are derived from basaltic sills, perhaps subvolcanic feeders to the Menzie Creek volcanic unit. On the other hand, since metabasites are spatially associated with green, possibly tuffaceous phyllites, some may be flows that accumulated in local flow and fine-grained hyaloclasite complexes.

Despite this ambiguity, there is no doubt volcanism did occur at times during the accumulation of Vangorda formation. The evidence is particularly clear in the Grum deposit where thin (1 mm to 1 cm), green, unmineralized, chloritic phyllites occur interlayered with sharp contacts in black, carbonaceous, sulphide-bearing quartzites. These chloritic rocks faithfully follow the layering in the ore and almost certainly were originally thin tuffs. The best evidence for the presence of tuffs is found in rare, green, chloritic phyllite interlayers found both in the ore and in other metasediments. These particular layers are a few to 10 cm thick and show rapid vertical colour gradation from dull, olive green to medium or dark grey more typical of the surrounding sediments.

Calc-silicates

One of the major problems in tracing Vangorda formation through the district is its variable metamorphic overprint. In areas of higher grade metamorphism, as near the Faro deposit, the dominant lithology is thinly and discontinuously banded, pervasively foliated, green, cream and purplish brown, hard calc-silicates. Typical mineral assemblages are quartz, tremolite-actinolite, plagioclase, biotite ± diopside ± calcite ± epidote. Calc-silicate outcrops are commonly druse covered, blocky and weather medium to light grey similar to the phyllites.

Table 4 compares the average bulk composition of representative calc-silicates and calcareous phyllite. When recast on a volatile-free basis, their compositions are essentially identical. The loss of CO_2 from the consumption of calcite during formation of calc-silicate minerals presumably accounts for the difference in volatiles (L.O.I.) between the two rock types.

A peculiar variant of calc-silicated Vangorda is found at several localities on the northeast flank of Anvil Range. These rocks are very fine-grained, thinly layered, pervasively foliated and have a characteristic cherty aspect. Despite their cherty appearance, these calc-silicates are no more siliceous than ordinary Vangorda calc-silicates (see Table 4, Col. B and C) and in thin section they are similar to other calc-silicates but so fine grained that their mineralogy is difficult to determine. These rocks are part of unit 4 of Gordey (1983) and crop out widely south of Two Pete Mountain (Fig. 1).

Depositional Environment

Like the underlying Mt. Mye formation, the depositional environment of Vangorda formation is equivocal. Its fine-grained, monotonous nature, more argillaceous character than its presumed equivalents to the east and southeast, and its paleogeographic setting suggest deposition in relatively deep water.

The thin bedding and lamination as well as grading and cross lamination within rare examples of Bouma cycles in equivalent strata outside the district is suggestive of some sediment transport by turbidity currents.

Contact Relationships and Internal Variation

The basal contact of the formation appears sharp, but is rarely exposed. At both Grum and Faro where the structure is reasonably well understood, the contact appears to be relatively sharp and occurs across the basal carbonaceous member within which there is a rapid downward transition of interlayered lithology from rocks typical of the Vangorda formation to those typical of the Mt. Mye.

At Faro, the basal carbonaceous member is a few to over 30 m thick and contains interlayers of transitional calc-silicates, amphibole-rich metabasic rocks, chloritic schists, marbles and pelites typical of Mt. Mye formation. The base of the formation is arbitrarily placed at the point where Mt. Mye formation schists with a normal grey colour are encountered. At Grum, there is also a basal carbonaceous member approximately 30 m thick which is variably dolomitic (presumably the protolith of the Faro transitional calc-silicates) and some chloritic metabasic rocks also occur. This basal unit at Grum is abruptly overlain by normal medium grey calcareous phyllite, but the base of the unit, unlike Faro, is the locus of one of the major ore lenses thus obscuring the normal formational contact relationship. Immediately beneath the ore layers are normal Mt. Mye phyllites.

Based on relationships at the Dy deposit, we have previously proposed a gradual, interlayered transition between the Mt. Mye and Vangorda formations over as much as 300 m vertically (Jennings *et al.*, 1980). We now suspect some of the apparent interlayering of calcareous and non-calcareous phyllite may be an artifact of the poorly understood structure there.

Geographic variation in the character of the formation occurs within the district. Compared to the area of the sulphide deposits on the south flank of the Anvil Arch (Fig. 3), the formation on the northeast flank is less calcareous and metabasites are less abundant and smaller; exhalative base metal-rich sulphide bodies are also conspicuously absent there though a small occurrence is known in Mye Creek (Fig. 5).

Age and Correlation

The formation crops out widely between the Anvil district and Coal River 500 km southeast (Fig. 1). Outside the Anvil district, the best accessible exposures are along the Nahanni Range Road west of the Mt. Billings Batholith between King and Sequence Creeks in Frances Lake map area (105 H) (Fig. 1). Metabasites are very minor in the formation everywhere outside the Anvil district northeast of the Tintina Fault.

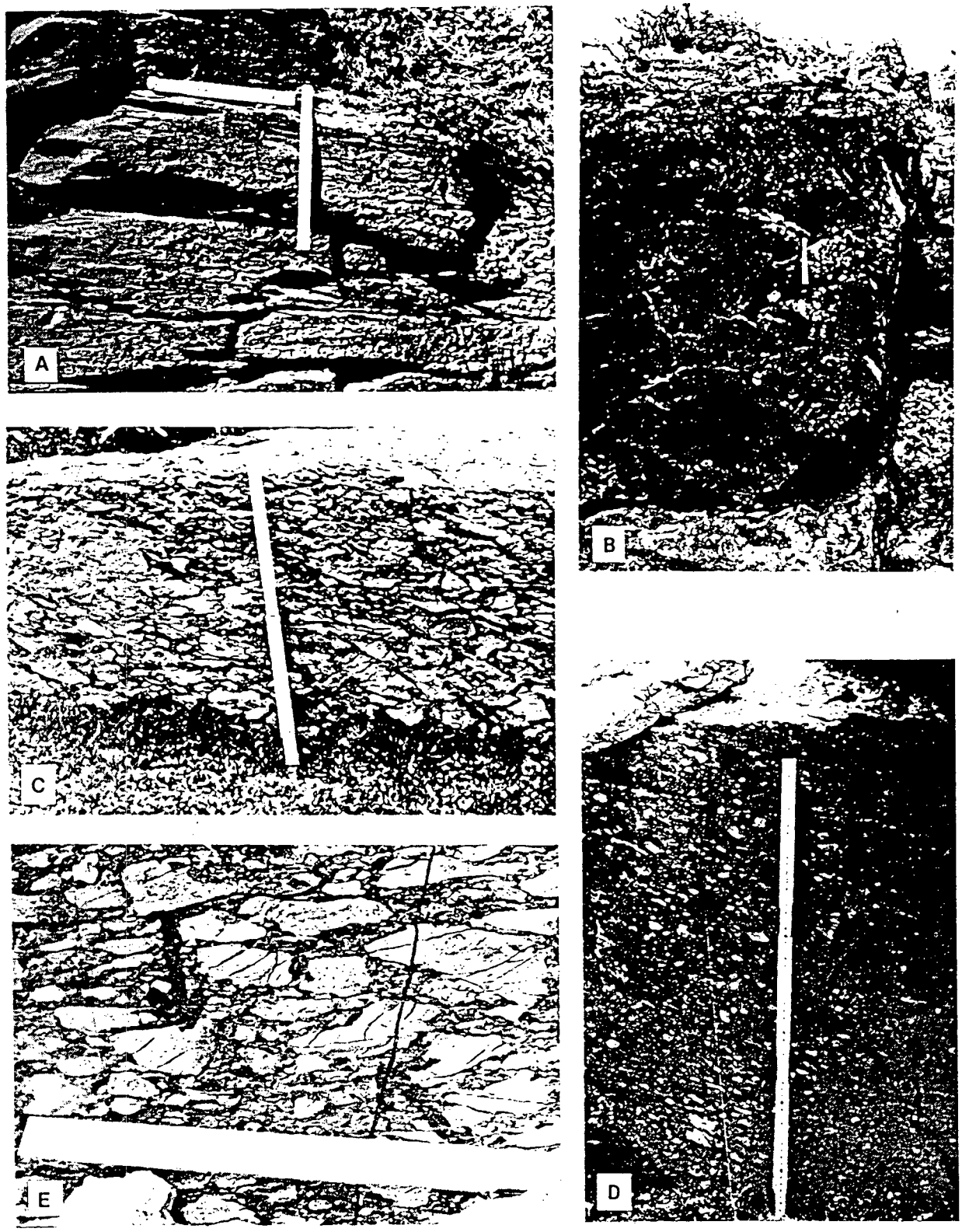


FIGURE 13. Typical Menzie Creek formation pillowed flows, (A) and (B), and breccias (C), (D) and (E). (B) shows unfoliated pillows. (A) shows more typical pillows toward the base of the unit where they are strongly flattened (into S_1): in (A), S_1 is horizontal and pillow margins are marked by zones of concentrated, crudely radial amygdules. (Rule is 20 cm on edge.) (C) shows the typical relief weathering of Menzie Creek breccias due to the strongly calcareous matrix; S_1 is horizontal with moderate flattening of clasts. (Rule is 40 cm long.) (D) is an example of less clast rich matrix support breccia; S_1 is gently inclined from left to right. (Rule is 60 cm long.) (E) is a close-up of a breccia in which some clasts have broken, dark rinds, possibly derived from non-amygdaloidal pillows; S_1 is horizontal. (Rule graduated in cm.) See Table 7 for explanation of structural terminology.

Similar rocks occur north of Mt. Hunt (unit 10 of Blusson, 1966) and on Simpson Tower in Frances Lake Map area; in southwestern Coal River Map area (unit 8a of Gabrielse and Blusson, 1969); and in northeastern Finlayson Lake map area (Fig. 1, unit uεOsl of Tempelman-Kluit, 1977). The Cambrian-Ordovician Kechika Group south of the Tintina Fault has long been noted to be similar to phyllites of the Anvil Range (Tempelman-Kluit, 1972) and the Vangorda formation presumably correlates with its lower portion at least in part (see also Gordey, 1981, p. 9).

The Rabbitkettle Formation (Gabrielse *et al.*, 1973) of Cambro-Ordovician age is similar to the Vangorda formation in its thinly layered, calcareous and silty nature, but is far less argillaceous.

On the basis of lithologic similarity to these better dated units, the Vangorda formation is thought to be, at least in part, upper Cambrian possibly extending to lowest Ordovician. We have found no evidence in the Anvil district for the pronounced, sub-upper Cambrian, regional unconformity at the base of the Rabbitkettle Formation (Gabrielse *et al.*, 1973) to the east. Strata as old as lower Cambrian, may thus be included in the Vangorda formation: specifically equivalents of part of unit εc of Gordey (1978) or the Hess River formation (Cecile, 1982).

Unit 3 of Tempelman-Kluit (1972) includes the Vangorda formation. Specifically, the upper member and the abundant graphitic rocks (*op. cit.* p. 6) appear to belong to the formation. The statement that thinly laminated silty limestone is abundant in the upper part of unit 3 (*op. cit.* p. 7) is a reflection of the more calcareous nature of the upper Vangorda formation. Some amphibolite facies portions of the Vangorda formation are included in unit 2 (*op. cit.*) particularly calc-silicates northwest of the Faro deposit.

Menzie Creek Formation

Introduction

Menzie Creek formation is a thick unit of resistant, grey weathering, dominantly basaltic metavolcanic rocks with intercalated black phyllite and slate. Major rock types present in subequal amounts are pillow lava, volcanic breccia and massive, amygdaloidal, commonly porphyritic flows.

A maximum thickness of 1.5 km seems likely. Locally, the formation is thin and appears to nearly lens out into a black shale package.

The best exposures of Menzie Creek formation are northeast of Anvil Batholith most easily accessed by helicopter. On the south flank of Anvil Arch, the unit is recessive with small outcrops within 1 or 2 km of the mine access road and the Blind Creek road northeast of Vangorda Fault zone.

Lithology

Well developed pillow lavas are common in the Menzie Creek formation (Fig. 13 A and B). Typically, they are 0.5 m in diameter and have 0.5 cm to 1 cm dark rinds. Radially elongated, calcite- and chlorite-filled anygdules 0.5 cm in diameter are developed around the periphery. The pillow core is finely to non-amygdaloidal, aphanitic, and non-porphyritic to porphyritic (feldspar and/or augite). Interpillow matrix is generally fine-grained, highly foliated, and chloritic. Fine breccia and minor red chert also occur. Pillow breccia is interlayered with or beneath pillow lavas at many localities. In the lower portions of the formation, pillows are highly flattened into the S_1 foliation. Well formed, undeformed pillows are the rule, higher in the formation.

The massive flows range from medium olive green to grey green to dark green to almost black and rarely, purple or red. They commonly contain 5 mm diameter calcite- and/or chlorite-filled amygdules and may be aphanitic or have feldspar or augite phenocrysts. The flows range from unfoliated and blocky to strongly foliated and fissile. A few exposures show individual flows with amygdule trains along their upper and lower contacts and massive or columnar jointed interiors. Rarely, massive flows have rubbly, flow-brecciated tops. Massive flows grade into flow breccias whose large angular fragments have matching margins separated by fine breccia with a nearly identical appearance. Massive flows are more abundant than pillow lavas in the upper part of the formation. Calcite amygdules are commonly much larger in flows from the upper part of the formation than in the lower.

Breccias of diverse and often obscure origin are widely developed in Menzie Creek formation (Fig. 13 C to D). Most breccias are homolithic, massive, ungraded and unstratified. Fragments are angular, usually equant and one to several centimetres across, although fragments to several metres are known. The weathering colour, amygdule or phenocryst content of the fragments vary, but most appear basaltic. Identifiable pillow fragments occur sparsely and in some cases, the fragments have broken across possible pre-brecciation weathering rinds. The matrix is fine fragmental basaltic material, now calcite- or dolomite-rich, typically weathering to a distinctive, rough, high relief surface (Fig. 13C). Both clast and matrix supported breccias appear to occur (discounting effects of metamorphic flattening). Where the basal contact of a breccia unit crops out, there is locally evidence of scour of interbreccia tuffs(?) and one example of a 0.5 m reverse graded zone was encountered. The thickness of individual breccia layers is difficult to determine because of lack of bedding. Individual units 30 m thick are defined and 5 m to 10 m high outcrops of homogeneous breccias are common.

Age and Correlation

The only direct evidence of the age of the Menzie Creek formation is provided by fossils from unit OSrr. This unit overlies the Menzie Creek with a poorly exposed, probably interdigitating contact. These fossils indicate that the Menzie Creek is early Ordovician or older. Lower Paleozoic, particularly Ordovician, mafic volcanic rocks have been described at several localities in and around eastern Selwyn Basin as recently summarized by Cecile (1982). From published descriptions, many of these occurrences are similar to Menzie Creek formation e.g.: unit 5 of Tempelman-Kluit (1970a) and the upper part of Gordey's (1981) Cambro-Ordovician assemblage.

The formation in Glenlyon map area to the northwest is more abundantly porphyritic; massive flows appear to predominate over breccia and pillowed basalt. Furthermore, Menzie Creek and Vangorda equivalents are more clearly interlayered. Vangorda and Menzie Creek formations (and minor Mt. Mye formation near Tay Mountain) in this area are equivalent to Campbell's (1967) Anvil Range Group.

Unit 8b? and all Anvil Range Group basalts outside the strip in Rose Mountain (Fig. 5) along Tintina Trench (G.S.C. Map 1261A, Tempelman-Kluit, 1972) are mainly Menzie Creek basalts. Analyses IIA-IID in Table II (*op. cit.*) are properly referred to Menzie Creek formation.

A comparable, thick accumulation of volcanic rocks in southwestern Selwyn Basin has not been recognized. The presence of Ordovician volcanic rocks and of large metabasite bodies in the Vangorda formation may be indicative of massive sulphide potential in underlying rocks.

Road River Equivalents and Related Strata

Introduction

Dark coloured metasedimentary rocks thought to be equivalent to the Road River Group (Cecile, 1982; Gordey *et al.*, 1983) are included in four separate map units in Figure 3. None of these areas have been studied in any detail.

Unit SDs

Unit SDs occurs in a narrow strip southwest of the belt of Menzie Creek formation on the southwest flank of Anvil Arch. The unit is very poorly exposed but its distribution is relatively well known due to its distinctive anomalous electromagnetic signature.

The few outcrops examined by the writers are recessive black, generally featureless, non-calcareous phyllite. Locally, thin bedding striping in shades of grey is developed on foliation surfaces.

TABLE 5. Menzie Creek formation metavolcanics

Sample Number	5535	5009	4505	4648	4506	4663	4198	1458	1617	Average
SiO_2	47.50	47.00	47.40	46.50	48.00	46.50	48.30	44.80	49.40	47.27
TiO_2	3.90	2.80	2.40	1.50	3.40	2.65	2.30	1.04	2.58	2.51
Al_2O_3	14.20	15.00	14.80	15.40	14.70	15.10	14.20	14.30	12.60	14.48
Fe_2O_3*	4.70	5.45	3.15	1.70	1.80	4.90	2.45	11.50	12.60	13.02
FeO	8.60	7.20	9.50	8.75	10.00	9.00	9.00	—	—	—
MnO	0.15	0.18	0.11	0.15	0.15	0.18	0.20	0.08	0.15	0.15
MgO	5.60	5.60	4.70	9.20	5.60	5.10	7.40	4.80	6.00	6.00
CaO	7.50	9.50	6.80	8.30	8.40	9.20	7.80	8.60	8.80	8.32
Na_2O	3.00	1.60	4.00	3.30	3.80	2.20	3.85	4.90	4.10	3.41
K_2O	0.95	0.10	0.25	1.60	1.30	0	0.50	0.45	0.50	0.63
P_2O_5	0.50	0.41	0.44	0.27	0.46	0.39	0.37	0.27	0.29	0.38
S	—	—	—	—	—	—	—	0.13	0.02	0.08
LOI	3.30	5.45	6.50	3.40	2.40	4.95	3.25	8.77	2.88	4.54
Total	99.90	100.29	100.25	100.07	100.01	100.17	99.62	99.64	99.92	
Zr ppm	220	180	185	135	190	160	160	156	188	175
Y ppm	12	(5)	5	(5)	10	6	(5)	27	27	11
Normalized for total = 100% and LOI + S = 0%										
SiO_2	49.17	49.56	50.67	48.10	49.18	48.83	50.12	49.37	50.92	49.55
TiO_2	4.04	2.95	2.57	1.55	3.48	2.78	2.39	1.15	2.66	2.62
Al_2O_3	14.70	15.82	15.82	15.93	15.06	15.86	14.73	15.76	12.99	15.19
Fe_2O_3	4.87	5.75	3.37	1.76	1.84	5.15	2.54	12.67	12.99	13.66
FeO	8.90	7.59	10.15	9.05	10.24	9.45	9.43	—	—	—
MnO	0.16	0.19	0.12	0.16	0.15	0.19	0.21	0.09	0.15	0.16
MgO	5.80	5.90	5.02	9.52	5.74	5.36	7.68	5.29	6.18	6.28
CaO	7.76	10.02	7.27	8.59	8.61	9.66	8.09	9.48	9.07	8.73
Na_2O	3.11	1.69	4.28	3.41	3.89	2.31	4.00	5.40	4.23	3.59
K_2O	0.98	0.11	0.27	1.66	1.33	0	0.52	0.50	0.52	0.66
P_2O_5	0.52	0.43	0.47	0.28	0.47	0.41	0.38	0.30	0.30	0.40
Total	100.01	100.01	100.01	100.01	99.99	100.00	100.00	100.01	100.01	

* Includes FeO calculated as Fe_2O_3 if FeO not given separately.
LOI = loss on ignition.
Analyses by Bondar-Clegg using XRF with Y checked by neutron activation.
( ) indicates less than the detection limit within parentheses.
All values are weight per cent unless otherwise noted.

An important, but volumetrically minor lithology is fetid, fine-grained, dark grey to black bioclastic limestone. The limestone occurs in lenses up to a metre thick but with uncertain lateral dimensions. The known localities occur in the lower part of the map unit. The limestone contains abundant crinoid ossicles, some of which have twin axial canals. The limestone has yielded conodonts of eary Middle Devonian age (Orchard, pers. comm. 1982; Cameron, pers. comm. 1977). Near Swim Lake, the unit contains very minor thin tan weathering dolomite similar to that in Unit OSrr (see below).

The upper and lower contacts are not exposed, but both are thought to be gradational. Metavolcanics similar to the Menzie Creek formation occur interlayered with the unit near its base. The upper portion appears to grade into black, grey and beige chert of the Earn Group.

Minor rock types in Menzie Creek formation include thin bedded, commonly graded, tuffs or fine, volcanic fragment-rich, epiclastic rocks with very minor interlayered, fine-grained, stratified breccia. Near the top of the formation, calcite- or dolomite-cemented basaltic sandstone, minor basalt cobble conglomerate and sandy grey limestone or orange weathering dolomite up to 10 m thick are interstratified with the volcanic assemblage. These sedimentary rocks and the abundance of large amygdules in nearby massive flows indicate, at least, local shoaling of the volcanic pile.

This description applies mainly to areas northeast of Anvil Batholith, where the formation is best studied. Southwest of Anvil Batholith, the formation's characteristic lithology is olive green, amygdaloidal, chloritic phyllite. Pillow lavas and breccia with lesser thin bedded tuff also occur, but unlike the northeast area, the Menzie Creek is interlayered with abundant black phyllite. This part of the formation is highly foliated, recessive and has not been studied in detail. The interlayered black phyllite gives a characteristically "busy" EM signature useful in mapping its extent in areas of poor exposure.

Volcanic rocks of Menzie Creek formation show a limited range of basaltic composition and were probably alkalic basalts originally (Table 7). The metabasalts are extensively carbonated to orange weathering quartz ± fuchsite (?) rock in the extreme case. Though the analyses in Table 5 are of least altered material, they sould be approached with caution. Andesite has been reported in Glenlyon map area (Fig. 1, Campbell, 1967) and may be present, but is not suggested in our analyses.

The abundance of breccia, greater thickness of the formation, evidence of shoaling, general lack of thin pelagic sedimentary interlayers and association with large discordant mafic plugs northeast of Anvil Batholith are interpreted to imply a volcanic centre in that area. A large area of pre-metamorphic bleaching (to sericite, quartz, carbonate) enclosing folded or foliaform stringers of quartz and calcite with sphalerite, pyrite, chalcopyrite and minor galena (KD deposit, Fig. 3, Mineral Occurrence No. 9) perhaps coincidentally occurs near this centre. This may be a minor occurrence of volcanogenic, fumarolic-type mineralization.

Unit SDa

Unit SDa occurs in a triangular fault-bounded area 14 km northeast of Mt. Mye. The upper and lower contacts are not exposed.

The lowest portion of the unit exposed is characterized by laminarly bedded, dolomitic siltstone about 100 m of which is present. A zone of poor exposure separates these siltstones from overlying massive orthoquartzite and dolomite. This interval may be underlain by dark shale. Medium-grained, well sorted pure orthoquartzite occurs in a bed or beds 10 m to 20 m thick. The orthoquartzite is overlain by about 30 m of medium crystalline light grey to white, white weathering massive dolomite. The dolomite has yielded Middle Devonian fossils (locality F3; Tempelman-Kluit, 1972).

The dolomite is overlain by an unknown thickness of thin bedded, dark grey to black, non-calcareous shale and siltstone with characteristic thin bedding striping on cleavage surfaces.

The dolomitic siltstone is identical to the basal portion of the late early Silurian to middle Devonian Askin Group (Wheeler, Green and Roddick, 1960) that crops out 150 km southeast of the Anvil district. The dolomite and quartzite are very similar to upper parts of the Askin Group. The Askin Group defines the

extent of the Cassiar Platform, and unit SDa contains the only strata in the Anvil District that resemble this important regional unit. The dark coloured sediments overlying the quartzite are very similar to strata of the basal Earn Group (Gordey *et al.*, 1983) examined by the writers southeast of Anvil District and in the Akie District (Jefferson *et al.*, 1983) of northeastern British Columbia (Fig. 2).

Unit OSrr

Unit OSrr occurs in an irregular area 15 km north-northeast of Mt. Mye. Approximately 250 m to 400 m of sequence is exposed there.

The basal two-thirds of the unit at that locality are black, non-calcareous, shale to phyllite. The upper third of the unit is brown weathering, dark grey shale with very minor tan weathering unlaminated dolomitic siltstone. Near the top of the unit is a 1 m to 30 m thick laterally discontinuous bed or beds of orthoquartzite. The quartzite is medium-grained, pure and massively bedded. It is similar to the quartzite of unit SDa, but the laminated dolomitic siltstone characteristic of unit SDa is not present in unit OSrr. The shales and tan weathering dolomitic siltstone of the upper part of the unit contain graptolites at several localities (including localities F1 and F2; Tempelman-Kluit, 1972) of middle Ordovician or early Silurian age. A few kilometres west of these localities, Gordey (1983) has recently discovered lower Ordovician graptolites from near the base of a similar shale sequence also divisible into lower black and upper brown weathering parts. Quartzite is not present there. The younger graptolitic rocks occur very close to the orthoquartzite and probably overlie it but the relative stratigraphic positions of these rocks are not well known due to poor outcrop. The quartzite is very similar to that of unit SDa, however, laminated dolomitic siltstone characteristic of the latter unit is absent. If unit SDa is equivalent to the Askin, as seems likely, then it is not likely that the quartzites correlate, as those of unit OSrr appear to be older.

The lower contact of unit OSrr is not well exposed. The distribution of local shale and volcanic float suggests that the unit is interlayered with the upper part of the Menzie Creek formation. Unit OSrr is also thought to overlie the Menzie Creek because of its northerly sheet dip, the regular asymmetric distribution of colour in the shales and the fact that Menzie Creek bedded tuffs and pillow lavas at many localities south of the belt of OSrr dip north and are north facing. The reader should consult Gordey (1983) for an alternative interpretation of this area.

Southeast of the locality just described, the unit consists of black shale to phyllite and drab black phyllitic chert (unit OSrr ? in Fig. 3). Near the top of this sequence is tan to orange weathering variably dolomitic quartzite (Sq?) and siltstone (locally irregularly laminated) that may be related to unit SDa.

The affinity of the map unit is uncertain in this area. Gordey (1983) considers most of this area to be underlain by rocks older than the graptolitic shales and a facies equivalent of the Menzie Creek and Vangorda formations. North of Orchay Pluton (Fig. 3), the black shale and chert sequence is underlain by calc-silicate and calcareous phyllite similar to Vangorda formation and basalt similar to Menzie Creek formation; thus, we consider the black shale and chert sequence to be younger than these formations.

Earn Group

Rocks tentatively considered equivalent to the Earn Group (Gordey *et al.*, 1983) occur in two belts on the northeast and southwest flanks of Anvil Arch respectively. The sequences in both areas are chert-rich. In the northeast, chert-bearing clastics are minor and a major limestone-bearing unit is present. On the southwest flank of the Anvil Arch, limestone is minor and chert pebble conglomerate is an important rock type.

In the southwestern belt, the Earn Group consists of black, grey, beige and green, thinly interbanded cherts and siliceous phyllite of similar colours. The dominant colour at the base of the unit is dark grey and black. The colour changes gradually up section to grey and beige dominant with increasing proportions of dull olive green chert so that the top of the unit is beige and green chert dominant. The lower half of the unit contains abundant chert pebble conglomerate and grit. Rocks of the Earn Group in this belt are very highly strained and the conglomerate clasts are strongly flattened into the generally layer parallel metamorphic foliation. Since folds in the thinly banded chert sequence are highly attenuated and rootless, it is commonly difficult to distinguish strongly deformed thin-banded chert from chert pebble to cobble conglomerate.

Near the top of the unit, minor grey calcareous phyllite, limestone and orthoquartzite are interlayered with the phyllitic cherts. Several tens of metres beneath the calcareous rocks is the most important of several layers of stratiform barite that occur through the Earn Group sequence on the southwest flank of the Anvil Arch. The barite is finely crystalline and medium to light grey. It is hosted by and interbanded with beige phyllitic cherts and like the cherts, it is strongly foliated. The barite horizons are up to 12 m thick and have been traced for several kilometres. Several other barite horizons of lesser extent occur beneath the major unit including a discontinuous one near the base of the Earn Group.

This chert and chert conglomerate sequence is considered correlative with the Earn Group on the basis of its lithologic similarity. The age of the sequence is perhaps bracketed by the occurrence of Middle Devonian fossils in rocks structurally beneath and Pennsylvanian or Early Permian fossils (see below) in rocks structurally overlying, however, it is yet to be demonstrated that this is a stratigraphic sequence. The upper and lower contacts of the Earn Group here are gradational colour changes.

Anvil Range Group

Our use of the term Anvil Range Group follows the redefinition by Tempelman-Kluit (1972) and his subsequent usage (Tempelman-Kluit, 1979). The Anvil Range Group was originally named by Campbell (1967) for rocks exposed in Glenlyon map area. The sequence to which the name was originally applied, we now consider Mt. Mye, Vangorda and Menzie Creek formations.

The Anvil Range Group consists of two units. An upper volcanic unit characterized by unfoliated but locally sheared, massive, but commonly finely brecciated, dense, fine-grained, dark green, commonly epidotized and hematite-veined basalt (Table 6). The basalt weathers to characteristic reddish brown, rounded, knobby but resistant outcrops. The basalt is underlain by ribbon-bedded green and red chert, tuffaceous chert and minor tuff. The contact between basalt and chert is intercalated as described by Tempelman-Kluit (1972). This sequence is seen only on the Rose Mountain ridge, but similar green cherts lacking associated basalt or significant red chert occur locally on the northeast flank of Anvil Range (not differentiated from uDM in Fig. 3).

The Anvil Range Group and Menzie Creek formation have been previously mapped as one unit. Basalts of the Anvil Range Group are distinguished from those of the Menzie Creek by their lack of appreciable amygdules, lack of diverse volcanic structures and textures, lack of metamorphic foliation, darker colour and distinctive weathering colour. The Anvil Range Group is only exposed on the Rose Mountain ridge. That locality is fairly typical of much of the unit in the belt from Faro to Watson Lake (Fig. 1) and we believe should be the Group's type locality. The basalts to the southeast, however, are quite clearly pillowed and not everywhere associated with red chert, for example in the Campbell Range (Fig. 1).

The Anvil Range Group bears a close spatial relationship to ultramafic rocks, layered and massive gabbro, diabase, locally as dyke complexes, rodingite and orange weathering, carbonated, fuchsitic ultramafics.

The prominent light grey weathering carbonates of Unit 8c of Tempelman-Kluit (1972) (PPc, Fig. 3) occur in Tintina Trench across Vangorda fault zone and may not be related to the Anvil

TABLE 6. Anvil Range Group volcanics

Sample Number	6064	6176	6322	4144	4260	Average
SiO_2	45.20	46.70	47.40	47.00	47.20	46.7
TiO_2	1.50	2.20	1.05	1.50	1.20	1.49
Al_2O_3	16.30	14.00	14.70	15.60	15.60	15.24
Fe_2O_3	13.30	4.85	2.15	2.30	3.30	12.05
FeO	—	9.00	7.85	7.60	6.45	—
MnO	0.15	0.32	0.17	0.15	0.17	0.19
MgO	5.80	7.40	8.70	10.40	7.20	7.90
CaO	10.50	9.20	11.50	8.00	11.80	10.20
Na_2O	3.10	3.50	2.35	3.15	1.90	2.80
K_2O	0.85	.80	0.35	0.25	.30	0.51
P_2O_5	0.10	0.20	0.13	0.20	0.15	0.16
LOI	3.05	1.60	3.50	3.55	4.60	3.26
Total	99.85	99.77	99.85	99.70	99.87	
Zr ppm	—	135	88	120	105	112
Y ppm	—	14	(5)	7	(5)	8
Normalized for total = 100% and LOI + S = 0%						
SiO_2	46.69	47.57	49.20	48.88	49.54	48.38
TiO_2	1.55	2.24	1.09	1.56	1.26	1.54
Al_2O_3	16.84	14.26	15.26	16.22	16.37	15.79
Fe_2O_3*	13.74	4.94	2.23	2.39	3.46	12.48
FeO	—	9.17	8.15	7.90	6.77	—
MnO	0.15	0.33	0.18	0.16	0.18	0.20
MgO	5.99	7.54	9.03	10.82	7.56	8.36
CaO	10.85	9.37	11.94	8.32	12.39	10.57
Na_2O	3.20	3.57	2.44	3.28	1.99	2.90
K_2O	0.88	0.81	0.36	0.26	0.31	0.52
P_2O_5	0.10	0.20	0.13	0.21	0.16	0.16
Total	99.99	100.00	100.01	100.00	99.99	

* Includes FeO calculated as Fe_2O_3 if FeO not given separately.
LOI = loss on ignition.
Analyses by Bondar-Clegg using XRF with Y checked by neutron activation.
( ) indicates less than the detection limit within parentheses.
All values are weight per cent unless otherwise noted.

Range Group. It appears to be part of the Yukon-Tanana Terrane, since at Grew Creek and Blackfox Bend (Fig. 1) on Pelly River it shares interlayered quartz grit with underlying members of the blue quartz grit-bearing Yukon-Tanana sequence.

Intrusive Rocks

Anvil Plutonic Suite

Late- and post-metamorphic intrusive rocks cutting the Anvil metamorphic complex occur as large plutonic bodies or as dykes, sills and plugs. Three major intrusions are recognized, Anvil Batholith, Orchay Pluton and Marjorie Pluton (Fig. 3). Collectively, they are termed the Anvil Plutonic Suite (Pigage and Anderson, 1985) and range in composition from granite to granodiorite with biotite, quartz, plagioclase and K-feldspar as ubiquitous phases. Variable amounts of hornblende and muscovite distinguish discrete intrusive phases (Pigage, pers. comm., 1982), but relationships between the phases are poorly understood. A description of the plutonic suite was first given by Tempelman-Kluit (1972) and a more recent description can be found in Pigage and Anderson (1985).

The Anvil Batholith is typically biotite-muscovite or biotite-hornblende quartz monzonite, either medium crystalline and equigranular or with coarse K-feldspar megacrysts. The vast majority of the batholith shows cross-cutting relationships to the S_2 foliation (see structure section) and post-dates the major deformations. Little, if any, contact metamorphic effects are seen such as hornfelsing or retrogression of regional metamorphic phase assemblages. Contacts of the batholith are sharp and non-migmatitic. These observations suggest a "hot-into-hot" intrusive relationship, implying the heat flow regime responsible for the second regional metamorphic event (see below) is related to the batholith. Very locally, margins of Anvil Batholith are weakly to moderately foliated by a relatively shallowly dipping foliation.

Orchay Pluton is smaller than Anvil Batholith but may be connected to it at depth beneath the crest of Anvil Arch. It is biotite-hornblende quartz monzonite texturally similar to Anvil Batholith and shows post-metamorphic, non-migmatitic intrusive contacts.

The Marjorie Pluton (Fig. 3) is mapped only in reconnaissance fashion. It includes hornblende-biotite quartz monzonite showing both medium-grained equigranular and coarsely porphyritic textures. Hornblende phenocrysts are locally coarsely crystalline, seived and irregular. Poikilitic, K-feldspar megacrysts are also common. Quartz phenocrysts characterize this suite and are commonly smoky. Cross-cutting relationships between the Marjorie and Orchay Plutons are uncertain because the contact area is very poorly exposed. Roddick and Green (1961) considered the Marjorie Pluton to be a subvolcanic equivalent of the South Fork Volcanics.

Anvil Dyke Suite

The Anvil Dyke suite has been studied in detail only near the Faro deposit. This discussion focuses mainly on that area, but most dykes in the district fall into one of the following categories. The members of the dyke suite are more abundant with depth or proximity to Anvil Batholith and may be related to it. All members of the dyke suite are post metamorphic and cut the Batholith, but their relative ages are poorly known.

The most voluminous members of the dyke suite are northeast-trending, porphyritic, medium to dark green hornblende diorite dykes which cut megacrystic quartz monzonites of the Batholith. The diorite body in the north end of the Faro open pit and the body immediately northeast of Faro deposit, zone 2, are among the largest examples (Fig. 29). Several diorite dyke sets cut the Faro deposit with a prominent set developed along the fault between zones 1 and 3 (Figs. 30 and 32). Elsewhere, hornblende diorite dykes commonly follow northeast-trending faults and fractures.

Intrusion of hornblende diorite dykes and sills in the calc-silicated Vangorda formation above zone 3 produced extensive brecciation locally involving the sulphide deposit (Fig. 21). This

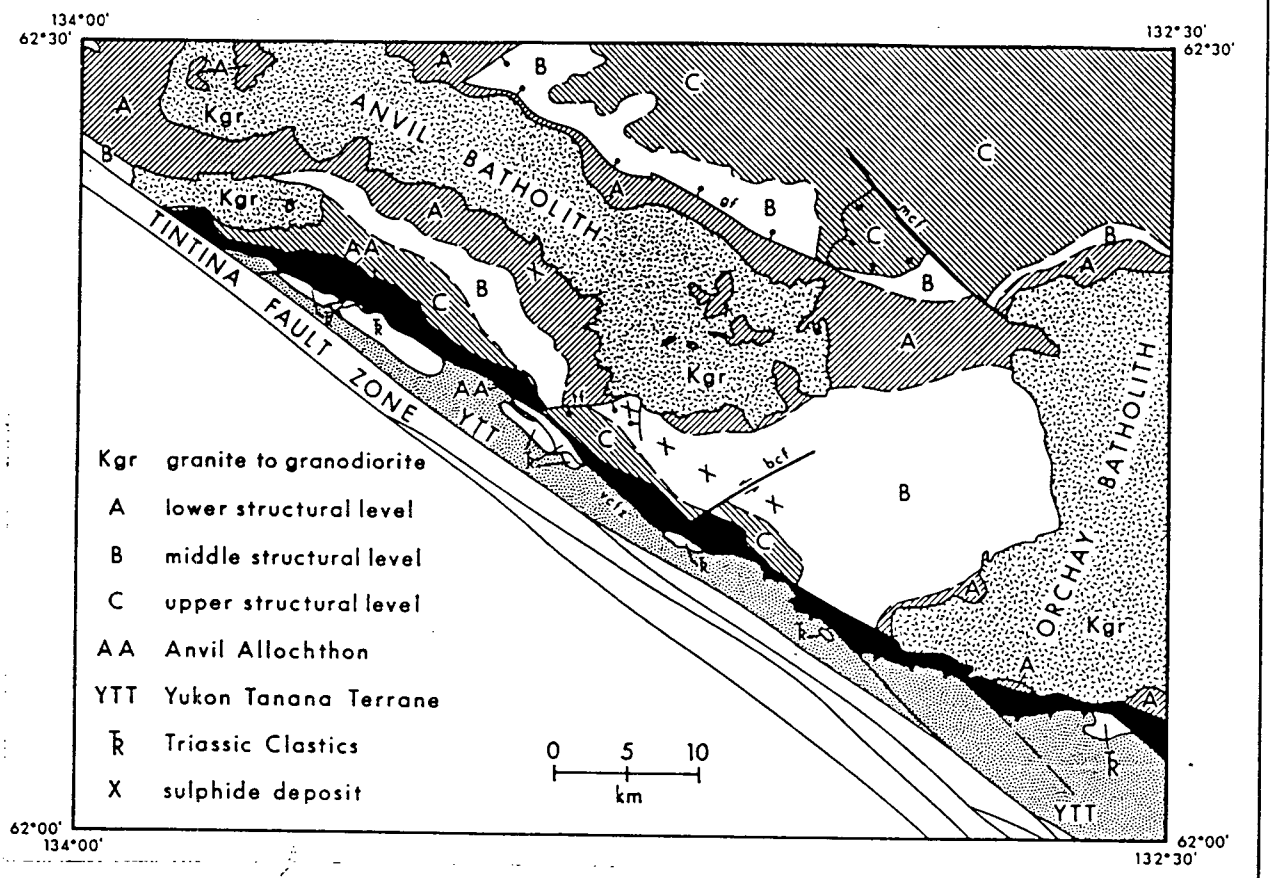


FIGURE 14. Distribution of the three structural levels of the Anvil District. AA is possibly allochthonous Anvil Range Group basalt and chert (Anvil Allochthon of Tempelman-Kluit, 1979). Black represents sheared mafic and ultramafic rocks of Vangorda Creek Fault zone. Triassic clastics are polymict conglomerates, shales and limestone found adjacent to Vangorda Creek Fault zone, see Tempelman-Kluit (1972) for descriptions. tf = Tie Fault, vcfz = Vangorda Creek Fault zone, bcf = Blind Creek Fault, mcf = Mye Creek Fault, gf = Graphite Fault.

brecciation presumably resulted from vapour pressure of the melt having exceeded confining pressure of the superincumbent strata and resulted in a coarse, angular, clast supported breccia with a rock flour and minor, devitrified, altered, chloritized diorite glass matrix. The age of the brecciation is at least post D_3 (see below). This breccia body is the only example known in the district; it occurs immediately adjacent to the Faro orebody and in cross section, the deposit can be interpreted to be zoned with respect to the centre of brecciation. The post-metamorphic age of the breccia shows the breccia forming event cannot be related to the ore-forming event since the ores are clearly pre-metamorphic. Rare diorite fragments occur in the breccia. However, unbrecciated diorite and minor medium-grained, equigranular, dark pink monzonite intrude the breccia, apparently following joint surfaces and post-dating the main stage of brecciation.

Intrusion of quartz-feldspar porphyry dykes, minor sills, and irregular intrusive masses and leucocratic tourmaline-garnet pegmatite dykes mark the last intrusive event. Both rock types crosscut hornblende diorite dykes northeast of the Faro deposit, but their relative ages are not known.

Quartz-feldspar porphyry also cuts quartz monzonite of Anvil Batholith north of the Dy deposit. The porphyry consists of smoky, grey or clear, euhedral and subhedral, locally doubly terminated and/or embayed quartz, subhedral feldspar and commonly biotite in a light coloured, generally aphanitic matrix. The smoky quartz-bearing character of these rocks and rocks of Marjorie Pluton may imply a genetic relationship and suggest the Marjorie Pluton is younger than Orchay Pluton. A similar, possibly younger quartz-feldspar porphyry plug occurs northeast of Anvil Batholith (unit TV in Fig. 3).

Well-foliated, garnet-bearing granitic sills up to a few metres thick occur in schists near the contact of Anvil Batholith. The occurrence of garnet and tourmaline in the late stage dykes as well as in the batholith itself reinforces the probable relationship between the plutonic and dyke suites.

The best and most recent K/Ar ages on rocks of the Anvil Batholith fall in the range 95 to 100 Ma (Pigage, pers. comm., 1982), an age range, in general confirmed and extended to other members of the plutonic suite by Rb/Sr work (Pigage and Anderson, 1985), though one sample of the Orchay phase yielded a single, questionable Rb/Sr isochron age of 61 Ma.

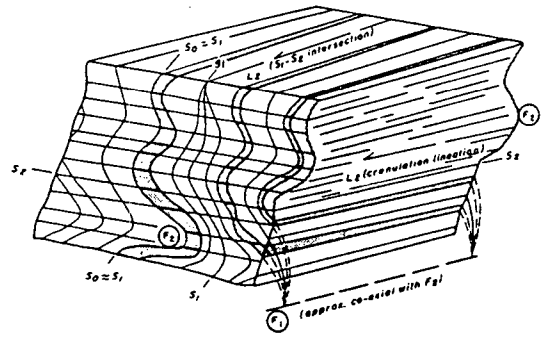
Structure

Introduction

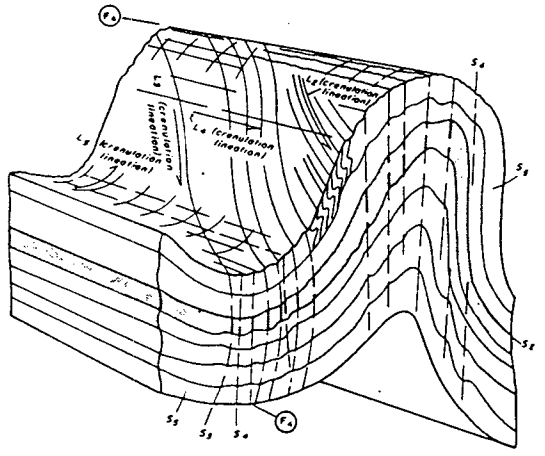
The Anvil District is a structurally complex polymetamorphic and polydeformational terrane. Metasediments of the district contain evidence for at least five phases of deformation of which the first two are the most significant in that they are penetrative, regionally developed and accompanied by regional metamorphism. They are further of great importance in that they significantly affect the shape and character of the orebodies.

The metasediments are domed to form a northwest-trending structural culmination, Anvil Arch, cored by Cretaceous granitic rocks of the Anvil plutonic suite (Fig. 3). Grade of metamorphism decreases in intensity radially outward and upward from the granitic rocks in the core of the arch. Middle amphibolite facies rocks occur near the plutonic core, but much of the district is greenschist facies.

The most prominent and characteristic fabric element of the metasediments of the Anvil District is a shallowly dipping foliation commonly sub-parallel to compositional layering. This foliation varies in its manifestation depending on depth in the structural sequence. Other deformational features likewise vary



A Schematic post-D_2 geometry



B Schematic post-D_5 geometry (F_3 and F_5 omitted)

FIGURE 15. Summary diagrams showing the fabric elements in rocks of the Anvil District:

$D_{1\text{-}5}$ refers to deformations 1-5.

$S_{1\text{-}5}$ refers to foliations (surfaces) formed during D_1 through D_5. S_0 is bedding.

$L_{1\text{-}5}$ refers to lineations formed during D_1 through D_5.

$F_{1\text{-}5}$ refers to folds and fold axes formed during D_1 through D_5.

See Table 7 for details of structural terminology.

(A) summarizes the post D_2 geometry and is an idealization of the greenschist facies phyllites of the middle structural level. (B) shows the post D_2 deformations, superimposed on near pervasive S_2 where parallel to compositional layering, and is an idealization of the amphibolite facies schists of the lower structural level.

according to depth in the pile. Structural position thereby provides a convenient framework for discussion of the fabric of rocks of the district. We divide the district into three gradational and somewhat arbitrary regimes: lower, middle and upper structural levels (Fig. 14).

In the lower level, amphibolite facies metamorphic rocks contain an intensely developed schistosity into which compositional banding is transposed on most observable scales. Development of features characteristic of this level is generally confined to the lower Mt. Mye formation, however, strata as high as the Menzie Creek formation are locally affected.

The middle level's rocks are generally in the greenschist facies with characteristic intensely developed crenulation cleavage. In many outcrops, banding is transposed into the dominant foliation but exceptions are numerous and there are many examples where the over-all dip of layering is at strong angles to the foliation over large areas. The middle level is best developed in the upper Mt. Mye formation and throughout the Vangorda formation.

In the upper structural levels, rocks were deformed at low or sub-greenschist facies and they commonly have a well developed phyllitic to slaty cleavage which can be found at high angles to well preserved bedding. In the upper levels, the characteristic low-angle cleavage noted above is present but very weakly developed and an earlier foliation is dominant. This structural level is best developed in the Menzie Creek and younger units.

Table 7 summarizes the nomenclature applied to various elements of the fabric of Anvil District rocks and the manifestation of these elements at the three structural levels referred to above. Figure 15 summarizes the geometric relationships of the fabric elements of rocks of the lower and middle structural levels.

The structure of the district has only been studied in detail on the southwest flank of the Anvil Arch where extensive drill control and aritificial exposures supplement the meager outcrop of the district. Reconnaissance work elsewhere demonstrates that the remainder of the district shows a similar structural style, but the specific geometry of these areas is known only in a most general way.

Lower Structural Level

The lower structural levels of the metamorphic pile are best exemplified by the area of the Faro deposit (Fig. 16). Here, S_2 is a penetrative schistosity axial planar to close to isoclinal folds in an earlier foliation (S_1) and compositional banding. S_1 and banding are largely transposed into S_2 with preservation only in the hinges of F_2 folds and particularly in lithons which are commonly only noticeable on a microscopic scale (Fig. 17). F_2 fold axes and the parallel L_2 crenulation lineation trend 300 degrees to 330 degrees plunging shallowly to the northwest. The L_2 direction is sub-parallel to the elongation of the Faro deposit. S_2 dips about 20 degrees to the southwest away from the core of the Anvil Arch and the batholith. The majority of F_2 folds verge southwest. Though mesoscopic D_2 folds are developed in ores of the Faro deposit and mesoscopic to microscopic folds are not uncommon in the host rocks, there is no evidence in the results of deep drilling near the deposit of any large-scale folds of that generation that could repeat the deposit or the stratigraphy of the host rocks. The over-all shape of the deposit may be the result of large intrafolial D_2 folds but the internal geometry is not well known. Like S_2, large-scale compositional layering also dips shallowly southwest but tends to dip more shallowly than S_2. This may be the result of unmapped northeast vergent F_1 folds that are expected from relations elsewhere in the district (see below) and would be parasitic to a larger first-phase fold postulated to explain the local map pattern north of the Faro deposit. Small-scale F_1 folds are not, however, widely preserved in the Faro deposit area, nor are they anywhere in the deeper parts of the sequence.

Three temporally and geometrically distinct post D_2 deformations are recognized in the Faro deposit area.

D_3 deformation and metamorphism produced a weak, non-penetrative metamorphic foliation, S_3 axial planar to F_3 folds in S_2 and compositional banding. S_3 strikes 150 degrees to 160 degrees and has a sub-vertical dip. F_3 fold axes plunge shallowly southwest parallel to a penetrative crenulation lineation, L_3. F_3 folds are close, parallel flexural slip folds in S_2 whose amplitudes vary from 10 cm to 10 m and wavelengths are up to 15 m.

D_4 deformation features include a non-penetrative, axial planar, metamorphic foliation, S_4, striking 110 degrees to 120 degrees and dipping sub-vertically to moderately southwest and a non-penetrative crenulation lineation parallel to F_4 fold axes. F_4 folds are open to close with doubly plunging axes trending 110 degrees to 120 degrees. Folds of this generation (Fig. 18A) are the largest recognized in the Faro deposit and complicate the over-all shape of the deposit (Figs. 30 and 31). Folds with amplitudes of 15 m to 40 m and wavelengths of 75 m have been recognized but their size varies laterally through the deposit. These fold amplitudes decrease rapidly with depth in the deposit, suggesting that significantly different mechanical properties between sulphides and host rocks controlled the folding. Small-scale northeast directed thrust faulting along pre-

TABLE 7. Summary of nomenclature and manifestation of structural features

Event	Nomenclature: Fabric Element	Nomenclature: Definition	Manifestation: Lower Structural Level	Manifestation: Middle Structural Level	Manifestation: Upper Structural Level	Orientation: SW Flank of Anvil Arch	Orientation: NE Flank of Anvil Arch	Associated Faulting	Associated Intrusive Activity	Associated Metamorphism
D_1	S_0	bedding	not preserved, transposed into S_2	rarely preserved, largely transposed into S_1 and intensely crenulated into D_2 folds	widely preserved bedding	over-all sheet dip of compositional units moderately to shallowly SW	over-all sheet dip of compositional units moderately to shallowly NE	possible syn-depositional growth faults	mafic sill emplacement	none
	S_1	planar structures formed during D_1	schistosity locally preserved in lithons and small D_2 folds (mostly)	phyllitic axial planar cleavage intensely crenulated by F_2	slaty to phyllitic cleavage axial planar to F_1 folds	moderately to steeply SW dipping in high levels	dips shallowly in higher levels, poorly known in deeper levels	small NE directed thrusts on N flank of range and possible large scale overthrusting on south flank emplacing Anvil Range Group	none identified	regional metamorphism greenschist to amphibolite facies
D_1	F_1*	folds formed during D_1	not well preserved on outcrop scale but inferred on larger scale	rarely preserved, generally tight to isoclinal folds S_0. Northeasterly vergent.	well developed close to tight folds in S_0	axial planes dip moderately SW, axes trend NW-SE sub-parallel to L_2	poorly known			
	L_1	linear structures formed during D_1	not preserved due to D_2 overprinting	rarely preserved as compositional striping on S_1, largely overprinted by D_2	compositional stripping in S_1 (S_0xS_1)	NW-SE sub-parallel to L_2	poorly known in lower levels - Trend NW-SE in upper levels			
D_2	S_2	planar structures formed during D_2	nearly pervasive schistosity axial planar to isoclinal folds in S_1 and compositional layering ubiquitous development	strongly developed crenulation cleavage axial planar to F_2 folds	weak crenulation cleavage not well developed in highest levels	shallow SW sheet dip	shallow NE sheet dip	none conclusively identified	possible intrusion of Anvil Batholith during waning stages	regional metamorphism greenschist to amphibolite Buchan facies series
	F_2	folds formed during D_2	small isoclinal rootless folds in compositional layering and S_1, common rootless isoclines in quartz veins. Larger scale folds probably present but not well documented.	intensely developed small scale folds in S_1 and compositional layering	not widely developed except as microscopic folds in S_1 related to L_2 crenulation lineation	axial planes parallel S_2, axes parallel L_2, commonly SW vergent	axial planes parallel S_2, axes L_2, vergence unknown			
	L_2	lineations formed during D_2	poorly preserved lineation due to (1) hinges of microlithons,(2) waviness on S_2 caused by hinges of quartzose layers in microlithons, and (3) onlap lineation	ubiquitous development of wrinkle lineation on S_1 in noses of F_2 and widely developed onlap lineation	weak wrinkle lineation on S_1	shallowly doubly plunging in direction 135° on average	shallowly doubly plunging in direction 135° on average			
D_3	S_3	planar structures formed during D_3	generally weak crenulation cleavage but more strongly developed locally in vicinity of larger folds	locally developed weak to moderate crenulation cleavage	not identified with certainty	moderate to steep SW sheet dip	not well known	none conclusively identified	possibly related to late stages of intrusion of Anvil Batholith	waning stages of D_2 metamorphism in lower levels, none in middle and upper levels
	F_3	folds formed during D_3	locally developed, close, flexural slip folds in S_2 with wavelength and amplitude of several cm. Larger folds near FARO deposit	mesoscopic folds not generally developed but broad regional warps in S_2 appear to be genetically related	not identified with certainty	axial planes parallel S_3, axes parallel L_3, generally NE vergent	not well known			
	L_3	lineations formed during D_3	coarse** wrinkle lineation in S_2 parallel to F_3 axes	fine** wrinkle (crenulation) lineation on S_2	not identified with certainty	shallowly doubly plunging in direction 155°	shallowly doubly plunging in direction 155°			

TABLE 7. Summary of nomenclature and manifestation of structural features

Nomenclature			Manifestation			Orientation		Associated Faulting	Associated Intrusive Activity	Associated Metamorphism
Event	Fabric Element	Definition	Lower Structural Level	Middle Structural Level	Upper Structural Level	SW Flank of Anvil Arch	NE Flank of Anvil Arch			
D_4	S_4	planar structures formed during D_4	similar to S_3	similar to S_3	weak crenulation cleavage only locally developed	strike 110°-120° dip moderately SW to subvertical	not well known	small northeast directed thrusts	possibly related to late stages of intrusion of Anvil Batholith and formation of Anvil Arch	as above
	F_4	folds formed during D_4	similar to F_3	similar to F_3	broad warps in S_1 and S_0 appear geometrically related	axial planes parallel S_4, axes parallel L_4, generally NE vergent	not well known			
	L_4	lineations formed during D_4	coarse wrinkle lineation on S_2	coarse wrinkle lineation on S_2	coarse wrinkle lineation on S_1 developed locally in lower parts of level	shallowly doubly plunging in direction of 110°-120°	shallowly doubly plunging in direction 110°-120°			
D_5	S_5	planar structures formed during D_5	fracture cleavage axial planar to small folds in S_2	fracture cleavage to close spaced jointing	not identified	strike 60° - 80°, subvertical dip	strike 60° - 80°, subvertical dip	normal faults trending 60°, possibly related to Tie Fault and other extensional faults	possibly Anvil Dyke Suite, especially 60° trending dykes	none
	F_5	folds formed during D_5	open chevron-style folds with amplitudes up to several tens of centimetres	not widely developed, local open, low amplitude folds on outcrop scale. Weakly developed chevron-style folding	not identified	axial planes parallel S_5, axes parallel L_5	unknown			
	L_5	lineations formed during D_5	weak coarse wrinkle lineation on L_2	very wide spread crenulation lineation on S_2 locally but generally only intersection of S_5 and S_2	not identified	doubly plunging in direction 60°-80°	doubly plunging in direction 60°-80°			

* F is also used to refer to the axial plane and axis of the fold depending on context.

** Coarse wrinkle (or crenulation) lineation (see Fig. 188) crests spaced about 0.5 cm, fine wrinkle lineations spaced about 1 mm or less.

existing S_2 surfaces occurred during D_4. Northeast and north of the Faro Deposit, F_4 folds with amplitudes of over 100 m occur (Figs. 16 and 30).

Features developed during the D_5 event occur only locally in the Faro deposit area. S_5 is a weak non-penetrative foliation axial planar to small folds in S_2. A weak crenulation lineation, L_5, parallels the fold axes and represents the intersection of S_5 with S_2. S_5 strikes 60 degrees to 80 degrees and dips subvertically. D_5 was associated with normal faults which cut the above thrusts.

Middle Structural Level

A partial cross section through the southwest flank of the Anvil Arch (Fig. 19) illustrates the features of the middle structural level of the terrane. The area of the Grum, Vangorda and Dy deposits (the Vangorda Plateau) is the best studied portion of this structural level and an appreciation of the over-all style of this area was essential to the discovery of the deeply buried Dy deposit and will be to its continuing delineation.

The most prominent feature of the cross section is the gross right way up panel of stratigraphic units forming the flanks of the Anvil Arch. Superimposed on this panel are several Z symmetry, northeast vergent, first-phase folds (F_1) in the over-all compositional layering (S_0) with amplitudes in excess of 500 m. Axes of these folds trend northwest-southeast and are shallowly doubly plunging. The axial surface of this fold generation is paralleled by a steeply southwest dipping foliation (S_1) which is cut and crenulated by a shallow southwest dipping, close spaced, younger foliation (S_2). This younger crenulation foliation is axial planar to ubiquitous, dominantly S symmetry, southwest vergent, folds (F_2) in S_1. These second generation folds are of significantly smaller wavelength and amplitude than the first generation folds and impart a macrolithon fabric to the rocks. The F_2 folds are approximately coaxial with F_1. F_2 axes are parallel to the L_2 crenulation which trends about 330 degrees on the average and plunges most commonly shallowly to the northwest but is doubly plunging over-all. L_2 is parallel to the elongation of each of the ore deposits and on a district scale follows the curvilinear trend of the deposits (Fig. 20).

A closer view of the same geometry and the structural style is provided by a representative cross section through the Grum deposit (Fig. 33). S_1 is axial planar to a megascopic, Z symmetry, tight to isoclinal, first phase antiform synform pair outlined by the contact of the Mt. Mye and Vangorda formations and the ore layers. Compositional layering (S_0) as well as S_1 are folded into close to tight, S symmetry folds whose axial plane parallels a younger shallow southwest dipping crenulation cleavage, S_2. The failure to recognize such a large-scale F_1 fold would lead to a quite different picture of the Grum deposit probably involving facies changes. Conversely, the inherent difficulty of convincingly demonstrating the presence of F_1 folds through the D_2 overprint greatly limits the ability to deduce the original geometry of these deposits.

Geometric relationships characteristic of the outcrop or mesoscopic scale at this structural level are illustrated in Figure 21. Figure 21A is one of the best examples of a refolded F_1 fold in the district. This is from an outcrop of laminarly banded metatuffs or altered green phyllite adjacent to a metabasite of the Vangorda formation. A phase one antiform-synform pair is refolded along shallow dipping axial planes paralled by the S_2 crenulation cleavage producing an over-all structure very similar to the previous Grum section. This outcrop demonstrates the importance of a detailed appreciation of small-scale structures as a guide to the interpretation of the expected shapes of unexposed sulphide deposits known only through widely spaced drill holes.

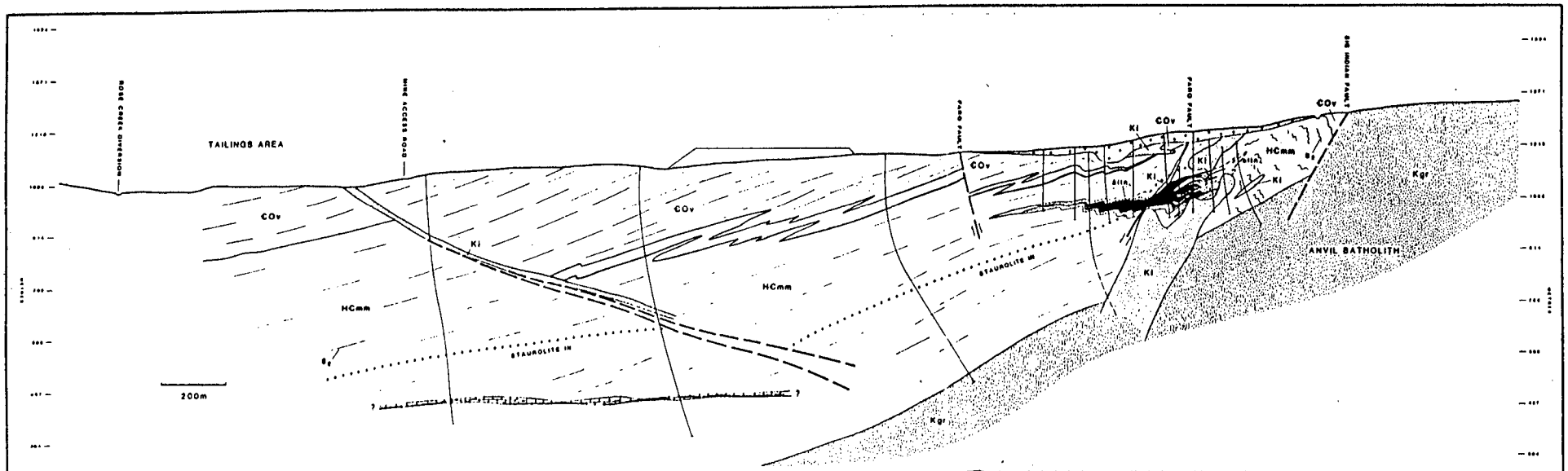


FIGURE 16. Cross section G-H (Fig. 20) through the Faro Deposit (same section line as Fig. 30) illustrates the large scale structural relations of the lower structural level. Note approximate parallelism of unit boundaries to S_1. Most Vangorda formation on this section is calc-silicate with the exception of the structurally highest portion near the mine access road. The dotted line shows the first appearance of staurolite in Mt. Mye schists. The metamorphic reaction surface and S_2 are approximately parallel to the contact of Anvil Batholith. The marble unit may be equivalent to the lower Cambrian archaeocyathid limestone of Selwyn Basin. In drill holes that intersect the marble near the Batholith it is altered to tactite and contains minor scheelite. The low dip of the fault in the southwest half of the section is apparent. Note the large scale post D_2 folds northeast of the Faro deposit.

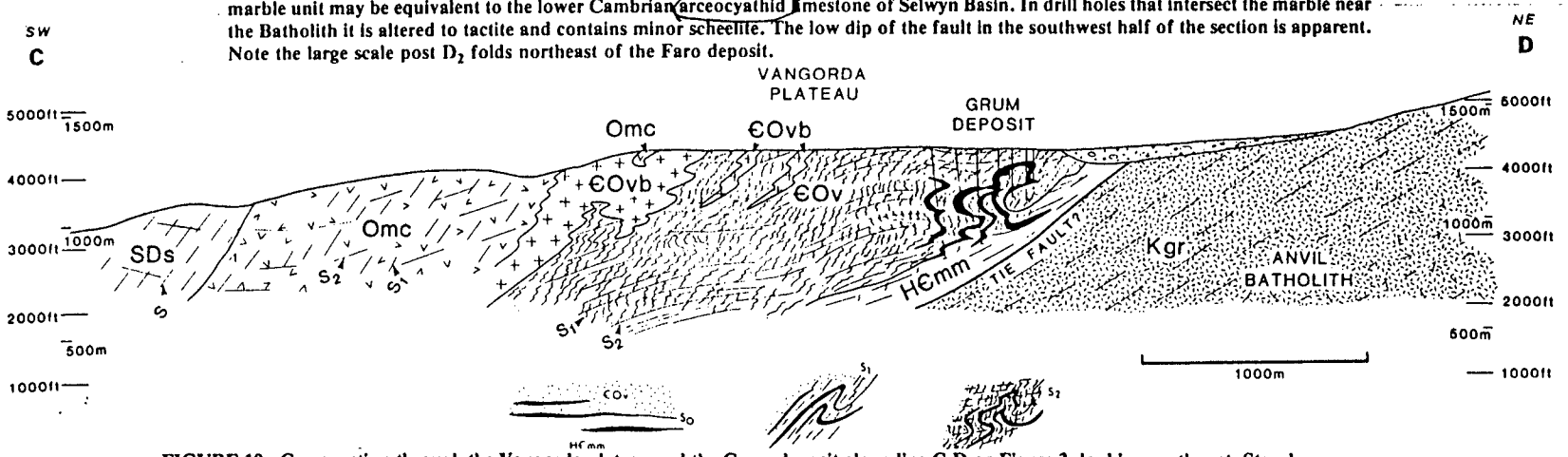


FIGURE 19. Cross section through the Vangorda plateau and the Grum deposit along line C-D on Figure 3, looking northwest. Steeply to moderately southwest dipping S_1 crenulated by shallowly dipping S_2 is typical of the structural relations of the middle structural level on the Vangorda plateau where greenschist facies rocks dominate. Post D_2 folds gently warp the S_2 foliation near Grum. The Grum deposit provides the best example of the F_1/F_2 interference pattern in the district. The deposit is involved in a large "Z" (or "N") shaped D_1 fold, refolded by "S" shaped D_2 folds. The inserts show the sequential development of Grum from a sequence of stacked en echelon ore layers parallel to S_0 through D_1 and D_2 to produce the geometry observed today.

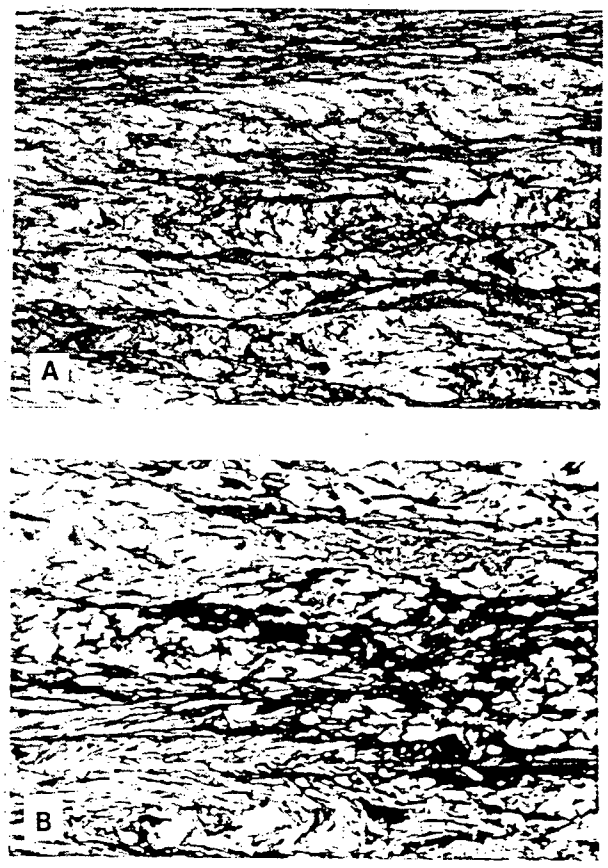


FIGURE 17. Typical microstructures of the lower structural level (B) and lower part of middle level (A). Photomicrographs of Mt. Mye formation phyllite (A) and biotite schist (B). Both specimens are pervasively S_2 foliated in hand specimen. In phyllites, S_1 preservation in thin section is clear and, with careful examination by hand lens, sometimes visible in hand specimen. In schists, S_1 preservation, even in thin section, is not commonly demonstrable except as inclusion trails in porphyroblasts. In hand specimens, S_1 is rarely seen.

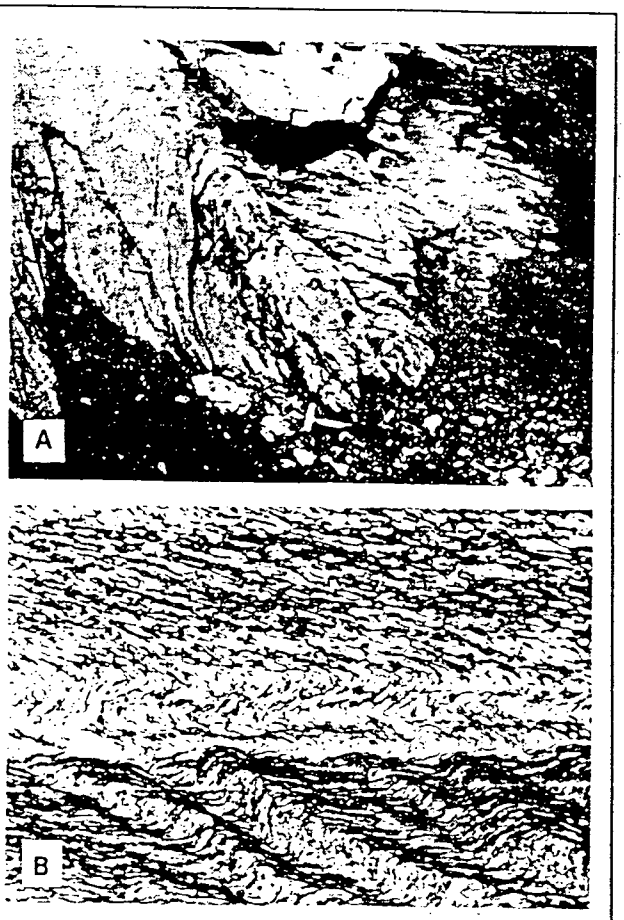


FIGURE 18. Examples of post D_2 structures in Anvil District rocks. (A) is a D_4 fold at the top of the Faro deposit, the photo was taken close to section 118 (Fig. 30). The folded element is pervasive S_2 in the altered wallrocks of the Faro deposit. S_4 is moderately developed as a crenulation cleavage. This example is from the lower structural level and illustrates the stronger development of post D_2 structures at that level. (B) is an example of small scale folding of S_2 in middle level rocks which imparts a wrinkle lineation to the S_2 surface and a very weak post D_2 crenulation cleavage where better developed. Folds similar to that in (A) are not commonly developed in the middle level. (Field of view 2 mm by 3 mm.)

Second phase folds on a variety of scales from macroscopic to microscopic are illustrated in Figures 22 and 23.

On the Vangorda Plateau and in all other areas of the middle structural level that have been examined, there is evidence of three distinct post D_2 deformation generations. A nearly pervasive fine wrinkle or crenulation lineation on S_2 is sub-parallel to L_2 over much of the district. This lineation represents the intersection of a weak non-penetrative foliation with S_2 and parallels the axes of small locally developed folds in S_2 whose axial surface is sub-vertical and parallel to the weak foliation.

A more widely spaced, less penetrative crenulation lineation trends more east-west and is due to the intersection of a weaker foliation with S_2. Axial planes of local, small related folds are sub-vertical.

A fracture cleavage to close spaced jointing trends approximately 60 degrees to 80 degrees and is only locally developed. Like the weak D_5 elements at Faro, this feature is commonly related to small faults.

These deformation features are not as intensely developed as those described previously in the Faro deposit area and it is not yet possible to make direct correlations with that area, but the geometric similarities are striking. Nowhere has the relative age of these features been worked out. Thus far, folds related to these generations have not proved to be of comparable importance to ore deposit shapes as those at Faro. The features are thought to be related to broad-scale warps in S_2 such as are shown in Figure 19.

Upper Structural Level

The upper structural level has not been studied in the same detail as the deeper portions of the pile in proximity to the ore deposits.

Progressively up-section on both flanks of the Anvil Arch, S_2 becomes less intensely developed and the dominant foliation becomes S_1 with only local S_2 development as a weak low angle cross-cutting crenulation foliation. Deep in the Menzie Creek formation, S_1 is well developed as a pervasive cleavage or a chloritic schistosity. Flattening of pillows and breccia clasts into this foliation is locally extreme.

On the north flank of the Arch, the development of S_1 also becomes much less intense up-section in the Menzie Creek formation. Near the top of the unit, virtually undeformed pillows are common and metamorphic foliation is rare, particularly in the larger of the two areas indicated as possible klippe in Figure 3. Tuffs interlayered with the Menzie Creek formation and shales interlayered with and overlying it commonly contain well preserved bedding cut by a slaty cleavage that is the equivalent of the S_1 chloritic foliation in the basaltic rocks. Some of this decrease in the effects of deformation is probably due to the more competent nature of the basaltic section, but a continuation of the upward decrease in strain away from the batholith already noted in the lower levels is apparent.

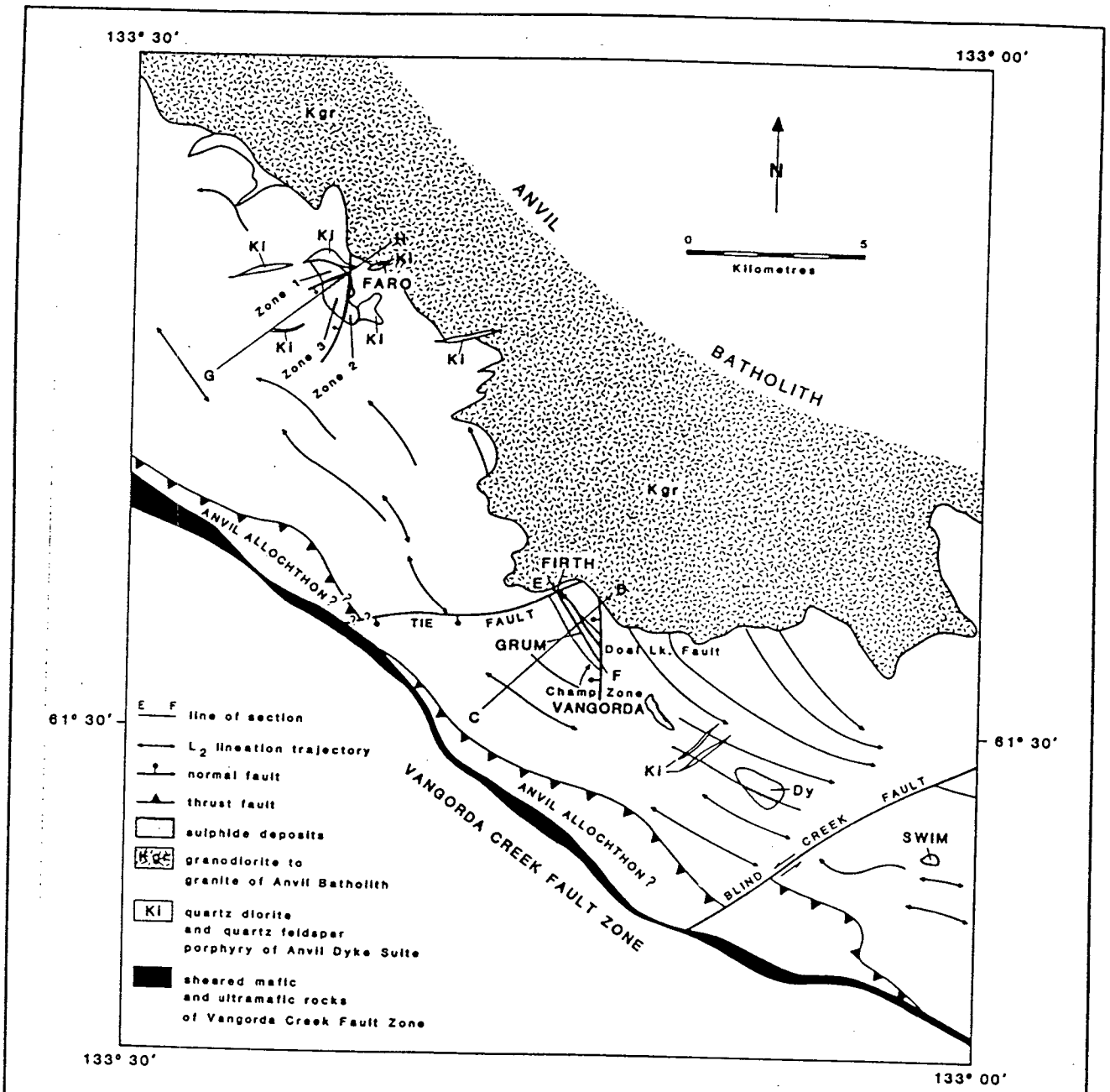


FIGURE 20. Map showing average L_2 lineation trajectories on the southwest flank of Anvil Arch. Each sulphide deposit is elongate parallel to the local L_2 and the over-all curvilinear trend of the deposits approximately parallels the regional trend of L_2. Section C-D is Figure 19, E-F is Figure 24 and G-H is Figure 16.

Post D_2 deformation features are not well developed in the upper structural levels. A fine crenulation lineation is commonly developed on S_1 and is due to the intersection of a steeply-dipping weak crenulation foliation trending 90 degrees to 130 degrees and axial planar to small folds in S_1 that are parasitic to the larger folds indicated in Figure 3. These folds appear to be due to post D_2 deformation, possibly D_4 at the Faro deposit.

Devonian and Mississippian strata on the north flank of the Anvil Range are thrown into northeasterly inclined northeast-verging asymetric folds with an axial planar slaty cleavage. These folds are associated with small northeast-directed thrust faults. The folds are thought to have formed during D_1 but this has not been established with certainty since this sequence is everywhere in fault contact with the older rocks to the southwest. This style of deformation appears to be present in strata as young as Triassic.

On the southwest flank of the Anvil Arch, Devonian and Mississippian strata show a different style of deformation. There, an intense phyllitic cleavage is developed with strong transposition of layering into the foliation. Coarse-grained chert pebble conglomerates are strongly flattened into this foliation. The foliation dips moderately to steeply southwest and is cut by a weak crenulation cleavage dipping shallowly southwest showing that the steeper foliation is S_1. A strong chloritic foliation is present throughout the underlying Menzie Creek formation as well. The extraordinary degree of foliation development and flattening in the Earn Group here may be due to proximity to the possible overthrust slab of Anvil Range Group and the Vangorda fault (see below).

Metamorphism

We have done little work on metamorphism in the district and refer the reader to Tempelman-Kluit (1972) for lists of assemblages and a map of metamorphic zonation. Regional metamorphism of the Buchan type (Miyashiro, 1961) accompanied the first two deformations with grade ranging from greenschist

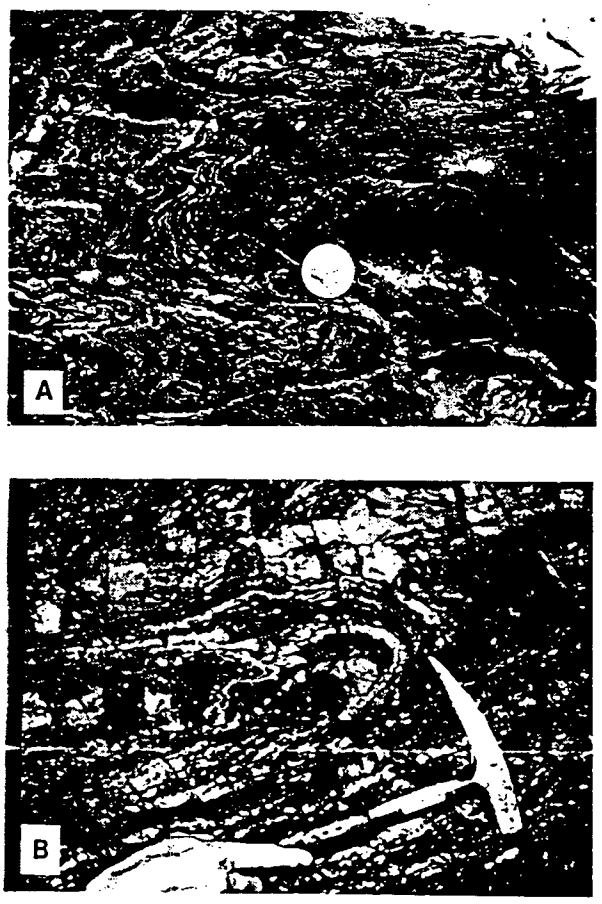


FIGURE 21. Examples of refolded F_1 folds in thinly banded green phyllites of Vangorda formation (A) and in banded sulphides of the Grum deposit (B). In (A), S_2 is slightly inclined toward the left (southwest) and S_1 sheet dip is inclined steeply to the southwest. Compare the "Z" shaped F_1 fold in (A) to the shape of the Grum deposit (Fig. 33) and the over-all structure of the Vangorda plateau (Fig. 19). The type 3 interference pattern of (A) typifies interference patterns in the District; (B) is an exception to this generalization.

through amphibolite facies. The degree of metamorphism attained during D_1 and D_2 appears to be comparable since mineral assemblages within and between lithons are comparable. Metamorphic grade decreases outward from a central metamorphic welt cored by Anvil Batholith. Immediately adjacent to the batholith, pelitic schists consist of the assemblage andalusite-staurolite-garnet-biotite-muscovite-quartz-plagioclase. Fibrolitic sillimanite and cordierite have been identified locally (Pigage, pers. comm., 1983). Metamorphic grade decreases to the muscovite chlorite zone of greenschist facies. In general, deeper stratigraphic units are more metamorphosed than their overlying units; however, isograds cross-cut stratigraphy on a large scale such that the base of the Vangorda formation is at greenschist facies at Grum, but at Faro, amphibolite facies is attained.

D_2 mineral assemblages at the Faro Deposit correspond to bathozone 2 or 3 of Carmichael (1978), suggesting a total pressure during metamorphism of approximately 3 kb. Limited sphalerite geobarometer work by Kuo (1976) corroborates this pressure range. This corresponds to a depth of burial of 9 km to 10 km, but evidence for only about 5 km of superincumbent section can be found in or around the district. This "missing" section may be accounted for by the former presence of overthrust slabs of allochthonous oceanic or arc terranes predicted to have existed in the area by recent tectonic models (Tempelman-Kluit, 1979).

Age of Deformation and Metamorphism

The age and timing of the various deformational events in Anvil District have not been resolved. The entire Paleozoic sequence is affected by both the D_1 and D_2 events. Rocks containing upper middle Devonian fossils display a steeply southwest dipping foliation, parallel to S_1, implying D_1 to be younger. If the Permo-Pennsylvanian age assignment to Anvil Range Group is correct (Tempelman-Kluit, 1972), D_1 may be this age or younger since phyllitic cherts at its base possess a similar steep foliation. These relationships suggest D_1 is, at its oldest, uppermost Paleozoic and not lower Paleozoic as previously suggested (Tempelman-Kluit, 1972). Emplacement of allochthons of Anvil Range Group in the adjacent Yukon Tanana Terrane and Pelly Mountains during uppermost Triassic or early Jurassic (Tempelman-Kluit, 1979) may imply a similar age for D_1.

By virtue of cross-cutting relationships, D_2 is younger than D_1. Their separation in time may not be great, as suggested by the similarity of new metamorphic minerals defining S_2 and those defining S_1, implying reorientation of maximum principal stress to the D_2 direction in a still hot, metamorphic pile.

Locally, foliated plutonic rocks developed along the southeastern margin of Anvil Batholith display a shallow dipping foliation, similar in orientation to S_2 in surrounding country rocks. This relationship, plus at least one roof pendant showing continuity of the S_2 foliation in the pendant with the shallow foliation in the plutonic rocks, suggests the D_2 event post-dates at least part of the intrusive suite. At many localities, the Anvil Batholith clearly cross-cuts S_2, thus complicating the relationship. It is appealing, but certainly premature, to suggest an early phase of Anvil Batholith is synkinematic with the D_2 event and therefore K/Ar and Rb/Sr ages of 95 to 100 Ma noted above for the plutonic rocks imply a Cretaceous age for the D_2 event.

Faults

Introduction

Two of the most significant faults of the Anvil District are the Tintina and Vangorda Fault Zones which together form the southwest boundary of the district. Northeast of these structures are many smaller faults of more local importance. These faults are of diverse orientations, but two trends are well developed: 60 degrees and 340 degrees. Many of these faults are moderately to steeply dipping normal faults that appear to be part of a post-metamorphic extensional fault system, perhaps related to the rise of Anvil Batholith. Some of the faults appear to have strike-slip displacement and may be related to offset on the Tintina Fault. Older faults, possibly related to D_1, are present locally.

Normal Faults

The best studied normal fault of the district is the Tie Fault (Fig. 3). This structure has been intersected by five diamond drill holes and can be mapped on the surface by an abrupt change in metamorphic grade. In drill hole intersections the fault consists of coherent, sheared, black phyllite with augen of carbonatized metabasite and vein quartz. The black phyllites allow the fault to be mapped on the surface by electromagnetic surveys. Its trace is a conductor trending 60 degrees, almost perpendicular to the usual trends of conductors in the vicinity. The Tie Fault has been defined laterally for 4 km and 1 km down dip. Based on subsurface data, the fault dips about 45 degrees southeast. The fault truncates the D_1 and D_2 folded Grum Deposit (Fig. 24); the Firth showing consists of portions of the Grum deposit caught in the fault zone along with mobilized mineralization. Along most of the fault zone, footwall amphibolite facies metamorphic rocks are juxtaposed against greenschist facies hangingwall rocks. The fault is spatially related to an irregular projection of the Anvil Batholith. Near the fault, granitic rocks have developed a mylonitic foliation marked by ribbon quartz and feldspar augen. In the subsurface, sheared rocks of the fault zone are cut by unsheared quartz-feldspar porphyry of the Anvil Dyke Suite. These relationships demonstrate that the fault is post-metamorphic, postdates D_2 and is probably closely tied in

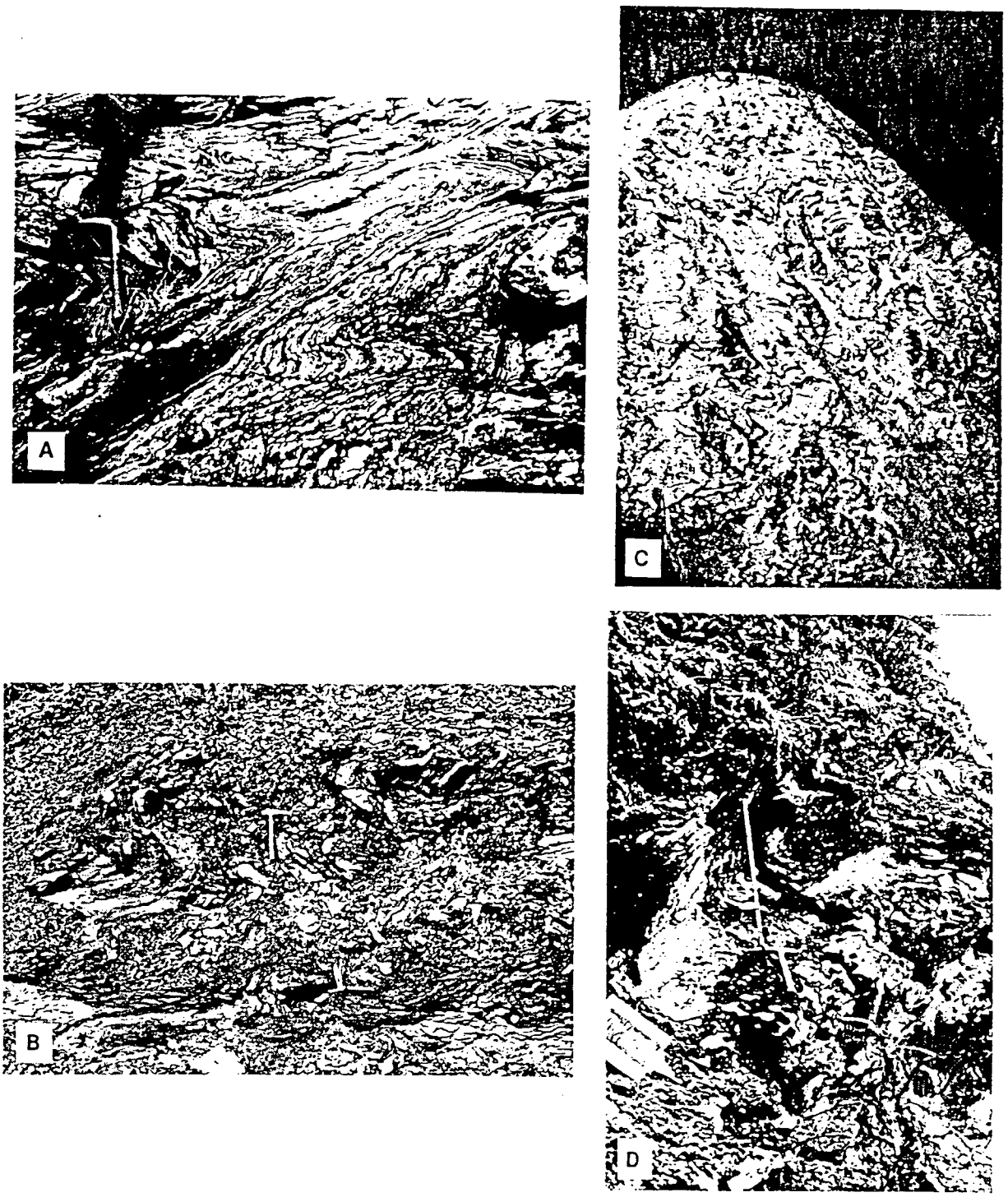


FIGURE 22. Typical mesoscopic structure of the middle structural level; D_2 folds of various scales in the Vangorda formation calcareous phyllites. Compare with small scale structures in Figure 23 and large scale structures of the Grum, Vangorda and Swim deposits, Figures 33, 34 and 36.

time to the late stages of emplacement of the Anvil Batholith. The magnitude of displacement on the fault is in the order of 1000 m (Fig. 24); its slip line appears to be almost down the faults dip.

A similar structure, the Doal Lake Fault (Figs. 20 and 24), truncates the southeast end of the Grum deposit, but this fault is marked by gouge rather than coherent fault rock. It trends north-south and dips about 40 degrees to the west.

A number of other major post-metamorphic faults similar to the Tie Fault are known to exist on the south flank of the Anvil Arch. These include the faults under the Dy and Swim deposits (Figs. 35 and 36 respectively) and one or more additional faults near the Grum. In most cases, these faults juxtapose older and more metamorphosed footwall against younger lower-grade hangingwall. The over-all fault pattern is not yet worked out and it is likely that several more major structures have yet to be recognized.

Northeast of the Anvil Batholith, there are a number of similar faults which are known only through reconnaissance surface geological mapping and geophysical surveys. The Graphite

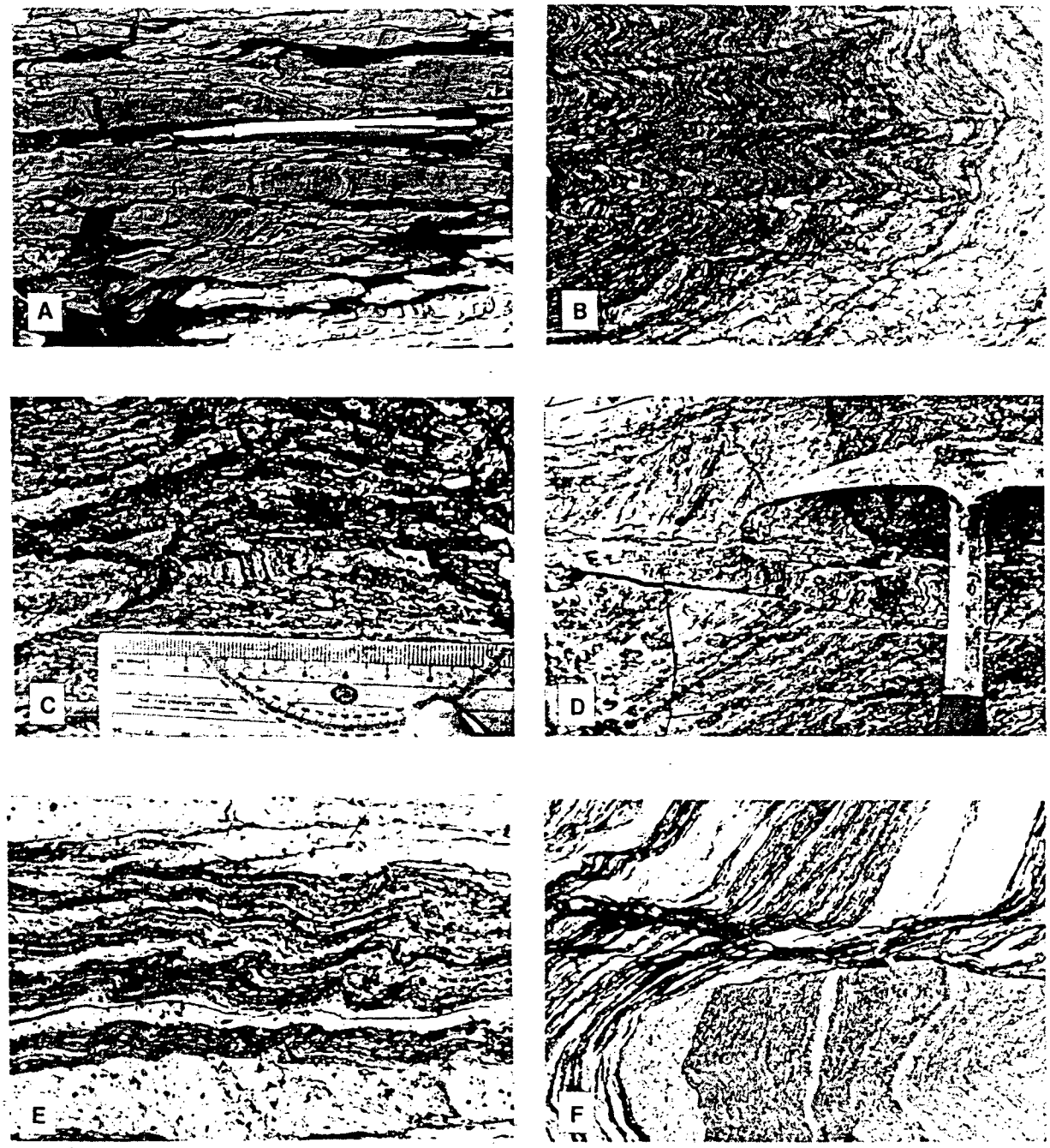


FIGURE 23. Comparison of mesoscopic and microscopic (all plane light, 2 mm by 3 mm view) structures of middle structural level phyllites. In all cases, S_2 is horizontal. (A) and (B) show typical lithon structure with dark, more carbonaceous S_2 folia separating lithons with folded S_1 parallel to compositional banding. (C) and (D) show phyllites with rare S_1 preservation in lithons separated by zones of pervasive S_2 (and D_1 micas rotated into S_2?). In (D), note post D_2 crenulations in S_2 and the darker, more carbonaceous nature of the pervasively S_2 foliated regions. (E) and (F) show the common small offset along S_2. In many cases, such offsets are apparent and probably result from pressure solution along S_2 resulting in the darker, carbonaceous micaceous residue. In some cases, however, there does appear to be slip along S_2 (but not necessarily during D_2). The microstructures of the dark horizontal band in (F) closely mimic the macroscale of Tie Fault Zone. All phyllites from Vangorda formation except (F) which is from uppermost Mt. Mye formation.

Fault (gf on Fig. 3) parallels the trend of the Anvil Batholith and along much of its length is marked by a prominent electromagnetic conductor due to the "smearing out" of the lower carbonaceous member of the Mt. Mye formation into the fault plane. Toward the fault's southeast end, progressively younger formations are juxtaposed against the middle part of the Mt. Mye formation showing stratigraphic omission of over 2000 m. At some localities, S_2 foliation and formational contacts are perpendicular across the fault. The fault is thought to dip moderately to steeply northeast, but the attitude, slip line and displacement on the fault are not known with certainty. The above observations suggest the northeast side is down dropped and that large displacements are implied. Like the Tie Fault, this structure is post-metamorphic.

A related structure, the Klunk Creek Fault (Fig. 3), occurs north of the graphite fault. This fault separates little metamorphosed northeast dipping and facing strata of the Menzie Creek formation from higher grade footwall calc-silicates of the

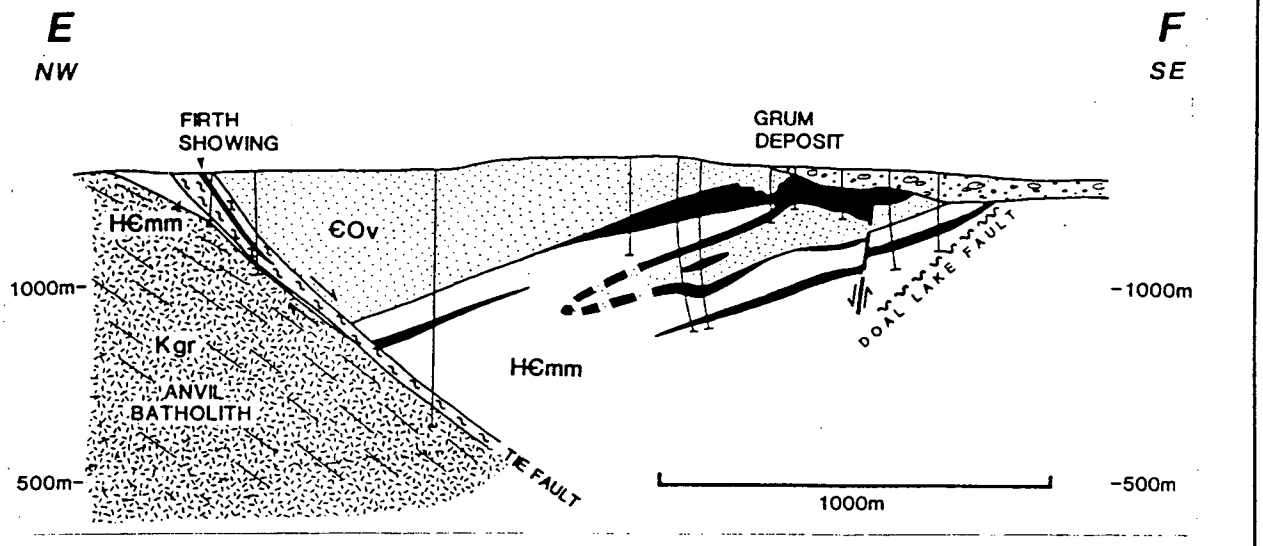


FIGURE 24. A diagramatic longitudinal section of Grum deposit showing the plunge of the Grum fold structure and the relationship of Grum to the Firth showing. Firth appears to represent slivers of Grum mineralization in a large extensional fault zone, the Tie Fault, that separates footwall amphibolite facies Mt. Mye formation and granitic rocks from hanging wall greenschist facies rocks of Vangorda and Mt. Mye formations. A similar fault, the Doal Lake Fault truncates the southeast end of the deposit. The Tie Fault and Doal Lake Fault together form the boundary between the lower and middle structural levels here.

Vangorda formation. The fault appears to subparallel S_2 in the calc-silicates and dips about 30 degrees to the southeast.

Also northeast of graphite fault is another possible member of this family of normal faults, the contact between map unit SDa and the Menzie Creek formation (Fig. 3). This contact appears to dip moderately to shallowly southeast based on intersection with topography. Bedding in map unit SDa dips west or southwest toward the fault with a stratigraphic omission of up to several hundred metres between Menzie Creek formation and the uppermost part of map unit SDa.

These faults appear to be part of a network of extensional faults that is related to the final stages of emplacement of the Anvil Batholith. They generally show down drop away from the core of the Anvil Arch and may be due to diapiric rise of the granitic and high-grade metamorphic core of the district through the lower-grade rocks flanking the Arch.

A myriad of other small faults with normal displacement occur throughout the district. Many of these appear to post-date the larger lower angle faults but still show evidence of being related to emplacement of the Anvil Dyke Suite.

The most important of these structures are the faults that bound the central graben of the Faro deposit, but there are many others with similar magnitudes of displacement that attract less attention.

Strike Slip Faults

The Blind Creek Fault (Tempelman-Kluit, 1972) is inferred to follow the linear 60-degree trending Blind Creek valley, Its existence is confirmed by offset of contacts, the trend of sulphide deposits and electromagnetic conductor patterns. The apparent sense of offset is left lateral and the amount of displacement is about 1 km.

Many other small faults with apparent strike-slip offset occur in the district—not all of these fall into any convenient geometric families. The trend and offset of the Blind Creek Fault is consistent with it being a second order wrench related to the Tintina Fault. The fact that many dykes and extensional faults related to the batholith also follow this trend perhaps suggest the batholith was emplaced when the stress regime of the Tintina was established.

Thrust Faults

Several small northeast directed thrust faults have been mapped in Earn Group strata along the northeast margin of the Anvil District by P.F. Lewis (1974). These faults are associated with close, northeasterly-inclined, northeast-vergent folds with a slaty axial planar cleavage. These thrusts appear to have formed during D_1.

A large allochthonous sheet floored by a shallowly dipping fault is interpreted to be present northeast of Anvil Arch (Fig. 3). The rocks of this sheet and those underlying it have a shallowly northeast dipping S_1 foliation and a dominantly more steeply northeast dipping bedding implying a Z shaped F_1 asymmetry and north or northeast D_1 vergence. This structural style is compatible with northeast-directed D_1 thrust faulting. Northwest of the area of Figure 3, we have mapped several other areas where rocks of the Menzie Creek and Vangorda formations appear to overlie Earn Group strata along shallowly dipping fault surfaces. All these faults emplace older on younger strata and thus have been assumed to be thrust faults. It is possible, however, that they are not thrusts but belong to the family of extensional faults described above and that the allochthonous sheet is actually a large gravity slide shed off the crest of the Anvil Arch.

The most significant potential overthrust occurs along the southeast edge of the district in the foothills of Rose Mountain. This fault is predicted on the basis of more regional mapping (see Tempelman-Kluit, 1979), but there is little evidence for it in the rocks of Rose Mountain. We have made numerous traverses in this area to look for evidence of the fault, but have found only a highly deformed sequence that grades from black and beige chert and chert conglomerate of the Earn Group to green beige and lesser red chert of basal Anvil Range Group. This problem has been recognized by Tempelman-Kluit (1979) who suggested that there may be both allochthonous and autochthonous Anvil Range Group. This is an attractive hypothesis but our regional mapping outside the Anvil District tends to confirm that the Anvil Range Group is not comfortably part of Selwyn Basin stratigraphy. It is more strongly linked to the Yukon-Tanana Terrane with which it is structurally interleaved at many localities.

For now all we can state with certainty is that if a thrust is responsible for emplacing the Anvil Range Group, it probably occurs within the highly deformed and flattened phyllitic chert sequence or perhaps in the black phyllites above the Menzie Creek formation (Figs. 3 and 14). Such a thrust does not occur at the base of the Anvil Range Group basalts since, as Tempelman-Kluit (1972) has demonstrated, the basalts and cherts interfinger.

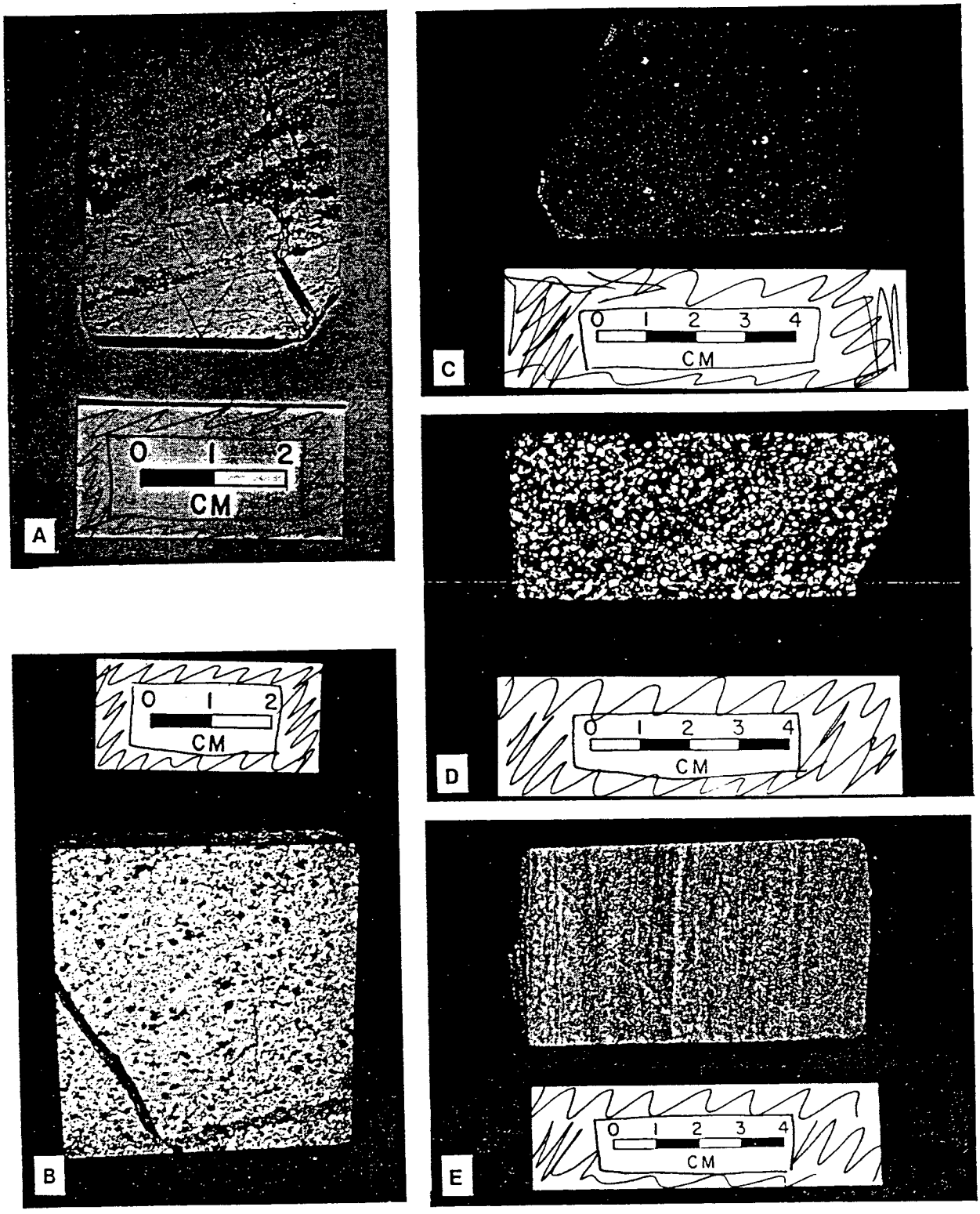
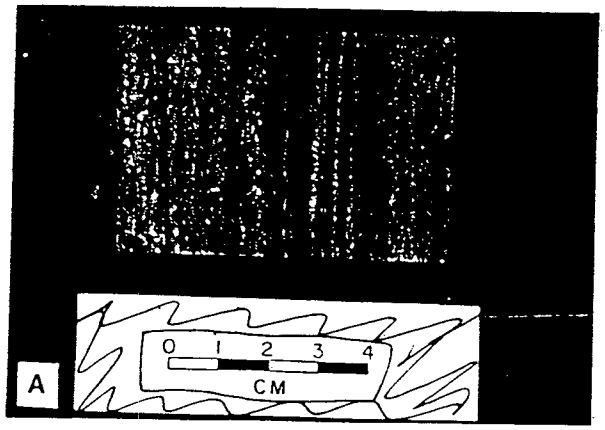
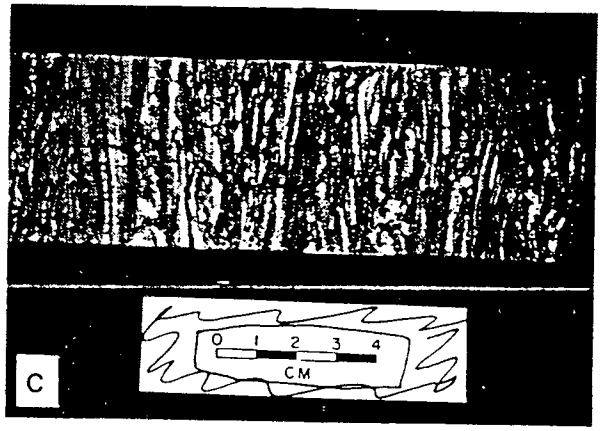
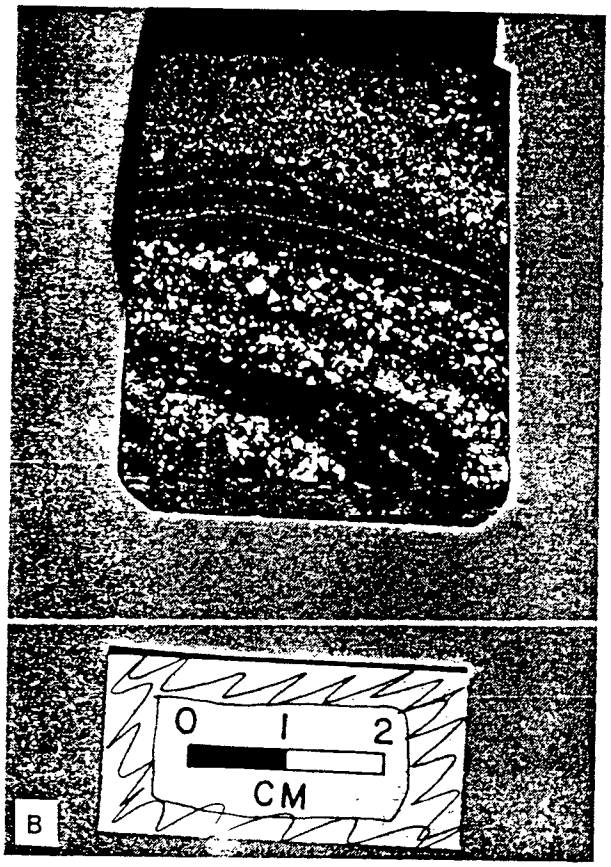


FIGURE 25. Massive sulphide lithofacies of the Anvil District deposits: (A) Banded massive pyritic sulphides from the Swim deposit. Dark material is largely sphalerite and galena, light is pyrite. Note the D_2 fold hinge and general transposition of layering into S_2 as is typical of massive sulphides. The pull apart structure approximately normal to S_2 is commonly developed in most very pyrite rich rocks especially at Faro, but not generally to this degree. (B) Homogeneous, but foliated and lineated, pyritic massive sulphide from the Faro deposit. Dark spots are magnetite porphyroblasts. The light material is pyrite, a network of grey quartz is developed between the pyrite grains. This is typical of the low-grade massive sulphides along the northeast edge of the Faro deposit. (C) High-grade pyritic massive sulphides from the Vangorda deposit. Light-coloured grains are pyrite in a matrix of dark galena and sphalerite. (D) The same lithology as (C) form, the Faro deposit illustrating the effect of metamorphic intensity on grain size (Tempelman-Kluit, 1970b). This is the buckshot ore (Campbell and Ethier, 1974). As lead-zinc content decreases, a network texture of galena and sphalerite surrounding pyrite porphyroblasts is developed. (E) Baritic massive sulphides form the Dy deposit. The light bands are dominantly pyrite and the grey bands barite, sphalerite and galena. Pure massive barite does not occur in the Anvil deposits; this is essentially as barite rich as the ore type becomes. Strongly developed, thin banding parallel S_2 is typical of this ore type except at Faro where compositional banding in all massive sulphides is less well developed.







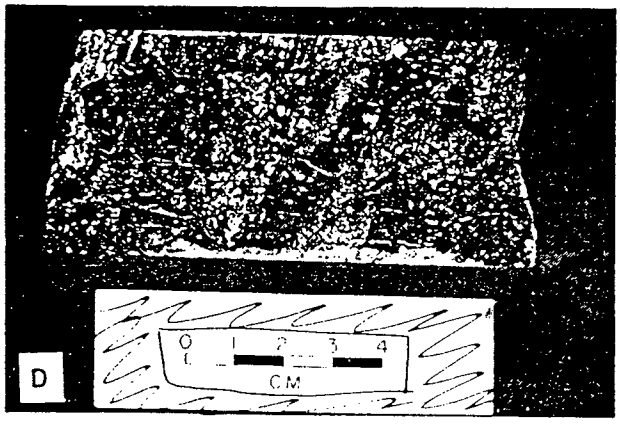


FIGURE 26. Quartzose, disseminated sulphide lithofacies of the Anvil District deposits: (A) Ribbon banded graphitic quartzite. Dark bands are fine-grained quartz and carbonaceous material with very minor sulphides. Light bands are coarser non-carbonaceous, quartz, sphalerite, galena and pyrite. Banding is parallel S_2. This example is from the Dy deposit. The grain size differential between Faro and other deposits is not as great for the quartz-rich ore type, as it is for the massive sulphides. (B) An unusually well banded example of pyrite rich ribbon banded graphitic quartzite. The thin sulphide banding may be transposed bedding however, similar zones of fine-grained sulphides are commonly better interpreted as high-strain zones where grain size reduction has occurred. Size grading within bands in this ore type (but not this sample) is not uncommon but the grains are recrystallized and the size gradation appears to relate more to compositional gradation. More quartz-rich bands commonly contain coarser sulphides than more sulphide-rich bands. Convincing sedimentary structures, if present originally, have not survived the deformational overprint. The three coarse bands at the bottom of the sample illustrate problematic bands widely developed in this ore type. Texturally this material resembles quartz sulphide veinlets, many examples of which can be found cutting the S_2 foliation. The majority of these bands, however, parallel S_2 (or S_1 where preserved in lithons); whether these foliation parallel bands are originally veinlets or beds is not resolved. (C) A sulphide poor micaceous pyritic quartzite. Banding is not as well developed in the non-carbonaceous quartzites. The bulk of the ore type is interpreted to be recrystallized siliceous exhalite, however, some, particularly the more micaceous examples, may be silicified and mineralized host meta-sediments. Some non-carbonaceous pyritic quartzite is demonstrably bleached ribbon banded facies; this is particularly well developed adjacent to small metabasite layers at Grum. (D) A more sulphide rich variant of the pyritic quartzite. This sample illustrates the typical occurrence of chalcopyrite in veinlets cutting S_2 in the more quartzose zones.

quartzose

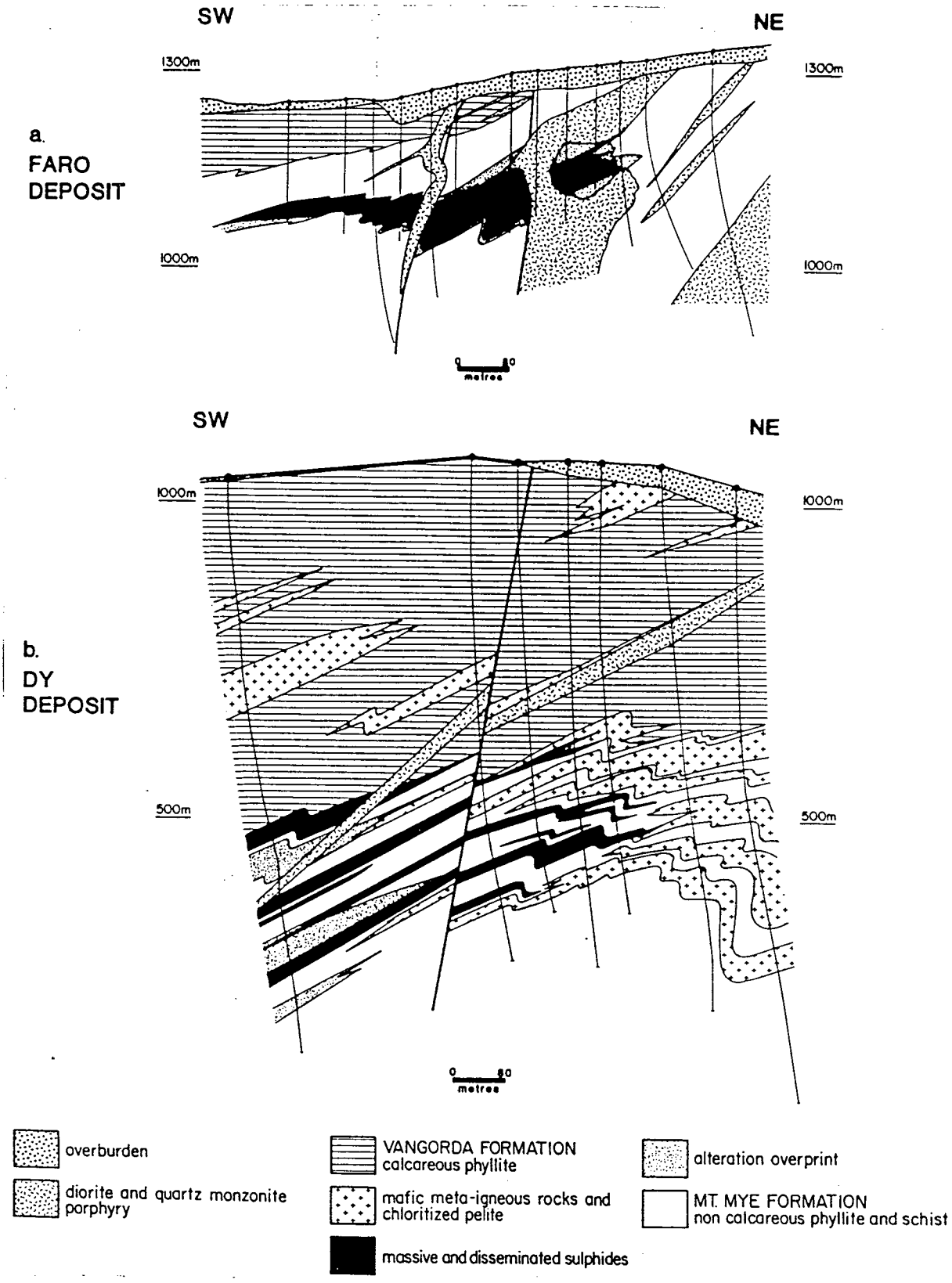


FIGURE 27. Cross sections of Faro and Dy showing the distribution of alteration. At Faro, the alteration is commonly equally developed in the hanging wall and footwall of the deposit, and in some places it is better developed in the hanging wall. At Dy, and all the other greenschist deposits, the alteration is more clearly footwall biased, but the situation is clouded by the multilayered nature of those deposits. At Dy, strong bleaching of the phyllites is best developed at the southwest edge of the deposit, perhaps indicating the presence of a feeder zone (B.V. Hall, pers. comm., 1981). The green phyllites at the northeast edge of the deposit are combinations of metabasites and probably altered (chloritized) calcareous pelites. This may be part of the same alteration package or a separate alteration related to later metabasite emplacement. A similar chloritic zone is developed at the northeast edge of the Grum deposit where metabasite is less abundant.

TABLE 8. Summary of tonnage and grade figures for Anvil District ore deposits as of June 1983*

	Tonnage x 10^6 tonnes	Pb (%)	Zn (%)	Ag (g/mt)	Cutoff (% Pb + Zn)
Faro (1)**					
Geological reserves before mining	57.6	3.4	4.7	—	5.0
Remaining geological reserves (1983)	33.0	3.0	4.6	36	4.0
Remaining open pit reserves (1983)	25.2	2.9	4.3	36	4.0
Grum (2)					
Geological reserves	30.8	3.1	4.9	49	4.0
Open pit reserves	16.9	3.0	4.9	47	4.0
Vangorda (3)					
Geological reserves	7.1	3.4	4.3	48	4.0
Open pit reserves	5.2	3.4	4.2	47	4.0
Dy (4)					
Geological reserves	20.3	5.7	7.0	82	9.0
Swim (5)					
Geological reserves	4.3	3.8	4.7	42	6.0
Total					
Geological reserves before mining	120.1	3.7	5.6	—	N/A
Remaining geological reserves (1983)	95.5	3.7	5.2	51	N/A
Remaining open pit reserves (1983)	47.3	3.0	4.5	41	4.0

* Compiled from various "in house" reports of Cyprus Anvil Mining Corp. and Kerr Addison Mines.
** Refers to the number on Figure 4.

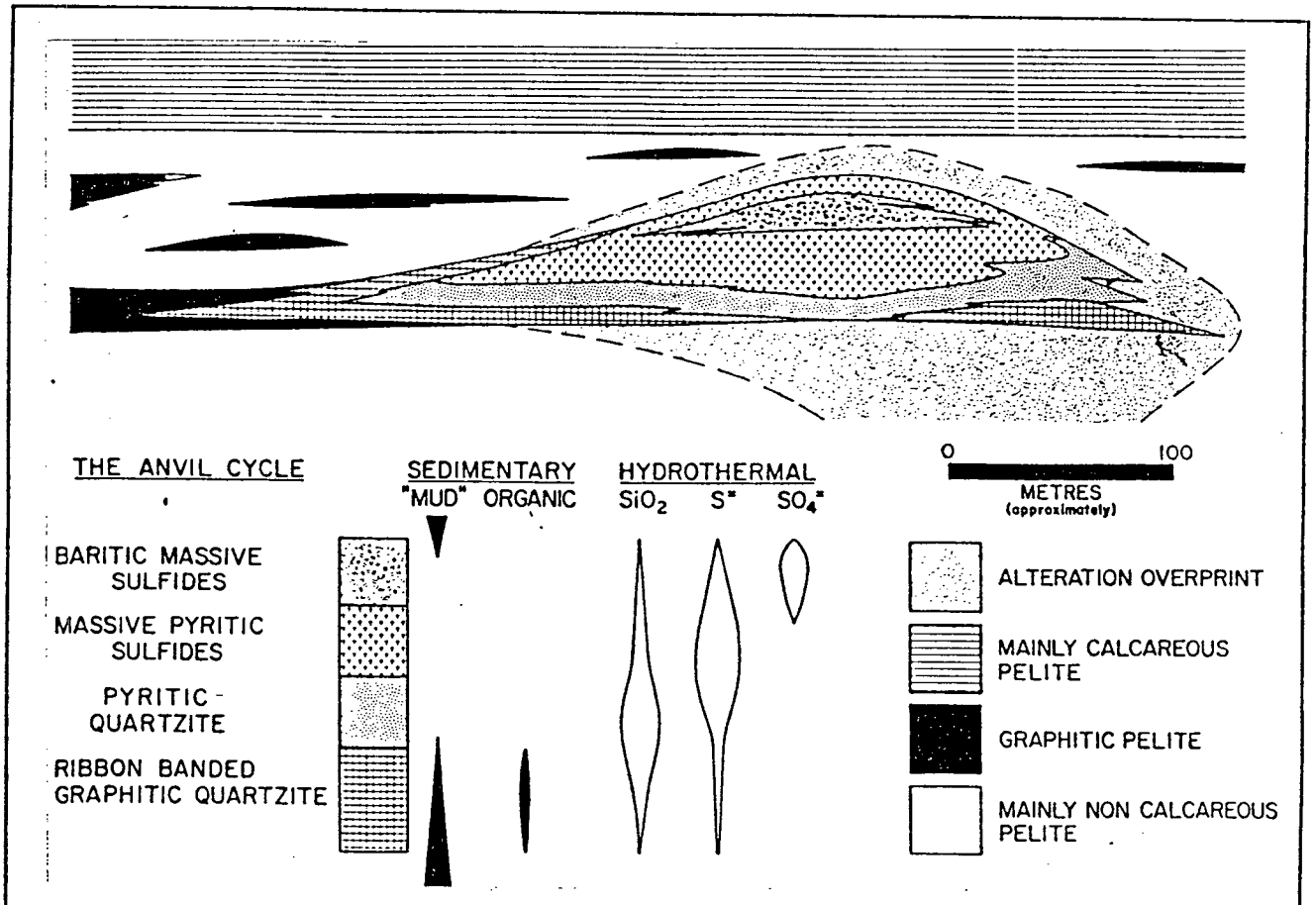


FIGURE 28. An idealized Anvil deposit based on cross sections of the Faro deposit. Such lateral and vertical zoning can be found to some degree in all deposits of the district. Massive sulphides are the central and upper lithofacies with peripheral and lower quartzose disseminated lithofacies grading outward toward graphitic phyllite. The asymmetry shown is not uncommon in the district and is evident both in cross and long sections at Faro. A ~~random drill hole~~ or sectional slice through the three-dimensional array of lithofacies implied here results in the characteristic Anvil Cycle. Diagramatically indicated are the competing sedimentary and hydrothermal input, as well as the evolution of the latter, which the cycle implies.

The section is greatly exaggerated vertically. The geometry depicted is speculative; there is no evidence preserved indicating an original pile with respect to bedding or any other geometry.

SP
Diagramm atically

Ore Deposits

General Description

The lead, zinc, silver deposits of Anvil Range are of the sediment-hosted, stratiform, massive pyritic sulphide type. They have been subjected to the complex structural and metamorphic history described above. They occur as a single, thick, sulphide lens with little or no interbanded metasedimentary rocks (e.g. Faro) or as multilayered deposits with several, approximately vertically stacked layers with substantial metasedimentary or metavolcanic interlayers within and between sulphide layers (e.g. Grum and Dy). An unfolded mineralized layer consists of an upper, often centrally positioned, massive, base metal-bearing sulphide facies and a lower and peripheral, disseminated, quartzose sulphide facies. Quartz is the main gangue mineral of the disseminated sulphide facies while barite and lesser quartz are the principal gangue phases in the massive facies. Present deposit lenths are generally two to three times the widths. Unfolded deposit dimensions range up to 4000 m across their amoeboid shapes. Individual sulphide horizons commonly are 10 m to 40 m in thickness. The upper and lower contacts of sulphide horizons are sharp but lateral extensions grade into the enclosing host rocks. All deposits show a variably developed, sericite/muscovite alteration overprint in the adjacent wallrocks.

The Anvil deposits are distributed through a 150 m stratigraphic interval straddling the boundary of the Mt. Mye and Vangorda formations in association with regionally developed, laterally discontinuous, siliceous graphitic (carbonaceous) phyllite units (Fig. 4). Individual sulphide lenses commonly appear to be the lateral facies equivalent of these graphitic phyllites. Some lenses of some deposits (such as the upper horizons of Grum) are basal to the carbonaceous phyllite units as well as being their partial lateral equivalents. In other cases, lateral equivalence of graphitic phyllite and ore lenses has not been established.

There are presently five known deposits along a prominent curvilinear trend on the south flank of Anvil Arch (Figs. 3 and 20). From northwest to southeast they are Faro, Grum, Vangorda, Dy and Swim. Additionally, two base metal deficient, sulphide occurrences, Sb and Sea, are also known. The Firth showing is a faulted part of Grum while the Champ Zone (Brock, 1973) is the subcrop of one of the upper Grum horizons at its southeast end (Fig. 20). Reserve figures for the deposits as of 1983 are given in Table 8.

Although the bulk of basaltic, meta-igneous rocks occur stratigraphically higher than the Anvil deposits, the first significant pulse of basic igneous activity is roughly coincident with the ore horizons (Fig. 4), suggesting at least a temporal relationship between ore formation and magmatism. Despite this, there is a generally poor spatial association of sulphide deposits and metabasic rocks. The Dy, and to a lesser extent, the Grum deposits are exceptions to this generalization and in this sense, the Anvil deposits are dominantly pelitic sediment-hosted.

Detailed geological and geophysical mapping and drilling suggest the linearly distributed deposits lie close to a northeasterly "pinch out" or "zero edge" of the associated graphitic phyllite. To date, no sulphide deposit lithofacies have been encountered in a moderate number (20 to 30) of drill holes through the ore-bearing horizon southwest of the deposit line. Taken together, these observations suggest some relationship between sulphide deposits, facies changes at reduced basinal margins and basic igneous activity.

Sulphide Lithofacies and Alteration Assemblages

There are numerous sulphide lithofacies which comprise all Anvil district deposits. The same facies, in variable proportions, form each deposit, suggesting a consanguineous origin for all deposits. The appearance of specimens of sulphide facies in different deposits varies primarily as a function of metamorphic grade. Two principal subdivisions are recognized in the Anvil ores, massive and quartzose disseminated sulphides. Brief descriptions of the rock types in each of these major subdivisions are given below.

Massive Lithofacies

Massive pyritic sulphides: banded (Fig. 25A) to homogeneous (Fig. 25B), commonly weakly foliated and/or lineated, massive pyrite with lesser sphalerite and galena. Total sulphide content is at least 60% and is commonly nearly 100%. Gangue consists of quartz ± barite ± carbonates (calcite, dolomite, ankerite). Accessory minerals include pyrrhotite, chalcopyrite, magnetite, arsenopyrite and marcasite. In the amphibolite facies, ores with abundant Pb/Zn commonly develop pyrite prophyroblasts in a matrix of dark reddish brown to black base metal sulphides (Fig. 25D).

Baritic, massive pyritic sulphides: strongly and thinly banded (Fig. 25E) massive sulphide/sulphate rock consisting of pyrite, galena, sphalerite and commonly magnetite in a gangue of off-white barite and lesser carbonates (calcite, dolomite, ankerite and probably barytocalcite). The amount of barite may be as high as 50%; non-sulphidic, massive barite does not occur in the Anvil deposits. There is a complete gradation between this and the above facies. This facies is usually quite high-grade (10% to 15% combined lead-zinc) but low-grade variants occur rarely. Sphalerite is characteristically honey coloured to reddish brown.

Carbonate-bearing, massive pyritic sulphides: similar to massive pyritic sulphides but contains 10% or more carbonate (calcite, dolomite, ankerite) either as interstitial gangue or as coarse patches and irregular blebs. This is a minor facies and is not known with certainty to be a primary depositional variant. The most common occurrence of coarse, beige to tan, ankerite patches may represent recrystallized original matrix carbonate or re-worked pre-synmetamorphic veins.

Pyrrhotitic massive sulphides: massive, finely crystalline, typically well foliated pyrrhotite with pyrite porphyroblasts and highly variable amounts of sphalerite and galena. Minor chalcopyrite is characteristic of this relatively copper-rich facies. Rounded to angular, rotated and foliated quarzite or quartz-vein clasts 2 cm or less in diameter are typical. This is a minor facies and is not known with certainty to be primary, as some pyrite in the massive facies may invert to pyrrhotite during regional metamorphism.

Breccia textures are more common in the massive pyritic and pyrrhotitic facies than in the barite- or carbonate-bearing facies. Pyritic breccias generally involve fragments (0.1 cm to 5.0 cm) of more quartzose or less base metal-rich pyritic facies in a massive pyrite plus base metal sulphide matrix. Fragments can be angular to subrounded, poorly sorted and may be either clast or matrix supported. In some cases, margins of fragments can be fitted back together. In all cases, the breccias are post-metamorphic since they involve variably oriented, foliated clasts. The origin of the breccias appears to be due to ductility contrasts between the affected rock types during sulphide flowage induced by deformation and metamorphism. These are clearly *not* primary breccias related to feeder zones or paleoslumps prior to sulphide lithification.

Friable and porous massive sulphides are relatively common and often degenerate to pyrite sand in open pit exposure and drill core. These friable ores originate by post-metamorphic groundwater leaching (especially near faults) of matrix carbonate or barite.

Quartzose Disseminated Lithofacies

Ribbon-banded, graphitic, pyritic quartzite: dark grey to black, well banded, sulphide-bearing quartzite (metamorphic usage). Bands are: (a) dark grey, very fine-grained, carbonaceous, phyllitic quartzite to siliceous phyllite (presumed metachert), and (b) light grey, quartz-sulphide (pyrite-sphalerite-galena) bands (Fig. 26A). These bands are usually 2 mm to 2 cm thick. Total sulphide content is commonly between 10% to 30% and ranges from 2% to 60%. Pyrite is usually the dominant species,

but higher-grade examples have sub-equal to base-metal dominant variants. Strong sulphide species differentiation between bands occur locally such that barren pyrite bands can be found, adjacent to bands rich in sphalerite or galena.

Pyritic quartzite: light grey, generally poorly banded, moderately to weakly foliated, micaceous quartzites with highly variable base metal and pyrite contents; pyrite contents are generally 10% to 40%, ranging between 5% and 60%. Although there is a complete gradation from massive to quartzose ores, there is usually little problem in separating this facies from the massive pyritic sulphides, because most examples have less than 40% total sulphides. A minor variant of this facies shows low pyrite (<2%) contents with base metal sulphides being predominant. Barite in major amounts is absent from the pyritic quartzites and carbonate species are uncommon. Chalcopyrite, pyrrhotite and/or magnetite-bearing varieties are common. Sphalerite in the high grade examples is characteristically a vibrant, reddish brown. A significant galena- and sphalerite-poor variant of the pyritic quartzites occurs in several deposits. This variant is generally copper rich and contains chalcopyrite mobilized into veinlets crosscutting the metamorphic foliation. In some deposits, this variant is also gold rich.

Post-metamorphic breccias are common in the disseminated sulphide lithofacies. Pyritic quartzite breccias are often spectacularly developed in the sphalerite-rich, high-grade facies, where again, ductility contrasts between the sulphide-rich and quartzite bands dictate ductile flow in the sulphides and brittle failure, rotation and brecciation of the quartzite. Less intensively developed incipient breccias show sulphide mobilization along bounding fractures as well as into D_2 or later cleavages.

Alteration

Both wallrocks and certain ore facies of the Anvil deposits are overprinted by a prominent, easily recognized, light beige, sericite/muscovite dominant alteration assemblage. This overprint facies is not a depositional unit and may have formed as a syndepositional reaction product between wallrocks and deposit-forming hydrothermal fluids; as a metamorphic reaction envelope during later regional metamorphism or as a combination of these processes. In the multi-layered deposits, this alteration overprint appears discontinuous and commonly is best developed in the footwall of a given lens or deposit as a whole. At Faro, a continuous envelope of this lithology encloses the entire deposit with local best development in the hanging wall (Figs. 27, 30 and 32).

Many mineralogical variants of the alteration facies are recognized, including siliceous, carbonate-bearing, talcose, chloritic, pyritic, pyrrhotitic, chalcopyrite-bearing, magnetite-bearing and base metal-bearing species. Careful attention has been paid to the distribution of these facies in an attempt to define feeder zones for all deposits, but with little success. Several instances of suspected pre-D_1 quartz-chlorite-pyrrhotite-chalcopyrite veins or stringers have been observed in the altered stratigraphic footwalls of several horizons (Swim deposit in particular), but not in sufficient abundance to define a stringer or feeder zone comparable to those of volcanogenic deposits. Recognition of a feeder zone is considerably hampered in this terrane by the polydeformational overprint. It may be that Anvil deposit feeder zones are simply broad and diffuse, not focussed and funnel shaped as in volcanogenic massive sulphide deposits. Alternatively, the extensive stratabound nature of the alteration envelope may imply its formation by downward percolation of pooled hydrothermal brines or by lateral migration along a permeable horizon laterally from a feeder.

In the multi-layered deposits at greenschist facies grade, all mineralogical variants of the alteration facies are commonly recognized, often the best degree of development in the footwall of a mineralized horizon. The only amphibolite-grade example, the Faro deposit, shows a much less varied phase assemblage (muscovite, quartz, pyrite ± marcasite) in altered rocks with development of a substantial hangingwall, as well as footwall alteration envelope. This simplified phase assemblage may be due to re-equilibration of the greenschist alteration assemblages at higher grades of metamorphism. The prominent hangingwall alteration may be due to continued, post-depositional, hydrothermal activity, to sulphurization or other metasomatic reactions in the wallrocks during metamorphism, perhaps caused by mobile sulphur from the inversion of pyrite to pyrrhotite in the deposit. It is interesting to note that the develpment of massive pyrrhotitic facies is greatest in the Faro deposit, which also shows the broadest, most well defined and most symmetrically developed alteration envelope.

Within the ore deposits, the ribbon-banded, graphitic, pyritic quartzites are locally "bleached" to the same light beige colour as other altered rock types. Alteration fronts cross-cut the well developed banding of this facies but preserve pre-alteration textures. At Grum, the bleaching of carbonaceous ore is common adjacent to carbonated metabasite bodies, but no such association applies to the bleached rock as a whole. It is this preservation of texture which allows the discrimination of altered ore facies from weakly disseminated base metal occurrences in altered wallrocks.

Idealized Anvil Deposit and Anvil Cycle

In addition to all deposits showing a spatial relation to the Mt. Mye/Vangorda boundary and having a variably developed alteration overprint, they have a distinct arrangement of sulphide lithofacies. This arrangement in a vertical and lateral sense is so commonly seen within and between deposits, that it has been termed the Anvil Cycle (Jennings *et al.*, 1980). Since the Anvil Cycle was first recognized in the Faro deposit, a generalized, pre-deformation cross section of this deposit (Fig. 28) will illustrate this cyclicity. The base of the cycle is marked by ribbon-banded, graphitic, pyritic quartzites succeeded upward by pyritic quartzites, massive pyritic sulphides and baritic massive pyritic sulphides. This array is also seen laterally with ribbon-banded, graphitic, pyritic quartzites forming the marginal or distal facies of a deposit inward to the baritic massive facies.

In open pit exposure, the distal ribbon-banded facies seem to tongue laterally over several tens of metres into equivalent, weakly to non-sulphidic, graphitic or carbonaceous, siliceous pelites suggesting a strong sedimentary component to this ore facies. The entire Anvil Cycle can be viewed as a competition between the background sedimentary and exhalative, hydrothermal systems as diagrammed in Figure 28. The ribbon-banded, graphitic, pyritic quartzites are thought to represent a sedimentary system-dominant phase in the evolution of a deposit with organic carbon-bearing, silica enriched pelitic sediments interleaved with initial sporadic, silica-dominant exhalative pulses. The Anvil Cycle rapidly evolves from this to an exhalite dominant system with first, silica dominant (pyritic quartzites), then sulphide dominant (massive pyritic sulphides) and finally sulphate/oxide-rich exhalative components (barite, and magnetite-bearing massive pyritic sulphides) overwhelming the sedimentary regime entirely.

Anvil Cycles are developed on a wide variety of scales and to varying degrees of completeness. The largest scale is that of a cross section through an entire deposit. A series of complete and partial cycles may cumulatively form a mega-cycle on the scale of a complete deposit, e.g. Faro, or on the scale of a single sulphide horizon within a multi-layered deposit, e.g. Grum or Dy, generating the concept of cycles within a cycle. Complete cycles are seen over as little as a one metre stratigraphic interval.

Facies zoning can be used in a tenuous way to indicate tops in polydeformed horizons to decipher fold patterns. The more complete the facies cyclicity shown, the greater is the degree of confidence. However, top directions defined by the distribution of Mt. Mye and Vangorda formation always take precedence.

Metal zoning in some cases crudely complements sulphide distribution in that the quartzose disseminated sulphide facies at the base of an ideal cycle tend to be zinc enriched, whereas the massive, upper facies are lead-silver enriched, particularly toward the uppermost baritic facies. Commonly, however, there

TABLE 9. Faro Deposit Synopsis

Stratigraphic Position:
Approximately 100 m below Mt. Mye/Vangorda formation contact; 30 m to 40 m beneath a graphitic schist unit in uppermost Mt. Mye formation; probably equivalent to lowest sulphide horizon at Grum.

Number of Horizons:
Essentially one; there is a minor upper horizon 10 m to 20 m above main horizon and multiple cycles in the main horizon.

Dimensions (present):
Approximately 2000 m long, 1000 m wide, 30 m average thickness.

Geological Reserves:

	Tonnes x 10^6	Pb (%)	Zn (%)	Ag (g/t)
(at 5% Pb + Zn cutoff) (before mining)	57.6	3.4	5.7	—
(at 4% Pb + Zn cutoff) (remaining)	33.0	3.0	4.6	36

Zoning:
Preliminary investigations suggest basal, quartzose disseminated sulphide facies enriched in zinc; upper massive facies Pb-Ag-$BaSO_4$ enriched. Possible S isotope zoning (Shanks *et al.*, in press).

Facies Distribution:
Weak asymmetric distribution of massive sulphides skewed slightly to northeast of deposit centreline in cross section. Most massive sulphide facies-rich deposit in district at 50% or greater; N.W. end shows mega-Anvil Cycle; deposit shows marked asymmetry in long section with northwest part baritic, central part massive pyritic sulphides dominant and southeast part ribbon-banded graphitic facies dominant.

Precious Metals Content:
Silver largely structurally bound in PbS; Ag enriched in massive sulphide facies; distribution of Au uncertain but appears to be lower grade than other deposits (Tolbert, pers. comm., 1983).

Feeder Zone:
None unequivocally defined.

Alteration Overprint:
Bleaching is broadly developed as an envelope, both hangingwall and footwall of deposit show strong alteration; qtz + musc + plag + /-py (marcasite) as dominant present-day alteration assemblage; major differences between alteration pattern at Faro and other deposits are degree of hangingwall development and simplicity of phase assemblage; alteration may be in part due to amphibolite facies metamorphic overprinting reactions and locally enhanced development in association with metabasites above the deposit. Local bleached schists associated with post-metamorphic faults and dykes.

Structural Regime:
On upper long limb of Z symmetry, northeasterly vergent, macroscopic first phase fold; general parallelism of S_0 and S_2 on this limb; only local F_2 fold development known to affect deposit outline but very common F_2 folds within deposit and deposit shape may be partly D_2 controlled; conspicuous, generally Z symmetry F_3 and F_4 folds crenulate entire deposit.

Faults:
Zone 3 is a graben bounded by post D_2 (and D_3?) normal faults; numerous other sets with relatively small displacement are known.

Metamorphic Grade:
Amphibolite facies; common index minerals in pelitic rocks include andalusite, staurolite and garnet; diopside occurs in silicated marbles and calc-silicate schist; ores more coarsely porphyroblastic than other deposits of district (Tempelman-Kluit, 1970b).

Metavolcanic Rocks:
Weak spatial association with deposit although first appearance of metabasite bodies is roughly coincident with deposit horizon; little metavolcanic rock interleaved with ores.

Remobilization Features:
Extensive brecciation in massive pyritic and pyrrhotitic sulphides as well as base metal sulphide-rich pyritic quartzite; breccias thought to originate from ductility contrasts between particularly sulphides and quartzite during post D_2 folding events; local fault breccias present; sulphide fills fractures and/or post D_2 fracture cleavage in immediate wallrocks of deposit (particularly brittle quartzites); scale of sulphide remobilization is tens of centimetres to several metres in narrow "veins" and is volumetrically insignificant; Faro deposit is intact with no known "rootless" folds dismembering deposit.

Intrusive Rocks:
Variably porphyritic medium greenish grey hornblende diorite to quartz diorite occurs as large elongated plugs or marginal phases of Anvil Batholith and relatively thin (1 m to 10 m) dykes or sills; prominent finely porphyritic beige smoky quartz-feldspar porphyry dykes also cut deposit and diorite suite. Dyke rocks appear to be related to a large area of explosive post D_4 breccia over central part of deposit.

Contact Metamorphic Features:
Massive pyritic sulphides largely inverted to massive pyrrhotitic sulphides in contact aureole of diorite plug at north end of deposit; aureole is 10 m to 15 m thick, and characteristically contains randomly-oriented, coarse pyrite cubes and clusters; single pyrite cubes to 10 cm on an edge and magnetite octahedra to 20 cm have been observed.

is no evidence in the assays of metal zonation in an individual horizon, despite strong facies zonation. Studies of metal zoning are greatly hampered by deposit structural complexity and are not yet available for all deposits.

On the basis of scanty and preliminary data, copper, and to a lesser extent gold, seem to be preferentially distributed in siliceous facies of the footwall-based alteration overprint or in the pyritic quartzite facies of the stratiform sulphides.

Deposit Synopses

In this section, the detailed characteristics and distinguishing features of each deposit are tabulated (Tables 9-13) and summarized opposite a reference cross section(s) of the deposit (Figs. 30-36).

Genetic Model

The Anvil deposits are examples of synsedimentary, stratiform, massive sulphide deposits and are considered to be of submarine exhalative origin. Evidence for their synsedimentary origin is ambiguous but includes:

1. The prevalent and well developed compositional layering or banding in most sulphide facies locally with large variation in proportions of sulphide species between bands.
2. The interlayering of sulphides with unmineralized metasedimentary and probable metavolcanic rocks, commonly on a scale of centimetres.
3. The occurrence of all deposits within a relatively restricted stratigraphic interval.
4. The curvilinear depositional array crudely spatially associated with graphitic or carbonaceous pelite facies changes perhaps at a reduced basinal margin.
5. The metamorphic and deformational overprints clearly show the ores are pre-metamorphic.

Reconnaissance studies by Kuo (1976) demonstrate the presence of chloride-rich fluid inclusions in barite, quartz, and sphalerite from several deposits (Faro, Grum, Vangorda) implying metalliferous brines played a role in deposit formation. The ubiquitous development of generally footwall-biased alteration envelopes suggests that these brines were relatively hot. The curvilinear deposit array may indicate control of sedimentary facies and basin geometry by synsedimentary faults which formed a hinge line and could have provided the locus of exhalative ore fluid migration into the basin(s).

Considerable effort has been devoted to the recognition of a discrete hinge line in the Anvil pile. No synsedimentary slump

breccia or dramatic thickening/thinning relationships of units overlying or underlying the ore horizon have been found. Soft-sediment breccias (if they existed) would not likely be recognizable through the metamorphic and deformational overprint. Likewise, the complex poorly understood internal geometry of the pile renders thickness estimates, of the original sedimentary succession as related to sub-basin margin definition, suspect. The only suggestion of hinge line location is provided by the curvilinear deposit trend itself and its crude relation to the distribution of reduced basinal graphitic pelites.

The ore deposits are thought to have formed from hot metalliferous brines discharged from submarine fumaroles localized along a synsedimentary fault or hinge line which developed in response to late Hadrynian or lower Cambrian extensional tectonism. This inferred rifting episode is thought to have influenced basinal geometry resulting in reduced, second-order facies truncating against the hinge line. Hydrothermal fluids are envisioned as moving up this fault zone and being exhaled into a relatively deep water, reduced marine basin which was receiving distal turbidite sedimentation. Sulphides may have been deposited from plumes along the hinge line (Type II, Sato, 1972) or from relatively dense exhaled brines ponded in local topographic depressions (third order basin) near the hinge (Type I, Sato, 1972). This model accounts for the crude associations of known deposits with apparent depositional limits of reduced sediments. The hinge line or related fault sets could have provided the channelways for the first pulse of basic magmatism associated temporally with the deposits (or vice versa).

Whatever synsedimentary model is devised for these deposits, the mineralizing process must operate repetitively over a time long enough for 150 m of compacted (and deformed) section to accumulate.

Basin Evolution and Source of Ore Fluids

We have previously suggested (Jennings *et al.*, 1980) that since the northern Cordillera may have evolved following a Wilson-like cycle of rifting followed by collison (see Monger and Price, 1979; Tempelman-Kluit, 1979, for recent models of Cordilleran evolution), the Anvil district may be underlain by red beds and evaporites deposited in rift basins on Precambrian, continental crust. This postulated shallow marine and continental sequence may have been overlain, as the rift basin deepened by thick relatively coarse turbidites passing upward through fine clastic sediments capped by deep water shales. Mt. Mye formation represents the shaley upper member of this proposed stratigraphic cycle, while the "Grit Unit", part of which is presumed to extend beneath the Mt. Mye in Anvil Range, forms the upper part of the turbidite package. Evaporite/redbed sequences are present in the Proterozoic of Mackenzie Mountains below the Rapitan Group (Eisbacher, 1981; Aiken, 1982), but their extent beneath "Grit Unit" is unknown.

This cyclic arrangement would provide an attractive reservoir-seal situation within which connate waters in the sub-Mt. Mye reservoir could evolve into hot, metalliferous fluids by dissolution of older evaporites to become highly saline. These brines became gradually geothermally heated interacting with the clastic reservoir rocks to leach metal from such sources as feldspar grains, pigmenting agents of red beds (Carpenter, 1979), interbedded shales and adsorbed metals on grain surfaces. These fluids may have gradually become geopressured as well.

With renewed extensional tectonism, ancient basinal boundary faults and related structures were reactivated breaching the Mt. Mye producing reduced basins localizing carbonaceous pelitic assemblages. The evolved geothermally-heated fluids in the reservoir moved up these fracture systems to be exhaled on the sea floor and accumulated with the reduced pelitic basinal sediments. Basaltic volcanic and intrusive rocks probably moved up the same conduits to accumulate contemporaneously with the ores. In this sense, volcanism is entirely passive, simply reflecting the over-all tectonic environment.

TABLE 10. Grum Deposit Synopsis

Stratigraphic Position:
From approximately 50 m below Mt. Mye/Vangorda formation contact to about 100 m above this contact; lowest sulphide horizon 30 m to 40 m below main graphitic phyllite; another horizon immediately below this graphitic phyllite; other horizon(s) within Vangorda formation.

Number of Horizons:
Three main horizons; one subsidiary horizon; others possible.

Dimensions:
2000 m by 500 m by 350 m thickness contains known sulphide horizons. Original dimensions of sulphide layers up to 2000 m by 1000 m by 30 m.

Reserves:

	Tonnes x 10^6	Pb (%)	Zn (%)	Ag (g/t)
(at 4% Pb + Zn cutoff)				
Open pit	16.9	3.0	4.9	47
Total geological	30.8	3.1	4.9	49

Zoning:
No definitive studies; reconnaissance suggests pattern similar to Faro but many exceptions; suggestions (Modene, 1982) of Pb increasing upward between horizons.

Facies Distribution:
Massive sulphide facies within each of three main superimposed or stacked horizons stepped off to southwest going up section; much stronger development of ribbon-banded graphitic pyritic quartzites in all horizons than in other deposits of district, especially Faro and Dy.

Precious Metal Content:
Ag in PbS and $Cu_{12}As_4S_{13}$ (Carson, 1977) and enriched in massive facies; over-all distribution of Ag and Au unknown in individual horizons, wallrocks or deposit as a whole but tends to follow total sulphide content and to some extent grade. Average Au approximately 0.8 g/t in ore.

Feeder Zone(s):
None unequivocally defined for any horizon; heavily altered and mineralized wallrocks in footwall of lowest horizon may be related to a feeder zone. Abundant weakly mineralized stringers below main horizon.

Alteration Overprint:
Well developed especially below deepest horizons; all variants well developed. White mica dominant in southwest, chlorite in northeast.

Structural Regime:
Forms first phase antiform/synform pair; part of a large F_1, Z shaped fold; strong F_2 interference pattern; broad open flexural slip(?) folds warp S_2 in deposit vicinity.

Faults:
Numerous shallowly dipping, post D_2 faults dismember deposit into discrete domains; offsets related to steep faults seem relatively minor. The Tie Fault truncates the deposit at its northwest end and Firth appears to represent slivers of Grum in this fault zone.

Metamorphic Grade:
Greenschist facies dominantly; lower parts of deposit transitional to amphibolite facies with first appearance of staurolite and andalusite in pelitic rocks. This change commonly occurs across a low-angle fault.

Remobilization Features:
Brecciation as in Faro deposit; local and minor sulphide remobilization along fractures, cleavages and faults. Possibility of major sulphide flowage during D_2 to form masses up to 200 m by 600 m by 20 m but not certain.

Intrusive Rocks:
Mainly hornblende quartz diorite dykes; lesser monzonitic dykes particularly in lower parts of deposit near Anvil batholith, marginal phases of which are encountered in deeper drill holes. Intrusive rocks over-all are minor.

Contact Metamorphic Features:
None.

Isotope studies of ore leads in stratiform deposits of Selwyn Basin including the Anvil deposits by Godwin and Sinclair (1982), show a crustal affinity as inferred from their radiogenic character. Detailed analysis of lead isotopes of the Anvil deposits alone supports the hypothesis that: (1) the majority of

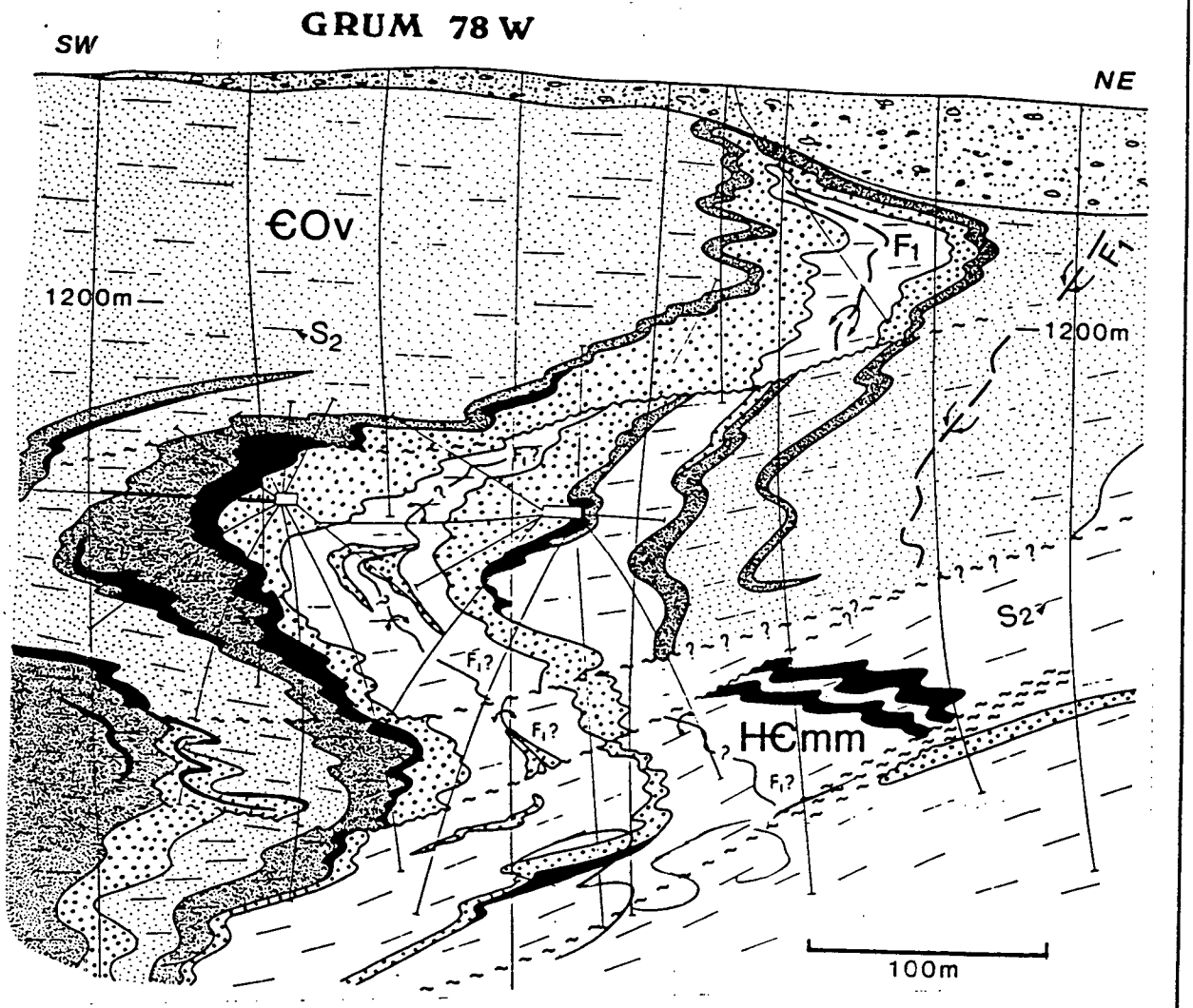


FIGURE 33. Vertical cross section 78 W through the Grum deposit viewed along a 315 degree azimuth. The deposit forms a complex F_1/F_2 interference pattern which, despite the density of drilling, is not yet completely resolved, particularly in the core of the deposit near the northeasterly underground workings. The F_1 closure just beneath the overburden is confirmed on several densely drilled sections down fold plunge to the northwest. At least some of the shallowly dipping faults shown have slip lines directed across the plane of the cross section such that they "telescope" different deposit domains and when viewed in a single cross section, appear not to make sense. The relative abundance of quartzose disseminated sulphides at Grum is evident in this section. Most of the massive sulphide in the main horizon just beneath the Vangorda formation is baritic; the massive sulphides are more abundant to the southeast. Black is massive sulphide, coarse stipple is quartzose disseminated sulphides, fine dense stipple is carbonaceous phyllite.

the lead in the deposits was derived from an orogenic to upper crustal source and that, (2) correction of the least thoranogenic leads for their Phanerozoic development histories shows they are identical to leads in shales and sandstones from modern enclosed basinal environments (Ryan, pers. comm.). These findings are compatible with the basinal brine leaching model proposed above.

Origin of the Anvil Cycle

Sulphide facies ordering in the form of Anvil Cycles may reflect a relatively local, but consistently recurring environment of sulphide deposition; consistent and systematic brine evolution in the hydrothermal fluid reservoir, or a combination of these.

One theoretical way to produce an Anvil Cycle involves sulphides precipitated in equilibrium with a brine following a positive trajectory on an fo_2-pH stability diagram. Figure 37, after Rye and Ohmoto (1974), illustrates this qualitative, conceptual relationship. For an ore fluid in the pyrite stability field at fo_2-pH conditions at or near the carbon buffer exhaled into a reduced (carbon-stable) basinal environment, a quartz-carbon-muscovite-pyrite assemblage would be stable (Point A, Fig. 37), approximating the lowermost unit of a cycle (ribbon-banded, graphitic, pyritic quartzite).

Increasing Fo_2 and pH of the ore fluid would cause precipitating sulphides to move away from the graphite stability field toward B where a quartz-muscovite-pyrite assemblage approximating pyritic quartzites and massive pyritic sulphides would be stable. Earlier formed graphitic sediments (including the ribbon-banded facies) coming in contact with evolved ore fluids of this composition during successive exhalative pulses would alter to carbon-free, muscovite dominant assemblages typical of the alteration overprint facies. Continued fluid evolution along this fo_2-pH path would result in a quartz-pyrite-barite ± magnetite assemblage (Point C, Fig. 37) similar to the baritic pyritic sulphides at the top of a cycle.

This fo_2-pH trend and resultant ore facies could be generated in various ways. It could result from convective mixing of more oxidized, higher pH sea water with ponded ore fluids producing stratification in the brines and resultant cyclicity in the ores. Mixing of hot brines with relatively cold sea water will lower the brine temperature, also favouring barite deposition (Ohmoto, 1972).

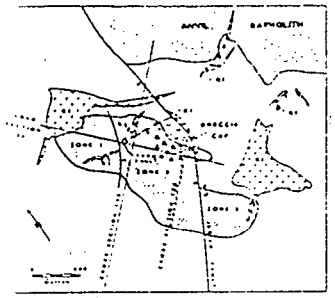


FIGURE 29. A reference map of the Faro Deposit showing the location of the sections (Figs. 30 to 32). The deposit outline is the vertical projection of the limits of the sulphide deposit. Zones 1 to 3 are indicated. Zones 1 and 2 are mined out, remaining reserves are within Zone 3. See text for a discussion on the breccia cap. The unit Ki northwest of section 118 is mostly quartz diorite, the unit southeast is quartz feldspar porphyry.

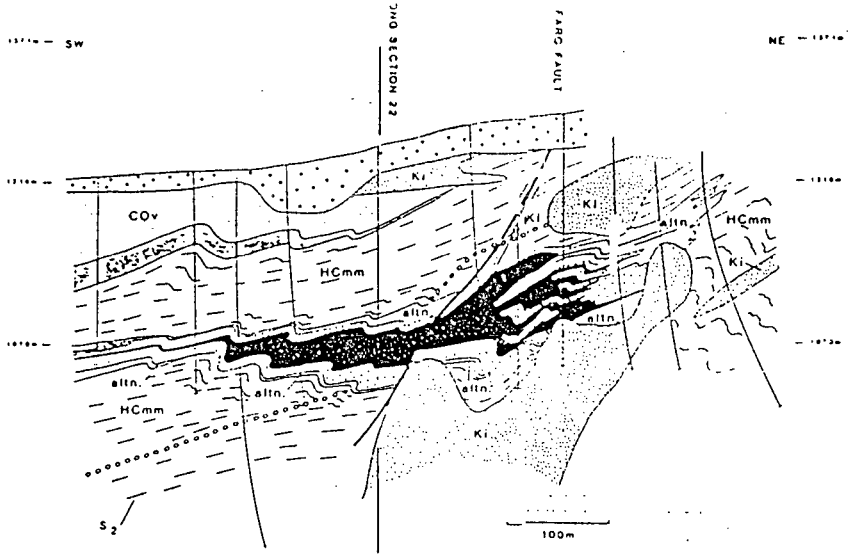


FIGURE 30. Vertical cross section 118 of the Faro deposit, looking northwest, no vertical exaggeration. The present pit outline is not shown. Black is massive sulphides; coarse stipple is quartzose disseminated sulphides; grey is carbonaceous phyllite; altn. = white mica envelope (bleached altered phyllites). Northeast of Faro Fault most massive sulphides are low grade and transitional into quartzose sulphides with high-grade bands at the top of the deposit and scattered through the remainder. Southwest of the Faro Fault the massive sulphides are mostly [illegible] the upper half is variably baritic. On this and all other sections of the Faro deposit pyrrhotitic sulphides are well developed in the southwest part of the deposit where the massive sulphides thin rapidly. The basal and peripheral quartzose unit is largely ribbon banded graphitic quartzite. The folds in S_2 and the deposit outline are probably D_4 folds. Unit O_c on this section is all calc-silicate. The dotted line approximates the first appearance of staurolite in Mt. Mye schists.

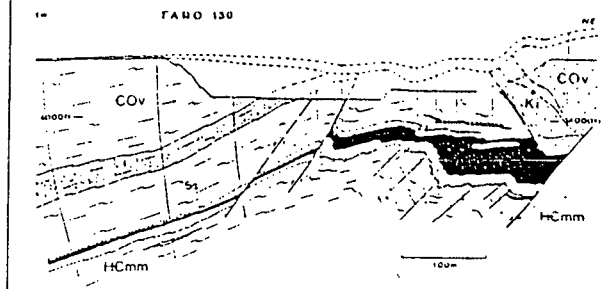


FIGURE 31. Vertical cross section 130 of the Faro deposit, looking northwest, no vertical exaggeration. The pit outline shown is as of the June 1982 interruption of mining. Units are the same as those of Figure 30. The triangles indicate the breccia cap (Fig. 29 and text). In this portion of the deposit, a thin upper horizon is separate from the remainder of the deposit. The fault at the northeast end of the section is part of the system that separated zones 3 and 2 (Fig. 29). The distribution of sulphide facies is essentially the same as that of Figure 30 with barren pyrite common northeast of the large D_4 fold in the base of the deposit and pyrrhotitic sulphides abundant for about 150 m southwest of the fold.

pyrrhotitic

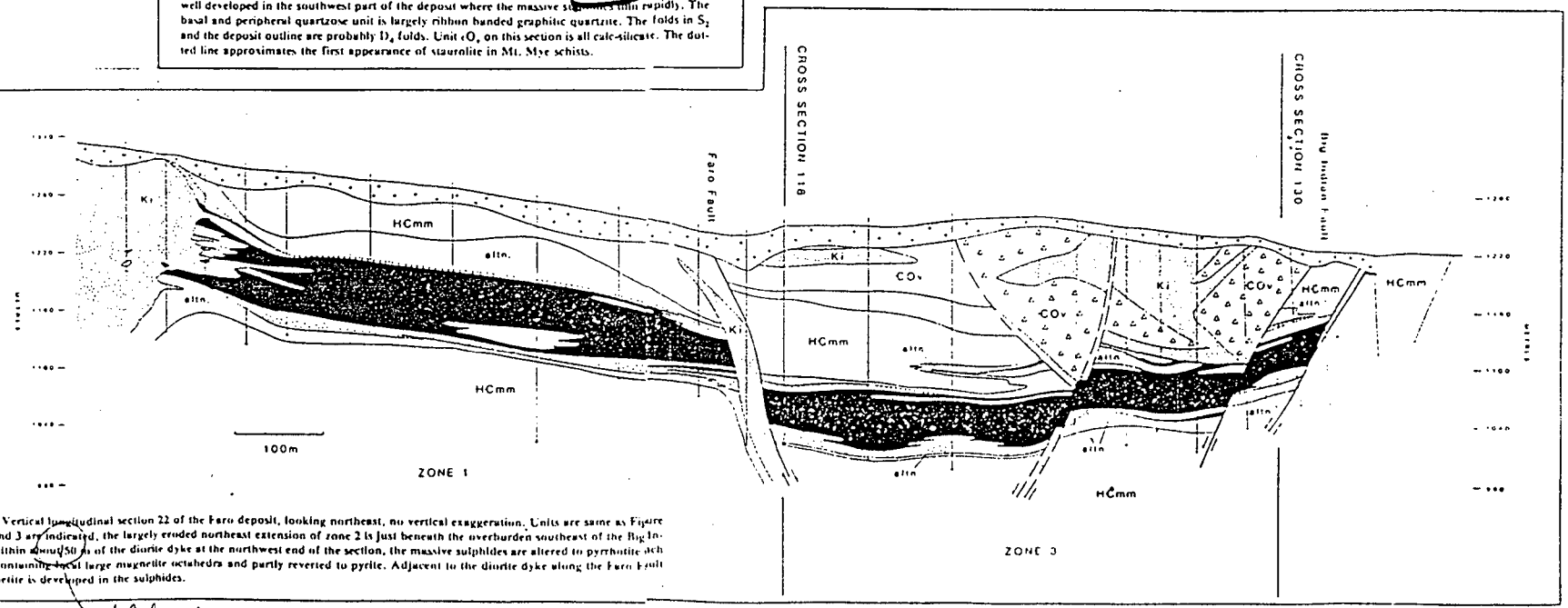


FIGURE 32. Vertical longitudinal section 22 of the Faro deposit, looking northeast, no vertical exaggeration. Units are same as Figure 30. Zones 1 and 3 are indicated, the largely eroded northeast extension of zone 2 is just beneath the overburden southeast of the Big Indian Fault. Within about 50 m of the diorite dyke at the northwest end of the section, the massive sulphides are altered to pyrrhotite-rich assemblages containing local large magnetite octahedra and partly reverted to pyrite. Adjacent to the diorite dyke along the Faro Fault massive magnetite is developed in the sulphides.

TABLE 11. Vangorda Deposit Synopsis

Stratigraphic Position:
Immediately at base of and approximately 50 m to 75 m below Mt. Mye/Vangorda formation contact; main horizon most probably at same stratigraphic interval as lowest horizon at Grum and equivalent to Faro; no horizons known in Vangorda fm above basal carbonaceous member. Basal carbonaceous member of Vangorda fm very well developed and thick.

Number of Horizons:
Two principal horizons, numerous smaller horizons or lenses.

Dimensions:
Approximately 1000 m long, 200 m wide, 25 m average thickness but highly variable.

Geological Reserves:

	Tonnes x 10^6	Pb (%)	Zn (%)	Ag (g/t)	Cu (%)	Au (g/t)
(at 4% Pb + Zn cutoff)	7.1	3.4	4.3	48		0.75

Zoning:
No definitive studies.

Facies Distribution:
Tops indicated by Anvil Cycles and local stratigraphic facing imply main portion of deposit is overturned; over-all structure of deposit imperfectly known. This facies relationship is poorly known.

Precious Metals Content:
Ag in PbS as in all deposits; suggestion of Au enrichment in pyritic quartzites in structural footwall (stratigraphic hangingwall) of main horizon; spatially coincident with thickest development of baritic ore. These quartzites are in stratigraphic footwall of higher smaller ore lenses, but position uncertain. Average Au content of quartzite approximately 1 g/t.

Feeder Zones:
None defined.

Alteration Overprint:
Widespread with substantial alteration in hangingwall of lower horizons (but footwall to higher, smaller horizons). Strong silicification and impregnation by pyrite, pyrrhotite and magnetite.

Structural Regime:
Main part of deposit is possibly overturned and appears to lie on D_2 Z symmetry short limb of megascopic S symmetry F_2 fold; no F_1 folds presently known.

Faults:
Most cross sections imply steep commonly northeast-dipping faults of unknown continuity; a north-south-trending normal fault truncates the deposit at its N.W. end.

Metamorphic Grade:
Greenschist to depth of current drilling in main part of deposit.

Metavolcanic Rocks:
Metabasites and altered (carbonatized) metabasites present in deposit in average amounts along with probable meta-tuffs.

Remobilization Features:
Internal, generally small scale brecciation as seen in other deposits; possibility of flowage in baritic facies on scale of hundreds of metres, but uncertain.

Intrusive Rocks:
Negligible.

Contact Metamorphic Features:
None.

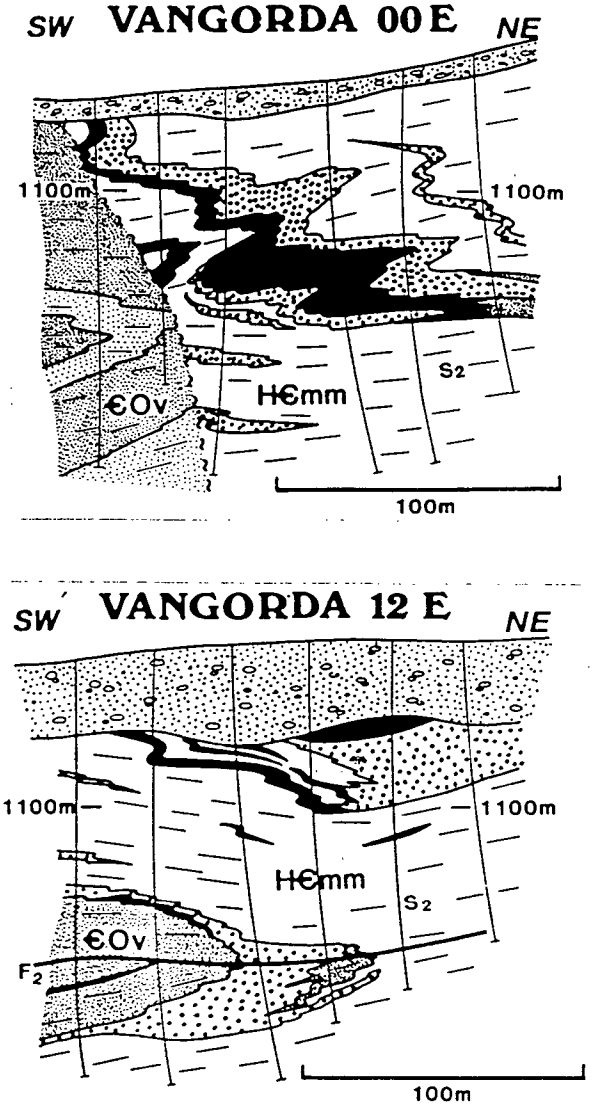


FIGURE 34. Vertical cross sections of the Vangorda deposit, looking northwest, no vertical exaggeration. Units are the same as Figure 33. (A) Cross section 00E. The strike of the fault at the southwest end of the section is at a small angle to the trend of the section; it downdrops the deposit but since it is superimposed on the overturned limb of a large second phase fold the throw appears opposite. (B) Cross section 12E (about 400 m southeast of 00E). The disseminated sulphides just beneath the overburden are low in lead-zinc but relatively enriched in copper and gold. Pyrite > pyrrhotite > magnetite are all developed in the quartzite and the quartzose matrix of the rock may represent silicified and bleached host metasediment rather than recrystallized cherty exhalative mineralization. The structure on this section, hence the stratigraphic position of the quartzite relative to massive sulphides is not resolved. The quartzite is certainly one of the best candidates in the district for a siliceous footwall feeder zone. The massive sulphides just beneath the overburden correlate with the main massive sulphide horizon on section 00E. This interpretation of the deposit structure is essentially the same as one first developed independently by Kerr Addison geologists in 1977. Alteration is not shown separately on these sections but most Mt. Mye phyllites (Hcmm) are bleached off-white with muscovite-rich assemblages or less intensely bleached to light green with muscovite chlorite rich assemblages, both assemblages containing minor disseminated pyrite or pyrrhotite.

Alternatively, the Anvil Cycle could form by repetitive release of a fluid whose composition changes through time in a regular fashion as it is released from a deep-seated reservoir and need bear no relationship to sea floor depositional conditions. Many causes of fluid variation could be proposed that may relate more to conditions, fluid and rock composition at the site of ore fluid evolution, the manner of ore fluid reservoir tapping, or possible fluid mixing during transport to the sea floor.

Conclusions

Strata of Anvil District have been shown to be likely North American because of their association with, and correlation to, well understood Selwyn Basin stratigraphy. In this light, the

Anvil package is considered only slightly suspect. This stratigraphic package is a coherent, layered sequence about 5 km thick, conveniently divisible into an upper and lower sequence.

The lower sequence is subdivided into three regionally mappable units from late Precambrian to Silurian age. A monotonous 2 km thick sequence of variably metamorphosed, non-calcareous phyllites and pelitic schists of Mt. Mye formation forms the base of the Anvil pile. These rocks are correlated with similar pelitic assemblages beneath Rabbitkettle Formation northeast of the district toward Mackenzie Platform. Mt. Mye formation is overlain by a 1 km thick assemblage of calcareous phyllites and lesser basaltic volcanic rocks of Vangorda formation. Vangorda formation is much more argillaceous than Rabbitkettle Formation with which it is correlated. Stratiform lead-zinc-silver deposits of Anvil District occur within a 150 m thick interval straddling the Mt. Mye/Vangorda contact and are associated with reduced basinal pelites. The deposits are sediment hosted, and not directly related to the basaltic volcanic component of the pile. Calcareous phyllites of Vangorda formation are interleaved with and overlain by a 1 km thick, basaltic metavolcanic sequence named Menzie Creek formation. Shales, slates and siltstones interbedded with a wide variety of Menzie Creek volcanic rocks are lithologically identical to Road River strata and yield fauna of lower Ordovician to Lower Silurian age. On this basis, Menzie Creek formation is correlated with Road River Group. The Menzie Creek volcanic facies are similar to alkaline basaltic assemblages of similar age elsewhere in Selwyn Basin but were included in the Anvil Range Group of the upper stratigraphic division of the Anvil pile by earlier workers. The term Anvil Range Group should be restricted to younger (possibly Permo-Pennsylvanian), suspect, alkaline basalts overlying a thick, vari-coloured phyllitic chert sequence forming Rose Mountains immediately northeast of Vangorda Creek and Tintina Fault Zones. Rocks of the lower stratigraphic division in Anvil Range are thought to represent a deep, marine basinal sequence of shales, siltstones and minor mafic volcanic and intrusive rocks which accumulated on a trailing continental margin subject to repeated episodes of extensional tectonism during basin evolution.

The ore deposits and enclosing host rocks of Anvil District are polydeformed, twice regionally metamorphosed and intruded by a 100 m.y. granitic plutonic suite which is syn- or late-kinematic with respect to at least the second metamorphic event.

A characteristic vertical and lateral zonation of sulphide lithofacies, the Anvil Cycle, is common to all Anvil sulphide deposits. Quartzose, variably carbonaceous disseminated sulphide-bearing facies typify the basal and marginal facies of a deposit or given horizon in a multi-layered deposit. Massive pyritic sulphide and baritic facies succeed the disseminated facies, occupying the upper and more central area of a sulphide layer. The consistently recurring facies assemblage of the Anvil Cycle may imply repetitively occurring physicochemical factors at the site of sulphide deposition or in the reservoir site of brine evolution.

All deposits have a variably developed, white-mica-dominant wallrock alteration envelope that is commonly best developed in the footwall. This alteration may represent hot ore fluid/wallrock interaction at the time of sulphide deposition; a metamorphic reaction envelope between the sulphides and enclosing pelites, or a combination of both. To date, the distribution of this alteration assemblage has not revealed credible feeder zones for any deposit.

The Anvil deposits form a prominent curvilinear array in plan and are associated with anomalous development of graphitic pelites in the transition zone between Mt. Mye and Vangorda formations. These graphitic assemblages appear to thin dramatically immediately northeast of the curvilinear deposit line. The linear distribution of known deposits, their association with facies changes involving reduced basinal assemblages and the first recognizable pulse of basaltic volcanism are compatible with a synsedimentary exhalative genetic model.

TABLE 12. Dy Deposit Synopsis

Stratigraphic Position:
Multilayered deposit spanning very poorly defined transition zone from Mt. Mye to Vangorda fm.; uppermost horizon within Vangorda fm., remainder of horizons in Mt. Mye fm.; current data inadequate to define Mt. Mye/Vangorda boundary accurately.

Number of Horizons:
At least three, up to five; current drilling density and resultant limitations of structural interpretation preclude resolution.

Dimensions (present):
Length 2200 m; width 1800 m; 200 m thickness contains known sulphide horizons.

Geological Reserves:

	Tonnes x 10^6	Pb (%)	Zn (%)	Ag (g/t)	Cu (%)	Ag (g/t)
(at 9% Pb + Zn cutoff)	21.1	5.5	6.7	84	0.12	0.95

Zoning:
No definitive studies.

Facies Distribution:
Internal structure of deposit too poorly understood to allow evalution; reasonable development of Anvil Cycles; anomalous development of carbonate-bearing, pyritic, massive sulphides and to a lesser degree baritic, pyritic, massive sulphides; development of graphitic phyllite demonstrably less than in Swim, Vangorda and Grum deposits.

Precious Metal Content:
Ag in PbS; PbS preferentially enriched in massive sulphide facies, particularly in baritic facies; Au follows same trend.

Feeder Zones:
None defined (but see below).

Alteration Overprint:
Moderately to well developed; generally footwall biased with some overlapping of successive footwall on previous hangingwall; general suggestion of stronger development toward present southwestern margin of deposit perhaps implying proximity to a feeder zone (Fig. 27). Large areas of light olive green chloritic phyllites northeast of deposit may reflect alteration as well (Fig. 27).

Structural Regime:
Appears to lie on upper Z symmetry long limb of megascopic F_1 antiform; local superimposition of moderate scale F_2 folds; internal geometry of deposit poorly understood.

Faults:
Numerous steep faults cut the deposit but their orientation, distribution and displacements are unknown. Important shallowly dipping faults also present beneath the deposit.

Metamorphic Grade:
Dominantly greenschist facies; local portions of deposit transitional to amphibolite facies with first appearance of staurolite in pelitic rocks.

Remobilization Features:
Brecciation as in other deposits; no other features obvious.

Intrusive Rocks:
Numerous hornblende diorite and quartz feldspar porphyry dykes cut deposit with greatest density along a generally 60° trending zone along the east end of the deposit; monzonite and pegmatitic dykes common at greatest depths of drilling below deposit.

Contact Metamorphic Features:
None.

Acknowledgments

We thank the officers of Cyprus Anvil Mining Corporation and Dome Petroleum Ltd. for permission to present this paper. Particular thanks are given to Dr. J. Glenn Simpson for his years of support, assistance and guidance. Dr. Lee C. Pigage provided frequent counsel, ideas and collaborative field work for which we are indebted.

While the ideas, conclusions and shortcomings of this paper are the responsibility of the authors, we gratefully acknowledge the discussions with and extensive field work by many colleagues over the years. Thanks are given specifically to D.J. Hanson, J.B. Heslop, P.F. Lewis, J.S. Modene, G.A. Gorzynski, J.W. Mustard, W.J. Roberts, J.P. Franzen, B.V. Hall, R.S. Tolbert,

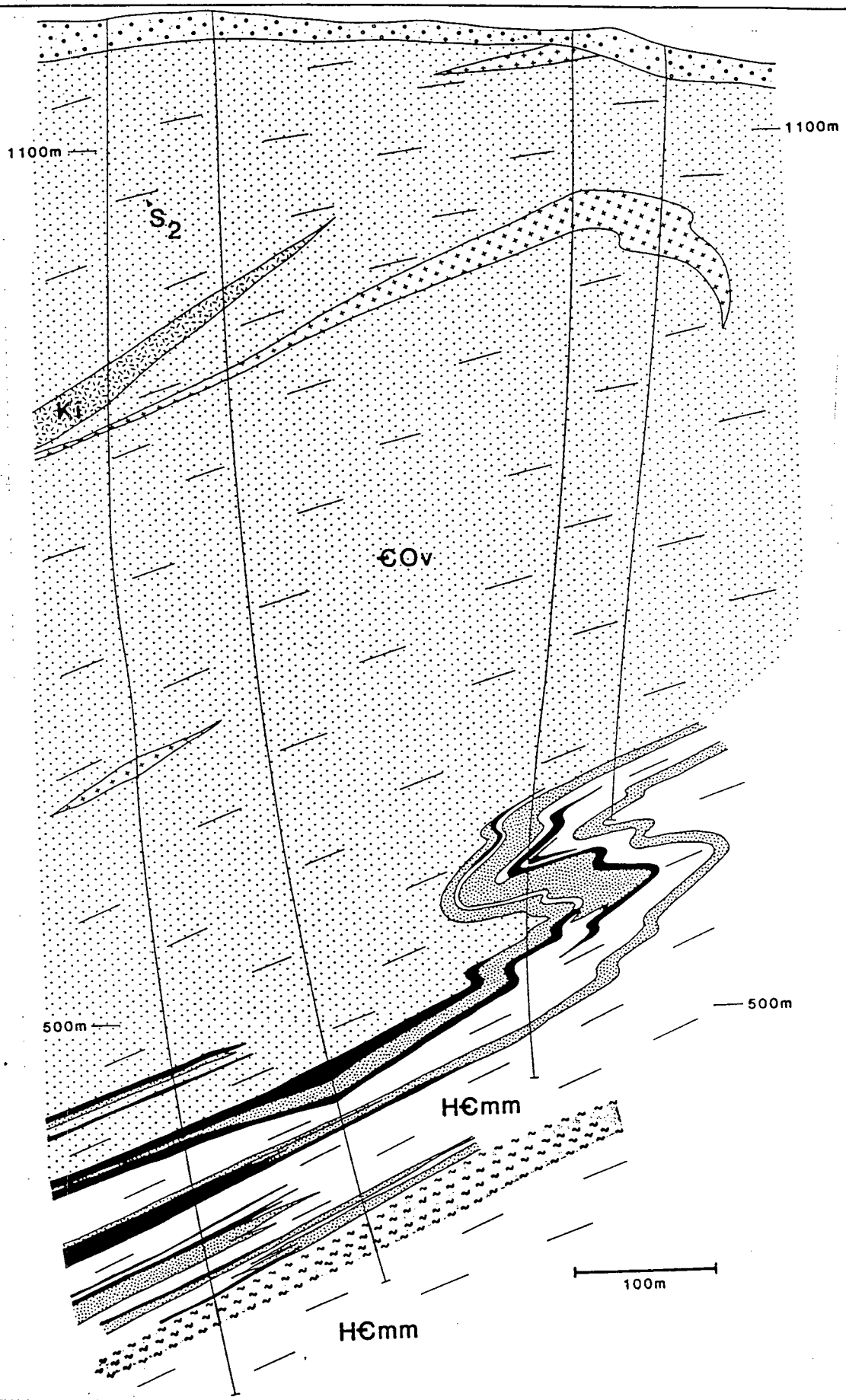


FIGURE 35. A vertical cross section (12 + 00E) of the Dy deposit, looking northwest, no vertical exaggeration. Modified from a section by B.V. Hall. Units are the same as those of Figure 33. The carbonaceous shear zone at the base of the deposit is identical to the Tie Fault shear zone and probably is another major extensional fault flooring the deposit. Alteration is not shown separately (Fig. 27).

J. Kier, P. Nakai, M.A. Stammers, M.O. Hampton, J. Gondi and P.M. Pettigrew.

Geophysical data interpretation and integration into the geological framework was achieved in cooperation with P.E. Walcott. Our understanding of both the regional and local geological setting of Anvil District benefited from numerous discussions with Dr. D.J. Tempelman-Kluit and Dr. S.P. Gordey of the Geological Survey of Canada and Dr. J.K. Mortensen of The University of British Columbia. Numerous drafts of this manuscript were typed whole or in part by M. Mardus, C. Kent, V. VanderPutt and J. Broeren. While the authors are listed alphabetically, they have contributed equally to this paper.

REFERENCES

AHO, A.E., 1966, Exploration methods in Yukon with special reference to Anvil District; *Western Miner, Vol. 39, April, pp. 127-148.*

AHO, A.E., 1969, Zinc-lead province of Yukon, *CIM Bull., Vol. 62, No. 684, April, pp. 397-409.*

AIKEN, J.D., 1982, Precambrian of the Mackenzie fold belt—a stratigraphic and tectonic overview; *in* Precambrian Sulphide Deposits; Geol. Assoc. Can., Spec. Paper 25, *pp. 149-161.*

BLUSSON, S.L., 1966, Frances Lake, Yukon Territory and District of Mackenzie; Geol. Surv. Can., Map 8-1967.

BLUSSON, S.L., 1968, Geology and tungsten deposits near the headwaters of Flat River, Yukon Territory and southwestern District of Mackenzie; Geol. Surv. Can., Paper 67-22.

BROCK, J.S., 1973, Geophysical exploration leading to the discovery of the Faro Deposit, Yukon Territory; *CIM Bull., Vol. 66, No. 738, Oct., pp. 97-116.*

BROCK, J.S., and ROBERTS, W.J., 1971, Exploration report, Tintina Anvil Project; unpublished report, Dynasty Exploration.

CAMPBELL, F.A., and ETHIER, V.G., 1974, Sulfur isotopes, iron content of sphalerites, and ore textures in the Anvil Ore Body, Canada; *Econ. Geol., Vol. 69, pp. 482-493.*

CAMPBELL, R.B., 1967, Geology of Glenlyon map-area; Geol. Surv. Can., Mem. 352, 92 p.

CARMICHAEL, D.M., 1978, Metamorphic bathozones and bathograds: a measure of the depth of post-metamorphic uplift and erosion on the regional scale; *Amer. Jour. Sci., Vol. 278, pp. 769-797.*

CARPENTER, A.B., 1979, Interim report on lead and zinc in oil field brines in the central Gulf Coast and in southern Michigan; Amer. Inst. Min. Metall., Preprint No. 79-95.

CARSON, D.J.T., 1977, Geological and mineralogical investigation of the metallurgy of the Grum orebody, Yukon Territory; unpublished report, Kerr Addison Mines, 47 p.

CECILE, M.P., 1982, The lower Paleozoic Mistry Creek embayment, Selwyn Basin, Yukon and Northwest Territories; Geol. Surv. Can., Bull. 335, 78 p.

CHISHOLM, E.O., 1957, Geophysical exploration of a lead zinc deposit in Yukon Territory; *in* Methods and case histories in mining geophysics, Sixth Commonwealth Mining and Metallurgy Congress, *pp. 269-277.*

CLARKE, F.W., 1924, Data of geochemistry; U.S. Geol. Surv., Bull. 770, 841 p.

CONEY, P.J., JONES, D.L., and MONGER, J.W.H., 1980, Cordilleran suspect terranes; *Nature, Vol. 288, pp. 329-333.*

EISBACHER, G.H., 1981, Sedimentary tectonics and glacial record in the Windermere Supergroup, Mackenzie Mountains, northwestern Canada; Geol. Surv. Can., Paper 80-27, 40 p.

FLOYD, P.A., and WINCHESTER, J.A., 1978, Identification and discrimination of altered and metamorphosed volcanic rocks using immobile elements; *Chemical Geology, Vol. 21, pp. 29-306.*

GABRIELSE, H., and BLUSSON, S.L., 1969, Geology of Coal River map area, Yukon Territory and District of Mackenzie (95 D); Geol. Surv. Can., Paper 68-38, 22 p.

GABRIELSE, H., BLUSSON, S.L., and RODDICK, J.A., 1973, Geology of Flat River, Glacier Lake and Wrigley Lake map areas; Geol. Surv. Can., Mem. 366, 153 p.

GODWIN, C.I., and SINCLAIR, A.J., 1982, Average lead isotope growth curves for shale hosted zinc-lead deposits, Canadian Cordillera; *Econ. Geol., Vol. 77, pp. 675-690.*

GORDEY, S.P., 1978, Stratigraphy and structure of the Summit Lake area, Yukon and Northwest Territories; *in* Current Research, Part A; Geol. Surv. Can., Paper 78-1A, *pp. 43-48.*

GORDEY, S.P., 1979, Stratigraphy of southeastern Selwyn Basin in the Summit Lake area, Yukon Territory and Northwest Territories; *in* Current Research, Part A; Geo. Surv. Can., *pp. 13-16.*

TABLE 13. Swim Deposit Synopsis

Stratigraphic Position:
Approximately 20 m below Mt. Mye/Vangorda formation contact in uppermost Mt. Mye formation immediately below thick graphitic phyllite unit; probably equivalent to main horizon at Grum. Basal carbonaceous rocks to Vangorda formation very well developed.

Number of Horizons:
One, possibly a second thin footwall horizon; multiple Anvil cycles in higher horizons.

Dimensions:
Approximately 400 m long, 300 m wide (measured along F_2 fold profile), 10 m average thickness.

Geological Reserves:

	Tonnes x 10^6	Pb (%)	Zn (%)	Ag (g/t)
(at 4% Pb + Zn cutoff)	4.3	3.8	4.7	42

Zoning:
No definitive study.

Facies Distribution:
Uncertain as part of the deposit may be offset by shallow fault flooring deposit; suggestion of massive sulphide and baritic massive sulphides centrally located in main horizon.

Precious Metal Content:
Silver largely in PbS; no data on systematics of Ag and Au distribution.

Feeder Zone:
A few identified pre-D_1 and many pre-D_2 quartz-chlorite-chalcopyrite-pyrrhotite veinlets in footwall of main lens may represent a feeder but this is uncertain.

Alteration Overprint:
Generally weakly to moderately developed in stratigraphic footwall only.

Structural Regime:
Deposit in hinge of megascopic southwesterly closing F_2 fold hinge on inferred Z symmetry long limb of northeasterly vergent F_1 antiform; deposit floored by shallowly southwesterly dipping thrust or extensional fault.

Faults:
Local steep faults of minor significance inferred from drilling; main fault of exploration importance is the low-angle fault noted above, which appears to truncate, and may offset a portion of the deposit.

Metamorphic Grade:
Greenschist facies above low-angle fault transitional to amphibolite facies approximately 100 m below same.

Metavolcanic Rocks:
Metabasites and related metatuffs (?) above deposit at immediate base of Vangorda Formation; dull light medium green chloritic phyllite unit forms deposit footwall and structural footwall of shallow fault beneath deposit; this unit of uncertain origin, may be tuffaceous or a carbon-deficient weakly chloritized pyllite (altered by ore-bearing fluids?); chloritic unit similar to that developed northeast of Dy deposit and near metabasites of District.

Remobilization Features:
Internal brecciation in sulphides as seen in other deposits; no other notable features.

Intrusive Rocks:
Minor hornblende diorite dykes.

Contact Metamorphic Features:
None.

GORDEY, S.P., 1981, Stratigraphy, structure and tectonic evolution of southern Pelly Mountains in the Indigo Lake area, Yukon Territory; Geol. Surv. Can., Bull. 318, 44 p.

GORDEY, S.P., 1983, Thrust faults in the Anvil Range and a new look at the Anvil Range Group, south central Yukon Territory; *in* Current Research, Part A; Geol. Surv. Can., Paper 83-1A, *pp. 225-227.*

GORDEY, S.P., ABBOTT, J.G., and ORCHARD, M.J., 1982, Devono-Mississippian (Earn Group) and younger strata in east central Yukon; *in* Current Research, Part B; Geol. Surv. Can., Paper 82-1B, *pp. 93-100.*

IRVINE, T.N., and BARAGAR, W.R.A., 1966, A guide to the chemical classification of the common volcanic rocks; *Can. Jour. Earth Sci., Vol. 8, pp. 523-548.*

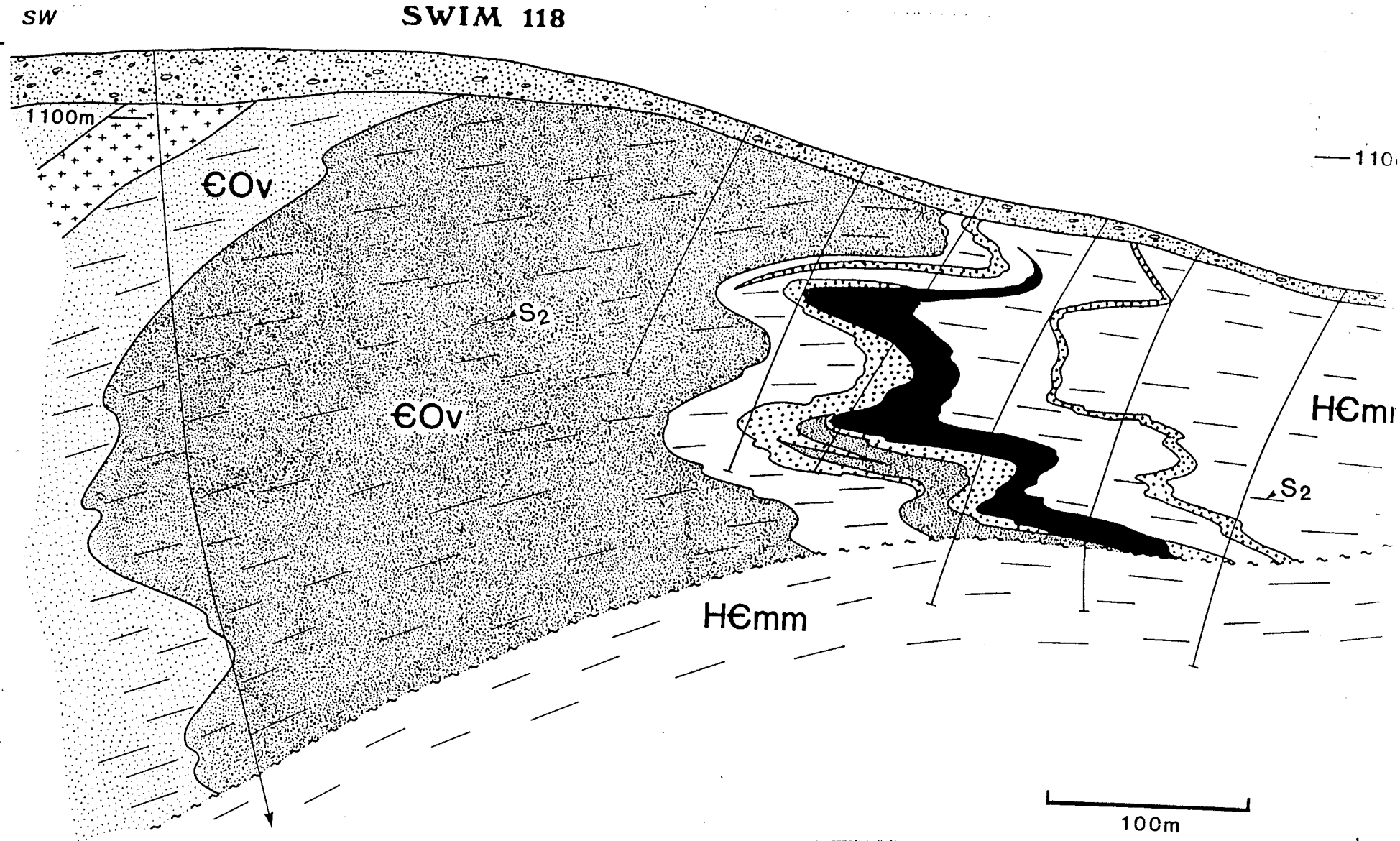


FIGURE 36. Vertical cross section 118 through the Swim deposit. The basal massive sulphides in the main horizon are divisible into an upper baritic portion and a lower non-baritic portion, underlain locally by a thin quartzose unit not differentiated here. Thus, the appearance of a reversed cycle is not real. The upper quartzose mineralization may represent the onset of a second incomplete (on this section at least) cycle or may simply be the result of an off-centre random slice through the idealized deposit shown in Figure 19 illustrating the difficulties and dangers in the uncritical usage of the cycle concept. The fault at the base of the deposit is a low angle one. Its displacement does not appear to be within the plane of the section and is a matter to be resolved by future exploration. Essentially the same fold geometry for Swim has been worked out independently by Kerr Addison geologists in 1975.

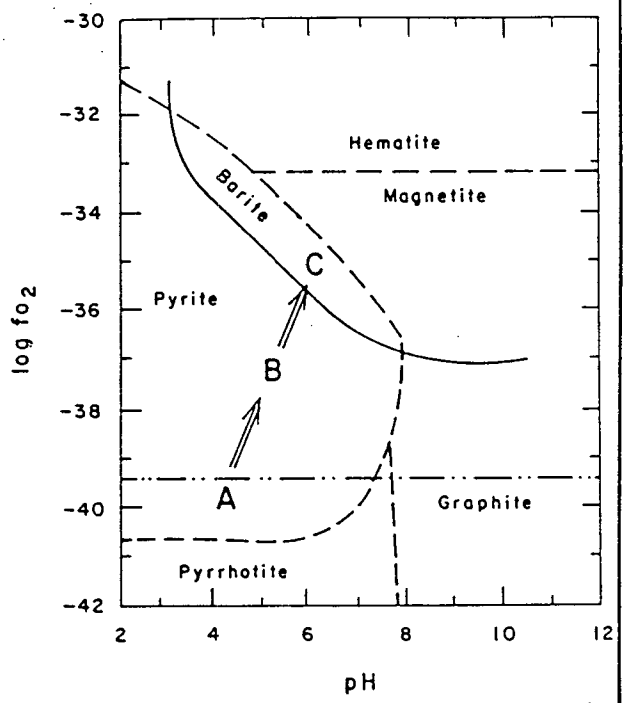


FIGURE 37. fO_2-pH diagram, modified from Rye and Ohmoto (1974), for T = 250°C, ionic strength = 1, ΣS = 0.01 m, m_{Ba++} = 0.001, fCO_2 = 1 atm. The path A>B>C would explain the sequence of lithologies of the Anvil Cycle. At "A", graphite and pyrite are stable; thus ribbon banded graphitic quartzite could form. At "B", graphite is no longer stable but massive and quartzose pyritic sulphides could form. At "C", barite-bearing massive sulphides could form, the common association of magnetite with barite bearing massive sulphides follows from this path.

JEFFERSON, C.W., KILBY, D.B., PIGAGE, L.C., and ROBERTS, W.J., 1983, The Cirque barite-zinc-lead deposits, northeastern British Columbia; *in* Sangster, D.F. (ed.), Short Course in Sediment-hosted Stratiform Lead Zinc Deposits, Mineralogical Association of Canada, Short Course Handbook, Vol. 8, May, *pp. 121-140.*

JENNINGS, D.S., JILSON, G.A., and PIGAGE, L.C., 1980, Anvil Range stratigraphy, south central Yukon Territory; (prog. with abst.), Cordilleran Section, Geol. Assoc. Can., Jan. 1980, pp. 16-17.

KUO, S.L., 1976, Geology and geochemistry of stratabound ore deposits in south central Yukon Territory and southwestern District of Mackenzie, Northwest Territories; Unpubl. Ph.D. thesis, Univ. of Alberta, Edmonton.

KUO, S.L., and FOLINSBEE, R.E., 1974, Lead isotope geology of mineral deposits spatially related to the Tintina Trench, Yukon Territory; *Econ. Geol., Vol. 69, pp. 806-813.*

LECOUTEUR, P., 1973, A lead isotope study of ore deposits from the East Kootenay District, B.C. and the Anvil District, Yukon Territory, Unpubl. Ph.D. thesis, Univ. of B.C.

LEWIS, P.F., 1974, A report on the reconnaissance geology and geochemistry—Anvil Range program, Yukon Territory, unpublished report, Ridgemount Mining Corp., 31 p.

McCLAY, K.R., and ELLIS, P.G., 1983, Deformation and recrystallization of pyrite; *Mineralogical Magazine, Vol. 47, pp. 527-538.*

MIDDLETON, G.V., 1960, Chemical composition of sandstones; *Bull. Geol. Soc. Amer., Vol. 71, pp. 1011-1026.*

MIYASHIRO, A., 1961, Evolution of metamorphic belts; *Jour. Pet., Vol. 2, pp. 277-311.*

MODENE, J.S., 1982, Origin and sulfur isotope geochemistry of the Grum deposit, Yukon Territory, Canada; Unpubl. M.Sc. thesis, Univ. of Wisconsin, 158 p.

MONGER, J.W.H., and PRICE, R.A., 1979, Geodynamic evolution of the Canadian Cordillera—progress and problems; *Can. Jour. Earth Sci., Vol. 16, pp. 770-791.*

MONGER, J.W.H., PRICE, R.A., and TEMPELMAN-KLUIT, D.J., 1982, Tectonic accretion and the origin of the two major metamorphic and plutonic belts in the CAnadian Cordillera; *Geology, Vol. 10, pp. 70-75.*

MORTENSEN, J.K., and JILSON, G.A., 1983, Evolution of the Yukon-Tanana terrane: Evidence from southeastern Yukon Territory; *Geology, Vol. 13, pp. 806-810.*

MORTON, P.C., 1973, Geochemistry of bedrock and soils in the vicinity of the Anvil Mine, Yukon; unpubl. M.Sc. thesis, Univ. of B.C., 207 p.

OHMOTO, H., 1972, Systematics of sulfur and carbon isotopes in hydrothermal ore deposits; *Econ. Geol., Vol. 67, pp. 551-579.*

PEARCE, J.A., and CANN, J.R., 1973, Tectonic setting of basic volcanic rocks determined using trace element analyses; *Earth and Planetary Science Letters, Vol. 19, pp. 290-300.*

PETTIJOHN, F.J., 1963, Chemical composition of sandstones—excluding carbonate and volcanic sands; *in* Data of Geochemistry, 6th ed., U.S. Geol. Surv. Prof. Paper 440-S, 19 p.

PIGAGE, L.C., and ANDERSON, R.G., 1985, The Anvil plutonic suite, Faro, Yukon Territory; *Can. Jour. Earth Sci., Vol. 22, pp. 1204-1216.*

RODDICK, J.A., and GREEN, L.H., 1961, Tay River map area, Yukon Territory; Geol. Surv. Can., Map 13-1961.

RYE, R.O., and OHMOTO, H., 1974, Sulfur and carbon isotopes in ore genesis: a review, *Econ. Geol., Vol. 69, pp. 826-842.*

SATO, T., 1972. Behaviors of ore forming solutions in Seawater; *Mining Geol., Vol. 22, pp. 31-42.*

SHANKS, W.C., III, WOODRUFF, L.G., JILSON, G.A., JENNINGS, D.S., MODENE, J.S., and RYAN, B.D., Sulfur and lead isotope studies of stratiform Zn-Pb-Ag deposits, Anvil Range, Yukon Territory: Basinal brine exhalation and anoxic bottom-water mixing; *Econ. Geol., in press.*

SHAW, D.M., 1956, Geochemistry of pelitic rocks III: major elements and general geochemistry; *Bull. Geol. Soc. Amer., Vol. 67, pp. 919-934.*

TEMPELMAN-KLUIT, D.J., 1970a, Stratigraphy and structure of the "Keno Hill Quartzite" in Tombstone River - Upper Klondike River map areas, Yukon Territory; Geol. Surv. Can., Bull. 180, 102 p.

TEMPELMAN-KLUIT, D.J, 1970b, The relationship between sulfide grain size and metamorphic grade of host rocks in some stratabound pyritic ores; *Can. Jour. Earth Sci., Vol. 7, pp. 1139-1345.*

TEMPELMAN-KLUIT, D.J., 1972, Geology and origin of the Faro, Vangorda and Swim concordant zinc-lead deposits, central Yukon Territory; Geol. Surv. Can., Bull. 208, 73 p.

TEMPELMAN-KLUIT, D.J., 1977, Quiet Lake (105 F) and Finlayson Lake (105 G) map areas, Yukon Territory; Geol. Surv. Can., Open File 486.

TEMPELMAN-KLUIT, D.J., 1979, Transported cataclasite, ophiolite and granodiorite in Yukon Territory: evidence of arc-continent collision; Geol. Surv. Can., Paper 79-14.

WHEELER, J.O., GREEN, L.H., and RODDICK, J.A., 1960, Finlayson Lake map area, Yukon Territory; Geol. Surv. Can., Map 8-1960.

APPENDIX B

GEOLOGY AND MINERAL DEPOSITS OF SOUTHERN YUKON

Dirk Tempelman-Kluit, Regional Geologist
Department of Indian Affairs and Northern Development
Whitehorse, Yukon

INTRODUCTION

This report includes a summary of the mineral exploration history of Yukon, an outline of the geology of its southern part, and brief descriptions of the most important mineral occurrences. The report brings together current ideas of the geology and examines the metal deposits in this context. This account is intended as an introduction to exploration geologists, prospectors and interested laymen to provide an overview of Yukon's mineral industry. It is not a source of detailed data, or an exhaustive treatment; references to sources are included.

Yukon's mineral resource base is broad with world class reserves of zinc-lead (Anvil and Howard's Pass), important stores of copper (Casino, Minto), a near monopoly in tungsten (Cantung, Mactung, Logtung, Dublin Gulch), a significant molybdenum deposit (Red Mountain) and a range of smaller gold, silver, tin, asbestos and barite occurrences. Only three districts are presently being mined.

EXPLORATION HISTORY

Mineral exploration in Yukon has evolved from an early stage of searching out high grade precious metals occurrences to exploring for large, relatively low grade deposits of base metals. In Yukon this switch came later than elsewhere in North America, partly because of the physical isolation in the early part of the century and because of its psychological remoteness. Exploration for gold and silver lodes began in the Territory following the Klondike Rush and attention focussed in the Wheaton and Conrad districts. In 1919, high grade silver mineralization was discovered on Keno Hill near Mayo. With the exception of some small rich occurrences of copper (in the Whitehorse copper belt) exploration concentrated on the precious metals and until the early 1950's Yukon was considered as a place with small high-grade silver deposits, but precious little else.

Opening of the Alaska Highway removed the physical and psychological distance of the Yukon and was soon followed by discovery of the Tom, Wellgreen (1952), and Vangorda (1953), which deposits stirred the imagination of prospectors. Although none of these occurrences were economic, they indicated an unrecognized potential for base metals in Yukon making it interesting to larger companies for the first time.

There followed a decade of regional prospecting that grew in intensity, and which resulted in discovery of the Clinton Creek, (18 million tonnes asbestos, 1957), Swim,(9 million tonnes 10% combined zinc and lead, 1963) and New Imperial (4.5 million tonnes 1.5% copper, 1964) deposits, and which culminated with finding of the Faro orebody, (57 million tonnes 10% combined zinc and lead, 1965).

Discovery of the Faro sparked the first massive exploration rush in Yukon (Figure 1) and in 1966 and 1967 large and small companies swarmed the Anvil Range. As is often the case, the rush itself contributed no

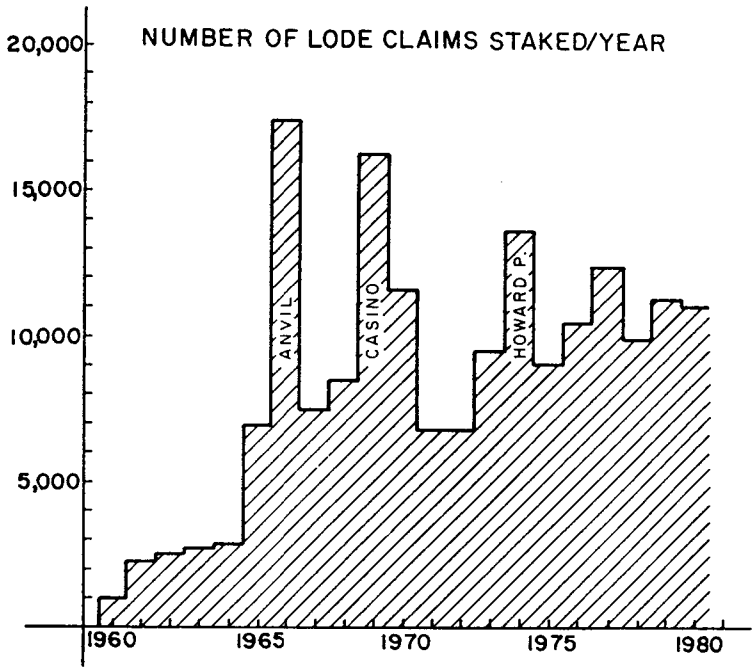


Figure 1a
New Lode Claims staked annually in Yukon between 1960 and 1980.

significant discoveries, and the exploration interest in the Anvil district cooled. Nevertheless, this stampede started the Territory on the rush phase in its exploration history and signalled a decade of grassroots exploration.

Recognition in 1968 of a large, low grade copper-molybdenum deposit near silver-lead showings known earlier, led to the Casino rush in the Dawson Range in 1969 and 1970. This exploration surge again involved large and small companies alike, and led indirectly to two subsequent discoveries (Minto and Williams Creek). Although the Casino deposit is presently uneconomic, it widened the metals base for Yukon exploration and indicates a potential for further finds of this type.

The third exploration rush in Yukon began as quietly as its predecessors with the finding in 1972 near Summit Lake, of fine-grained lead-zinc mineralization of a type not recognized before in Yukon, and in rocks not thought to be productive. This time exploration surged into the Mackenzie mountains, the most remote part of the Territory. This rush was also spurred by a change in politics in British Columbia that drastically altered the exploration interest there. This third rush, led directly to finding of two significant showings (Goz and Gayna) and a number of less important occurrences. It confirmed the Howard's Pass area as the second major lead-zinc district of Yukon. The Grum deposit (1974), the fourth in the Anvil district, was discovered almost incidentally at this time as a result of systematic drilling in the Anvil district.

The DY, another deposit in the Anvil Range was found in 1976 following careful follow-up work and drilling.

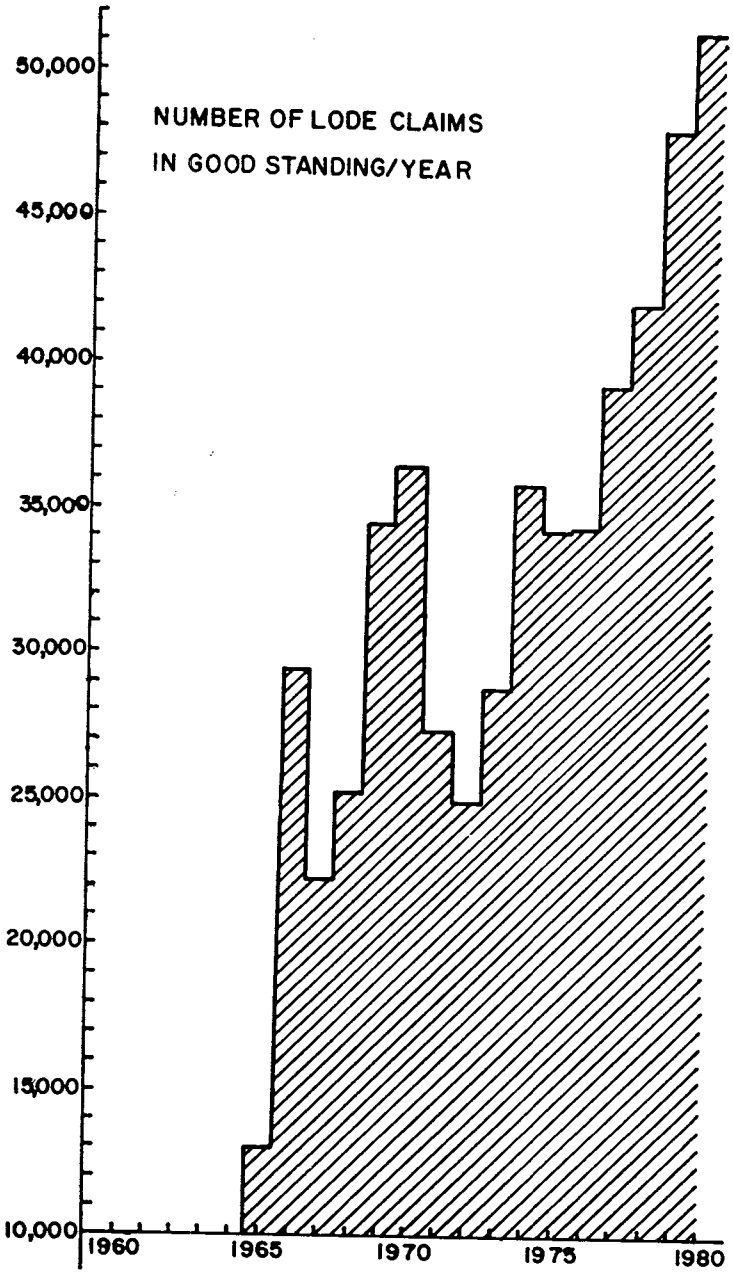


Figure 1b
Yukon Lode Claims in good standing between 1960 and 1980

In the mid-seventies, exploration shifted from the carbonate rocks of Mackenzie Platform to the shales of Selwyn Basin and the Jason, a stratabound lead-zinc deposit, was discovered in 1975. Later in the decade grass roots exploration declined in favour of more concentrated property work with increasing emphasis on drilling. As a result Logtung, Red Mountain and Clear Lake were found on old properties.

Mineral production in Yukon reflects the exploration history with an appropriate time lag (Figure 2). Before 1965, the mines at Keno and Galena Hill were Yukon's sole producers, and for decades accounted for the total annual output of mineral concentrates to a value of about $15 million. Opening of Clinton Creek (1968, 2500 tpd), added $10-$15 million a year, and production at New Imperial, which began the same year (1968, 2000 tpd), added $10 million annually. However, opening of the Anvil Mine (1969, 6000 tpd) overshadowed these developments , and led to a quantum jump in annual production so that Yukon now produces in the order of $300 million a year. Although this is a modest 1-1/2% of Canadian mineral production the figure has been increasing and the per capita production from minerals of the Territory (about $15,000) is the highest in the country.

GEOLOGY OF SOUTHERN YUKON

This introduction emphasizes the main elements of the geology of southern Yukon and intends to set the stage for the descriptions of mineral deposits that follow. The geology is treated in four steps: its subdivisions, their stratigraphy, the deformation and metamorphism and the overlap suites. Subdivisions of the geology are outlined in a sketch map and relations between the entities summarized. Stratigraphic columns giving the main divisions for each element follow and the important plutonic suites are characterized. The style of deformation and metamorphism are briefly treated. Sedimentary and volcanic units that overlap more than one element are indicated.

Southern Yukon is sliced into three parts by two northwest trending strike-slip faults, the Tintina and Denali faults (Figure 3) which localized 450 km and 250 km of dextral slip respectively during the Tertiary. Tectonic elements northeast of the Tintina fault recur southwest of it, but the Denali fault separates discrete terranes and probably follows a fundamental suture in most of Yukon. Both strike-slip faults localize narrow grabens which are Pliocene physiographic trenches. Tintina Trench is along Tintina fault and Shakwak Trench is along the Denali.

The geology includes two discrete parts (Figure 3); northeasternmost are strata deposited on the ancient North American continent and southwest of it are rocks formed as part of a Mesozoic arc on a foreign continental fragment now accreted to North America. The two parts are further divided (Figure 4) and the ancient North American element includes four subdivisions that are laterally intergradational and deposited as facies belts next to one another. These four parts are Mackenzie Platform, Selwyn Basin, Cassiar Platform and Nasina Shelf. The accreted part is also split into four entities northeast of Denali fault, namely the Yukon Cataclastic Complex, Whitehorse Trough, Yukon Crystalline Terrane and Coast Plutonic Complex. Southwest of the Denali are the Alexander Terrane and Gravina-Nutzotin Belt.

Subdivisions used here correspond closely to the classic divisions of the Canadian Cordillera. The Mackenzie Platform, as used here, is the Mackenzie Fold Belt. Selwyn Basin, Cassiar Platform, Nasina Shelf and Yukon Cataclastic Complex were grouped together in the classic Omineca Belt while Whitehorse Trough and Yukon Crystalline Terrane relate to the Intermontane Belt.

* The Clinton Creek mine was closed in 1978.

Stratigraphy of the Ancient North American Margin

Stratigraphy of the four ancient North American elements is given in Figure 4 and the lateral equivalence of units is indicated. Stratigraphic names in common use or lithologic descriptors are used to distinguish units. Mackenzie Platform includes a thick section of Precambrian clastic strata containing two angular unconformities. A thick Cambrian to Devonian carbonate succession overlies these, and Mississippian and younger clastic rocks (Imperial Formation) cover this carbonate in turn. Selwyn Basin includes shale, chert and basaltic volcanics, the so-called Road River Group, equivalent to thick carbonate on Mackenzie Platform. The Grit Unit, Atan and Sekwi Formations, beneath the Road River, resemble strata in the adjacent Platforms. The Devono-Mississippian "Black Clastic" or Earn Group, characteristically a chert conglomerate, is much thicker than, but equivalent to, the Imperial Formation. It is overlain by a condensed section of Carboniferous and Permian fine-grained clastics. Cassiar Platform exposes a succession dominated by Silurian and Devonian carbonate rocks resembling those in Mackenzie Platform. These overlie calcareous shale with intercalated volcanics of the Kechika Group; equivalents of the Road River. Mississippian strata are clastics like those of the Imperial Formation and Earn Groups to the northeast, but contain important accumulations of trachyte and felsic plug domes. A condensed upper Paleozoic succession of limestone and calcareous siltstone is seen in Cassiar Platform and Selwyn Basin. Upper Triassic calcareous siltstone lies disconformably across the older rocks in Mackenzie Platform, Selwyn Basin and Cassiar Platform. The only important regional unconformity seen across the three elements separates Lower Cambrian and Upper Cambrian or Lower Ordovician strata. Nasina Shelf includes three variably metamorphosed units laterally traceable into Cassiar Platform. Upper Paleozoic strata are absent.

Strata in the ancient North American elements were thrust to the northeast and folded during Late Jurassic and Early Cretaceous time. The rocks generally lack penetrative structures and the intensity of the deformation decreases toward the northeast. There is no evidence of earlier folding in the Paleozoic rocks, but the strata are locally cut by Mississippian normal faults. Precambrian strata of the Wernecke Supergroup were folded before deposition of the Pinguicula Group.

Only the southwestern elements of ancient North America are regionally metamorphosed. Metamorphism was of the Barrovian type (moderate temperature and pressure) and occurred through the Late Jurassic and Early Cretaceous.

Yukon Cataclastic Complex

Yukon Cataclastic Complex contains three assemblages of highly sheared and metamorphosed rocks that are not a stratigraphic sequence, but a structural stack (Figure 4). Shearing was penetrative enough that the units lack stratigraphic integrity. The rocks range from ultramylonite and blastomylonite, products of ductile deformation, to less strained equivalents so that the parent rocks are locally preserved. Lithologic units within the stack lack lateral continuity and can not be traced into either adjoining tectonic subdivision. Moreover, extensive sheets of the sheared rocks are thrust over the less deformed ancient North American strata of the Nasina Shelf and Cassiar Platform. The internal stratigraphy, depositional relations and age of the three units are unknown.

The three assemblages occur in consistent stacking order except where disrupted by younger faults. At the base are quartz muscovite schist and interleaved chlorite schist derived from sedimentary and volcanic rocks. This is the Klondike Schist or Nisutlin Allochthonous Assemblage. Structurally above it, Anvil Allochthonous Assemblage, includes amphibolite and serpentinite, a sheared ophiolite. Highest structurally is a slice of biotite granodiorite schist, a ductile deformed plutonic suite called Simpson Allochthonous Assemblage.

Metamorphism in Yukon Cataclastic Complex occurred with ductile deformation in the Late Triassic and Early Jurassic. The rocks locally contain eclogite and blueschist minerals which indicate extreme pressure but low or moderate temperatures of metamorphism.

Intermontane Belt and Yukon Crystalline Terrane

Whitehorse Trough contains three important units: the Cache Creek, Lewes River and Laberge Groups (Figure 4). The Cache Creek is a Pennsylvanian, Permian and Triassic basalt, limestone and chert unit. It is overlain by Upper Triassic basalt of the Lewes River Group. Thick reef buildups with fossil sponges, corals and algae make up the Upper Lewes River Group locally. The Laberge is a Lower Jurassic conglomerate and sandstone derived from the volcanic Lewes River and its plutonic roots.

Four units of metamorphic rocks make up Yukon Crystalline Terrane. In sequence upward they are a biotite schist, a marble, a graphitic quartzite and an amphibolite and ultramafic unit. The age of the rocks is unknown, but they likely represent a metamorphosed stratigraphic succession. They are homotaxial with the sequence in Nasina Shelf and it is tempting to consider the two broadly equivalent. Yukon crystalline Terrane was metamorphosed in the Paleozoic? by a Barrovian style event with folding, but no shearing.

Strata of Whitehorse Trough were probably deposited on, or at the edge of the matamorphic rocks of Yukon Crystalline Terrane, but the relations are obscured by young faults. Plutonic rocks that are considered the roots of the Lewes River volcanics intrude Yukon Crystalline Terrane. The Tantalus Formation, an Upper Jurassic to Lower Cretaceous conglomerate, dominated by resistate clasts, lies unconformably across Yukon Crystalline Terrane and Whitehorse Trough strata.

The Coast Plutonic Belt in Yukon contains one stratigraphic unit, the Kluane Schist, a biotite schist of Buchan metamorphic type (moderately high temperature and low pressure) intruded and metamorphosed by Ruby Range Batholith. The Kluane Schist can be traced into strata that resemble the Jurassic and Lower Cretaceous Dezadeash Group.

Intrusive Rocks

Plutonic rocks in southern Yukon can be divided into three lithologically distinct groups with restricted distribution (Figure 5). Oldest are hornblende granodiorite (Klotassin Suite) and related pink quartz monzonite intruded in the Upper Triassic and Middle Jurassic respectively. They form large

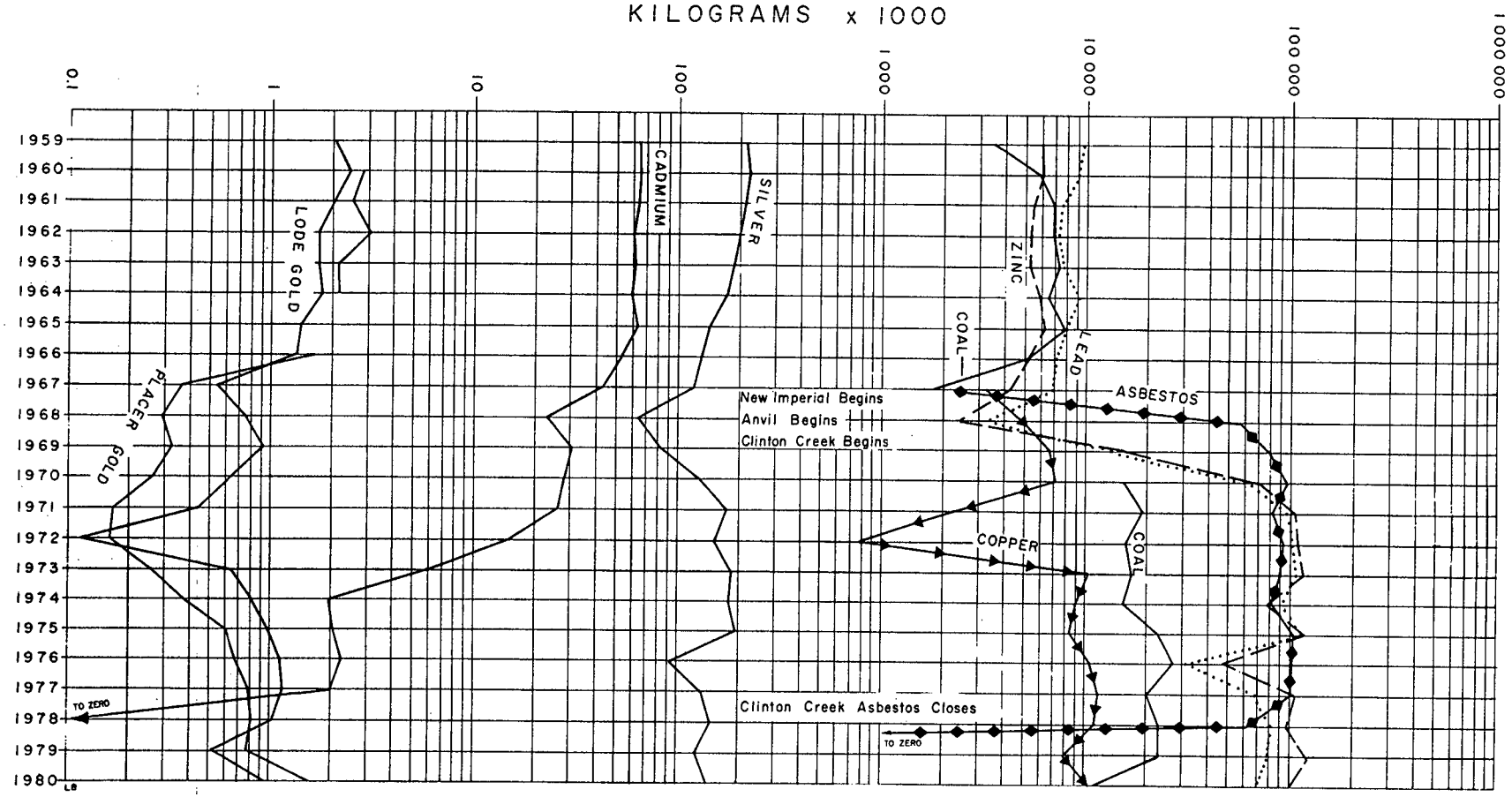
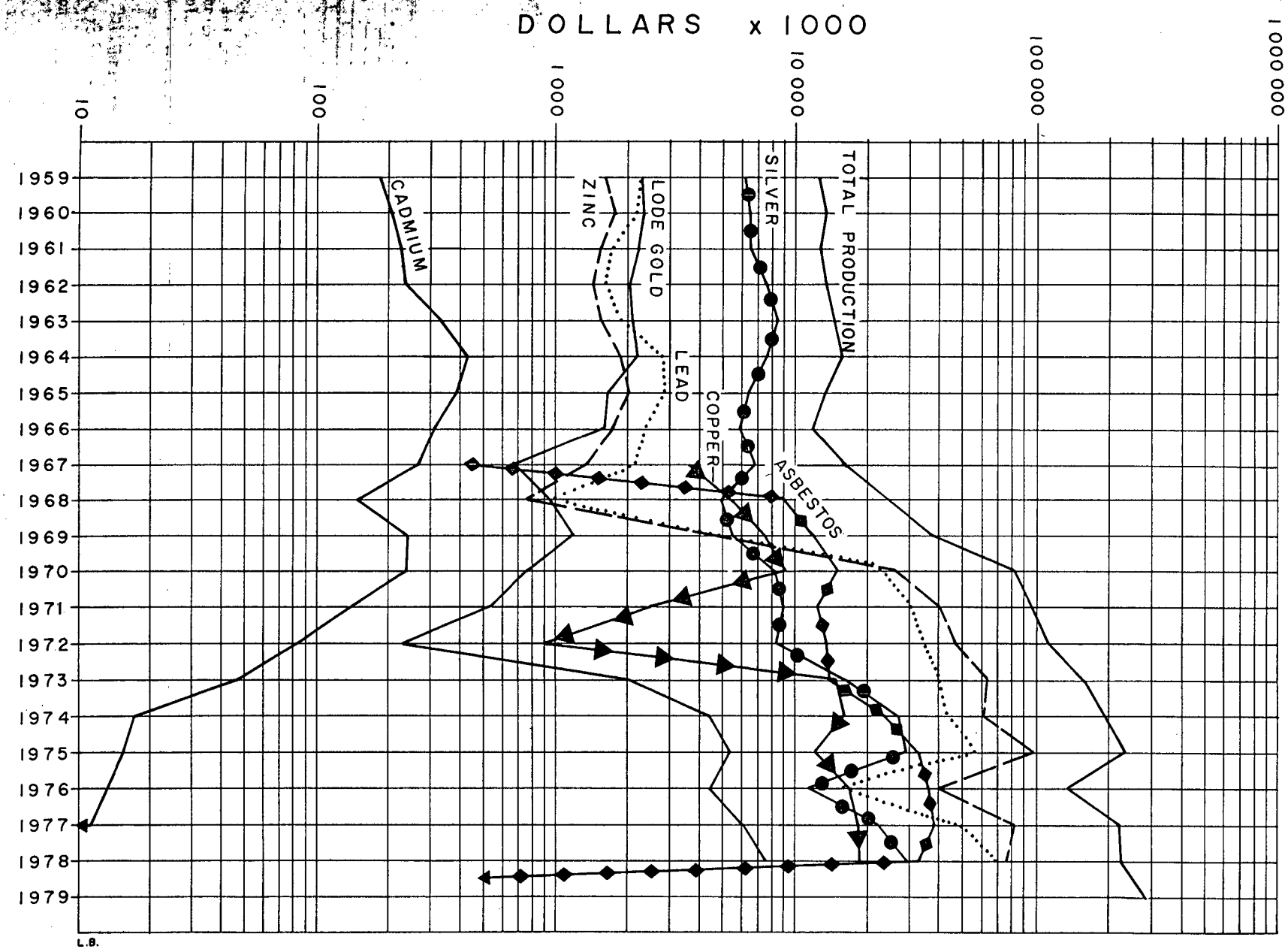


Figure 2a & 2b
Yukon mineral production for 1960 - 1980 (note semi-logarithmic scale).


DOLLARS x 1000
10
100
1000
10 000
100 000
1 000 000
1959
1960
1961
1962
1963
1964
1965
1966
1967
1968
1969
1970
1971
1972
1973
1974
1975
1976
1977
1978
1979
CADMIUM
ZINC
LODE GOLD
LEAD
COPPER
SILVER
ASBESTOS
TOTAL PRODUCTION
L.B.

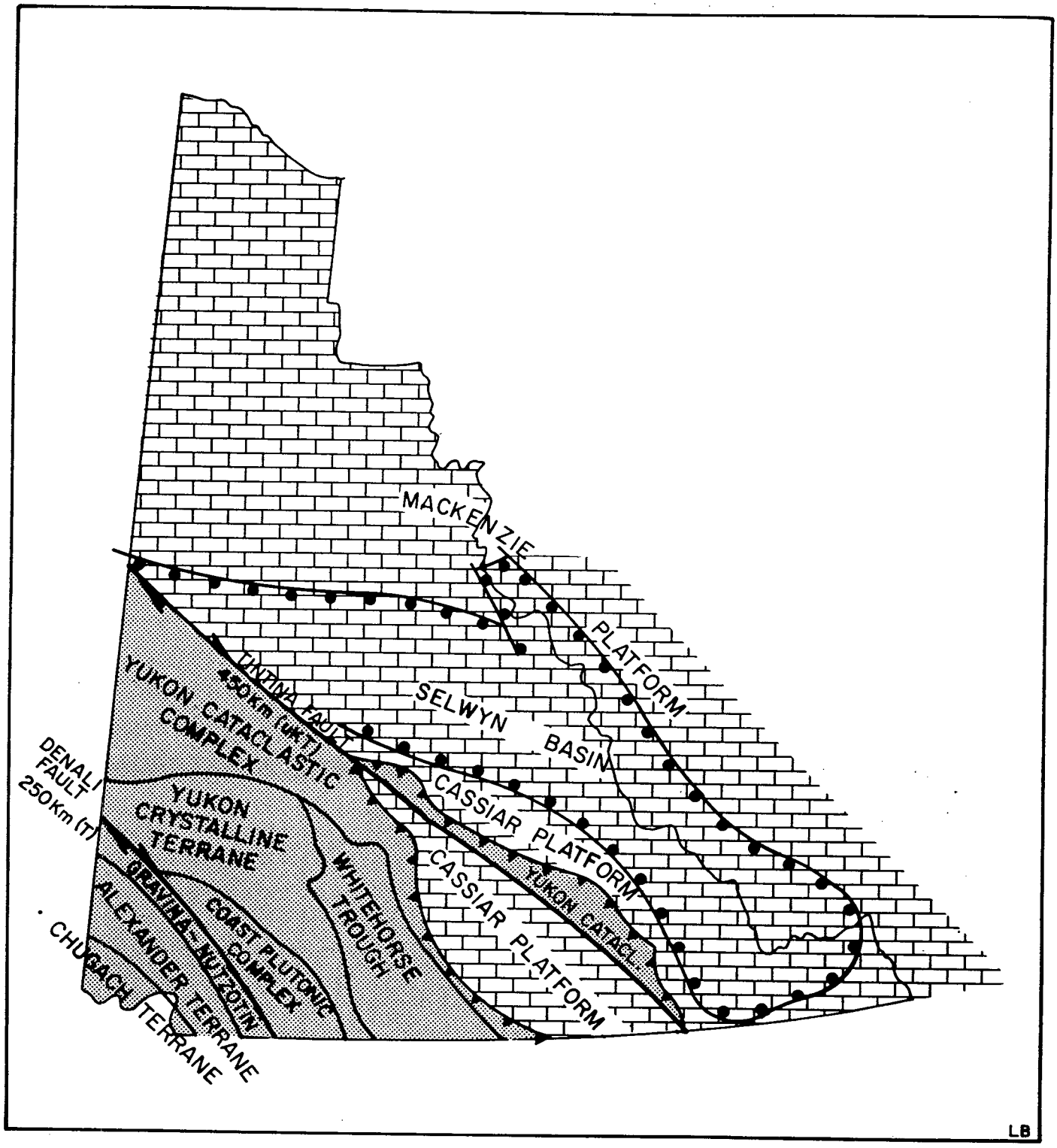


Figure 3
Sketch map of Yukon showing the subdivisions of the ancient North American margin on the northeast (brick pattern) and elements of the accreted southwest part (shaded).

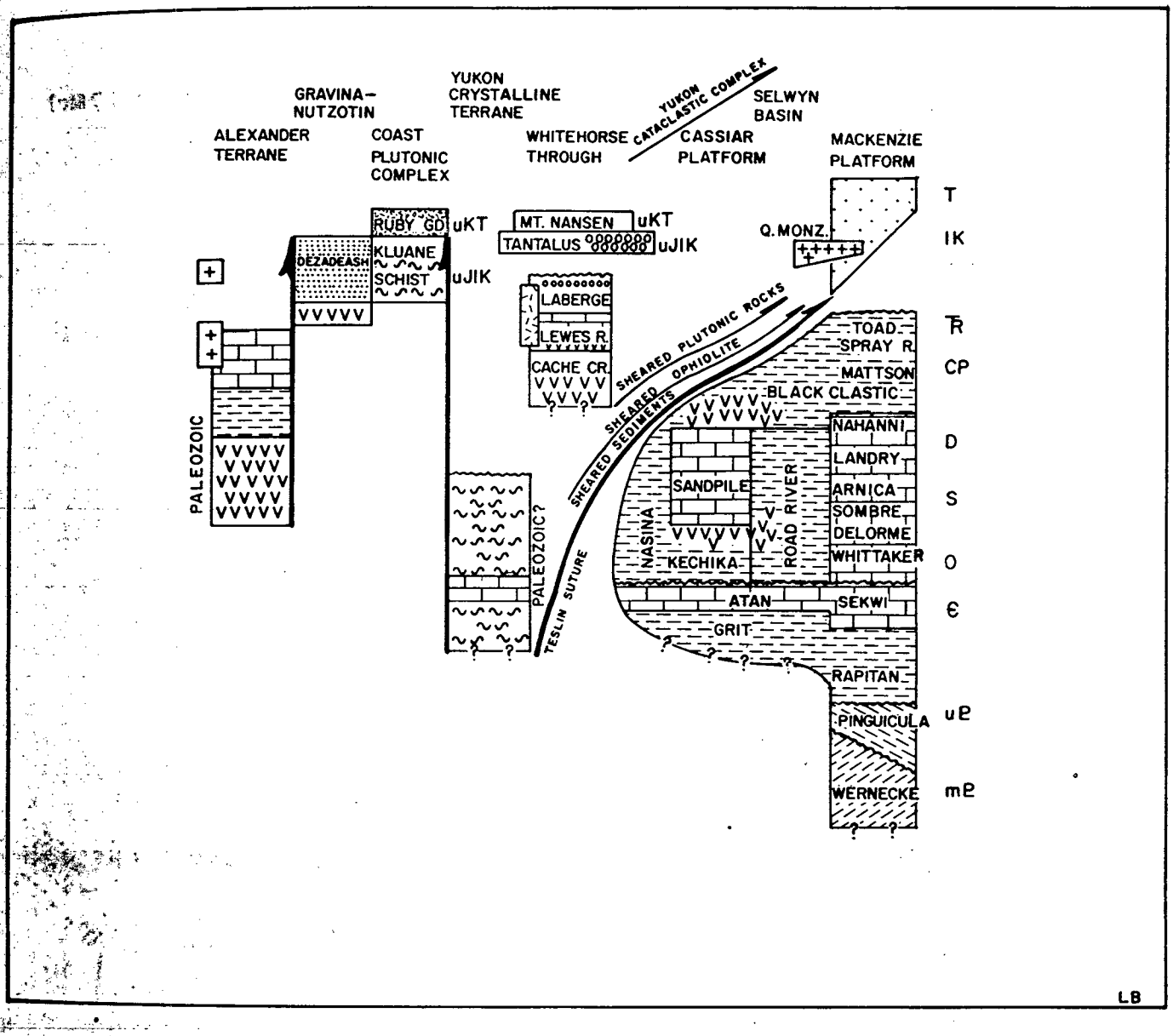


Figure 4
Columns showing the main stratigraphic units of the tectonic elements in Figure 3. Relations between elements are shown schematically.

discordant batholiths confined to Yukon Crystalline Terrane and parts of Whitehorse Trough. The hornblende granodiorite may be the subvolcanic root of the Lewes River volcanics.

The areally most extensive plutonic rocks are biotite quartz monzonite that cooled between 120 and 90 Ma, about the Early Cretaceous. This set, the classic Omineca Belt granites, is confined to the ancient North American elements with minor intrusions in Yukon Cataclastic Complex. The suite shows a general variation in mode of occurrence from northeast to southwest. In Selwyn Basin and parts of Mackenzie Platform are small, discordant plugs that have forcefully invaded and thermally metamorphosed the surrounding unmetamorphosed strata. Southwestward in Cassiar Platform and Nasina Shelf the plutonic suite forms large concordant batholiths with wide mantles of lit par lit gneiss centred on regional metamorphic culminations, which are arched up passively around the intrusions. The large batholiths of quartz monzonite are considered to be dominantly in situ melts derived by metamorphism of sedimentary rocks and the small discordant plutons are considered the mobilized parts of such melts intruded higher in the sequence.

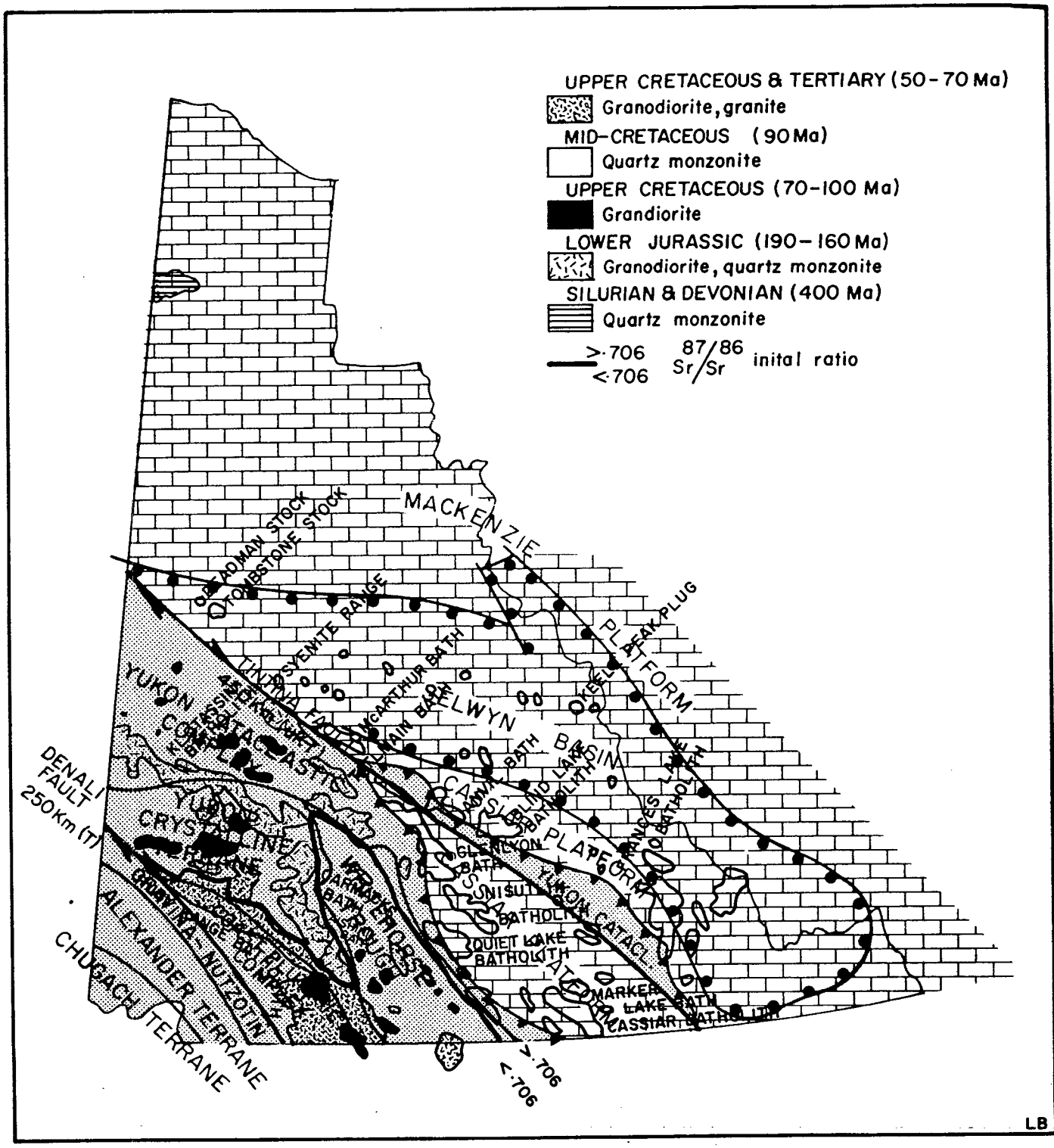


Figure 5

Sketch maps of the distribution of plutonic rocks in relation to the tectonic elements. The mid-Cretaceous suite is restricted essentially to the northeastern ancient North American margin and the other granitic rocks are confined to the accreted terrane.

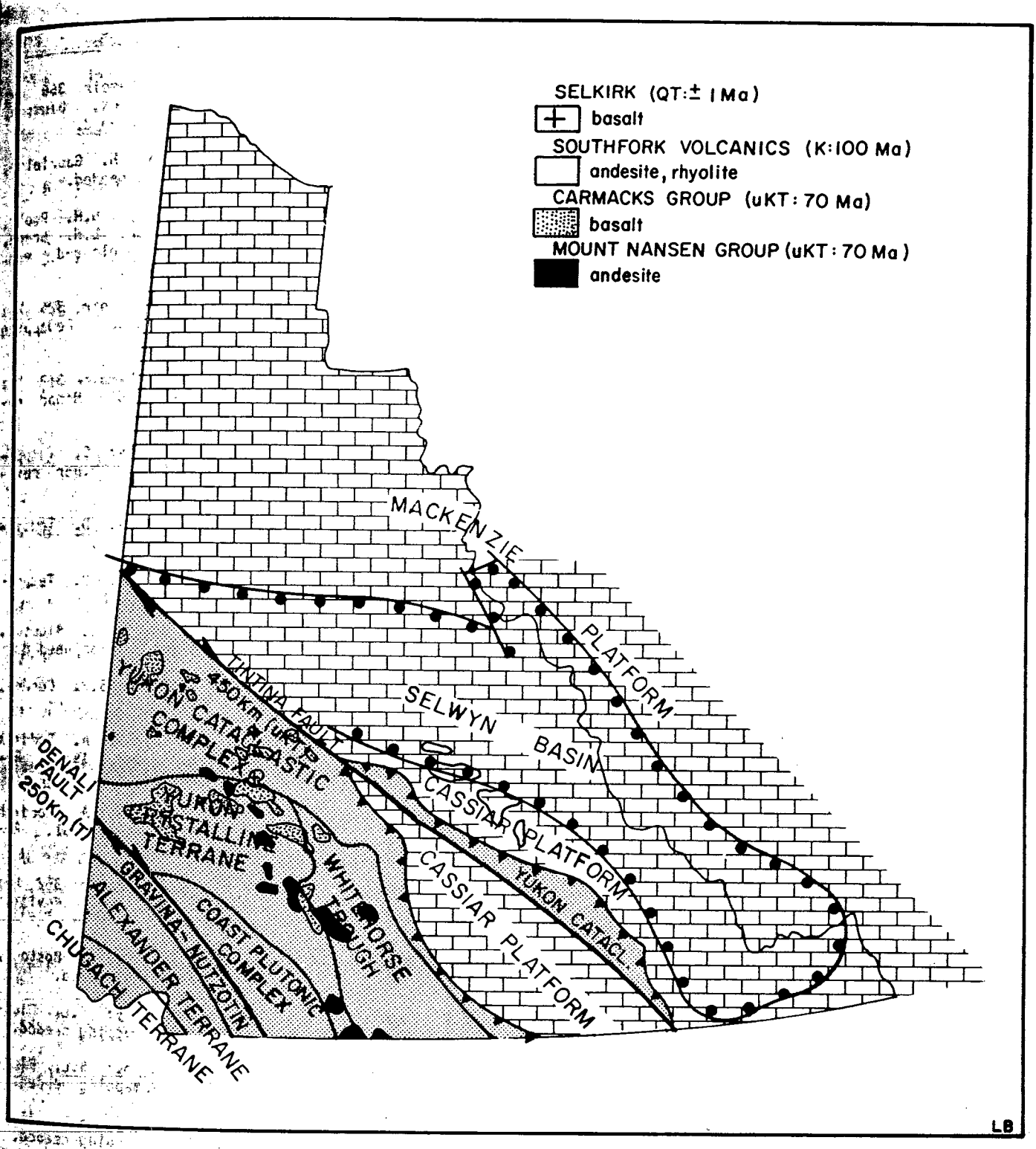


Figure 6
Sketch map of the distribution of Late Cretaceous and Tertiary volcanic rocks in relation to the tectonic elements.

The third set of granitic rocks includes hornblende granodiorite and alaskite-biotite granite respecively, the Ruby Range and Nisling Alaskite suites. They give radiometric cooling ages of about 60 Ma (Paleocene). Both suites are restricted to the Coast Plutonic complex and Yukon Crystalline Terrane. The granodiorite forms large heterogeneous batholiths and the alaskite occurs as small cross-cutting plutons.

The Upper Triassic and Paleocene suites are I type granites, derived by partial melting from oceanic crust; the Early Cretaceous quartz monzonite is S type, generated from continental crust and sedimentary strata by partial melting. Initial Sr_{87}/Sr_{86} ratios determined from the suites bear this out (Figure 5).

Cretaceous and Younger Volcanic Rocks

Four groups of Cretaceous and younger volcanic rocks are known in southern Yukon (Figure 6). Oldest are the probably mid-Cretaceous South Fork Volcanics. These andesites occur in a restricted area and are extrusive equivalents of the Cretaceous quartz monzonite. Most extensive are the Mt. Nansen and Carmacks volcanics. The first are explosive, intermediate to acid volcanics intruded through and laid across parts of the Yukon Crystalline Terrane, Whitehorse Trough and Coast Plutonic Complex. The Mt. Nansen Group is equivalent to the Hutshi and Skukum Groups; all are Paleocene and give radiometric ages between 70 and 55 Ma. The Carmacks Groups is a sequence of basalt flows and breccias, also of Paleocene age, that overlies the Mt. Nansen Group conformably and is extruded onto parts of Yukon Crystalline Terrane and Yukon Cataclastic Complex.

The Selkirk lavas and their equivalents, the Tuya (near Watson Lake) and Miles Canyon (near Whitehorse) are columnar jointed olivine basalt flows intercalated with Pleistocene glacial deposits. They form scattered small outcrops between the Tintina and Shakwak Trenches.

SOURCES OF ORIGINAL DATA

Geological maps are the basic data used in all aspects of mineral exploration. The initial mapping and the task of keeping the maps up to date is the job of the Geological Survey of Canada. Complete coverage of the bedrock geology at a scale 1:250,000 is now published, but the maps vary in vintage and completeness and therefore in current usefulness. Some maps are based on rapid reconnaissance, others on exhaustive study. Furthermore, understanding of Cordilleran evolution has changed in the last decade. Many of the areas need extensive remapping with revisions in the light of this new understanding. A list of the most recently published maps with subjective assessments of their current status follows:

NTS	Name	Reference and Status
95 C	La Biche	Map 1380 A by: R.J.W. Douglas, 1976. Status OK.
95 D	Coal River	Map 11-1968 by: H. Gabrielse, 1968. Minor revision needed.
95 E	Flat River	Map 1313 A and Memoir 366 by: Gabrielse, Roddick, Blusson. Minor revision needed.
95 L	Glacier Lake	Map 1314 A and Memoir 366 by: Gabrielse, Roddick, Blusson. Minor revision needed.
105 A	Watson Lake	Map 19-1966 by: H. Gabrielse, 1966. Revision needed.
105 B	Wolf Lake	Map 10-1960 by: W.H. Poole, J.A. Roddick and L.H. Green. Preliminary uncoloured map. Remapping needed.
105 C	Teslin	Map 1125 A and Memoir 326 by: R. Mulligan, 1963. Remapping needed.
105 D	Whitehorse	Map 1093 A and Memoir 312 by: J.O. Wheeler, 1961. Minor revision needed.
105 E	Laberge	Open File 578 by: D. Tempelman-Kluit, 1978. Minor revision needed.
105 F	Quiet Lake	Open File 486 by: D. Tempelman-Kluit, 1977. OK.
105 G	Finlayson Lake	Open File 486 by: D. Tempelman-Kluit, 1977. OK.
105 H	Frances Lake	Map 6-1966 by: S. L. Blusson, 1966. Major revision needed.
105 I	Nahanni	Open File 689 by: S.P. Gordey, 1980. OK.
105 J	Sheldon Lake	Map 12-1961 by: J. A. Roddick and L. H. Green, 1961. Remapping needed.
105 K	Tay River	Map 13-1961 by: J. A. Roddick and L. H. Green, 1961. Remapping needed.
105 L	Glenlyon	Map 1221 A and Memoir 352 by: R.B. Campbell, 1967. Revision needed.
105 M	Mayo	Map 890 A by: H. S. Bostock, 1947. Remapping needed.
105 N	Lansing	Open File 205 by: S.L. Blusson, 1974. Remapping needed.
105 O	Niddery Lake	Open File 205 by: S.L. Blusson, 1974. Remapping needed.
106 B	Bonnet Plume	Open File 205 by: S.L. Blusson, 1974. Remapping needed.
106 C	Nadaleen River	Open File 205, 206 by: S. L. Blusson, 1974. Remapping needed.
106 D	Nash Creek	Map 1282 A and Memoir 364 by: L. H. Green, 1972. Revision needed.

NTS	Name	Reference and Status
106 E	Wind River	Open File 279 by: D.K. Norris, 1975. Minor revision needed.
106 F	Snake River	Open File 279 by: D. K. Norris, 1975. Minor revision needed.
116 A	Dezadeash	Map 1019 A and Memoir 268 by: E. D. Kindle, 1953. Revision needed.
115 B	Kaskawulsh	Map 1143 A by: J.O. Wheeler, 1963.
116 F/G	Kluane	Map 1177 A and Memoir 340 by: J. E. Muller, 1967. Revision needed.
116 H	Aishihik Lake	Map 17-1973 and Paper 73-41 by: D. Tempelman-Kluit, 1974. Minor revision needed.
115 J/K	Snag	Map 10-1973 and Paper 73-41 by: D. Tempelman-Kluit, 1974. Minor revision needed.
115 N	Stewart River	Map 18-1973 and Paper 73-41 by: D. Tempelman-Kluit, 1974. Minor revision needed.
115 O	Ogilvie	Map 711 A by: H. S. Bostock, 1942. Remapping needed.
115 P	McQuesten	Map 1143 A by: H. S. Bostock, 1964. Remapping needed.
116 A	Larsen Creek	Map 1283 A and Memoir 364 by: L. H. Green, 1972. Revision needed.
116 B/C	Dawson	Map 1284 A and Memoir 364 by: L. H. Green, 1972. Revision needed.
116 F/G	Ogilvie	Open File 715 by: D.K. Norris, 1980. OK.
116 H	Hart River	Open File 279 by: D.K. Norris, 1975. OK.
116 I	Eagle River	Open File 715 by: D.K. Norris, 1980. OK.
116 J/K	Porcupine River	Open File 715 by: D.K. Norris, 1980. OK.
116 O/N	Old Crow	Open File 715 by: D.K. Norris, 1980. OK.
116 P	Trail River	Open File 715 by: D.K. Norris, 1980. OK.

The Geological Survey of Canada also undertakes syntheses of the regional geology and detailed studies of areas where geological problems require closer mapping. Recent synetheses include the 1:1,000,000 scale Geological Map of MacMillan River area (Open File 209) covering essentially all of southern Yukon and the Tectonic Assemblage map of the Canadian Cordillera (Open File 572). An overlay of the assemblage map also shows the important mineral deposits (Open File 573). A synthesis and model for the evolution of Yukon geology is given in G.S.C. Paper 79-14. Detailed mapping has been done in the Keno-Galena Hills area, the Anvil district and Tombstone area north of Dawson.

Descriptions of Yukon's mineral deposits can be found in a variety of publications of the Geological Survey of Canada and the Department of Indian Affairs and Northern Development. Many of the original reports are out of print, but they are reprinted in Bostock (1957). Mining and exploration development of the Territory during the period 1934 to 1940 were described by Bostock (1935, 1936, 1937, 1938, 1939, 1941). Between 1940 and 1960 no information was published. A report detailing this period and based on the unpublished summaries of mining recorders is being readied for publication by the Geology Section DIAND. Following 1960 developments have been reported annually. Reports for the period 1960-1970 are authoritative accounts of the geology of properties based on first-hand examination published as G.S.C. Papers; for 1960 and 1961 (Skinner 1961, 1962), for 1962 to 1965, Green and Godwin (1963, 1964) and Green (1965, 1966) and for 1966 to 1968, Findlay (1967,1969, 1969a).

In 1969 the role of reporting on mineral development devolved on the Department of Indian Affairs and Northern Development. The emphasis shifted to documenting exploration work done rather than first-hand accounts of the geology with a description of work performed. For 1969 to 1972 reports are by Craig and others (1972, 1975), for 1973 to 1975 by Sinclair and others (1975, 1975a); for 1976 by Morin and others (1977); for 1977 by Marchand and others (1978) and for 1978 by Morin and others (1980).

MINERAL OCCURRENCES

The following section characterizes the most important known mineral occurrences in Yukon, grouping them by commodity and by geological setting. Stratabound zinc-lead deposits and silver-lead-zinc veins, examined first, are essentially confined to strata of the ancient North American elements. Copper porphyries and skarns and gold lodes are restricted to the accreted terrane. Tungsten, tin and some molybdenum are associated with the Cretaceous quartz monzonite confined to the ancient North American elements. The stratigraphic setting of asbestos, barite, coal and iron deposits is also examined.

Tonnage and grade figures quoted in the text are the most recent available from published sources; they are rough guides to scale for comparison of the deposits.

DEPOSITS OF THE ANCIENT NORTH AMERICAN MARGIN

Stratabound Zinc-Lead

Zinc-lead occurs in five stratigraphic associations in Yukon (Figure 7). Four are in strata deposited on the ancient North American margin and the fifth is in accreted rocks. The four include Anvil-Howard's Pass type in Cambro-Ordovician strata, Tom-MM type in Mississippian beds, Quartz Lake type in the Grit Unit and Goz type in Lower Cambrian dolomite. Although of different age the first three, economically the most important, may have similar origins. The deposits occur in a variety of facies and differ in their post-mineralization history.

Five deposits are known in a 30 km long belt in the Anvil district.

Faro	57 m tonnes	5.72% Zn	3.40% Pb	37 gm/t Ag
Vangorda	10.3 m tonnes	4.96% Zn	3.18% Pb	51 gm/t Ag
DY	14.7 m tonnes	7.1 % Zn	5.6 % Pb	84 gm/t Ag
Grum	26 m tonnes	6.43% Zn	4.07% Pb	52 gm/t Ag
Swim	4.3 m tonnes	4.7 % Zn	3.8 % Pb	47 gm/t Ag

All are medium-to coarse-grained massive pyrite-sphalerite-galena lenses that dip moderately to the southwest (Tempelman-Kluit, 1972). On small and large scales the mineralization is conformable with the deformed and transposed bedding of the surrounding Cambro-Ordovician phyllite. The phyllite belongs in the Kechika Group of Cassiar Platform; in Anvil district this unit contains considerable interbedded volcanic tuff with which the deposits may be genetically related. The mineralization occurs on the southwest side of a 60 km long metamorphic-structural culmination, Anvil Arch, a feature related to the Early Cretaceous quartz monzonite. The deposits are regionally metamorphosed; the degree of metamorphism varies, matching that of the host rocks.

Several other occurrences, the JA-Sunset, Maxi (Marchand et al 1978, p. 64, p. 90) and Fin, have conformable sphalerite-galena in black slate probably equivalent to the Kechika Group. Although they are small they may be guides to further sulphides: all are close to the southwest edge of Selwyn Basin.

Three deposits, the Anniv, OP and XY (Marchand et al 1978, p. 69) are known at Howard's Pass (Summit Lake) near the N.W.T. border. They are lenses of extremely fine-grained galena-sphalerite, conformable with bedding in enclosing black graphitic slate. The slate is Ordovician and Silurian and part of the Road River Group; it lacks interbedded volcanics unlike Anvil. The deposits lie at the northeast edge of Selwyn Basin, near the boundary with Mackenzie Platform. Unlike the Anvil deposits and host rocks those at Howard's Pass are essentially unmetamorphosed, but a steeply dipping slaty cleavage cuts the rocks and the mineralization is partly mobilized into this cleavage. Howard's Pass reserves are in the order of several hundred million tonnes, but as yet no reliable figures have been published. Unlike Anvil, lead predominates over zinc and silver is a minor component.

A second set of stratabound zinc-lead deposits, the Tom-Jason (Carne, 1976), MM (Morin, 1977, p. 83-97) and Clear Lake occur in Mississippian strata of varied facies. The Tom-Jason are two physically separate galena-sphalerite-barite lenses in black shale of the lower Earn Group or "Black Clastic". Both are near the northeast margin of Selwyn Basin. Reserves at Tom are about 8 million tonnes with 8.5% lead and zinc each and 90 gm/t silver. The MM is in Cassiar Platform southwest of Tintina Fault. Its host are Mississippian felsic volcanics intercalated with black slate of the "Black Clastic", the same rocks as the Tom-Jason. The sequence is folded and imbricated by gently south dipping thrust faults. Three lenses of coarse-grained pyrite-sphalerite-galena-barite, each some metres thick and comformable with the transposed bedding , are known. The deposits and host are metamorphosed next to Nisutlin Batholith, an Early Cretaceous quartz monzonite.

At Clear Lake, fine-grained pyrite-sphalerite-galena occur conformably in black slate intercalated with volcanic rocks immediately south of Tintina Fault. The host is correlated with Mississippian strata of the Earn Group like those at MM, but differs in being unmetamorphosed. The deposit is speculated to contain 25 million tonnes of massive pyrite with subeconomic zinc-lead: a 13 m drill intersection grades 18.3% Zn, 2.15% Pb and 58.6 gm/t Ag.

Another type of lead-zinc deposit is characterized by the Quartz Lake or McMillan (Green, 1966, p. 72-74, Sinclair et al, 1976, p. 154-155), 80 km northeast of Watson Lake. Greenish grey slate of the upper "Grit Unit" (Late Proterozoic) is host to comformable fine-grained pyrite-sphalerite mineralization. The rock and sulphides are essentially unmetamorphosed, but bedding is transposed so that the mineralization is disrupted. One million tonnes of 10% Zn, 5% Pb, 56 gm/t material is known. The Matt Berry (Findlay, 1967, p. 63) has lenses of galena, sphalerite and pyrite enclosed by quartz mica schist. It may be the metamorphosed equivalent of Quartz Lake as the schist is likely the regionally metamorphosed "Grit Unit". The rocks are metamorphosed at the margin of the Frances Lake culmination related to Lower Cretaceous arching west of the Frances Lake Batholith. At Matt Berry about 400,000 tonnes of 9% Zn, with 133 gm/t silver are indicated.

Several carbonate breccia hosted zinc-lead ocurrences are known in Mackenzie Platform; that at Goz Creek (Reeve, 1977) is an important example. Pale coloured, coarsely crystalline sphalerite with minor galena occurs as fracture fillings and breccia matrix within dolomite of the Lower Cambrian Sekwi or

Backbone Ranges Formation. The mineralization may be Mississippi Valley type or it may be emplaced in zones precipitated by fluids under pressure. The Goz may be more properly considered part of the cavity filling type of mineralization instead of the stratabound type. Drill indicated reserves are 11 million tonnes at 8% Zn with minor lead and essentially no silver.

The fifth zinc-lead type is exemplified by the Holly showing 50 km west of Dawson. Medium-grained sphalerite and galena are confined to a quartz rich layer conformable with the flaser fabric in quartz muscovite schist. The host is Nisutlin Alochthonous Assemblage of the Yukon Cataclastic Complex. The mineralized layer is less than a metre thick, but can be traced for hundreds of metres. Zinc predominates over lead and silver content is low. The mineralization was probably mobilized with quartz during stages of ductile strain and was sheared and metamorphosed in later stages. Several like occurrences are known, but all appear small with limited potential. Other examples are the Fyre (Findlay, 1967, p. 59) and Hoo (Sinclair and Gilbert, 1975, p. 85) in the Pelly Mountains. Each is a tectonically dismembered, sheared and recrystallized sulphide deposit. While the Holly is a sheared remobilized sulphide the Fyre and Hoo are sheared metamorphosed deposits still in their original host rocks.

Vein and Fracture Filling Silver-Lead-Zinc Deposits

Like the stratabound zinc-lead deposits the silver bearing lead-zinc veins are largely restricted to the ancient North American margin (Figure 7). They are found in various strata within or close to Selwyn Basin and range from fracture fillings to breccia zones. Silver veins occur in three districts, the Keno-Galena Hills camp, the Pelly Mountains and the Nadaleen range. Isolated deposits scattered widely beyond these districts are Mt. Hundere, Bomber, Mosquito Creek, Logjam and Plata. None of the vein occurrences are associated with, or demonstrably mobilized from the known massive sulphide bodies. The highest silver grades are found in the Keno-Galena Hills camp and other silver mineralization is traditionally compared to it. Silver to lead ratios at Keno-Galena Hill average 120:1 (gm/t silver: % lead). In most other districts in Yukon this ratio is nearer 30:1.

Yukon's silver mineralization is probably Late Cretaceous or Tertiary. That at Keno-Galena Hills, the Nadaleen Range, the Pelly Mountins and the Plata is alike and may be of roughly the same age. None of the mineralization is enclosed by strata with which the mineralization is genetically related and the ores are not deformed although the enclosing rocks generally are. This implies the mineralization post-dates the mid-Cretaceous deformation. The same absence of deformation is seen at the Bomber and Mosquito; host rocks at the Bomber are Cretaceous and those at Mosquito were strained in the Middle Jurrassic. Plutonic or volcanic rocks that might be mineralizing agents are absent at all the camps or far from the ores. The silver may be hydrothermally emplaced from host rock fluids circulating from the surface without an introduced energy source.

Veins on Keno-Galena Hills (Boyle, 1965) follow near vertical, northeast trending faults in a southward dipping sequence of the Keno Hill Quartzite, a Lower Cretaceous orthoquartzite. The veins pinch out in the underlying "Lower Schist", an Upper Jurassic phyllite and in the overlying "Upper Schist", a thrust sheet of Nisutlin Allochthonous Assemblage. A number of strong veins have been found. Some like the Hector-Calumet and Comstock-Porcupine systems can be traced on strike for four km or more and have been mined to depths of 300 m below surface. Mineralization consists of early pyrite, arsenopyrite and quartz followed by more voluminous sphalerite, galena, argentiferous tetrahedrite and locally ruby or wire silvers in siderite gangue. The district has been mined from innumerable workings since 1916 and 5,602 tonnes of silver, 252,954 tonnes of lead and 137,772 tonnes of zinc have been extracted to date.

The Keno-Galena Hills camp is on the south limb of the McQuesten Anticline, a broad east-northeast trending fold with 10 km amplitude, broken along its hinge by the vertical McQuesten fault. On the north limb of the anticline are several occurrences such as the Shanghai and UR (Green, 1965, p. 19) where silver is found in lead-zinc veins within Keno Hill Quartzite. The structures are as promising as those on Keno Hill, but the mineralization is poorer in silver. Lookout is a property on Mt. Haldane west of Galena Hill, (Green, 1965, p. 16-18) where the same type of silver mineralization is found in fractures in Keno Hill Quartzite.

Twenty-five km northwest of Galena Hill are the Peso and Rex (Green, 1965, p. 20-22) veins, two strong east trending structures with a paragenesis like that in the Keno-Galena Hill camp except that it contains jamesonite as a common constituent. The veins cut highly sheared metamorphosed rocks of Nisutlin Allochthonous Assemblage (Upper Schist) and are part of the system of mineralized veins that contain gold in the valley of Dublin Gulch. Some 140,000 tonnes grading 648 gm/t Ag and 3.7% Pb have been proved by drilling.

In the Davidson Range, 30 km northeast of Keno Hill, are several properties with silver bearing galena veins. They include the Rambler, Forbes, Cameron and Clark (Craig and Laporte, 1972, p. 19-20). All are enclosed in Keno Hill Quartzite except the Clark which is hosted by slate and gritty strata that may be Upper Paleozoic. Roughly 300,000 tonnes grading between 180 and 300 gm/t silver with about 5.5% lead and 5% zinc are indicated and inferred at the Clark.

The Val, Vera and Craig (see elsewhere this report) are the main properties in the Nadaleen Range. As in the Pelly Mountains coarse crystalline galena and sphalerite with minor argentiferous tetrahedrite occur as irregular lenses and as fillings of weak fractures in a variety of strata to which they are genetically unrelated. Vera host rocks are ankeritic algal laminated dolomite of the Gillespie Lake Group (Proterozoic); on the Val they are light grey, sugary dolomite of the Cambrian to Devonian Mackenzie Platform and at the Craig showings the veins are hosted in silicified dolomite that is probably Paleozoic. At the Vera about 270,000 tonnes, with roughly 300 gm/tonne silver have been blocked out.

Lenses of massive galena and argentiferous tetrahedrite occur in folded and thrust faulted Paleozoic sedimentary rocks within Selwyn Basin on the Plata property (Morin et al, 1977, p. 111-114). The mineralized lenses follow irregular brecciated zones and are not fracture fillings; they lack structural control. Bulk samples from three showings returned between 5000 and 7500 gm/tonne silver and 70% lead.

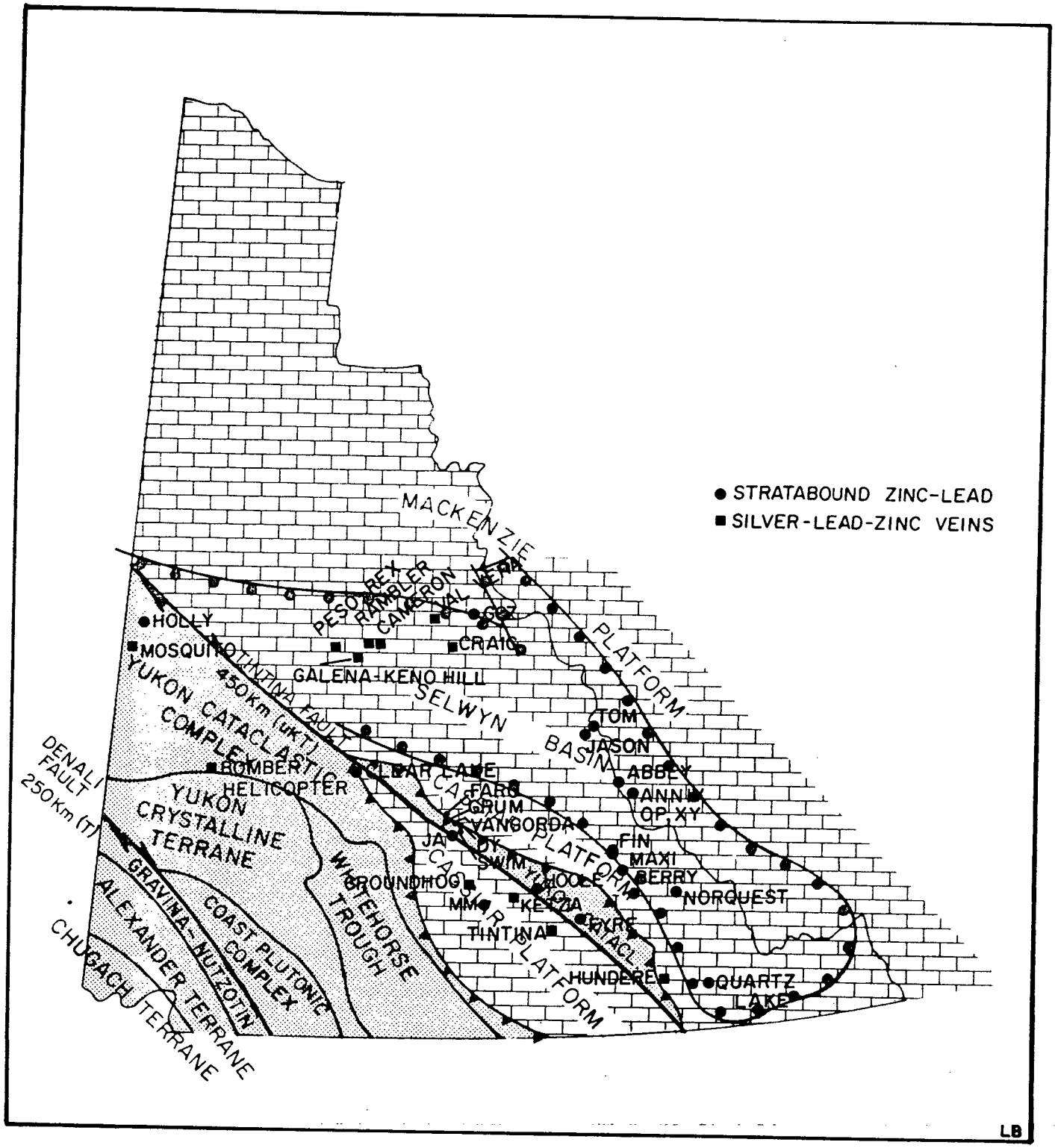
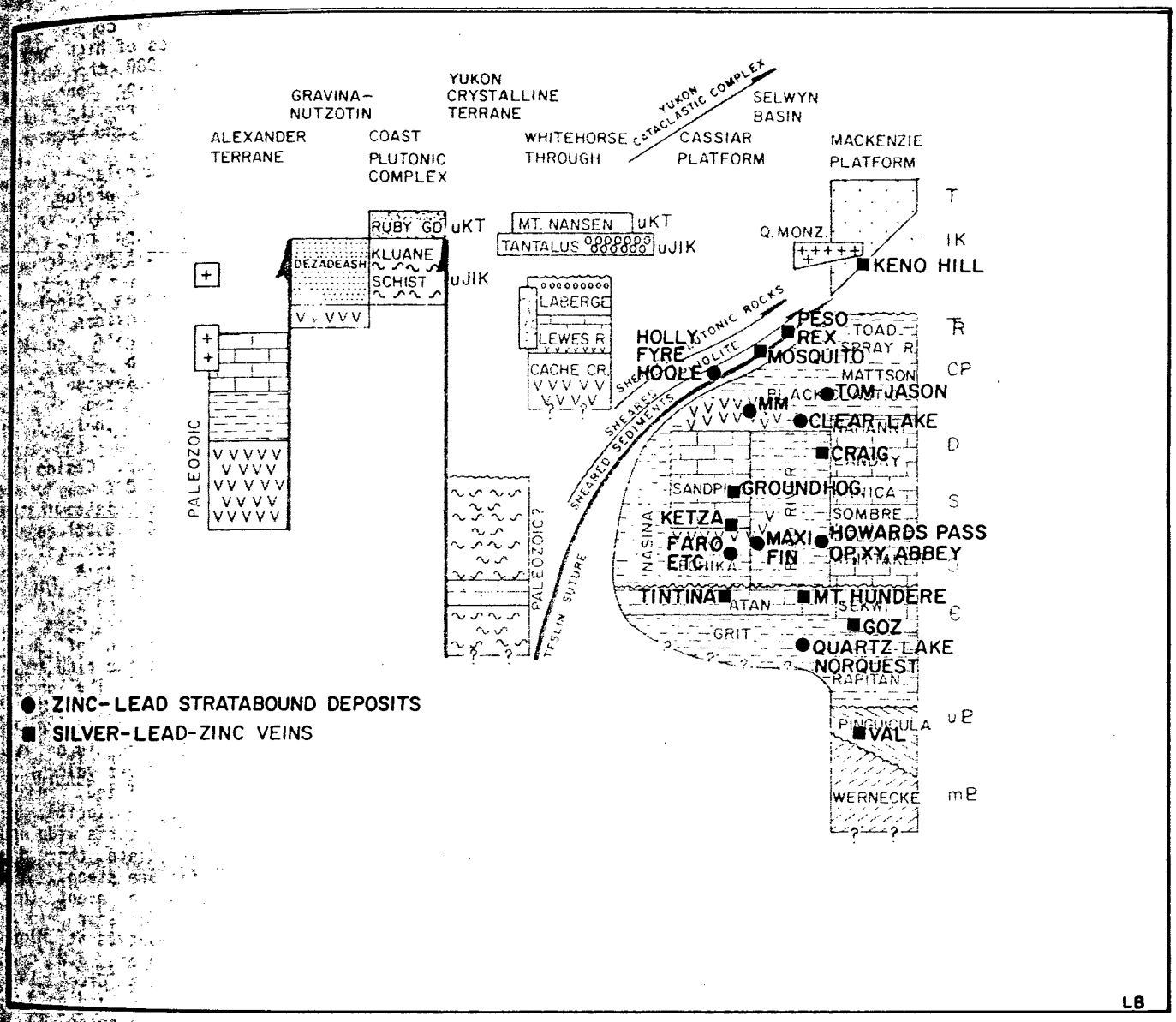


Figure 7a & 7b

Sketch map and columnar sections to show the distribution of stratabound zinc-lead deposits and silver-lead-zinc veins in relation to the tectonic elements. Note that these deposits are restricted to the ancient North American margin.



LB

The most encouraging silver properties in the Pelly Mountains are Tintina, Ketza and Groundhog. At Tintina (Green and Godwin, 1963, p. 26-29) coarse-grained galena and brown sphalerite with argentiferous tetrahedrite occurs as irregular shaped and variously oriented lenses and fills small veins. The host is limestone of the Lower Cambrian Atan Formation in Cassiar Platform. It is repeated by northeast directed thrust faults and folded, and a Cretaceous quartz monzonite plug intrudes the limestone about 1 km north of the showings. Some 90,000 tonnes with 620 gm/t silver, 6% lead and 10% zinc are indicated.

At Ketza River (Green, 1966, p. 64-68) medium-grained galena and sphalerite with argentiferous tetrahedrite in a gangue of siderite and quartz fill irregular fractures and form pods in various Paleozoic strata of Cassiar Platform. Some mineralization is in phyllite of the Kechika Group, some in Siluro-Devonian dolomite and siltstone and another showing is in Devono-Mississippian slate and volcanic rocks. In the "A vein" about 170,000 tonnes are indicated with 12% lead and 527 gm/t silver.

On the Groundhog (Findlay, 1969, p. 46-47), 30 km west of Ketza, massive coarse-grained galena with minor pyrite in quartz siderite gangue occurs as irregular fracture fillings or lenses enclosed by Siluro-Devonian dolomite (Sandpile Formation in Cassiar Platform). A 60 x 5 m shoot grading 266 gm/t silver and 14.7% lead has been outlined.

At Mount Hundere (see elsewhere this report and Abbott, 1977), 55 km north of Watson Lake, a lens of massive coarsely crystalline galena and sphalerite, is crudely conformable with bedding in Lower Cambrian limestone of the Atan Formation. The showings are exposed in a structural culmination that may lie above a covered intrusion and as such they may be mantos or skarns rather than vein occurrences. About 71,000 tonnes with 73.1 gm/t silver, 15.6% lead and 18.9% zinc have been outlined.

The Bomber, Helicopter and Mosquito differ from the other silver bearing veins because they are in strata that are part of the accreted system. This type of mineralization has escaped intensive exploration so far. Mineralogically they resemble other silver -lead-zinc deposits but the host rocks differ. The Bomber-Helicopter (Findlay, 1967, p. 32-34) showings in the Dawson Range are a series of silver bearing veins in wide sheared zones near Casino. On the Bomber is a 45 m wide, northwest trending, near vertical shear zone with several subparallel mineralized veins which are up to 3 m wide locally. The shear zone cuts equigranular medium-grained saussuritized biotite hornblende granodiorite in a Cretaceous part of Klotassin Batholith. The veins contain lenses of massive sulphides, mainly galena with less sphalerite, pyrite and chalcopyrite in quartz barite gangue. A 50-tonne hand sorted sample of mineralization contained 4991 gm/t silver and 68.0% lead. The Helicopter is like the Bomber, and in the same host. The mineralization may be genetically related to the Mount Nansen Group and to the Casino porphyry copper occurrences.

At Mosquito Creek (Craig and Laporte, 1972, p. 32-34), 60 km west of Dawson, silver bearing galena veins cut the Pelly Gneiss. Two northeast trending veins 1/2 to 1 m wide are known. One, traced discontinuously for about 1000 m, has average grades of 707 gm/t silver, 0.96 gm/t gold and 19.95 lead for 50 m along the vein. The Pelly Gneiss is a Devonian granodiorite metamorphosed and partly mobilized in the Cretaceous. Near the showings the rocks are invaded by a small monzonite plug, probably subvolcanic to the Carmacks basalt and therefore Paleocene. The mineralization may be genetically related to this plug.

DEPOSITS IN THE ACCRETED SYSTEMS

Copper Skarns, Porphyries and Massive Sulphides

In contrast to the zinc-lead deposits and the silver bearing veins, which are confined essentially to ancient North American strata, copper concentrations occur largely in the accreted arc system (Figure 8). Four important groups and one minor type are known. Whitehorse copper type are skarns in Upper Triassic limestone, Casino type are porphyry coppers associated with the Late Cretaceous to Tertiary Mount Nansen group, Minto type are porphyries in Triassic hornblende granodiorite and Hart River is a massive sulphide in Proterozoic volcanics.

Whitehorse Copper skarns are developed in a 15 km long belt from dolomite of the Lewes River Group where it is intruded by Cretaceous hornblend granodiorite on the west side of Whitehorse Trough (Kindle, 1964). Two skarns, a grossular-diopside-tremolite mixture and a magnetite rich variety are found. Copper occurs in both as massive lenses or disseminations of bornite and chalcopyrite with less common minerals such as valeriite. Gold is present locally as are scheelite and molybdenite. Copper in the skarns is concentrated by the granodiorite, but whether the metal is derived from this intrusive or from the invaded sedimentary and volcanic rocks is unknown. Volcanics of the Lewes River Group have exceptional copper backgrounds. Lewes River limestone continues far northwest of Whitehorse and is locally invaded by granodiorite, but although skarns exist they lack significant copper.

Seven deposits were mined in the copper bel between 1900 and 1920 and 153,000 tonnes of high grac were shipped. From 1964 to November, 1980 the White horse copper belt has produced 8.5 million tonnes c ore at an average grade of 1.40% copper from the Littl Chief, Arctic Chief, War Eagle, Black Cub and Keeweena deposits.

Several small skarns, genetically unrelated to th Whitehorse copper type, but similar in mineralogy ar known near Hopkins Lake. They are chalcopyrite bornite lenses in tremolite-diopside skarn made fro possibly Cambrian marble in Yukon Crystalline Terran next "Klotassin Suite" granodiorite.

Casino type are classic porphyries (Sinclair 1978) and include several deposits: besides Casin (Craig and Laporte, 1972, p. 55-57) itself are Mt Cockfield (Craig and Laporte, 1972, p. 64), Cas (Marchand et al , 1978, p. 70-71), Yukon Revenue (Crai and Laporte, 1972, p. 79-84) and Mount Nansen in th Dawson Range. Each contains disseminated chalcopyrit and molybdenite within subvolcanic parts of the Lat Cretaceous to Paleocene Mount Nansen Group. Casino has 160 million tonnes at 0.37% copper and 0.04% molybdenum and at Cash, an area 2500 m x 800 m has dissseminatec chalcopyrite and molybdenite at about 0.2% copper equivalent.

Minto type (Sinclair, 1977) includes Minto, Williams Creek (Abbott, 1971) and STU (this report elsewhere) in a 40 km long belt northeast of Carmacks. The occurrences are identical, consisting of chalcopyrite and bornite disseminated in biotite rich zones within foliated hornblende granodiorite. The granodiorite makes up Carmacks Batholith a pluton of Upper Triassic to Lower Jurassic Klotassin granodiorite intruded in Yukon Crystalline Terrane. The pluton may be the deeply eroded root of the Lewes River volcanics. At each occurrence several mineralized zones, conformable with the foliation in the granodiorite, are known. These zones are generally a few metres wide and one or two hundred metres long; at Minto they dip moderately, but at Williams Creek dips are steep. The deposits may be genetically related to an event that metasomatized the rocks emplacing K-feldspar widely about Middle or Late Jurassic time. Reserves at Minto are 6.5 million tonnes at 1.86% copper, 3.2 gm/t silver, 0.46 gm/t gold and at Williams Creek 14.5 million tonnes at 1% copper with low silver and gold.

Hart River (Morin, 1978) is a steep-dipping 30 m thick, 200 m long lens of massive pyrite, pyrrhotite, sphalerite and chalcopyrite in siliceous black argillite of the Proterozoic Gillespie Lake Group. The strata are invaded by diabase dikes, and basalt is interbedded with the host rocks, so that the deposit may have a proximal exhalative origin. About 520,000 tonnes with 1.45% copper, 3.65% zinc, 0.87% lead, 45 gm/t silver and 1.25 gm/t gold have been proven.

The Pike (Findlay, 1967, p 60-62) is an interesting occurrence of veinlets and disseminated arsenopyrite, chalcopyrite, pyrite, galena and sphalerite at the edge of a small quartz feldspar porphyry belonging with the South Fork Volcanics. As the only known showing in these rocks it is an untested indicator of their potential. The mineralized zone is estimated to contain 2,250 tonnes per vertical foot averaging 0.6% copper and 70 gm/t silver.

Gold Veins

Gold lodes in Yukon occur in four districts: on Montana Mountain near Carcross, in the Mount Nansen area west of Carmacks, on Dublin Gulch north of Mayo and in the Klondike (Figure 8). At Montana and Mount Nansen the mineralization is in, and probably genetically related to, the Late Cretaceous to Paleocene Mount Nansen Group; in the other districts the enclosing rocks are incidental hosts. Three occurrences outside the main camps are the AJ, Cache Creek and Moosehorn. Mount Nansen and Montana gold is in some of the youngest felsic volcanics laid across the accreted part of the Cordillera; that in the Klondike is part of the Mesozoic subduction complex accreted to North America. At the AJ and Dublin Gulch the host rocks differ and are incidental, the gold is likely derived from, and mobilized by, Cretaceous quartz monzonite that had no extrusive component. The most exciting possibilities are with the Klondike type which may be as widespread as their host.

Montana Mountain near Carcross hosts a number of gold bearing quartz sulphide veins mined at various times since early this century (Green, 1966, p. 55-60; Findlay, 1967, p. 46-50; also see elsewhere this report). Arctic Caribou, Big Thing and Peerless are the main properties on the north side of the mountain and Venus and Vault are part of a more southerly vein system. The veins range from narrow discrete, single structures, to wider stockworks of branching veinlets and contain pyrite, arsenopyrite and sphalerite with minor galena and chalcopyrite in quartz gangue. Well mineralized zones average 30 gm/t gold and 500 gm/t silver. The Arctic Caribou vein system dips gently or moderately northwest and is enclosed in medium-grained hornblende granodiorite, a Paleocene plutonic phase of the Mount Nansen Group. The Venus vein, traced for 1600 m, dips moderately west-northwest in intermediate to acid volcanic rocks of the Mt. Nansen Group. Reserves at Venus (1980) are 108,000 tonnes with 6.84 gm/t gold and 205.3 gm/t silver with lead, zinc and cadmium values.

Gold veins of the Mount Nansen district include the Laforma and Guder on Freegold Mountain, and the Webber, Huestis and Brown-McDade near Mount Nansen 25 km south. Most of these deposits were high graded in the mid-sixties.

At Laforma (Green, 1965, p. 28-31) gold occurs in a northeast trending quartz vein that cuts Jurassic granodiorite invaded by Paleocene quartz-feldspar porphyry dikes. About 60,000 tonnes at 13 gm/t gold are probable. Several similar showings are known of which Guder is one of the most promising. On the Webber (Green, 1965, p. 35-36) two steeply southwest dipping veins, ranging from a single structure to a branching stockwork 2 or 3 m across the containing quartz with arsenopyrite, pyrite, galena and sphalerite are found. Average grade of the veins is 12 gm/t gold and 690 gm/t silver. The host rock is schist of Yukon Crystalline Terrane that is most likely Late Precambrian, but these schists are cut by quartz feldspar porphyry dikes (Mount Nansen Group) with which the mineralization is associated. The Huestis, just southwest of the Webber, has the same host rocks and vein mineralization of the same mineralogy and grade, but the veins dip steeply northeast.

At Brown-McDade (Findlay, 1969, p. 35-38), 2 km to the east of Webber, a steeply southwest dipping shear zone in Middle Jurassic biotite quartz monzonite carries lenses of quartz with arsenopyrite and pyrite. Gold is concentrated in the footwall. About 50,000 tonnes at 11.5 gm/t gold and 183 gm/t silver proven and probable were known in 1970. The mineralization is probably related to the Tertiary Mount Nansen Volcanics nearby and not the enclosing quartz monzonite.

On the south side of Dublin Gulch is a branching network of quartz arsenopyrite veins that cut sheared metamorphic rocks (Nisutlin Assemblage) on the northern flank of the Potato Hills stock, a Cretaceous quartz monzonite. The vein system can be traced for 2.5 km although individual veins are only 100 or 200 m long. Veins have sharp boundaries and are between 10 cm and 1 m wide. Most trend northeast and dip moderately northwest. Gold values between 10 and 30 gm/t gold, over widths near 1 m, are common. (MacLean, 1914, p. 128-158). The veins contain quartz, arsenopyrite, pyrite and gold and are generally oxidized with much scorodite. Jamesonite, like that in the silver bearing Peso and Rex veins, 6 km to the west, is found in the centres of some of the veins. Mostly likely the mineralization of the argentiferous Peso-Rex and the auriferous Dublin Gulch vein systems is genetically related to the Potato Hills Stock.

The Lone Star is the best known lode gold occurrence in the Klondike (McLean, 1914, p. 20-37). Irregular white quartz lenses or "sweats", as much as a metre thick, are interfoliated with quartz muscovite schist (Klondike Schist) and contain gold in a 200 m long, 3 m wide zone. The quartz lenses make up about a quarter of the rock and contain disseminated pyrite and gold. The property was mined in 1910; 2300 tonnes milled averaged between 5 and 6 gm/t gold. The Mitchell and Violet Groups (Bostock, 1957, p. 348-349) also in the Klondike, have gold in quartz lenses in the Klondike Schist like the Lone Star. The occurrences are not simple veins, but structurally disconnected, transposed remnants of veins sweated from the schist while it was sheared and metamorphosed about the Early or Middle Jurassic. In this respect the deposits resemble Holly type lead-zinc occurrences. The gold was probably mobilized from the enclosing schist with the quartz. Minor gold values are also found in the schist. Quartz lenses like those that contain the gold are widespread in the Klondike Schist and this suggests the possibility of mineralization elsewhere in these rocks.

At the AJ (Morin et al, 1977, p. 142) and Thor (this report) several arsenopyrite bearing quartz veins cut hornfelsed slate and quartzite of the Grit Unit (Late Proterozoic). The showings are at the east and west margins of the Antimony Mountain stock, a Cretaceous quartz monzonite. The veins are between 1/2 and 2 m wide and may average near 30 gm/t gold with some silver. Similar mineralization with the same gold content is known on the Thor claims at the northwest side of the Antimony Mountain stock in the same host. Like that at Dublin Gulch the veins are probably related to the quartz monzonite.

On Cache Creek (Skinner, 1961, p. 34-40) in the Pelly Mountains a 200 m long, 4 m wide lens of pyrrhotite, arsenopyrite, pyrite and chalcopyrite is found near a fault that separates Lower Cambrian limestone from Eocambrian, greenish grey slate. About 70,000 tonnes grading 10 gm/t gold are known. The

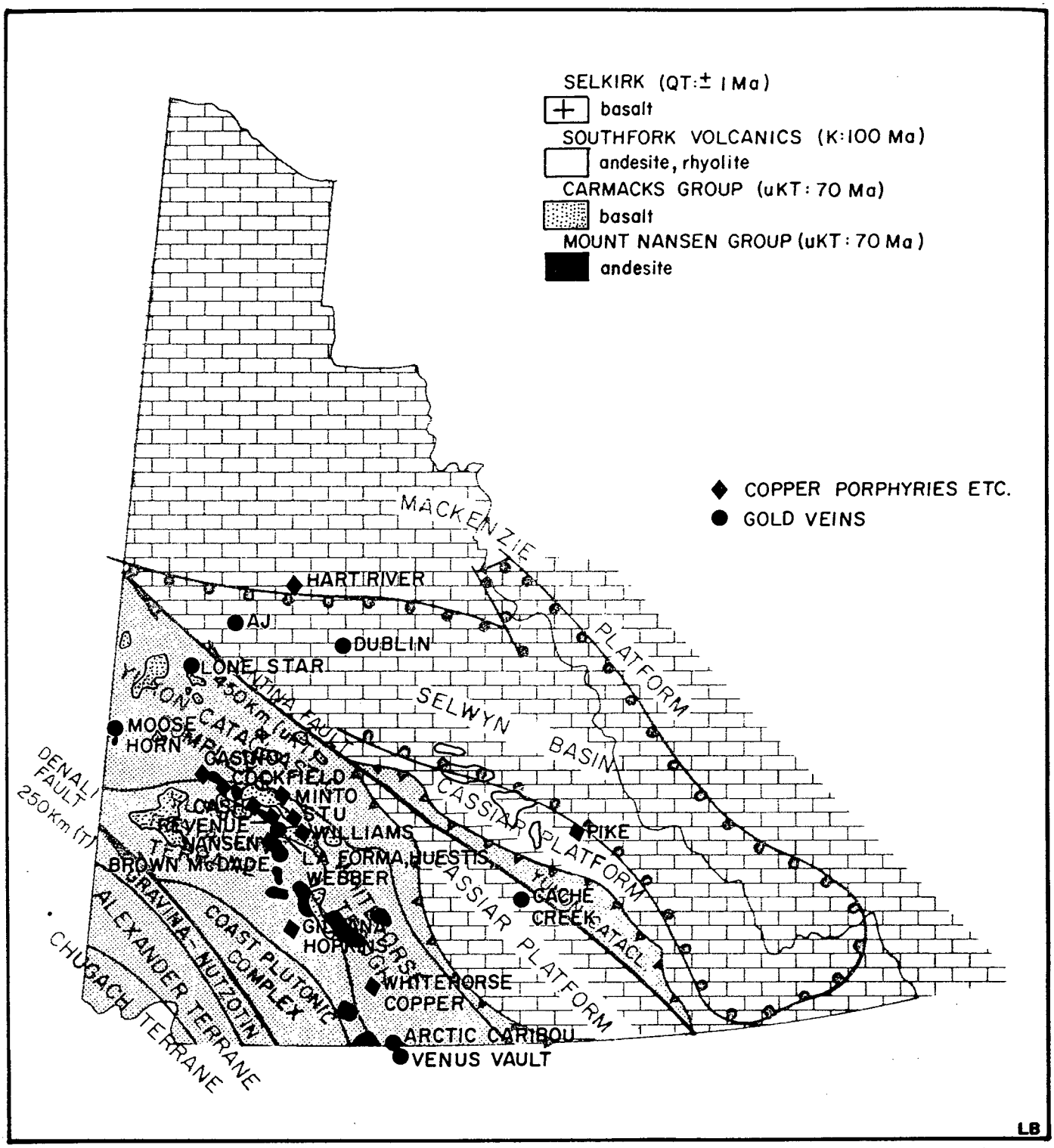
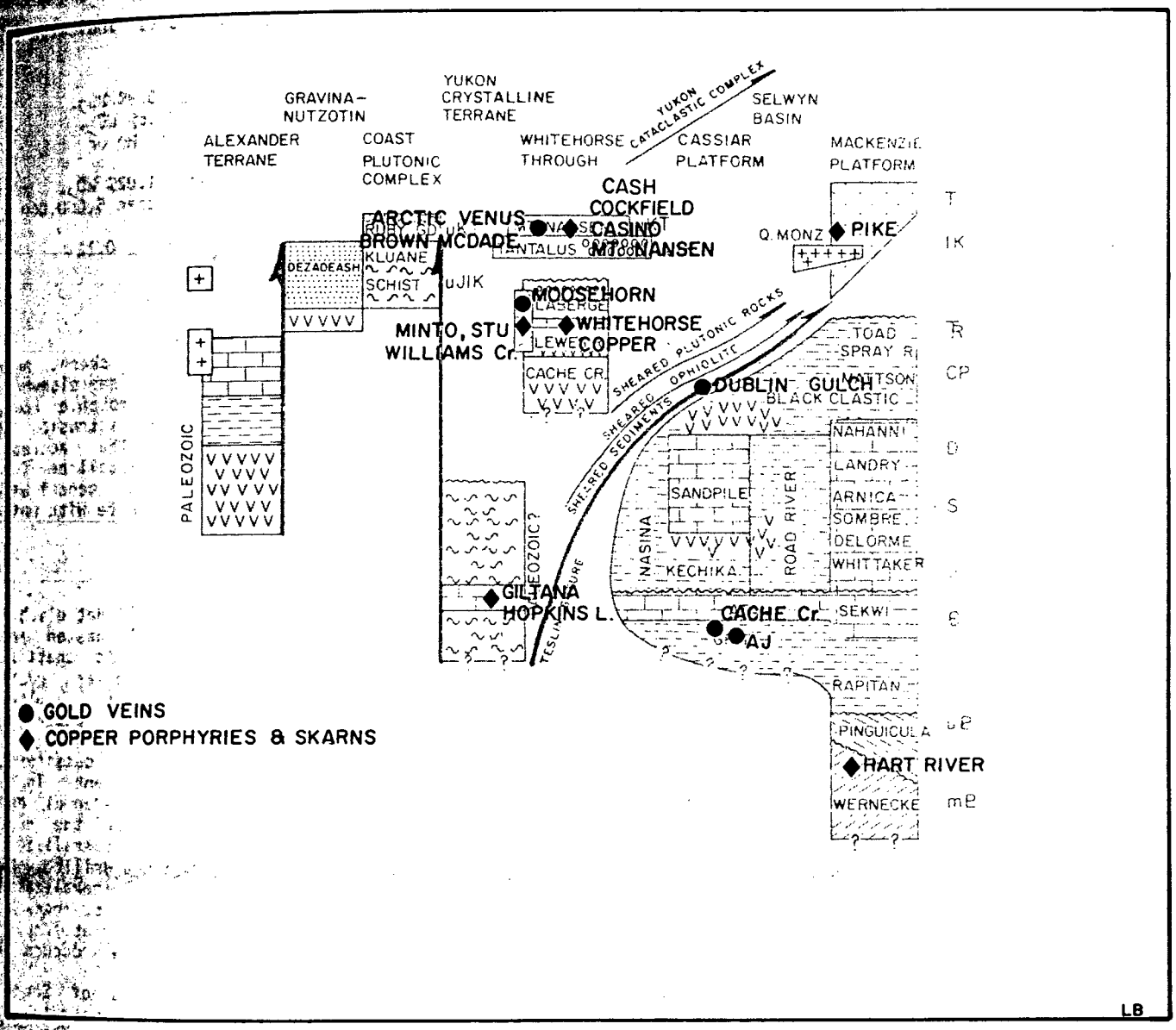


Figure 8a & 8b

Sketch map and columnar sections to show the distribution of copper and gold deposits in relation to the tectonic elements. Note that these occurrences cluster in the accreted terranes. Contrast this with Figure 7.



mineralization is probably fracture controlled and may be related to the silver showings of the Ketza area.

Auriferous quartz veins with arsenopyrite, galena, boulangerite and sphalerite are known in the Moosehorn Range (Morin et al, 1977, p. 33-46). The veins trend generally northwest, are 10 or 20 cm wide, and cut granodiorite that is part of the composite Klotassin Batholith. Gold values between 30 and 250 gm/t gold have been obtained across the veins. The host rocks are incidental and the mineralization may be related to Tertiary hornblende porphyry dikes that cut the Mesozoic granodiorite and which are part of the Carmacks Group.

The potential for bulk tonnage gold in Yukon is perhaps best in areas of known vein occurrences and peripheral to porphyry copper-molybdenum showings. Both these criteria suggest that the Mount Nansen Group warrants careful prospecting. The Klondike Schist is a second important target unit for such occurrences. Strata peripheral to some of the Cretaceous quartz monzonite plugs may stand a close look for bulk gold.

DEPOSITS ASSOCIATED WITH CRETACEOUS QUARTZ MONZONITE

Tungsten, tin and molybdenum deposits in Yukon are spatially and genetically associated with the Cretaceous quartz monzonite intruded in the ancient North American margin (Figure 9). From northeast to southwest a gross zoning of these deposits is evident. Most tungsten occurrences are found at the margins of the small discordant plutons in the northeastern part of the quartz monzonite belt. Tin occurrences are

known only in the central and southwestern parts of the plutonic belt and molybdenum, with tungsten, is found in the southwest part where the large semiconcordant batholiths occur. The reason for this deposit zoning is not known.

Tungsten

Yukon has an unusual number of significant tungsten deposits including Mactung (Findlay, 1969b, p. 52-53; Sinclair and Gilbert, 1975, p. 19-20; Harris, 1977) Potato Hills (elsewhere this report) and Logtung (Marchand et al, p. 78). A current producer, Cantung (Blusson, 1968), is just outside Yukon in the Northwest Territories. Other Yukon occurrences include the Boot and Marmot south of Finlayson Lake, the Bailey south of Frances Lake (elsewhere this report), Stormy Mountain (Skinner, 1961, p. 41-42) and Risby (Morin et al, 1980, p. 37-38) in the Pelly Mountains, the Clea and IVO (elsewhere this report) northwest and southeast of Cantung respectively and the Fidler on the Yukon-B.C. border. Each occurrence is intimately associated with a quartz monzonite pluton of the extensive mid-Cretaceous suite that is confined to the ancient North American part of the Cordillera. Cantung, Mactung and IVO are next to comparatively small discordant plutons at the northeast edge of Selwyn Basin and Potato Hills, Boot, Risby, Bailey and Stormy are at the margins of the more concordant, larger intrusions near the southwest side of Selwyn Basin or in Cassiar Platform.

In most showings (i.e. Cantung, Mactung, IVO, Risby, Bailey, Storm and Clea) tungsten occurs as scheelite in massive, coarse-grained garnet diopside tremolite skarn with pyrrhotite and minor chalcopyrite. The skarns are developed from calcareous strata, mostly shaly parts of the Lower Cambrian Atan and Sekwi Formations or the limy shale of the Cambro-Ordovician Kechika Group-Rabbitkettle Formation. Few tungsten bearing skarns are developed from the thick Siluro-Devonian carbonate or in other limestones intruded by the quartz monzonite.

The Potato Hills, Boot and Marmot showings are also closely associated with Cretaceous quartz monzonite plutons, but their hosts are not the Lower Paleozoic ancient North American strata. Instead the highly sheared rocks of Yukon Cataclastic Complex thrust above the "in place" strata contain the skarns. At Potato Hills limy horizons (but not the marbles) within Nisutlin Allochthonous Assemblage are converted to tungsten skarn and at the Boot a part of Anvil Allochthon that originated as basalt has been transformed to skarn. The skarns have similar mineralogy to the others, but are not the massive rocks of the other deposits and tend to be fine-grained; many retain the strongly layered fabric of their cataclastic precursor.

Logtung (Marchand et al, 1977, p. 78) and Fidler differ from the other tungsten showings in their geology. Logtung is a porphyry deposit with scheelite and molybdenite disseminated in a stockwork of quartz veins in one of the Seagull intrusions, a quartz monzonite stock of the Cretaceous suite. Logtung has its host rocks and porphyry style in common with the Red Mountain molybdenite occurrence. At Fidler, quartz veins with wolfranite, galena, cassiterite, scheelite, fluorite, pyrite and minor other sulphides cut Lower Cambrian limestone (Atan Formation) northeast of the Cassiar Batholith, but no intrusive rocks are exposed nearby.

The size of some of the deposits is indicated in the following table.

Mactung: indicated 27,000,000 tonnes 0.9% WO_3.
Bailey: indicated 270,000 tonnes @ 0.96% WO_3.
Stormy: probable 13,500 tonnes @ 0.73% Mo or 15,300 tonnes @ 1.5% WO_3.
Cab-Risby: possible 310,000 tonnes @ 1.02% WO_3.
Potato Hills: possible-probably more than 5,000,000 tonnes @ 0.5% WO_3.
Logtung: geological 160,000,000 tonnes @ 0.12% WO_3 0.052% MoS_2.
Fidler: geological 30x30 m @ 8.45% WO_3.

Several small chalcopyrite bearing skarns near Hopkins Lake also contain some scheelite (see elsewhere this report). They are hosted in a probable Lower Cambrian marble metasomatized next to an intrusion of the Triassic Klotassin suite within the accreted terrane. These occurrences in Yukon Crystalline Terrane are a second tungsten belt in Yukon, genetically unrelated to the Cretaceous quartz monzonite with which the others are associated.

Tin

Cassiterite is known near the Seagull Batholith in southern Yukon and in the Dublin Gulch-McQuesten area north of Mayo. In both areas the tin is spatially associated with the Cretaceous granite and quartz monzonite. None of the occurrences are explored sufficiently to be sure of their size. The occurrence on Tin dome (Dublin Gulch) is the best documented (Thompson, 1945). Here tourmaline and cassiterite occur in narrow fractures between fragments in an irregular shaped breccia zone. The incidental host rocks are schist of Nisutlin Allochthon on the north side of the Potato Hills Stock and the mineralization is genetically related to it. Though not drilled, the showing has been explored on surface and mineralization is known over an area 60 m x 250 m. The host rocks are fresh and the mineralization stops abruptly at fracture edges. Cassiterite in the McQuesten area occurs in skarns near small basic intrusive bodies.

Two showings near the northwest end of Seagull Batholith (see elsewhere this report) illustrate the variety of mineralization styles seen there. The JC is a cassiterite bearing skarn within limy strata of Nisutlin Allochthon above the gently dipping contact of the quartz monzonite. The MC has a swarm of parallel, cosely spaced fractures, each a few millimetres wide partly filled with cassiterite, within thermally metamorphosed schists above Seagull Batholith.

Molybdenum

Several porphyry copper occurrences in which molybdenite is an important constituent along with chalcopyrite are known in the Dawson Range. These include Casino, Cash and Mount Cockfield which occur within Mount Nansen group subvolcanic strata (Sinclair, 1978). Other deposits with significant molybdenite as the second mineral are the scheelite-molybdenite porphyry at Logtung and the skarn of Stormy Mountain. These deposits, characterized elsewhere are related genetically to the Cretaceous quartz monzonite.

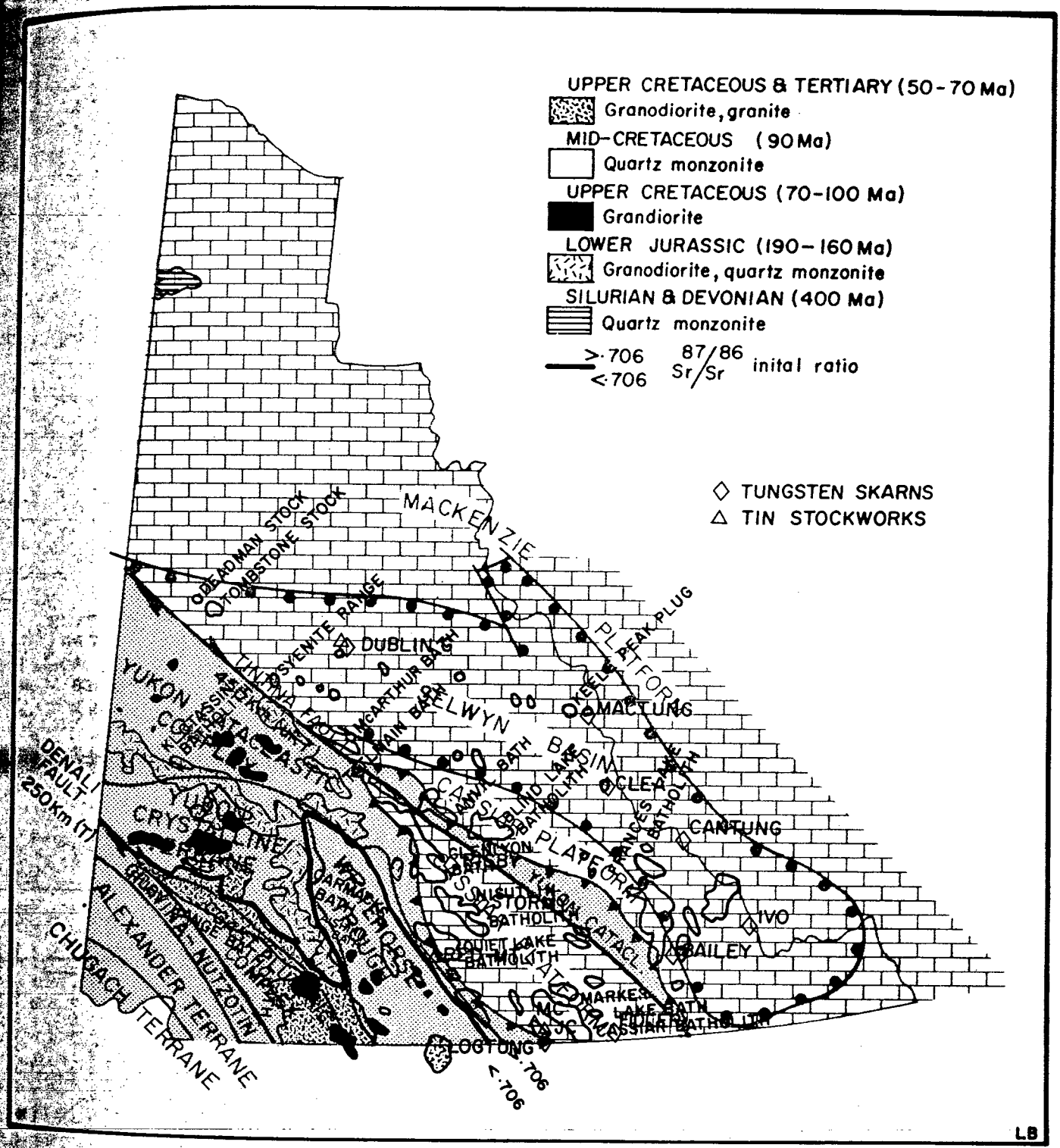


Figure 9

Sketch map to show the distribution of tungsten and tin deposits in relation to the plutonic rocks and tectonic **elements**. Occurrences of tungsten and tin are related to the mid-Cretaceous quartz monzonite that intrudes the **ancient** North American margin.

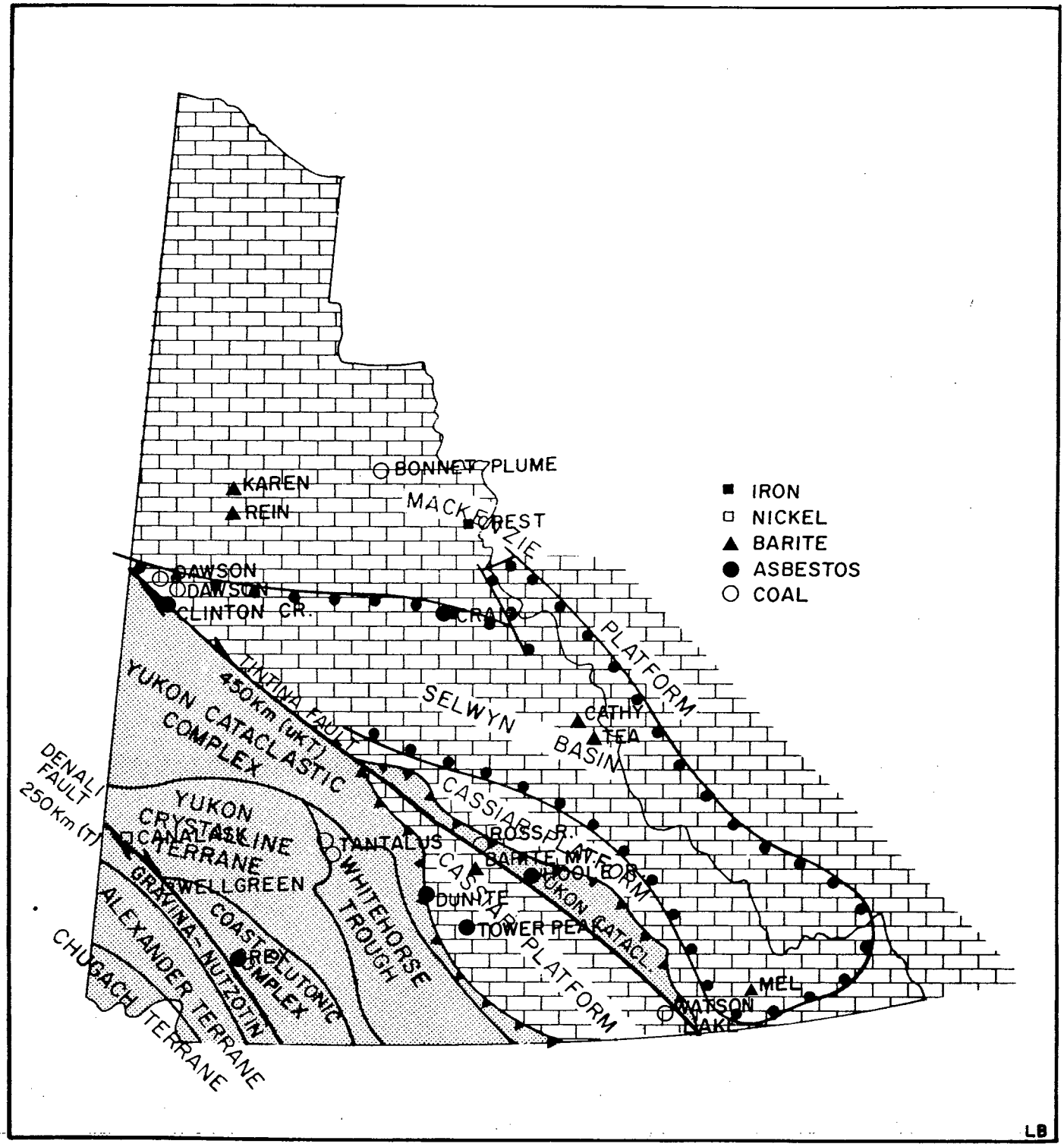
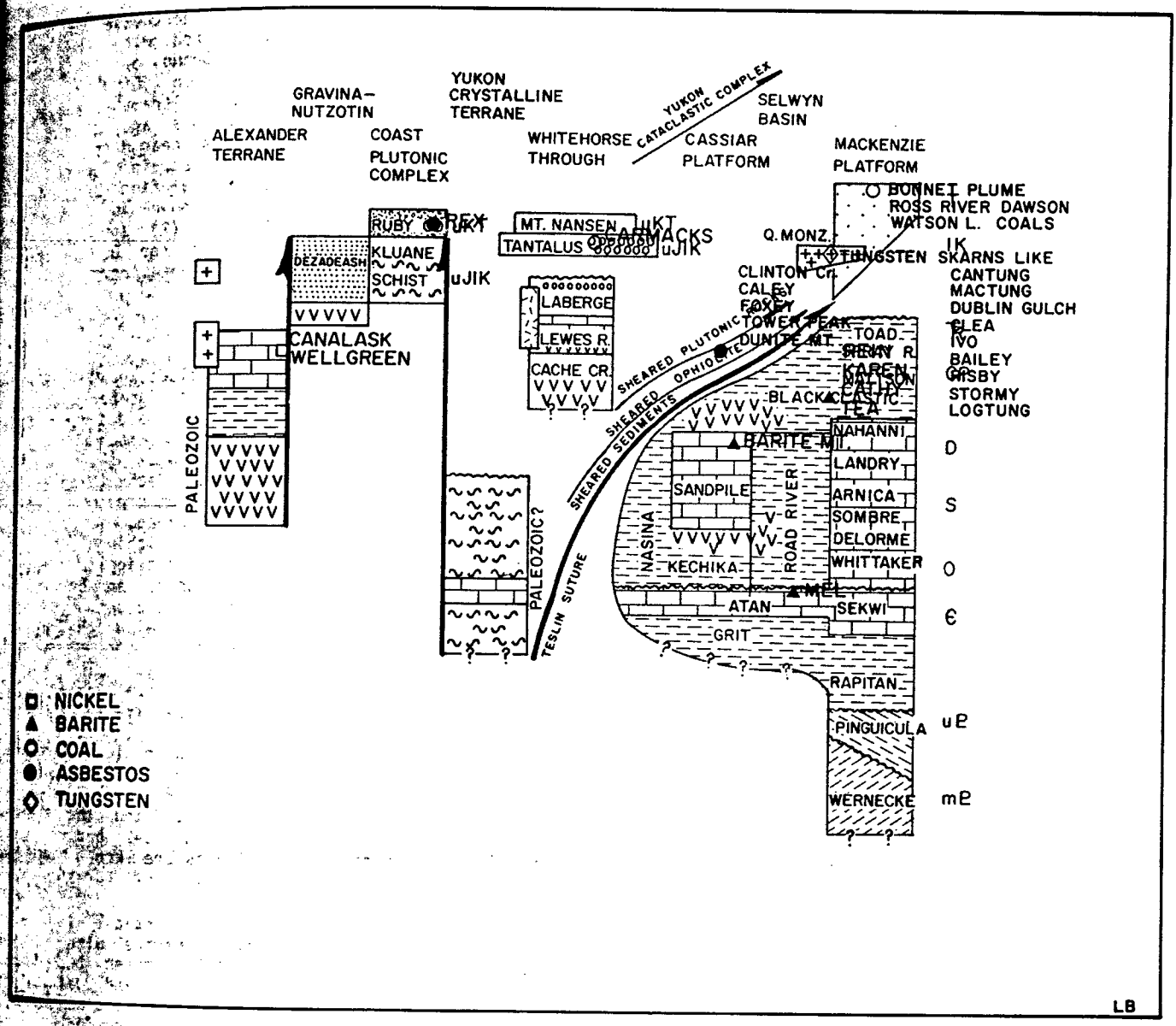


Figure 10a & 10b

Sketch map and columnar sections to show the distribution of iron, nickel, barite, asbestos and coal deposits.


GRAVINA–
NUTZOTIN
YUKON
CRYSTALLINE
TERRANE
YUKON CATACLASTIC COMPLEX
SELWYN
BASIN
ALEXANDER
TERRANE
COAST
PLUTONIC
COMPLEX
WHITEHORSE
THROUGH
CASSIAR
PLATFORM
MACKENZIE
PLATFORM
BONNET PLUME
ROSS RIVER DAWSON
WATSON L. COALS
RUBY
MT. NANSEN
TANTALUS
Q. MONZ.
TUNGSTEN SKARNS LIKE
CANTUNG
MACTUNG
DUBLIN GULCH
FLEA
IVO
BAILEY
GO
MSBY
STORMY
LOGTUNG
DEZADEASH
KLUANE
SCHIST
uJIK
LABERGE
LEWES R.
CACHE CR.
CANALASK
WELLGREEN
PALEOZOIC
PALEOZOIC?
CLINTON Cr.
CALEY
FOSSIL
TOWER PEAK
DUNITE MT.
SHEARED PLUTONIC
SHEARED OPHIOLITE
SHEARED SEDIMENTS
TESLIN SUTURE
TOAD
GRAY R.
KAREN
WATSON
CASTLE
FLEA
BLACK
BARITE MT.
NAHANNI
LANDRY
ARNICA
SOMBRE
DELORME
WHITTAKER
SEKWI
SANDPILE
NASINA
KECHIKA
ROAD RIVER
ATAN
GRIT
RAPITAN
PINGUICULA
WERNECKE
D
S
O
€
uP
mP
NICKEL
BARITE
COAL
ASBESTOS
TUNGSTEN
LB

Red Mountain (Craig and Laporte, 1972, p. 121) is Yukon's sole molybdenite deposit per se. A stockwork of quartz veins within quartz monzonite is host to disseminated molybdenite and pyrite with few other sulphides. An area 1000 m x 300 m contains nearly 0.1% MoS_2 to depths about 1000 m. The quartz monzonite host is an outlying stock of the Quiet Lake Batholith and is part of the Cretaceous suite associated with the ancient North American margin. As such, Red Mountain is genetically comparable to the Logtung deposit.

MISCELLANEOUS OTHER DEPOSITS

Iron

Crest (Dahlstrom, 1972; Green and Godwin, 1963, p. 15-18) is an iron deposit estimated to contain 30 or 40 billion tonnes of strippable, high phosphorous ore with 40% to 50% iron. It is at the headwaters of Snake River near the Northwest Territories border (Figure 10). Hematite and jasper iron formation occur in 120 m interval in the lower part of the Rapitan Group. The Rapitan is a Proterozoic pebbly mudstone of possible glacial origin correlated roughly with the "Grit Unit" and deposited on the ancient North American element in Mackenzie Platform. The unit is unconformably overlain by Ordovician dolomite and only erosional remnants are preserved beneath this unconformity in the area of interest. Crest, Yukon's sole iron deposit, is presently too remote for mining and its high phosphorous is a problem in smelting.

Nickel

Two nickel deposits, Wellgreen (Campbell, 1977) and Canalask (Findlay, 1969, p. 65-68) occur 60 km apart in the Kluane Ranges immediately southwest of Shakwak trench (Figure 10). They are in serpentinized ultramafic sheets within Permian sedimentary and volcanic strata. Nickeliferous pyrrhotite with pentlandite, sphalerite, pyrite and chalcopyrite forms massive lenses and are disseminated in the volcanic rocks. Wellgreen contained 650,000 tonnes with 2.05% nickel, 1.42% copper before mining. During 1972-1973, 170,000 tonnes with 2.30% nickel, 1.40% copper, 2.02 gm/t platinum and 0.073% cobalt were milled.

A$bestos

Deposits of asbestos are associated with four sets of ultramafic rocks. Most showings are in bodies of the areally extensive alpine-type ophiolites that are part of the Anvil Allochthonous Assemblage of Yukon Cataclastic Complex (Figure 10). They include the Clinton Creek (Htoon, 1976) and several other showings near Dawson (Foxy, Caley, Tjop), the Tower Peak, Hoole River and Dunite Mountain showings in the Pelly Mountains and small occurrences south and west of Frances Lake. Cassiar Asbestos, in northern B.C. also belongs to this group. In all the showings asbestos occurs as fillings of irregularly oriented fractures of varied width that post-date the strain fabric in the serpentinite. The host rocks are probably Late Paleozoic and the asbestos was likely emplaced during final tectonism when the strata were thrust over the ancient North American margin about the Jura-Cretaceous.

Two or three small showings northeast of Ma Lake are in ultramafics associated with the Pe sylvanian-Permian Cache Creek Group of Whiteho Trough. The Rex near Haines Junction (Findlay, 19 p. 55-56) is enclosed by the third ultramafic suite, Alaskan type body (?) of Cretaceous age within Coast Plutonic Complex. Like those near Marsh Lake peridotite lacks the penetrative strain fabric t characterizes many of the ultramafics in An Allochthon. Finally, asbestos is known in serpent ized peridotite of Early Paleozoic (?) age near northern edge of Selwyn Basin where the Dawson fa exposes possible oceanic material that floors part the Basin (Craig property).

Barite

Yukon's barite occurrences include the Mel, Bar Mountain, Tea, Karen, Rein, Cathy and Barite; none currently being mined. They include bedded and v types, but all are in ancient North American Paleoz strata close to the edges of Selwyn Basin (Figure 1 The bedded variety includes the Tea, Cathy (Sinclair al, 1976, p. 29), Rein and Barite occurrences, wh thin-bedded to laminated fine-grained, light g barite forms stratum-confined lenses within black sl stratigraphically low in the Mississippian "Bl Clastic" or Earn Group. The lenses can be tra laterally for hundreds of metres and are commonly t of metres thick. They interfinger with the bar strata laterally and up section and the barite simply a facies of the black slate unit. The bed deposits are stratigraphically and geographically cl to the Tom-Jason bedded lead-zinc-silver-barite posits (Carne, 1979). Two showings of the same t and in the same host rocks are known in the Pe Mountains northwest of Mount Cook. The Tea conta about a quarter million tonnes of direct shipp barite with a specific gravity of 4.24 and the Bar showing has 2.7 million tonnes of 84% barite w 12.14% SiO_2. Several barite lenses are known on Rein where a million tonnes or more of barite oc close to the surface.

The Mel (Carne, 1976)is a vertical lens coarse-crystalline, white, sparry barite with gal and sphalerite. It is sandwiched between the Lo Cambrian Sekwi Formation (limestone) and calcare slate of the Kechika Group (Cambro-Ordovicia Although it follows a stratigraphic contact there is interfingering of mineralized and unmineralized str and the deposit is hydrothermally mobilized. Some the wall rocks contain disseminated sulphides barite and this may be the source of the mobilized l of massive barite. About 5 million tonnes grad 52.1% barite with 2.05% lead and 5.6% zinc indicated at the Mel.

On Barite Mountain (Green and Godwin, 1964, p. south of Ross River a dozen steep dipping veins coarsely crystalline white barite between 30 cm and thick cut Siluro-Devonian dolomite of Cassiar Platfor The veins are confined to a fractured zone that is hanging wall of a thrust bringing the carbonate ab the lower black slate of the Earn Group. The miner ization may be mobilized from a stratigraphic source the slate into the fractured carbonate above thrust. If so, mobilization occurred about the Ea Cretaceous. Size is limited, but the veins essentially pure barite.

[redacted] occur in three stratigraphic associations in [redacted] subbituminous coal in Eocene strata along [redacted] trench, thermal coal in Late Cretaceous rocks [redacted] Plume basin and bituminous coal in the [redacted] Cretaceous Tantalus Formation of Whitehorse Trough [redacted] 10). A list and general review of Yukon coal [redacted] occurrences is given by Campbell, 1967.

The coals in Tintina Trench are found in immature [redacted] Eocene strata near Dawson, Ross River and [redacted] Lake. The coals formed in swamps and are [redacted] in fluviatile strata deposited in strike-slip [redacted] controlled basins along Tintina Fault. Although these [redacted] deposits may be small, their size is incompletely [redacted] They are the subject of a recent study by D. [redacted] 1980. Subbituminous coal is also known south of [redacted] on Matson Creek in Eocene (?) beds and near Big [redacted] and just 10 km northwest of Carmacks in Pliocene [redacted] beds.

The largest coal deposit in Yukon occurs as three [redacted]-horizontal seams within Late Cretaceous and Early [redacted] fluviatile beds deposited in the fault [redacted] controlled Bonnet Plume basin (Long, 1978). The [redacted] has been drilled on a 1 km grid and more than [redacted] million tonnes of thermal grade high voltile, low [redacted] low sulphur coal has been outlined.

Between Carmacks and Braeburn and west of White-[redacted] showings of coking coal are found in fluviatile [redacted] grain conglomerate of the Tantalus Formation. [redacted] deposit at Tantalus Butte, near Carmacks, has been [redacted] intermittently since early this century, first to [redacted] fuel for Yukon River steamers and in the last [redacted] to dry zinc-lead concentrates of the Faro mill. [redacted] coal is known in the upper nonmarine part of the [redacted] Laberge Group.

Uranium

Uranium in Yukon occurs in two associations, in or around heterolithic breccia pipes that cut Proterozoic strata and as veins in or near the Cretaceous intrusive rocks. Breccia pipe deposits (Morin et al, p. 101-107) (Archer and Schmidt, 1978) (Bell and Delaney, 1977) include the Nor, Loon, Igor, Thor, Bond, Pterd and Otter in the Wernecke and Richardson mountains. The pipes predate the Rapitan Group and are therefore Proterozoic. They are subcircular in plan and a km or two across. The host rocks are thin-bedded shale siltstone and dolomite of the Wernecke and Pinguicula Groups. Breccia in the pipes contains a variety of clasts of the Proterozoic strata in fine matrix that lacks an introduced volcanic component. The pipes host two types of mineralization. The early phase is interstitial to breccia fragments and is dominated by hematite and chalcopyrite and locally includes cobaltite. The later mineralization includes pitchblende and brannerite which occur in narrow irregular fractures that cut the breccia. The occurrences are interesting prospects, but are presently subeconomic.

Uranium occurrences related to the Cretaceous intrusions include the Ting, Noting and A and AB properties 40 km north of Dawson and the Jove a similar distance to the south. Those north of Dawson have uraninite in narrow fractures within tinguaite, a distinctive phase of the Tombstone and Deadman stocks. These plutons are dominantly syenite unlike the quartz monzonite that makes up most of the other intrustions of the same age. The occurrences are subeconomic. The Jove contains metaautunite in fractures within sheet-like intrusions of Cretaceous quartz monzonite that cut the Pelly Gneiss.

References

See BIBLIOGRAPHY this volume.